

National Library of Canada

Acquisitions and Bibliographic Services Branch

395 Wellington Street Ottawa, Ontario K1A 0N4 Bibliothèque nationale du Canada

Direction des acquisitions et des services bibliographiques

395, rue Wellington Ottawa (Ontario) K1A 0N4

Apartile Votre reference

Our file Notice references

#### NOTICE

The quality of this microform is heavily dependent upon the quality of the original thesis submitted for microfilming. Every effort has been made to ensure the highest quality of reproduction possible.

If pages are missing, contact the university which granted the degree.

Some pages may have indistinct print especially if the original pages were typed with a poor typewriter ribbon or if the university sent us an inferior photocopy.

Reproduction in full or in part of this microform is governed by the Canadian Copyright Act, R.S.C. 1970, c. C-30, and subsequent amendments.

### **AVIS**

La qualité de cette microforme dépend grandement de la qualité de la thèse soumise au microfilmage. Nous avons tout fait pour assurer une qualité supérieure de reproduction.

S'il manque des pages, veuillez communiquer avec l'université qui a conféré le grade.

La qualité d'impression de certaines pages peut laisser à désirer, surtout si les pages originales ont été dactylographiées à l'aide d'un ruban usé ou si l'université nous a fait parvenir une photocopie de qualité inférieure.

La reproduction, même partielle, de cette microforme est soumise à la Loi canadienne sur le droit d'auteur, SRC 1970, c. C-30, et ses amendements subséquents.



## UNIVERSITY OF ALBERTA

# REGULATION OF ACTION POTENTIAL IN AMPHIBIAN SYMPATHETIC NEURONES

BY



# **BALVINDER SINGH JASSAR**

A THESIS SUBMITTED TO THE FACULTY OF GRADUATE STUDIES AND RESEARCH IN PARTIAL FULFILMENT OF THE REQUIREMENT FOR THE DEGREE OF DOCTOR OF PHILOSOPHY.

DEPARTMENT OF PHARMACOLOGY
EDMONTON, ALBERTA.
FALL, 1993.



Acquisitions and Bibliographic Services Branch

395 Wellington Street Ottawa, Ontario K1A 0N4 Bibliothèque nationale du Canada

Direction des acquisitions et des services bibliographiques

395, rue Wellington Ottawa (Ontario) K1A 0N4

Your file. Votre reference

Our file Notic reference

The author has granted an irrevocable non-exclusive licence allowing the National Library of Canada to reproduce, loan, distribute or sell copies of his/her thesis by any means and in any form or format, making this thesis available to interested persons.

L'auteur a accordé une licence irrévocable et non exclusive Bibliothèque permeitant à la nationale du Canada reproduire, prêter, distribuer ou vendre des copies de sa thèse de quelque manière et sous quelque forme que ce soit pour mettre des exemplaires de cette disposition thèse la des personnes intéressées.

The author retains ownership of the copyright in his/her thesis. Neither the thesis nor substantial extracts from it may be printed or otherwise reproduced without his/her permission. L'auteur conserve la propriété du droit d'auteur qui protège sa thèse. Ni la thèse ni des extraits substantiels de celle-ci ne doivent être imprimés ou autrement reproduits sans son autorisation.

ISBN 0-315-88328-6



UNIVERSITY OF ALBERTA

**RELEASE FORM** 

NAME OF AUTHOR:

Balvinder Singh Jassar

TITLE OF THESIS:

Regulation of action potential in amphibian

sympathetic neurones.

DEGREE:

Doctor of Philosophy

DEGREE AWARDED:

Fall, 1993

Permission is hereby granted to the UNIVERSITY OF ALBERTA LIBRARY

to produce single copies of this thesis and to lend or sell such copies for private,

scholarly or scientific research purposes only.

The author reserves all other publication and other rights in association with

the copyright in the thesis, and except as hereinbefore provided neither the thesis nor

any substantial portion thereof may be printed or otherwise reproduced in any

material form whatever without the author's prior written permission.

Balvinder Singh Jassar

Boling Jossak

3504-25th Avenue

Edmonton, Alberta.

Dated: May 26, 1993

#### UNIVERSITY OF ALBERTA

#### FACULTY OF GRADUATE STUDIES AND RESEARCH

The undersigned certify that they have read, and recommended to the Faculty of Graduate Studies And Research for acceptance, a thesis entitled "Regulation of Action Potential in Amphibian Sympathetic Neurones" submitted by Balvinder Singh Jassar in partial fulfilment of the requirement for the degree of Doctor of Philosophy in Pharmacology.

(Dr. P.A. Smith; Supervisor)

P. Dmich.

(Dr. W.F. Dryden)

(Dr. T. Gordon)

(Dr. R.B. Campenot)

(Dr. E. Cooper; External

Examiner)

Swan Mg Dum

(Dr. S.M.J. Dunn; Committee

Chair)

Dated: May 26, 1993



#### **ABSTRACT**

Ionic currents through Ca<sup>2+</sup> and K<sup>+</sup> channels help to determine the integrative properties of nerve cells. These channels are susceptible to 'endogenous' regulation due to intrinsic properties of ion channels and neurones as well as 'exogenous' modulation by neurotransmitters, neuromodulators and perhaps also by trophic factors.

This thesis describes aspects of ion channel regulation in bullfrog sympathetic ganglion (BFSG) B-neurones. The duration of the afterhyperpolarization (ahp) which follows the action potential (ap) was frequency-dependent; the duration recorded when the neurone was stimulated at 0.5Hz was much shorter than that recorded when the neurone was stimulated at 0.012Hz. This phenomenon was attributed to an *intrinsic* property of Ca<sup>2+</sup> channels; a slow inactivation process which resulted in a frequency-dependence of whole-cell Ca<sup>2+</sup> currents (I<sub>Ca</sub>). The frequency-dependence of ahp correlated very well with the estimated frequency-dependence of Ca<sup>2+</sup> influx. Ca<sup>2+</sup>-induced Ca<sup>2+</sup> release did not seem to contribute to the frequency-dependence or to the generation of the ahp following a single a.p. because drugs which block Ca<sup>2+</sup> release from intracellular stores had minor and variable effects.

Axotomy increases the amplitude and duration of the a.p. and decreases the duration and amplitude of ahp in BFSG B-cells. The mechanism of this effect was examined using whose cell patch-clamp and voltage-clamp methods. Fura-2 spectrophotometric measurements showed that the concentration of intracellular  $Ca^{2+}$  in the cell body was not changed after axotomy. N-type  $Ca^{2+}$  currents exhibited increased inactivation and  $I_{Ca}$  amplitude was reduced to approximately 52%

of control. The  $Ca^{2+}$ -activated  $K^+$  currents,  $I_C$  and  $I_{AHP}$  were also decreased as a consequence of this reduction in  $I_{Ca}$ . The delayed rectifier  $K^+$  current  $(I_K)$  was reduced and the transient  $K^+$  currents,  $I_A$  and  $I_{SA}$  were practically absent from axotomized neurones. The amount of M-current  $(I_M)$  and sodium current  $(I_{Na})$  increased after axotomy whereas leak conductance was not affected. These results explain the effects of axotomy on the shape of a.p. and show that the properties of the  $Ca^{2+}$  channels, several different  $K^+$  channels and  $Na^+$  channels are **differentially** regulated by contact of sympathetic nerves with their target organ ('exogenous' regulation).

#### ACKNOWLEDGEMENT

First and foremost, I would like to express my sincerest thanks to Dr. Peter Smith for his ongoing moral support, confidence in me as a scientific investigator and guidance throughout the period of investigation. I also like to thank him for the financial support provided for travel to Calgary for attending a course in electrophysiological techniques and to Toronto to Dr. Pennefather's laboratory for carrying out experiments and biophysical analysis.

I am greatly indebted to Dr. Peter Pennefather (University of Toronto) for the use of his laboratory and equipment for microspectrofluorometric measurement of intracellular calcium. I would also like to thank him for helping me in modelling of ionic currents, providing mathematical derivations for describing slow inactivation of calcium currents and in interpretation of the data. To Dr. Steve Ross for his help in intracellular calcium measurements. To Dr. Paul Adams (State University of New York) and Dr. S.W. Jones (Case Western Reserve University) for their critical comments on manuscripts before submission to Journal of Physiology. I also wish to thank Dr W.F. Dryden, Dr. T. Gordon, Dr. W.F. Colmers, Dr Susan Dunn and Dr. R.B. Campenot for serving on my Ph.D thesis and examination committees and for providing feedback on the progress of the project.

To my friends Jeffery Zidichouski, Hisinyo Chen, Sam Kombian, Murat Oz, Manju Bhat, Gloria Klapstein, Rory McQuiston, Susan Fu and Mukaila Raji for their enlightening discussions from time to time. To Dave Ogden, Sam Grazziano and Nick Diakiw, the people in department of pharmacology workshop for machining

different small components as required and help in electronic troubleshooting.

I express my thanks to Natural Sciences and Engineering Research Council, Alberta Heritage Foundation for Medical Research and University of Alberta for providing studentship. My sincerest thanks to Medical Research Council of Canada for providing Postdoctoral Fellowship for Ph.D. training.

Lastly, I would like to extend my heartiest thanks to my family who held their confidence in my ability to the earnest and always stood by and supported me financially and morally. Special thanks to my parents who inculcated in me a great deal of self-confidence, patience and reasoning nature without which this project could not have been completed.

# TABLE OF CONTENTS

CHAPTER 1. Introduction.	
1.1 General Introduction.	2
1.2 Ion channel: biophysics, pharmacology, structure, modulation	
and regulation.	4
1.2.1 Sodium channels.	4
1.2.1.1 Biophysical characteristics and pharmacology of sodium	
channels.	4
1.2.1.2 Structural features of sodium channels.	6
1.2.1.3 Modulation and regulation of sodium channels.	8
1.2.2 Calcium channels.	10
1.2.2.1 Biophysical characteristics and pharmacology of calcium	
channels.	10
1.2.2.2 Structural features of calcium channels.	14
1.2.2.3 Modulation and regulation of calcium channels.	15
1.2.3 Potassium channels	17
1.2.3.1 Biophysical characteristics and pharmacology of potassium	
channels.	17
1.2.3.1.1 Delayed rectifier K <sup>+</sup> currents.	17
1.2.3.1.2 Transient voltage-dependent K <sup>+</sup> currents.	19
1.2.3.1.3 M-current (I <sub>M</sub> )	20
1.2.3.1.4 Calcium-activated potassium currents.	22

1.2.3.2 Structural features of potassium channels.	25
1.2.3.3 Modulation and regulation of potassium channels.	28
1.2.4 Inwardly-rectifying Na <sup>+</sup> /K <sup>+</sup> current.	28
1.3 Intracellular calcium.	29
1.4 Developmental regulation of ion channels.	33
1.5 Dependence of ion channels on an intact axon.	36
1.6 Rationale and statement of the problem.	40
1.7 References.	44
Chapter 2. Changes in sodium and calcium channel activity following	
axotomy of B-cells in bullfrog sympathetic ganglion.	81
2.1 Summary.	82
2.2 Introduction.	84
2.3 Methods.	85
2.4 Results.	91
2.4.1.1 Effects of axotomy on I <sub>Ba</sub> .	91
2.4.1.2 Pharmacology of Ba <sup>2+</sup> currents before and after	
axotomy.	96
2.4.1.3 Effects of axotomy on inactivation of I <sub>Ba</sub> .	102
2.4.1.4 Effects of axotomy on activation and deactivation of $I_{Ba}$ .	114
2.4.2 Effects of axotomy on I <sub>C</sub> .	117
2.4.3 Effects of axotomy on I <sub>Na</sub> .	123
2.5 Discussion.	131

2.5.1 Mechanism of axotomy-induced spike broadening.	131
2.5.2 Changes in $I_{Ba}$ and $Ca^{2+}$ channels.	132
2.5.3 Changes in I <sub>Na</sub> .	135
2.5.4 Effects of axotomy on ion channels.	136
2.6 Appendix.	138
2.7 References.	140
Chapter 3. Changes in potassium channel activity following axotomy	
of B-cells in bullfrog sympathetic ganglion cells.	147
3.1 Summary.	148
3.2 Introduction.	151
3.3 Methods.	153
3.3.1 Electrophysiological recording.	153
3.3.2 Intraceilular calcium measurements.	156
3.3.3 Modelling.	157
3.4 Results.	157
3.4.2 Effects of axotomy on $I_M$ and $I_{leak}$ .	158
3.4.3 Effects of axotomy on $I_A$ and $I_{SA}$ .	162
3.4.4 Effects of axotomy on $I_C$ .	163
3.4.4.1 $I_C$ evoked with 50ms pulses from $-40$ mV.	164
3.4.4.2 I <sub>C</sub> evoked with short pulses.	170
3.4.5 Effects of axotomy on I <sub>K</sub> .	177
3.4.6 Effects of axotomy on I <sub>AHP</sub> .	180

3.5 Discussion.	
3.5.1 Resting membrane potential and excitability.	183
3.5.2 Changes in $I_C$ after axotomy.	186
3.5.3 Changes in I <sub>K</sub> .	195
3.5.4 Changes in I <sub>AHP</sub> .	196
3.5.5 Concluding comments.	196
3.6 Appendix.	
3.7 References.	200
Chapter 4. Slow frequency-dependence of action potential	
afterhyperpolarization in bullfrog sympathetic ganglion	
neurones.	208
4.1 Summary.	209
4.2 Introduction.	210
4.3 Material and methods.	212
4.3.1 Intracellular recording.	212
4.3.2 Whole-cell patch-clamp recording.	214
4.4 Results.	216
4.4.1 Frequency-dependence of the a.h.p.	216
4.4.2 Effects of drugs on frequency-dependence of the a.h.p.	219
4.4.3 Frequency-dependence of Ca <sup>2+</sup> influx.	222
4.4.4 Frequency-dependence of Ca <sup>2+</sup> spikes.	233
4.4.5 Significance of a.h.p. frequency-dependence.	233

4.5 Discussion.	236
4.6 References.	239
Chapter 5. General discussion.	245
5.1 Introduction.	246
5.2 Frequency-dependence of action potential	
afterhyperpolarization.	246
5.3 Axotomy-induced changes in ion channels.	247
5.3.1 Changes in Ca <sup>2+</sup> channels.	248
5.3.1.1 Phosphorylation state of channels.	248
5.3.1.2 Changes in channel macromolecules and or G-protein	
activation.	249
5.3.1.3 Cytoskeleton and Ca <sup>2+</sup> channels.	250
5.3.2 Changes in Na <sup>+</sup> channels.	250
5.3.3 Changes in Ca <sup>2+</sup> -activated K <sup>+</sup> channels.	251
5.3.4 Changes in voltage-activated K <sup>+</sup> channels.	253
5.4 Intracellular calcium.	254
5.5 Dedifferentiation and axotomy.	255
5.6 Dependence of ion channels on an intact axon.	256
5.7 Possible mechanisms of axotomy-induced changes.	257
5.7.1 Trophic factors.	258
5.7.2 Activity and activity-dependent changes in second	
messengers.	259

5.7.3 Changes in gene expression and cytoskeletal disruption.	260
5.7.4 Inflammation and axonal transport.	260
5.8 Conclusions and future experiments.	261
5.9 References	268

# LIST OF TABLES

1. Components of inactivation of  $I_{Ba}$ .

# LIST OF FIGURES

## CHAPTER 2.

1.	Effects of axotomy on Ba <sup>2+</sup> currents.	92-93
2.	Comparison of $I_{\mbox{\footnotesize{Ba}}}$ in control and axotomized neurones.	94-95
3.	Comparison of the effects of 200nM $\omega\text{-conotoxin}$ on $I_{\text{Ba}}$ in	
	control and axotomized neurones.	97-98
4.	Voltage-dependence of the effects of dihydropyridines on	
	I <sub>Ba</sub> in control and axotomized neurones.	100-101
5.	Effects of $I_{Ba}$ evoked from different holding potentials.	103-104
6.	Effects of axotomy on time-dependence of onset and	
	recovery from inactivation.	107-108
7.	Effects of axotomy on voltage-dependence of inactivation of	
	$I_{Ba}$ .	112-113
8.	Effects of axotomy on kinetics of activation and deactivation	
	of I <sub>Ba</sub> .	115-116
9.	Comparison of I <sub>C</sub> in a typical control and a	
	typical axotomized neurone.	118-119
10.	Effects of axotomy on I <sub>C</sub> .	121-122
11.	Effects of axotomy on I <sub>Na</sub> .	124-125
12.	Effects of axotomy on voltage and time-dependence of	
	development of inactivation of I <sub>Na</sub> .	127-128
13.	Effects of axotomy on voltage and time-dependence of	

## CHAPETR 3.

1.	Effects of axotomy on I <sub>M</sub> .	159-160
2.	I <sub>C</sub> evoked in a typical control and a typical axotomized	
	neurone by applying 50ms depolarizing command pulses	
	from a holding potential of -40mV.	165-166
3.	Effects of axotomy on $I_{\rm C}$ evoked with long (50ms) command	
	pulses from a holding potential of -40mV.	167-168
4.	I <sub>C</sub> evoked in a typical control and a typical axotomized	
	neurone by applying 3ms depolarizing command pulses	
	from a holding potential of -80mV.	171-172
5.	Effects of axotomy on $I_C$ evoked with brief (3ms) command	
	pulses from a holding potential of -80mV.	173-174.
6.	Effects of axotomy on I <sub>K</sub> .	178-179
7.	Effects of axotomy on I <sub>AHP</sub> .	181-182
8.	I-V curves of $I_C$ and $I_{Ca}$ used in simulations.	189-190
9.	Results of I <sub>C</sub> simulations.	192-193

## CHAPTER 4.

- Frequency-dependence of a.h.p. duration in bullfrog
   sympathetic ganglion cells.

  217-218
- 2. Effects of caffeine and ryanodine on frequency-dependence

	of a.h.p. duration.	220-221
3.	Frequency-dependence of Ca <sup>2+</sup> currents recorded using the	
	whole-cell patch-clamp technique.	223-224
4.	Frequency-dependence of Ba <sup>2+</sup> currents recorded using the	
	whole-cell patch-clamp technique.	226-227
5.	Comparison of the effects of stimulus interval on normalized	
	a.h.p. duration and normalized tail current area.	229-230
6.	Frequency-dependence of Ca <sup>2+</sup> spike duration.	231-232
7.	Effects of frequency-dependence of a.h.p.	
	duration on excitability.	234-235

## LIST OF ABBREVIATIONS

a.p. action potential

ahp afterhyperpolarization

BDNF brain-derived neurotrophic factor

BFSG bullfrog sympathetic ganglion

C coulomb (unit of charge)

[Ca<sup>2+</sup>]<sub>i</sub> intracellular calcium concentration

[Ca<sup>2+</sup>]<sub>o</sub> extracellular calcium concentration

cDNA complementary DNA

CHO chinese hamster ovary

CICR calcium-induced calcium release

C<sub>in</sub> input capacitance

C<sub>m</sub> membrane capacitance

cm<sup>-2</sup> per square centimeter

CNTF ciliary neurotrophic factor

d duty cycle of 'Axoclamp' amplifier

DNA deoxyribonucleic acid

DUM dorsal unpaired median (neurones)

e elementary electronic charge

E<sub>Ca</sub> calcium equilibrium potential

E<sub>Na</sub> sodium equilibrium reversal potential

E<sub>K</sub> potassium equilibrium potential

exp

exponent

F

frequency

F<sub>350</sub>, F<sub>380</sub>

fluorescence intensity at 350nm and at 380nm

**FGF** 

fibroblast growth factor

Fura-2AM

Acetomethoxy-ester of Ca<sup>2+</sup>-sensitive dye, Fura-2

g

(voltage-clamp) gain

G

conductance

GAP-43

growth-associated protein (43 KD)

 $G_{\mathbf{C}}$ 

C (maxi  $G_{K,Ca}$ ) conductance

 $G_{Ca}$ 

calcium conductance

**GHK** Equation

Goldman-Hodgkin-Katz Equation

 $G_{K}$ 

delayed rectifier conductance

 $G_{K,Ca}$ 

calcium-sensitive K<sup>+</sup> conductance

 $G_{M}$ 

M-current conductance

 $G_{Na}$ 

sodium conductance

HTMR

high threshold mechanoreceptor

**HVA** 

high voltage-activated (calcium channels)

Hz

Hertz

I

current

 $I_A$ 

fast, transient K+ current

I<sub>AHP</sub>

voltage-insensitive Ca2+-activated K+ current

 $I_{Ba}$ 

barium current through Ca2+ channels

 $I_{C}$ 

voltage-sensitive Ca<sup>2+</sup>-activated K<sup>+</sup> current

I<sub>Ca</sub> calcium current

 $I_H$ ,  $I_Q$ ,  $I_f$  hyperpolarization activated Na<sup>+</sup>/K<sup>+</sup> current

I<sub>K</sub> delayed rectifier K<sup>+</sup> current

IL-1 interleukin-1

I<sub>M</sub> muscarine-sensitive K<sup>+</sup> current

I<sub>Na</sub> sodium current

I<sub>SA</sub> slow, transient K<sup>+</sup> current

k Boltzmann's cnstant

K<sub>D</sub>, K<sub>d</sub> dissociation constant

l litre

LVA low voltage-activated (calcium channels)

MAP microtubule-associated protein

 $\mu$ F microfarad

ml millilitre

mm millimeter

mM millimolar

 $\mu$ M micromolar

mRNA messenger RNA

ms millisecond

mS millisiemer

 $\mu$ S microsiemen

nA nanoampere

NGF nerve growth factor

nm nanometer

nM nanomolar

nS nanosiemen

osm/kg osmols per kilogram

pA picoampere

pF picofarad

pS picosiemen

R<sub>in</sub> input resistance

 $R_{min}$  minimum ratio of  $F_{350}/F_{380}$ 

RMP resting membrane potential

 $R_{max}$  maximum ratio of  $F_{350}/F_{380}$ 

RNA ribonucleic acid

T absolute temperature

 $\tau_{\rm act}$  time constant for activation

 $\tau_{\text{Deact}}$  time constant for deactivation

V voltage or potential

V<sub>E</sub> peak clamp error in voltage-clamp

V<sub>o</sub> voltage for half-maximal activation or inactivation

V<sub>C</sub> command voltage

 $V_m$  or  $V_M$  membrane voltage

V<sub>S</sub> steady-state error in voltage-clamp

z valency (of gating particle)

## **DRUGS AND CHEMICALS**

4-AP 4-aminopyridine

ATP adenosine triphosphate

BaCl<sub>2</sub> barium chloride

BAPTA 1-2-bis(2-aminophenoxy)ethane-N,N,N',N'-

tetraacetic acid

cAMP (cyclic-AMP) adenosine 3':5'-cyclic monophosphate

CaCl<sub>2</sub> calcium chloride

CdCl<sub>2</sub> cadmium chloride

CCCP carbonyl cyanide m-chlorphenylhydrazine

cGMP guanosine 3':5'-cyclic monophosphate

CsOH caesium hydroxide

DMSO dimethylsulfoxide

EGTA ethylene glycol bis-N,N,N',N'-tetraacetic acid

FCCP carbonyl cyanide

p-trifluoromethoxyphenylhydrazine

GTP guanosine triphosphate

GTP-γ-S guanosine-5'-[3-thiol]-triphosphate

HEPES N-2-hydroxyethyl piperazine N'-2-ethanesulfonic

acid

KCl potassium chloride

IP3 inositol 1,4,5-trisphosphate

LHRH leutinizing hormone releasing hormone

MgCl<sub>2</sub> magnesium chloride

MnCl<sub>2</sub> manganese chloride

NaCl sodium chloride

NMG.Cl N-methyl D-glucamine chloride

PDB phorbol dibutyrate

PKA protein kinase A

PKC protein kinase C

PKI protein kinase inhibitor

PMA phorbol 12-myristate 13-acetate

STX saxitoxin

TEA Br tetraethyl ammonium bromide

Tris tris(hydroxymethyl)aminomethane

TTX tetrodotoxin

CHAPTER 1.

INTRODUCTION

#### 1.1 GENERAL INTRODUCTION

The electrophysiological properties of neuronal cell membranes are determined by the activity of the ion channels that are present in them. These properties are exhibited in the form of local, graded potentials (excitatory synaptic potentials, inhibitory synaptic potentials, electrotonic potentials etc.) which are important for communication within the same neurone or action potentials which are the universal language of communication between the neurones and the target cell. Action potentials result from the intricate kinetic activity of different ion channels as a result of voltage- or Ca<sup>2+</sup>-dependent activation, inactivation, and/ or deactivation (Hodgkin & Huxley, 1952; Yamada, Koch & Adams, 1989; Belluzzi & Sacchi, 1991). The shape of the action potential and the membrane properties display a considerable degree of variability in different neuronal types which reflect the contribution of different ion channels as a result of their relative abundance and their specific kinetic properties. The contribution and kinetic properties of various ion channels are subject to regulation and modulation by various endogenous and exogenous influences. The changes brought about by such interactions will affect the currents through different ion channels which will be reflected as a change in the shape of the action potential and other membrane properties like resting membrane potential, conduction velocity, threshold for generation of an action potential. Thus, various voltage - and Ca<sup>2+</sup>-activated channels play a crucial role in determining the integrative and membrane properties of the neurone.

Biophysical, biochemical and molecular biological approaches have been used

to investigate the properties of ion channels. Biophysical characterization of ionic currents, using electrophysiological techniques (recording of whole-cell, single channel and gating currents etc.) and pharmacological tools, has been a fruitful approach to describe the mechanisms and kinetics of activation, deactivation and inactivation. However, there has recently been tremendous progress in the field of molecular biology and the combination of these techniques with biochemical and biophysical methods has proven very successful in identifying structural (molecular) correlates of activation, deactivation and inactivation (Catterall, 1988). For example, the 'gating particles" proposed by Hodgkin & Huxley (1952) now have real structural counterparts in ion channel macromolecules in the S4 segment of the  $\alpha$ -subunit of Na<sup>+</sup> channels (Noda, Shimuzu, Tanabe, Takai, Kayano, Ikeda, Takahashi, Nakayama, Kanaoko, Miniamino, Kangawa, Matuso, Raftery, Hirose, Inayama, Hayashida, Miyata & Numa, 1984). Many of the ion channels which occur in different types of neurones have been purified, their amino-acid sequences elucidated and cDNA's for different subunits cloned. Recent technological advances in the fields of biophysics and molecular biology have enabled us to address the question of whether changes and differences in the electrophysiological properties of neurones reflect changes and differences in ion channels which arise at the transcriptional, translational or posttranslational level.

To understand the mechanism/s of changes in the active membrane properties of a neurone induced by a physiological stimulation or by a pathological situation like injury, it becomes necessary to investigate these changes at the level of ion channels.

Therefore a general overview of the biophysical and pharmacological properties, structural features, regulation of expression and modulation of ion channels is in order. To keep this description to a manageable size, the brief general review is focused on the regulation and modulation of those ion channels which occur in bullfrog sympathetic ganglion (BFSG) cells. An additional section on regulation of intracellular Ca<sup>2+</sup> as it relates to channel function and neuronal survival is also presented.

Previous work in our laboratory has shown that axotomy alters electrophysiological properties of BFSG B-cells (Kelly, Gordon, Shapiro & Smith, 1986; Gordon, Kelly, Sanders, Shapiro & Smith, 1987; Shapiro, Gurtu, Gordon & Smith, 1987). However, the basic mechanism/s underlying these changes has not been investigated so far. Therefore, the investigation of the axotomy-induced changes in ionic currents in these cells has been the major focus of this thesis as it relates to the exogenous regulation of ionic currents.

1.2 ION CHANNELS: BIOPHYSICAL CHARACTERISTICS, PHARMACOLOGY, STRUCTURE, MODULATION AND REGULATION

#### 1.2.1 Sodium Channels

## 1.2.1.1 Biophysical Characteristics and Pharmacology of Sodium Channels

Voltage-sensitive sodium currents (I<sub>Na</sub>) play a fundamental role in the

generation and propagation of a.p.s. Almost all neurones investigated elicit sodium dependent action potentials (Frankenhaeuser & Huxley, 1964; Barrett & Crill, 1980; Kostyuk, Veselovsky & Tsyndrenko, 1981; Bossu & Feltz, 1984; Ishizuka, Hattori & Akaike, 1984) and the underlying  $I_{Na}$ s recorded from different cell types do not show as much diversity in their kinetic properties as the  $Ca^{2+}$  and  $K^+$  currents. Single channel recordings (Sigworth & Neher, 1980) and measurements of macroscopic gating currents (Armstrong, 1981; Armstrong & Bezanilla, 1974) have proven useful in elucidating the kinetic properties of these channels. These studies were the first to suggest a molecular basis for the voltage-dependence of the states and state transitions.  $I_{Na}$  starts to activate at about -30mV, reaching a maximum at +10mV.  $I_{Na}$  exhibits fast, voltage-dependent activation and inactivation which is consistent with its role in the generation of the action potential and also with its role, in part, for the rapid repolarizing phase.

In BFSG B-cells cells, more than 80% of the total  $I_{Na}$  is sensitive to TTX (Jones, 1987a). There are thus two kinds of sodium currents described in these cellstetrodotoxin (TTX)-sensitive and TTX-resistant. Activation of of  $I_{Na}$  is voltage-dependent and very fast; the current peaks in <1ms.  $I_{Na}$  exhibits two types of inactivation: fast and slow. Both the fast and slow inactivation are voltage-dependent (Jones, 1987a). The fast inactivation is complete at potentials positive to -40mV in less than 10ms. Removal of this component of inactivation is also very fast (almost complete removal of inactivation at -80mV in less than 10ms;  $t_{1/2}$  value of 1-2ms). The slow inactivation process is distinct from the fast inactivation: a long (30s)

depolarization to -20mV inactivates nearly all of the current, but half maximal recovery now requires about 5s at -80mV. The TTX-resistant component of  $I_{Na}$  shows slower kinetics. It activates at slightly more negative potentials and inactivates more slowly than the TTX-sensitive component. TTX-resistant  $I_{Na}$  has also been reported in other preparations like denervated or cultured skeletal muscle (Harris & Thesleff, 1971; Pappone, 1980; Gonoi, Sherman & Catterall, 1985), cardiac muscle (Brown, Lee & Powell, 1981), leech neurones (Kleinhaus & Pritchard, 1976) and vertebrate sensory neurones (Kostyuk *et al.*, 1981).

## 1.2.1.2 Structural Features of Sodium Channels

Although no structural data are available for Na<sup>+</sup> channels in BFSG cells, the purification of the channel protein and elucidation of the structure was possible because of its high affinity for TTX and STX (saxitoxin) and the abundance of the protein in various different tissue preparations like eel electroplax (Agnew, Levinson, Brabson & Raftery, 1978; Hartshorne & Catterall, 1981). Molecular biological studies have shown that Na<sup>+</sup> channels are more diverse than expected from the properties of  $I_{Na}$  recorded from different cell types (Trimmer & Agnew, 1989). After some early controversy, there is now a consensus that Na<sup>+</sup> channels comprise three different kinds of subunits; one  $\alpha$  and two different  $\beta$  subunits. The  $\alpha$ -subunit is the main pore-forming structure of the channel. The basic structure of the Na<sup>+</sup> channel can be described as follows (Noda *et al.*, 1984): The channel  $\alpha$ -subunit consists of four repeats of the basic channel-building element. Each repeat consists of

sequence of six hydrophobic and intervening hydrophillic amino acid sequences (S1-S6). The intervening hydrophillic segments form the portions of the channel that extend from the membrane into the intracellular and extracellular aqueous solutions. One of the putative membrane-spanning segments, S4, which is well-conserved among different types of voltage-sensitive ion channels, has a striking pattern of positively charged amino acids, usually arginine, every third residue which would be ideally suited to form the voltage sensor of the channel. Mutagenesis experiments have borne out this speculation. Mutation of some of the S4 basic residue/s to neutral ones reduces sensitivity of the channel to voltage (Stumer, Conti, Suzuki, Wang, Noda, Yahadi, Kubo & Numa, 1989). However, mutations of the neutral residues of this region (leucine in IIs4) also affect voltage-dependence of activation of Na+ channels (Auld, Goldin, Krafte, Catterall, Lester, Davidson & Dunn, 1990). Mutations in the hydrophillic segment located between repeats III and IV alter the inactivation kinetics of the channel (Stumer et al., 1989; Stumer, 1990), as do the antibodies directed to this segment of the protein (these antibodies are effective from the cytoplasmic side only; Vassilev, Scheuter & Catterall, 1988). Most structural hypotheses propose that the four repeats cluster together to surround a central pore. Each would thus be in a position to contribute to that pore's gating and to its permeability properties.

Various different kinds of  $\alpha$ -subunits have been described. For example, three different cDNA's for  $\alpha$ -subunits have been isolated from rat brain which encode three different types of Na<sup>+</sup> channels designated as type I, II & III (Noda *et al.*, 1984).

The  $\beta_2$ -subunit is covalently linked to the  $\alpha$ -subunit whereas  $\beta_1$  is not.  $I_{Na}$  recorded from Xenopus oocytes in which only  $\alpha$ -subunit has been expressed show slower kinetics. Co-expression of  $\alpha$  and  $\beta$  subunits results in expression of  $I_{Na}$  which exhibits the normal rapid activation and inactivation kinetics characteristic of the native Na<sup>+</sup> channels (Isom, DeJongh, Rebber, Offord, Charbonneau, Walsh, Goldin & Catterall, 1992).

## 1.2.1.3 Modulation and Regulation of Sodium Channels

Since the  $\alpha$ -subunit contains consensus phosphorylation sites for the c-AMP-dependent protein kinase (PKA) and protein kinase C (PKC),  $I_{Na}$  may be subject to modulation by cyclic nucleotide dependent kinases. Phorbol esters and activated purified protein kinase C (PKC) affect the voltage-dependent Na<sup>+</sup> channels expressed in Xenopus oocytes injected with chick brain RNA by shifting the voltage-dependence of activation to the right without affecting inactivation (Dascal & Lotan, 1991). This results in reduction of up to ~80% in peak  $I_{Na}$ . Phosphorylation by c-AMP-dependent protein kinase also reduces peak  $I_{Na}$  to 40-50% in membrane patches excised from rat brain neurones or from chinese hamster ovary (CHO) cells expressing type IIA Na<sup>+</sup> channels (Li, West, Lai, Scheuer & Catterall, 1992). Studies with neurotoxins like TTX, STX, batrachotoxin, grayanotoxin, brevitoxin, veratridine, aconitine have been useful in elucidating the mechanisms involved in activation and inactivation of Na<sup>+</sup> channels (Hille, 1992).

Na+ channels are clustered on axons in the initial segments and the area of

node of Ranvier in myelinated axons and in the area of axon hillock on neuronal soma (Wollner & Catterall, 1986). This clustering is dependent on Schwann cell contact in myelinated axons (Joe & Angelides, 1992). During the development of many neuronal types, the expression of Na<sup>+</sup> channels has been shown to be preceded by the expression of Ca<sup>2+</sup> channels because the Ca<sup>2+</sup>-dependent action potentials can often be elicited before Na<sup>+</sup>-dependent action potentials (Harris & Marshall, 1973; Spitzer & Lamborghini, 1976; Spitzer, 1979). Denervation of skeletal muscle leads to an increase in the number of TTX-insensitive Na+ channels (Harris & Thesleff, 1971; Sherman & Catterall, 1982). Axotomy also has been suggested to result in an increase the number of Na+ channels leading to an increase in the rate of rise and amplitude of a.p. (Pinter and Vanden-Noven, 1989; Gallego, Ivorra & Morales, 1987; Kuwada & Wine, 1981; Goodman & Heitler, 1979). The loss of electrical activity produced by TTX, botulinum toxin, local anaesthetics results in an increase in the number of Na<sup>+</sup> channels. This increase in Na<sup>+</sup> channels is a consequence of the increase in the de novo synthesis of channels induced by the changed intracellular c-AMP and Ca<sup>2+</sup> levels (Brodie, Brody & Sampson, 1989; Sherman & Catterall, 1984; Sherman, Chriva & Catterall, 1985).

Disruption of cytoskeletal elements has been suggested to affect the stability and thus expression of ion channels in the membrane. Selective breakdown of microfilaments by cytochalasin B or its derivatives has been shown to cause a reduction in the capability of the membrane to carry Na<sup>+</sup> ions as measured by V<sub>max</sub> of pure Na<sup>+</sup>-spikes (Fukuda, Kameyama & Yamaguchi, 1981). However, disruption

of microtubules by colchicine or vinca alkaloids did not have any effect or pure  $Na^+$ -spikes.

#### 1.2.2 Calcium Channels

## 1.2.2.1 Biophysical Characteristics and Pharmacology of Calcium Channels

The diversity of calcium channels in invertebrate (Hagiwara, 1983) and invertebrate neurones is well-established (Bean, 1989a; Planamer, Logothetis & Hess, 1989; Hess, 1990; Bertolino & Llinas, 1992; Miller, 1992). Voltage-dependent Ca<sup>2+</sup> channels in the plasma membrane, by controlling the Ca<sup>2+</sup> influx, play an important role in various intracellular Ca<sup>2+</sup>-activated processes like excitability, transmitter release, contraction, metabolism and gene expression. Three different types of Ca<sup>2+</sup> currents were distinguished in chicken sensory neurones on the basis of their voltage-dependent kinetic properties; pharmacology (Fox, Nowycky & Tsien, 1987a) and single channel characteristics (Fox, Nowycky & Tsien, 1987b), they were named L, N and T type.

L-type  $Ca^{2+}$ -current, in sensory neurones, activates at relatively positive potentials (positive to -10mV) and shows little inactivation during a sustained depolarization ( $\tau > 500 \text{ms}$  at 0mV). Because the voltage range for inactivation lies between -60 and -10mV, L-type  $Ca^{2+}$  current can be isolated from the other two types by using a more depolarized holding potential (-40mV). This current is blocked by 1,4-dihydropyridines like nifedipine, nitrendipine, nimodipine; phenylalkylamines

like verapamil; and benzothiazipines like diltiazem. The block by dihydropyridines is voltage-dependent and is relieved at potentials positive to 0mV (Jones & Jacobs, 1990; Pietrobon & Hess, 1990). However, another dihydropyridine compound, BayK 8644 is known to potentiate L-type Ca<sup>2+</sup> current and shifts the activation curve to the left by 10mV. L-type current flows through a rather large conductance channel (~25pS in 110mM Ba<sup>2+</sup>).

The second type of channels, N-type, are distinct in that they are found only in neurones. N-type currents, in sensory neurones, activate positive to -20mV and their inactivation range is -120 to -30mV (half maximal steady-state inactivation at about -70mV). Their inactivation is faster than L-type  $Ca^{2+}$ -current ( $\tau$  ~50-80ms). The whole cell N-type current can not be differentiated from the whole cell L-type current on the basis of activation and deactivation kinetics. N-type current, particularly in amphibian sympathetic neurones, is highly sensitive to block by  $\omega$ -conotoxin GVIA from a fish hunting marine snail, *Conus geographus*. The single channel conductance of N-type channels is ~13pS in 110mM Ba<sup>2+</sup>.

The third type of  $Ca^{2+}$ -channels described by Fox et al. (1987a & b) are T-type. These are 'tiny' channels with a single channels conductance of ~8pS. Their activation range is positive to -70mV. The inactivation range lies between -100 and -60mV with a time constant of ~20.50ms. Based on their activation voltages, T-type channels are also called 'low voltage activated' (LVA) channels whereas L- and N-type channels are called 'high voltage activated' (HVA).  $Cd^{2+}$  is more effective than  $Ni^{2+}$  in blocking HVA channels whereas in case of LVA channels,  $Ni^{2+}$  is more

effective than Cd<sup>2+</sup> (Tsien, Lipscombe, Madison, Bley & Fox, 1988). The pyrazine diuretic, amiloride, inhibits T-type current in mouse neuroblastoma cells and chick dorsal root ganglion neurones (Tang, Presser & Morad, 1988).

Besides these three kinds of channels found in sensory neurones, another kind of Ca<sup>2+</sup> current, called P-type, was found in Purkinje neurones of cerebellum (Llinas, Sugimori & Cherksey, 1989a). This type of channel has also been found to occur in other central and peripheral neurones (Mintz, Adams & Bean, 1992a). This current is resistant to block by dihydropyridines and ω-conotoxin GVIA but is sensitive to a spider toxin, ω-Aga-IVA agatoxin, from the funnel-web spider *Agelenopsis aperta* (Llinas, Sugimori, Lin & Cherksey, 1989b; Mintz, Venema, Swiderek, Lee, Bean & Adams, 1992b). The channel is also blocked by Cd<sup>2+</sup> and Co<sup>2+</sup> and is high voltage-activated.

Bovine adrenal chromaffin cells exhibit two different kinds of  $I_{Ca}$ - standard current and facilitation current (Artalejo, Dahmer, Perlman & Fox, 1991). The standard current shows no voltage-dependent inactivation, however, it does show marked current-dependent inactivation. Recruitment of facilitation current by 200ms prepulses to +120 mV increases whole-cell current by an average of 60%. Prepulses longer than 800ms start to inactivate the facilitation current. The facilitation current is like L-type current in some respects. Another kind of  $I_{Ca}$ , called B-type, has been found to occur in bovine cardiac sarcolemma (Rosenberg, Hess & Tsien, 1988). These channels open at negative membrane potential (-100mV), have a single channel conductance of  $\sim$ 7pS at 0mV to 10pS at -100mV, and has very long open

times (>100ms). Additional features of B channels are that they do not 'rundown' during prolonged recordings, are insensitive to BayK 8644 and do not discriminate between Ba<sup>2+</sup> and Ca<sup>2+</sup>. Thus the diversity of Ca<sup>2+</sup> channels is starting to unravel before us as more and more tissues are being investigated.

Inactivation of  $I_{Ca}$  has very interesting properties. Three different kinds of inactivation have been described in different cell types (Eckert & Chad, 1984; Chad, 1989). One of these is  $Ca^{2+}$ -dependent inactivation of  $I_{Ca}$ . This is suggested to be caused by activation of a phosphatase such as calcineurin by the Ca2+ entering the cell as a result of depolarizing command pulse (Armstrong, 1989). This can be overcome by including pseudosubstrates for the enzymes like 'leupeptin', Ca2+ buffers like EGTA or BAPTA and some ATP in the patch pipette (Chad & Eckert, 1986; Belles, Malecot, Heschler & Trautwein, 1988). The second type of inactivation is the voltage-dependent inactivation similar to that seen with other voltage-dependent channels. This kind of inactivation is removed by holding the cell at hyperpolarized potentials (-90mV and below). In BFSG B-cells, voltage-dependent inactivation of whole-cell  $I_{Ba}$  exhibits three distinct components ('fast',  $\tau$  <50ms; 'intermediate',  $\tau$ >100ms; 'slow',  $\tau$  >700ms; Werz, Elmslie & Jones, in press). The third type of inactivation is current-dependent inactivation and is dependent upon the charge entering the cell (Marks & Jones, 1989b). The presence of multiple components of inactivation of Ca2+ channels makes it rather difficult to study the kinetics of each different component in isolation.

Although there are various different kinds of Ca<sup>2+</sup> channels, all these types

are not found in each cell type. In BFSG B-cells, two types of  $I_{Ca}$  can be distinguished on the basis of their pharmacological sensitivities. Only about 20% of total  $I_{Ca}$  flows through L-type channels and the majority of the current (>89%) flows through N-type  $Ca^{2+}$  channels. The whole-cell current recorded from these cells exhibits voltage-dependent inactivation (Jones & Marks, 1989a).

#### 1.2.2.2 Structural Features of Calcium Channels

Most of the information about Ca2+ channel structure comes from work on L-type channels (dihydropyridine binding protein) from skeletal muscle and cardiac muscle. The channel molecule is a multimeric protein consisting of four distinct subunits:  $\alpha$ -1,  $\alpha$ -2 /  $\delta$ ,  $\beta$  &  $\gamma$ . Heterologous expression of different channel subunits, alone or in combination with each other, in different cell lines and in Xenopus oocyte has provided information about the functional significance of each subunit in the channel complex (Nargeot, Dascal & Lester, 1992). The  $\alpha$ -1 subunit is capable of forming a channel-like structure by itself, but the kinetic properties of such a channel are different from that of the native channel and the currents activate and inactivate slowly. However, the co-expression of the  $\alpha$ -1,  $\alpha$ -2 /  $\delta$ ,  $\beta$  and  $\gamma$  subunits together results in expression of Ca2+ channels with kinetic properties (activation, deactivation and inactivation) similar to the native channels (Varadi, Lori, Schultz, Varadi & Schwartz, 1991; Singer, Biel, Lotan, Flockerzi, Hofmann & Dascal, 1991). Thus α-2  $/\delta$ ,  $\beta$  and  $\gamma$  subunits play a significant regulatory role in channel function. Also the amplitude of I<sub>Ca</sub> is much greater in oocytes in which various subunits are expressed together than the ones in which only  $\alpha$ -1 subunit is expressed (Catterall, 1991). Rat brain expresses a heterogeneous family of 4 distinct classes of calcium channels called A, B, C & D (Snutch, Leonard, Gilbert, Lester & Davidson, 1990) whose  $\alpha$  subunits are homologous to the  $\alpha$ -1 subunit of skeletal muscle L-type  $Ca^{2+}$  channel. Most recently, a cDNA has been isolated from rat brain which is thought to encode a  $Ca^{2+}$  channel  $\alpha$ -1 subunit, designated rbB-1 (Dubel, Starr, Hell, Ahlijanian, Enyeart, Catterall & Snutch, 1992). Immunoprecipitation data, together with the exact correspondence between expression of rbB-1 and N-type  $Ca^{2+}$  channels in different cell lines suggests that this cDNA may be the one that encodes for  $\alpha$ -1 subunit of the N-type  $Ca^{2+}$  channel.

### 1.2.2.3 Modulation and Regulation of Calcium Channels

The  $\alpha$ -1 subunit and  $\beta$  subunit of  $Ca^{2+}$  channels contain consensus phosphorylation sites which render them subject to modulation by different kinases and phosphatases. Modulation of the inactivation of  $Ca^{2+}$  channels by phosphatases has already been mentioned above. The  $\alpha$ -1 like subunit of an  $\omega$ -conotoxin-sensitive brain calcium channel has been shown to be phosphorylated by cAMP-dependent protein kinase and protein kinase C (Ahiljanian, Striessnig, Catterall, 1991). Phosphorylation has been shown to increase the amount of inactivation of whole-cell  $I_{Ca}$  in bullfrog sympathetic ganglion B-cells (Wertz, Elmslie & Jones, 1992; Werz *et al.*, *in press*). This effect is likely to be a result of an increase in the proportion of channels which are phosphorylated and thus in an 'inactivating mode' (Plummer &

Hess, 1991). Various neurotransmitters which act via activation of cAMP-dependent kinase or protein-kinase C have been shown to affect  $I_{Ca}$  in different neuronal types, presumably through a phosphorylation mechanism. Calcium channels are coupled with G-proteins as application of GTP-γ-S slows the activation kinetics and attenuates I<sub>Ca</sub> (Scott & Dolphin, 1986; Dolphin & Scott, 1987; Dolphin & Scott, 1989; Ikeda & Schofield, 1989; Elmslie, Zhou & Jones, 1990). Recent evidence using double pulse protocols has revealed that the effect of GTP-γ-S can be partially reversed by a strong depolarizing prepulse (Scott & Dolphin, 1990; Elmslie et al., 1990). The slowing by GTP-y-S may be due to the dissociation of activated G-protein (Scott & Dolphin, 1990) or a shift in equilibrium between different gating states of the channel which have different opening probabilities depending on activation of G-protein (Delcour & Tsien, 1993; see also Bean, 1989b). Recently Yang & Tsien (1993) have reported enhancement of I<sub>Ba</sub> through N- and L-type Ca<sup>2+</sup> channels by activation of protein kinase C in BFSG cells. However, since the concentration of phorboldibutyrate (PDB;  $1\mu$ M) used in this study was rather high, these effects may have resulted from non-specific effects of PDB. Ca2+ channels are thus subject to modulation by changing levels of various second messengers.

Selective disruption of microtubules by application of colchicine or vinca alkaloids results in selective reduction of V<sub>max</sub> for Ca<sup>2+</sup> spikes (Fukuda *et al.*, 1981). Thus Ca<sup>2+</sup> channels are probably anchored by or to microtubules. Calcium channels are not distributed uniformly over the entire membrane surface of the neurones. L-type channels have been shown to be clustered to form "hotspots" which promote

morphological changes in neuronal growth cones (Lipscombe, Madison, Poenie, Reuter, Tsien & Tsien, 1988; Silver, Lamb & Bolsover, 1990).

#### 1.2.3 Potassium channels

### 1.2.3.1 Biophysical Characteristics and Pharmacology of Potassium Channels

The diversity and ubiquity of  $K^+$  channels is well-established (Rudy, 1988). Several different kinds of voltage-dependent  $K^+$  channels have been described in different neuronal types (Adams & Galvan, 1986). In addition,  $Ca^{2+}$ -activated  $K^+$  channels and inward rectifier  $K^+$  channels have also been identified. Based on their kinetic properties and pharmacological sensitivities, six different kind of  $K^+$  currents have been identified in BFSG B-cells- 1) Delayed Rectifier  $K^+$  current ( $I_K$ ); 2) Fast, Transient Outward  $K^+$  current ( $I_A$ ); 3) Slow Transient Outward  $K^+$  current ( $I_{SA}$ ); 4) Muscarine-sensitive  $K^+$  current ( $I_M$ ); 5)  $Ca^{2+}$  -activated voltage-sensitive  $K^+$  current ( $I_C$ ) and 6)  $Ca^{2+}$ -activated voltage-insensitive  $K^+$  current ( $I_{AHP}$ ). A brief review of these is given in the following section.

# 1.2.3.1.1 Delayed Rectifier K<sup>+</sup> current

This is the first of all the known K<sup>+</sup> currents that was recorded in squid giant axon by Hodgkin & Huxley (1952). This type of current has been recorded in several different preparations like skeletal muscle, cardiac muscle and different neuronal types (reviewed in Rudy, 1988). The current has been designated as delayed rectifier

because of its kinetic properties. Upon sustained depolarization, the current starts to activate with a sigmoidal time-course i.e. the rising phase is slower as compared with other voltage-gated conductances. In BFSG, it activates at voltages positive to -40mV (Adams, Brown & Constanti, 1982) and activation is shifted to more positive voltage range in whole-cell recordings (Goh, Kelly & Pennefather, 1989). In wholecell recording, I<sub>K</sub> activates at voltages positive to -30mV and activation becomes faster with increasing depolarization. The classical description of the delayed rectifier  $K^+$  current ( $I_K$ ) deals with it as a non-inactivating current (Hodgkin & Huxley, 1952), however, IK in BFSG B-cells does show slow voltage-dependent inactivation (Adams et al., 1982; Lancaster & Pennefather, 1987). Inactivation is almost complete at -40mV and is almost completely removed at potentials below -80mV (Adams et al., 1982; Lancaster & Pennefather, 1987; Xu & Adams, 1992). In the frog node of Ranvier, classically considered to exhibit a single K<sup>+</sup>-current, macroscopic kinetic and pharmacological studies have established that there are at least three types of K<sup>+</sup>currents (Dubois, 1981; Dubois, 1983).  $I_K$  was described as a current responsible for repolarization of the action potential in squid axons (Hodgkin & Huxley, 1952) and has been suggested to contribute in determining resting membrane potential in intracardiac parasympathetic neurones (Xu & Adams, 1992). However, in BFSG cells the kinetic properties of I<sub>K</sub> preclude it from playing any significant role in action potential repolarization (Goh et al., 1989) or in determining the resting membrane potential (Adams et al., 1982). I<sub>K</sub> in BFSG is sensitive to external application of tetraethyl-ammonium ( $K_D=1mM$ ) but is insensitive to 4-aminopyridine (1mM; Adams

et al., 1982; Adams & Galvan, 1986). The current is however sensitive to external application of low millimolar concentrations of 3,4-diaminopyridine (Goh et al., 1989).

# 1.2.3.1.2 Transient Voltage-dependent K<sup>+</sup> Currents

The fast, transient outward  $K^+$  current ( $I_A$ ) was first described in the neurons of the mollusc *Anisodoris* by Connor & Stevens (1971; *see also* Neher, 1971). The main characteristics of  $I_A$  in BFSG are its rapid activation ( $\tau = 5 \text{ms}$ ) and inactivation kinetics ( $\tau = 50 \text{ms}$ ). The current activates at potentials positive to -60mV and is completely inactivated at -40mV. Thus the activation and inactivation voltage range show little overlap around the resting membrane potential. Since the voltage for the steady-state half-inactivation for  $I_A$  in BFSG B-cells is -110mV, hyperpolarization removes inactivation and subsequent depolarization briefly activates  $I_A$  (Adams *et al.*, 1982).  $I_A$  in molluscan and in a variety of vertebrate ganglionic, hippocampal, sensory and central neurones is very sensitive to 4-aminopyridine ( $K_D = 1 - 2 \text{mM}$ ) but in BFSG neurones it is insensitive to up to 1mM 4-aminopyridine (*but see also* Rudy, 1988).

The second type of transient outward  $K^+$  current is the slow one  $(I_{SA})$ . The activation and inactivation voltage range for this current are similar as for  $I_A$ , however, its activation and inactivation are slow. This current was identified in the paravertebral sympathetic ganglion cells of *Rana pipiens* (Selyanko, Zidichouski & Smith, 1990b) and was not reported in BFSG cells under two-electrode voltage-clamp (Adams *et al.*, 1982). The current appears after some time of recording in the whole-

cell mode and is enhanced in freshly-patched cells following application of muscarine. Thus, it seems that it is a genuine current and not just an artifact arising from whole-cell recording conditions. Similar currents have been recorded from neonatal rat nodose ganglion neurones (McFarlane & Cooper, 1991).

Owing to their kinetic properties and voltage-dependence, these transient outward currents ( $I_A \& I_{SA}$ ) contribute neither to the resting membrane current nor to the action potential repolarization in BFSG cells. However,  $I_A$  has been proposed to contribute to the repolarization of the action potential in rat superior cervical ganglion cells and in rat hippocampal neurones (because the resting potential of these cells is more negative than that of BFSG cells i.e. -60 to -70mV). The kinetics of  $I_A$  closely resembles those of the fast, voltage-dependent Na<sup>+</sup> current and can be described with an equation similar to that used for the  $I_{Na}$  in squid axon (Belluzi & Sacchi, 1988; Belluzi & Sacchi, 1991; Traub, Wong, Miles & Michelson, 1991).

## 1.2.3.1.3 M-current $(I_M)$

This current was first described in BFSG B-neurones by Adams & Brown (1980) as a muscarine-sensitive non-inactivating K<sup>+</sup> current which started to activate close to the normal resting membrane potential of the cells. A careful detailed voltage-clamp study of the properties of I<sub>M</sub> was carried out subsequently by Adams et al. (1982). This current has also been identified in other preparations like rat superior cervical ganglion neurones (Constanti & Brown, 1981; Belluzzi, Sacchi & Wanke, 1985), guineapig olfactory cortical neurones (Constanti & Galvan, 1983), rat

hippocampal pyramidal neurones (Halliwell & Adams, 1982) and toad stomach smooth muscle (Sims, Clapp, Walsh & Singer, 1990a; Sims, Clapp, Walsh & Singer, 1990b).

 $I_{\rm M}$  shows both time and voltage dependence, giving rise to characteristic time-dependent relaxations in the macroscopic current responses to rapid changes in membrane potential. In BFSG neurones,  $I_{\rm M}$  is a non-inactivating K+ current with an activation range between -60mV and -10mV with a half-activation at -35mV. The voltage-sensitivity can be described by a simple Boltzmann distribution for a single multivalent gating particle (Adams *et al.*, 1982; Selyanko, Smith & Zidichouski, 1990a).  $I_{\rm M}$  activates and deactivates along a single exponential time course which depends upon voltage, maximizing at ~150ms at -35mV at 22°C. However, a recent study, using "noise analysis" and "curve fitting" shows that the macroscopically recorded  $I_{\rm M}$  has three distinct components which suggests that the M-channel may have at least four kinetic states (Marrion, Adams & Gruner, 1992).  $I_{\rm M}$  exerts a strong potential-clamping effect at membrane potential subthreshold to excitation (Adams *et al.*, 1982).

Although  $I_M$  is not a  $Ca^{2+}$ -activated current, the level of  $I_M$  at a given potential is subject to modulation by intracellular  $Ca^{2+}$  levels. Elevation of intracellular  $Ca^{2+}$  from a resting level of around 55nM to 150nM increases  $I_M$  whereas further increase in intracellular  $Ca^{2+}$  leads to a reduction of  $I_M$  (Marrion, Zucker, Marsh & Adams, 1991).  $I_M$  can be blocked by  $Ba^{2+}$  (1-2mM) and is susceptible to modulation by several neurotransmitter-like agents such as

acetylcholine, ATP, UTP, somatostatin, angiotensin, LHRH and its analogues and substance P (Jones, 1985; Jones, 1987b; Brown, 1988; Rudy, 1988; Kurenny, Chen & Smith, 1992). Although the single channel conductance of M-channel has not been recorded unequivocally, the estimates from noise analysis suggest a single channel conductance of about 1.6pS in SCG neurones (Owen, Marsh & Brown, 1989) and 3pS in neuroblastoma hybrid cells (Neher, Marty, Fuduka, Kubo & Numa, 1988). However putative M-channels recorded from isolated patches from cultured rat superior cervical ganglion neurones have been shown to exhibit different conductance levels (Stansfeld, Marsh & Brown, 1990). Single channel conductances recorded from cell-attached patches from dissociated rat superior cervical ganglion cells show three different levels of 7pS, 12pS and 19pS. However, it is not clear yet whether these different conductance levels pertain to the different subconductance states of the same channel or to different channel types (Selyanko, Stansfeld & Brown, 1992).

### 1.2.3.1.4 Calcium-activated Potassium Currents

The  $Ca^{2+}$  influx through voltage-dependent  $Ca^{2+}$  channels which open in response to depolarization, is responsible for activation of  $Ca^{2+}$ -activated  $K^+$  channels in most neuronal types. This may be a powerful protective mechanism to limit  $Ca^{2+}$  influx imposed by membrane depolarization. There are two types of  $Ca^{2+}$ -activated  $K^+$  channels in BFSG neurones- voltage-sensitive ( $I_C$  or maxi  $G_{K,Ca}$ ) and voltage-insensitive ( $I_{AHP}$ ).

Large-conductance  $Ca^{2+}$ -activated  $K^+$  channels (maxi  $G_{K, Ca}$  or  $I_C$  channels)

were first recorded in adrenal chromaffin cells (Marty, 1981) and subsequently characterized in rat skeletal muscle (Pallotta, Magleby & Barrett, 1981), in bullfrog B-cells (Adams *et al.*, 1982) and in rat sympathetic neurones (Smart, 1987; Belluzi & Sacchi, 1990). These channels are easily identified on the basis of their large conductance of ~ 200pS in 100-200mM K<sup>+</sup>, high selectivity for K<sup>+</sup> over Na<sup>+</sup>, and sensitivity of channel gating to both intracellular Ca<sup>2+</sup> and membrane voltage (McMannus, 1991). I<sub>C</sub> channels typically require micromolar concentrations of Ca<sup>2+</sup> to open, and their sensitivity to Ca<sup>2+</sup> increases with membrane depolarization. In most tissues, maxi-K<sup>+</sup> channels are moderately voltage-dependent (e-fold increase in open probability per 10-15mV, Latorre, Oberhauser, Labarca & Alvarez, 1989). I<sub>C</sub> has been characterized in a wide variety of preparations and has been shown to be responsible for the fast repolarization of the action potential in BFSG cells (see Adams *et al.*, 1982; Adams & Galvan, 1986; Lancaster & Pennefather, 1987).

Moczydlowski & Latorre (1983) conducted an elegant study on the activation kinetics of I<sub>C</sub> channels isolated from skeletal muscle sarcoplasmic reticulum and incorporated into lipid bilayer. They report that different maxi-K<sup>+</sup> channels from the same preparations can show a three- to fivefold variation in Ca<sup>2+</sup>-sensitivity when examined under identical experimental conditions. This suggests the presence of multiple classes of maxi-K<sup>+</sup> channels in the same preparation. However, this could as well be the result of spontaneous shifts in gating of single maxi-K<sup>+</sup> channels (Moczydlowski & Latorre, 1983). The Hill coefficient from the relationship between Ca<sup>2+</sup> concentration and open probability of the channel suggests 2-4 Ca<sup>2+</sup> binding

sites in the absence of Mg<sup>2+</sup> and 4-6 Ca<sup>2+</sup> binding sites in the presence of Mg<sup>2+</sup> that are involved in gating of the channel (see Table 1 in McMannus, 1991). I<sub>C</sub> channels can be blocked by nanomolar concentrations of charybdotoxin, a toxin from the venom of the scorpion Leiurus quinquestriatus var. hebraeus (Miller, Moczydlowski, Latorre & Phillips, 1985). External application of millimolar concentrations of tetraethylammonium also block the channel (Lancaster & Adams, 1986; Storm, 1987; Brown & Higashida, 1988).

I<sub>AHP</sub> channels, which are also called SK channels (small K<sup>+</sup> channels; Latorre et al., 1989), are responsible for generating the current that underlies the slow afterhyperpolarization that follows the action potential (Pennefather, Lancaster, Adams & Pennefather, 1985; Lancaster & Adams, 1986; Goh & Pennefather, 1987; Lancaster & Pennefather, 1987; Lancaster, Nicoll & Perkel, 1991; Schwindt, Spain & Crill, 1992). SK channels are more sensitive to Ca2+ than maxi-K+ channels but are insensitive to voltage. As a consequence of this, under depolarized conditions, as occur at the peak of the action potential, the maxi-K+ channels are more sensitive to  $\mathrm{Ca^{2+}}$  than the SK channels (Blatz & Magelby, 1987). Since  $\mathrm{I}_{\mathrm{AHP}}$  or SK channels are sensitive to intracellular Ca2+ concentrations and are insensitive to membrane potential, they can provide a standing current and contribute to the membrane potential under conditions when intracellular Ca2+ is increased. Single channel conductance of SK channels between different preparations varies typically between 10-20pS (McMannus, 1991). SK channels ( $I_{AHP}$ ) channels are sensitive to nanomolar concentrations of apamin, a toxin from the venom of honey bee Apis mellifera

(Hugues, Romey, Duval, Vincent & Lazdunski, 1982; Kawai & Watanabe, 1986) but not to charybdotoxin or millimolar concentrations of external tetraethylammonium (up to 2mM).

### 1.2.3.2 Structural Features of Potassium Channels

Major advances have been made in understanding the domains and amino acid sidechains important for the function of voltage-gated K<sup>+</sup> channels, by combining recombinant DNA techniques with pharmacological and electrophysiological approaches. The recent cloning of several cDNAs encoding K<sup>+</sup> channels, derived from Drosophila, Aplysia, Xenopus, mouse, rat and human mRNA or DNA, has revealed very similar primary sequences for the derived K<sup>+</sup> channel proteins (reviewed in Pongs, 1989). Voltage-activated K<sup>+</sup> channel protein is about a quarter of the size of the Na<sup>+</sup> and Ca<sup>2+</sup> channel protein. The deduced amino acid sequences of the K<sup>+</sup> channels are similar in several respects to each of the sequences of the four internally homologous repeats of the Na<sup>+</sup> and Ca<sup>2+</sup> channels (Catterall, 1988). A K<sup>+</sup> channel and a single homologous repeat of a Na<sup>+</sup> or a Ca<sup>2+</sup> channel have similar hydropathy profiles. Like the Na<sup>+</sup> and Ca<sup>2+</sup> channels, there are six possible membrane-spanning stretches. The fourth putative membrane-spanning stretch, S4, is atypical because the hydrophobic sequence is interrupted by a cationic residue (arginine or lysine) at every third or fourth position. S4 is thought to act as a voltage sensor (Stumer et al., 1989). The conservation of S4 sequence along with considerable similarity in amino acid sequences between various voltage-gated

channels mark the voltage-activated Na<sup>+</sup>, Ca<sup>2+</sup> and K<sup>+</sup> channels as related members of a common gene family. K<sup>+</sup> channels are tetrameric proteins. The diversity of K<sup>+</sup> channels results not only from an extended gene family as seen in Drosophila & mouse (Wei, Covarrubias, Butler, Baker, Park & Salkoff, 1990) but also through alternative splicing of RNA as is observed in mammalian central nervous system (Luneau, Williams, Marshall, Levitan, Oliva, Smith, Antanavage, Folander, Stein, Swanson, Kaczmarek & Buhrow, 1991). The four subunits of a K<sup>+</sup> channel may be generated by the same gene or by similar but different genes (Isacoff, Jan & Jan, 1990; Ruppersberg, Schroter, Sakmann, Stocker, Sewing & Pongs, 1990). Different types of K<sup>+</sup> chnnel current can be generated by different levels of a single cRNA (Honore, Attali, Romey, Lesage, Barhanin & Lazdunski, 1992). Injection of low cRNA concentrations into Xenopus oocytes led to expression of a transient K<sup>+</sup> current and injections of high concentrations of the same cRNA led to noninactivating K+ current. The sustained mode might have resulted from channel clustering involving cytoskeletal elements (also see section 1.2.3.3).

Mutagenesis and expression studies have been useful in identifying the structures in the channel which underly the kinetic properties of different voltage-activated K<sup>+</sup> channels. Hydrophobic substitutions in the S4 sequence alter voltage-dependent gating in the "shaker" K<sup>+</sup> channels expressed in *Xenopus* oocytes (Lopez, Jan & Jan, 1991; McCormack, Tanouye, Iverson, Lin, Ramaswami, McCormack, Campanelli, Mathew & Rudy, 1991) and incremental reduction of positive charge within the S4 region results in a corresponding decrease in gating charge (Logothetis,

Movahedi, Satler, Lindpaintner & Nadal-Ginard, 1992). Two types of inactivation have been identified in "shaker" K<sup>+</sup> channels. "N-type" inactivation corresponds to the 'fast' inactivation and "C-type" to 'slow' inactivation. The N-type inactivation is abolished by mutations that either alter or delete the NH2-terminus (Hoshi, Zagotta & Aldrich, 1990). N-type inactivation was restored in a non-inactivating mutant Shaker channel expressed in Xenopus oocyte by internal application of a synthetic peptide, with the sequence of the first 20 residues of the (inactivating type) "shaker B" (ShB) alternatively spliced variant (Zagotta, Hoshi & Aldrich, 1990). Trypsintreated peptide and the peptides with sequences derived from the first 20 residues of the non-inactivating form did not restore inactivation suggesting that the residues in this cytoplasmic domain are involved in inactivation by occluding the pore as suggested by the "ball and chain" model of inactivation. C-type inactivation may be modified by the nature of the last amino acid residue of H5 region. The presence of alanine in the alternative COOH-terminal segments S6 is critical for C-type inactivation (Hoshi, Zagotta & Aldrich, 1991). Deletions in the amino and carboxy terminal sequences can alter and restore activation and inactivation properties of the delayed rectifier K<sup>+</sup> channels (VanDongen, Frech, Drewe, Joho & Brown, 1990). The cDNA clones for voltage-activated channels are available and the cDNA for the calcium-activated K<sup>+</sup> channels has recently been cloned and expressed (Adelman, Shen, Kavanaugh, Warren, Wu, Larutta, Bond & North, 1992).

### 1.2.3.3 Modulation and Regulation of Potassium Channels

The effects of various neurotransmitters show that K<sup>+</sup> channels are subject to modulation by intracellular levels of second messengers and G-proteins (Kaczmarek & Levitan, 1987; Rudy, 1988). For example, Ca<sup>2+</sup>-activated K<sup>+</sup> channels are sensitive to intracellular Ca<sup>2+</sup>. Phosphorylation affects the voltage-dependence of the delayed rectifier K<sup>+</sup> channels in squid axon resulting in an increase in whole-cell current (Augustine & Bezanilla, 1990; Perozo & Bezanilla, 1991). The presence of divalent cations (in mM concentration) is necessary for optimal activation of voltage-activated K<sup>+</sup> channels (Armstrong & Lopez-Barneo, 1987; Begenisich, 1988; Marrion *et al.*, 1991; Sanguinetti & Jurkiewicz, 1992). Destruction of the cytoskeletal elements with cytochalasin D, colchicine or botulinum C2 toxin prevents expression of the sustained mode of the K<sup>+</sup> channel in *Xenopus* oocytes suggesting that the sustained mode obtained at high RNA concentrations corresponds to channel clustering involving cytoskeletal elements (Honore *et al.*, 1992). The exact mechanism/s linking channel clustering with sustained mode of the K<sup>+</sup> channel is not known.

# 1.2.4 Inwardly-Rectifying Na<sup>+</sup>/K<sup>+</sup> current

Tokimasa & Akasu (1990) have identified a cyclic-AMP regulated inwardly-rectifying current in dissociated BFSG neurones that activates on hyperpolarization which was called  $I_H$ . This current is similar to  $I_h$  in dorsal root ganglion neurones (Mayer & Westbrook, 1983),  $I_Q$  in hippocampal neurones (Halliwell & Adams, 1982),  $I_h$  in sino-atrial node cells (Yanagihara & Ishawa, 1980) and  $I_f$  in Purkinje fibres

(DiFrancisco, 1981a & b). The current in frog neurones was observed as a non-inactivating, inwardly-rectifying Na<sup>+</sup>/K<sup>+</sup> conductance which progressively activated in nominally calcium free medium which contained about 20mM Na<sup>+</sup> and approximately 70mM K<sup>+</sup>. Steady-state activation of current occurs between -60 and -130mV with half-maximal activation at -90mV. The reversal potential of  $I_{\rm H}$  was around -20mV and it activated with a time constant of 2.8s at -90mV at 22°C. Intracellular loading of GTP- $\gamma$ -S (30-500 $\mu$ M) led to progressive activation of  $I_{\rm H}$ . The current can be regulated by basal activity of adenylyl cyclase, presumably through protein kinase A, since forskolin (10 $\mu$ M), intracellular application of cyclic-AMP (3-10 $\mu$ M), bath application of dibutyryl cyclic-AMP (1mM) and 3-isobutyl-1-methylxanthine (0.1-1.0mM) increased the maximal conductance by causing a depolarizing shift in the voltage-dependence of activation/deactivation time constants of  $I_{\rm H}$ .

#### 1.3 INTRACELLULAR CALCIUM

Intracellular Ca<sup>2+</sup> levels are dynamic and fluctuate in response to a variety of physiological and pathological stimulii (Miller, 1991; Henzi & MacDermott, 1992). These are kept within submicromolar range by complex interactions between Ca<sup>2+</sup> influx through plasma membrane mediated by receptor- and or voltage-operated Ca<sup>2+</sup> channels, intracellular free Ca<sup>2+</sup> in the cytosol, storage in intracellular Ca<sup>2+</sup> stores and release therefrom via clease channels. Intracellular Ca<sup>2+</sup> in the cytosol is buffered by the calcium binding proteins like calmodulin, calbindin, calreticulin,

parvalbumin etc. The buffering capacity of the cytoplasm is limited and very small. Since high levels of  $Ca^{2+}$  are cytotoxic, it is important that intracellular  $Ca^{2+}$  can be controlled by either extrusion through the membrane or sequestration into the intracellular stores. This involves  $Ca^{2+}$  storage organelles which include  $Ca^{2+}$  pumps,  $Ca^{2+}$  storage proteins and  $Ca^{2+}$ -release channels.

Intracellular Ca2+ can thus increase as a result of influx of Ca2+ through receptor and voltage-activated Ca2+ channels and/or due to release from intracellular stores. Pharmacologically, three distinct intracellular pools of Ca<sup>2+</sup> have been identified in neurones. These are- 1) caffeine-sensitive 2) inositol 1,4,5-trisphosphate (IP3)-sensitive and 3) carbonyl cyanide p-trifluoromethoxyphenylhydrazine- (FCCP) or cabonyl cyanide m-chlorphenylhydrazine- (CCCP) sensitive (Miller, 1991). The FCCP- and CCCP-sensitive pool is located in the mitochondria. Although it is known that the caffeine- and IP3-sensitive pools are located in smooth endoplasmic reticulum, the exact location within this compartment and physical correlates of these pools are not yet clearly identified. The priming of Ca<sup>2+</sup>-induced Ca<sup>2+</sup> release process by application of caffeine results in prolongation of afterhyperpolarization duration in rat and frog sympathetic neurones and this effect can be blocked or reversed by application of blockers of Ca<sup>2+</sup>-release channel like ryanodine, dantrolene and ruthenium red (Kuba & Nishi, 1976; Kuba, 1980; Kuba, Morita & Nohmi, 1983; Thayer, Hirning & Miller, 1988; Kawai & Watanabe, 1989). Similarly IP3 induced intracellular release of Ca<sup>2+</sup> can be blocked by IP3 receptor antagonists like heparin. The contribution of these different stores is variable in different neuronal types. For example, release of caffeine-sensitive pool does not result in repetitive Ca<sup>2+</sup> oscillations in rat dorsal root ganglion neurones (Thayer et al., 1988; Thayer & Miller, 1990) whereas it is an effective stimulus for setting up such oscillations in frog sympathetic neurones (Kuba & Nishi, 1976; Kuba, 1980; Lipscombe et al., 1988; Friel & Tsien, 1992a & b). This suggests that caffeinesensitive pool in frog sympathetic neurones can be important in modulating intracellular Ca<sup>2+</sup> signals resulting from Ca<sup>2+</sup> influx from outside under physiological conditions. In contrast, the mitochondrial Ca2+ pool seems to be more important in rat dorsal root ganglion cells. IP3-sensitive pool has relatively smaller capacity since triggering of this pool raises intracellular Ca2+ levels by less than 100nM (Pfaffinger, Leibowitz, Subers, Nathanson, Almers & Hille, 1988). This pool is involved in responses to agonists that work through phosphoinositide hydrolysis like muscarine, LHRH etc. Caffeine- and FCCP-sensitive pools are relatively larger as compared with IP3-sensitive ones. The threshold for triggering of these pools is around 200nM (intracellular calcium level). Triggering of any of these two pools leads to an explosive increase in intracellular Ca<sup>2+</sup> to 500-600nM and can start Ca<sup>2+</sup> oscillations.

The rise in intracellular Ca<sup>2+</sup> has been shown to play an important role in various physiological and pathological processes (Henzi & MacDermott, 1992). Intracellular Ca<sup>2+</sup> levels rise only transiently in response to exposure to 10mM KCl or to an applied electric field or after cutting the axon (Davenport, Dou, Rehder & Kater, 1992) which suggests the presence of and interaction between voltage-sensitive Ca<sup>2+</sup> channels and an active extrusion and sequestration mechanism. The rise in

intracellular Ca<sup>2+</sup> levels in BFSG cells has been shown to be frequency-dependent. The source of intracellular Ca<sup>2+</sup> during action potential generation is extracellular and these neurones can buffer large changes in intracellular Ca<sup>2+</sup> during and following train of stimulation (Heppner & Fiekers, 1992).

Although an increase in intracellular Ca2+ to micromolar levels for prolonged periods is cytotoxic, a sustained increase in intracellular Ca<sup>2+</sup> within certain limits (250-500nM) promotes survival of ciliary ganglion neurones which would otherwise have died during development (Collins, Schmidt, Guthrie & Kater, 1991). This is consistent with the 'set point hypothesis' for Ca<sup>2+</sup> which states that higher levels of Ca<sup>2+</sup> above normal (i.e. around 150-300nM) are conducive to the growth and survival of the neurones and growth stops when intracellular Ca<sup>2+</sup> level returns to normal or below normal (Mattson & Kater, 1987; Kater & Mills, 1991). Similarly, cultured sympathetic neurones which are dependent on nerve growth factor for their survival can be rescued in the absence of nerve growth factor if intracellular Ca2+ is maintained at high levels i.e 200-400nM (Koike & Tanaka, 1991). The survival of chick embryo nodose neurones is regulated by intracellular Ca2+ both prior to and after the onset of neurotrophic factor dependence, but the survival-promoting effects of neurotrophic factors are not mediated by intracellular Ca2+ (Larmet, Dolphin & Davies, 1992). Reduction of intracellular Ca<sup>2+</sup> kills early neurotrophic factorindependent chick embryo nodose neurones, but has little effect on older neurones growing in the presence of brain-derived neurotrophic factor. The survival of these neurones, shortly before they become dependent on brain-derived neurotrophic factor, can be enhanced by depolarization-induced Ca<sup>2+</sup> influx through L-type channels. Also increased levels of intracellular Ca<sup>2+</sup> have been shown to activate immediate-early genes which can then promote activation of other genes which may be responsible for repair and regeneration (Morgan & Curran, 1988; Murphy, Worley & Baraban, 1991).

## 1.4 DEVELOPMENTAL REGULATION OF ION CHANNELS

Developmental changes in ion channel expression have been studied in different neuronal types in an attempt to identify the developmental timetable of such changes in order to arrive at a general hypothesis which may explain their mechanism. Microelectrode studies on Rohon-Beard neurones from amphibian embryos and dorsal unpaired median (DUM) neurones from grass-hopper embryos show that the action potentials change from Ca<sup>2+</sup>-dependent to Na<sup>+</sup>-dependent as these neurons grow (Spitzer, 1979). This suggests that the developmental expression of Na<sup>+</sup> channels is preceded by Ca<sup>2+</sup> channels and the density of I<sub>Ca</sub> decreases whereas density of I<sub>Na</sub> incraeses in these neurons. However, exceptions to this rule were later found in avian neural crest cells (Bader, Bertrand, Dupin & Kato, 1983) and in *Ambystoma* spinal neurones (Barish, 1986) where Ca<sup>2+</sup> current density increases during development.

Systematic studies conducted on different neuronal preparations provide information about the developmental timetable of ion channels. For example, tetrodotoxin-insensitive  $I_{Na}$  was more likely to be present in dorsal root ganglion

neurons from younger animals whereas tetrodotoxin-sensitive component of I<sub>Na</sub> was more common in the same type of neurones from older animals (Roy & Narahashi, 1992). In motoneurones, the density of I<sub>Na</sub> increases between E6 and E11 resulting in an increase in action potential amplitude; and IA increases about 20-fold between E4 and E11 (resulting in a decrease in the duration of the action potential) whereas  $I_K$  remains unchanged (McCobb, Best & Beam, 1990).  $I_K$  has been shown to increase during neural development in cultured amphibian spinal neurones (Barish, 1986).  $I_A$  has been found to be the last voltage-activated current to develop in embronic rat sympathetic neurones from superior cervical ganglion (Nerbonne, Gurney & Rayburn, 1986). I<sub>A</sub> increases by approximately 100% whereas I<sub>SA</sub> decreases to approximately 40% and I<sub>K</sub> does not change in rat sympathetic neurones during the first two postnatal weeks (McFarlane & Cooper, 1992). The expression of low voltage-activated Ca2+ channels occurs prior to expression of the classical high voltage-activated Ca2+ current in cultured chicken dorsal root ganglion cells and ciliary ganglion cells (Gottman, Dietzel, Lux, Huck & Rohrer, 1988) and in cultured immature hippocampal pyramidal neurons (Thompson & Wong, 1991).

On exposure to chemical agents like cyclic-AMP, ouabain or nerve growth factor (NGF), PC12 cells acquire a neurone-like morphology and undergo differentiation. For instance, exposure of these cells to NGF leads to a preferential increase in the number of N-type Ca<sup>2+</sup> channels (Usowicz, Porzig, Becker & Reuter, 1990). Different trophic factors exert different effects on neurite outgrowth and sodium channel expression in PC12 cells (Pollock, Krempin & Rudy, 1990). NGF

and basic fibroblast growth factor increase the density of Na+ channels. However, this increase is not necessary for the neurite outgrowth. Epidermal growth factor and cyclic-AMP do not cause or support such an increase in Na+ channel density. NGF has been suggested to regulate the duration of the action potential in mature sensory neurones: withdrawl of NGF prolongs, and exposure to anti-NGF antiserum accelerates the onset of the longer lasting action potentials elicited by simple withdrawl of NGF (Chalazonitis, Peterson & Crain, 1987). In contrast, NGF treatment results in increase in duration of the falling limb of the spike in HTMRs (dorsal root ganglion cells that innervate high threshold mechanoreceptors) compared with untreated controls or animals treated with pre-immune rabbit serum (Ritter & Mendell, 1992). Thus it seems that the ion channels underlying the action potentials in different neuronal types are regulated differentially by NGF. However, NGF may not be solely responsible for controlling the electrophysiological properties of BFSG cells in explant cultures. Absence of NGF in the culture medium promoted a reduction in afterhyperpolarization amplitude and duration and an increase in spike width. However, addition of NGF did not reduce the duration of the action potential back towards normal whilst addition of anti-NGF antibodies promoted further attenuation of afterhyperpolarization amplitude (Traynor, Dryden & Smith, 1992). This suggests that the regulation of channel expression may be under differential control by the same trophic factor. Thus it is tempting to speculate that the timetable of ion channel expression during development may be a result of the timecourse of expression of receptors for trophic factors and the production of trophic factors. Furthermore, this change in ion channel expression during development may have physiological relevance for processes such as growth and migration of cells to their definitive places. L-type channels have been shown to be involved in migration and differentiation of neural crest cells in explants of neural tube and neural crests from embryos of salamanders *Ambystoma maculatum* and *Ambystoma mexicanum* (Moran, 1991). N-type Ca<sup>2+</sup> channels play a selective role in migration of post-mitotic cerebellar granule cells. These cells initiate migration only after the expression of N-type channels on their plasmalemmal surface and ω-conotoxin specifically inhibited their directed migration whereas inhibitors of L- and T-type Ca<sup>2+</sup> channels; and Na<sup>+</sup> and K<sup>+</sup> channels had no effect (Komuro & Rakic, 1992).

# 1.5 DEPENDENCE OF ION CHANNELS ON AN INTACT AXON

Developing neurones, after reaching their respective definitive locations in the body, make connections with appropriate target organs through their axon terminals which are then responsible for maintaining the differentiated properties of the adult neurones (Lieberman, 1971; Gordon, 1983). Disruption of this connectivity and interaction of the neurone with its target organ through processes like axon transection (axotomy) brings about changes in the morphological, biochemical and electrophysiological properties of the neurone (Gordon, 1983). The changes induced in the soma of the surviving neurone have been described as 'cell body reaction' (Grafstein, 1983). These changes may be specifically geared for enhancing

regeneration and regrowth back to the target organ. Some of the axotomy-induced changes in the electrophysiological properties are reversed by re-establishment of connection after regeneration (Kelly, Bisby & Lukowiak, 1988; Morale, Ivorra & Gallego, 1985). The exact mechanism/s underlying this process have not been clearly identified. One working hypothesis is that axotomy reverts the mature differentiated neurone to a dedifferentiated state. This dedifferentiated state may resemble an immature neurone.

Axotomy-induced alterations in morphological and biochemical characteristics have been well-studied in different neuronal types. It leads to changes in gene expression which are appropriate for a non-communicating and non-transmitting, growing neurone. The expression of mRNAs required for production and synthesis of neurotransmitters are down-regulated and the mRNAs responsible for synthesis and production of material required for growth of axon and neurites are upregulated. Literature is replete with examples of studies of this kind (Fawcett & Keynes, 1990; also see Titmus & Faber, 1990). Axotomy may also result in disruption of cytoskeletal elements because interaction with appropriate target organ has been shown to prevent abnormal cytoskeletal changes in neurones (Doe ing, 1992).

Axotomy results in changes in the active and passive membrane properties which have diverse time courses and sequelae in different neuronal types (Titmus & Faber, 1990). For example, axonal conduction velocity decreases in cat spinal α-motoneurones (F-type; Kuno, Miyata & Munoz-Martinez, 1974; Foehring, Sypert & Munson, 1986; Pinter & Vanden-Noven, 1989); frog spinal motoneurones (Farel,

1978) whereas it increases in bullfrog sympathetic ganglion C-cells (Shapiro et al., 1987) and in hamster spinal dorsal root ganglion C-cells (Gurtu & Smith, 1988). Similarly, whole-cell input resumance increases in cat spinal  $\alpha$ -motoneurones (F-type; Kuno et al., 1974; Foehring et al., 1986); in S-type sectors motoneurones (Kuno et al., 1974) and in lumbar motoneurones (Pinter & Vanden-Noven, 1999) whereas it decreases in cranial hypoglossal motoneurones (Takata, Shohara & Fuita, 1980) and in hamster spinal dorsal root ganglion short action potential neurones (Gurtu & Smith ,1988). Action potential duration and amplitude increase in goldfish Mauthner cell (Titmus & Faber, 1986); in crayfish motoneurones (Kuwada & wine, 1981); in locust motoneurones (Goodman & Heitler, 1979) and in BFSG B-cells (Gordon et al., 1987) whereas it decreases in guineapig vagal visceral motoneurones (Lawaind, Werman & Yarom, 1988). Action potential afterhyperpolarization duration increases in medial gastrocnemius motoneurones (F-type; Foehring et al., 1986) and in lumbar motoneurones (Pinter & Vanden-Noven, 1989) whereas it decreases in cat cranial carotid motoneurones (Gallego, Ivorra & Morales, 1987); BFSG B-cells (Gordon et al., 1987) and in guinea pig vagal visceral motoneurones (Lawaind et al., 1988).

Based on current-clamp studies, axotomy has been suggested to increase I<sub>Na</sub> in cat cranial glossopharyngeal sensory neurones (Gallego *et al.*, 1987); in goldfish Mauthner cell (Titmus & Faber, 1986); crayfish motoneurones (Kuwada & Wine, 1981) and in locust motoneurones (Goodman & Heitler, 1979). Similarly, a functional loss of Ca<sup>2+</sup>-activated K<sup>+</sup> channels has been suggested to be responsible for an increase in the duration of the action potential and a decrease in the

amplitude and duration of afterhyperpolarization observed following axotomy in BFSG B-cells (Kelly et al., 1986). In guinea pig vagal visceral motoneurones, axotomy has been suggested to result in a decrease in I<sub>C</sub> and a loss of I<sub>A</sub> (Gallego et al., 1987). However, a voltage-clamp study of the effects of axotomy showing a direct effect on most of the ion channels that are involved in a.p. generation has not been conducted so far. There are only a few scattered reports about the effects of axotomy on ion channels (McFarlane & Cooper, 1992). For instance, axotomy has been shown to increase the density of leak channels without any effect on the channel properties in leech AP neurones (Simoni, Pellegrini, Cecconi & Pellegrino, 1990). Thus a systematic voltage-clamp study of the effects of axotomy on ion channels is essential to start to understand the effects of axotomy on membrane properties of the neurones. Other relevant reasons are discussed in subsequent chapters.

With this knowledge about the properties of ion channels which occur in BFSG B-cells and various aspects of their regulation and modulation, we are now in a position to investigate and discuss the molecular mechanisms of the regulation of the action potential in these neurones which include the axotomy-induced changes in the membrane properties and the frequency-dependent modulation of action potential afterhyperpolarization.

#### 1.6 RATIONALE AND STATEMENT OF THE PROBLEM

This thesis is focused on regulation of the action potential and its afterhyperpolarization. The electrophysiological properties vary between different neuronal types due to the differences in relative abundance and kinetic properties of the ion channels that are involved. These ion channels are subject to regulation and modulation by various 'exogenous' and 'endogenous' influences.

Transection of the axon (axotomy) results in loss of interaction between the neurone and its target organ, thus removing some 'exogenous' influences. This leads to various morphological, biochemical and electrophysiological changes in the cell body (Lieberman, 1971; Titmus & Faber, 1990). This 'cell body reaction' which has been interpreted as a neurone's attempt to regenerate an axon in order to reconnect to its target is probably common to all neuronal types. This 'teleological' argument would suggest that similar changes should take place and the mechanism underlying these changes should be similar in different neuronal types. However, the changes observed in the electrophysiological properties of various neuronal types show considerable variation (Titmus & Faber, 1990).

Since the contribution and relative abundance of various membrane conductances differ in different neuronal types, the apparent diversity in electrophysiological response to axotomy may be secondary to these differences. Alternatively, the variety in response may result from different effects of axotomy on similar ion channels. Therefore a comprehensive and systematic study of the effects of axotomy on ion channel properties in any single neuronal type is in order as a first

step towards formulating a unified hypothesis for the basic mechanism/s of axotomy-induced changes. Since the shape of the action potential depends on contribution from different ion channels and their intricate kinetic properties, it becomes difficult to determine from the changes in action potential shape as to which ion channels are affected and how. Therefore, it is necessary to study the different currents in isolation.

The first obvious question which can be asked is exactly which ion channel/s is/are affected by axotomy? Secondly, are all the ion channels affected similarly? i.e, is the activity of some of the ion channels increased whereas that of others decreased? Thirdly, is the change in whole-cell currents due to a change in the number of ion channels or due to change in the kinetic properties of the ion channels? Fourthly, are the changes observed in whole-cell currents (where wash-out of currents is usually a concern) commensurate with the changes observed in the action potential shape with microelectrode recordings? To answer these questions we recorded whole-cell currents and carried out a quantitative biophysical analysis of the activity of various ion channels in bullfrog sympathetic ganglion B-cells. These neurones were selected as a preparation because the ionic currents underlying an a.p. have been well characterized (Adams et al., 1982; Lancaster & Pennefather, 1987; Goh & Pennefather, 1987); current-clamp studies on the effects of axotomy have been conducted on these cells (Kelly et al., 1986; Gordon et al., 1987; Shapiro et al., 1987) and the B-cells can be differentiated easily from the other cell type (C-cells; small intensely fluorescent cells) present in these ganglia (Nishi, Soeda & Koketsu, 1965; Dodd & Horn, 1983). The activity of various ion channels ( $Ca^{2+}$ -activated and  $Ca^{2+}$ -sensitive  $K^+$  channels) depends on intracellular  $Ca^{2+}$ , therefore it is necessary to investigate whether axotomy leads to changes in intracellular  $Ca^{2+}$  levels.

The most obvious change induced by axotomy is a decrease in the amplitude and duration of the afterhyperpolarization which follows the action potential. The action potential afterhyperpolarization is the result of activation of a voltage-insensitive Ca<sup>2+</sup>-activated K<sup>+</sup> conductance and is quite sensitive to intracellular Ca<sup>2+</sup> levels. Thus it is likely to be influenced by Ca<sup>2+</sup> influx and intracellular Ca<sup>2+</sup> release under various physiological and pathological situations. Therefore it becomes relevant in this connection that how stable is the action potential afterhyperpolarization in BFSG B-cells? Thus the questions which can be asked include how does afterhyperpolarization vary with stimulus frequency? What is the basis of the variability in afterhyperpolarization duration / and amplitude? Is the change in afterhyperpolarization due to change in Ca<sup>2+</sup> influx or is it due to change in intracellular Ca<sup>2+</sup> release? What is the basis of the change in Ca<sup>2+</sup> influx, if any? Does Ca<sup>2+</sup>-induced Ca<sup>2+</sup> release affect afterhyperpolarization in BFSG B-cells when the action potentials are evoked singly?

The study on axotomy addresses the 'exogenous' regulation of action potential in BFSG B-cells which is the result of presence of an intact axon and its interaction with the target. It was conducted to test the hypothesis that the properties of the ion channels in BFSG B-cells are differentially regulated by contact of sympathetic nerves with their target organ and the changes observed after axotomy is not a simple

'dedifferentiation' process. Although it is well-established that axotomy alters action potential shape in a variety of neuronal types, this work represents the first voltage-clamp study of this effect. This study also aims at enhancing our understanding of the mechanisms of the response of neurones to injury. These findings represent a crucial step in our understanding of the mechanisms underlying some aspects of the 'exogenous' regulation of the action potential and the response of neurones to injury. The study on frequency-dependence of action potential afterhyperpolarization relates to its 'endogenous' regulation and the fact that afterhyperpolarization duration varies with stimulus frequency (at low frequencies between 0.5 to .011Hz). This suggests that this variation of afterhyperpolarization duration with frequency might have physiological relevance and be important in determining the 'signal to noise' ratio at different frequencies of stimulation.

### 1.7 REFERENCES

ADAMS, P.R. & BROWN, D.A. (1980). Luteinizing hormone-releasing factor and muscarinic agonists act on the same voltage-sensitive K<sup>+</sup>-current in bullfrog sympathetic neurones. *British Journal of Pharmacology* **68** 353-355.

ADAMS, P.R.; BROWN, D.A. & CONSTANTI, A. (1982). M-currents and other potassium currents in builfrog sympathetic neurones. *Journal of Physiology* **330** 537-572.

ADAMS, P.R. & GALVAN, M. (1986). Voltage-dependent currents of vertebrate neurones and their role in membrane excitability. In *Advances in Neurology* Vol. 44 Eds. A.V. Delgado-Escueta; A.A. Ward Jr.; D.M. Woodbury & R.J. Porter. Raven Press. New York. pp 137-170.

ADELMAN, J.P.; SHEN, K.; KAVANAUGH, M.P.; WARREN, R.A.; WU, Y.; LAGRUTTA, A.; BOND, C.T. & NORTH, R.A. (1992). Calcium-activated potassium channels expressed from cloned complementary DNAs. *Neuron* 9 209-216.

AGNEW, W.S.; LEVINSON, S.R.; BRABSON, J.S. & RAFTERY, M.A. (1978). Purification of the tetrodotoxin-binding component associated with the voltage-sensitive sodium channel from *Electrophorus electricus* electroplkax membranes.

Proceedings of the National Academy of Sciences of USA 75 2606-2616.

AHLIJANIAN, M.K.; STRIESSNIG, J. & CATTERALL, W.A. (1991). Phosphorylation of an alpha-1 like subunit of an w-conotoxin-sensitive brain calcium channel by cAMP-dependent protein kinase and protein kinase C. Journal of Biological Chemistry 266 20192-20197.

ARMSTRONG, C.L. & LOPEZ-BARNEO, J. (1987). External calcium ions are required for potassium channel gating in squid neurons. *Science* 236 712-714.

ARMSTRONG, C.M. (1981). Sodium channels and gating currents. *Physiological Reviews* **61** 644-683.

ARMSTRONG, C.M. & BEZANILLA, F. (1974). Charge movement associated with the opening and closing of the activation gates on Na channels. *Journal of General Physiology* **63** 533-552.

ARMSTRONG, D.L. (1989). Calcium channel regulation by calcineurin, a Ca<sup>2+</sup>-activated phosphatase in mammalian brain. *Trends in Neuroscience* 12 117-122.

ARTALEJO, C.R.; DAHMAR, M.K.; PERLMAN R.L. & FOX, A.P. (1991). Two types of Ca<sup>2+</sup> currents are found in bovine chromaffin cells: facilitation is due to

recruitment of one type. Journal of Physiology 432 681-707.

AUGUSTINE, C.K. & BEZANILLA, F. (1990). Phosphotylation modulates potassium conductance and gating current of perfused giant axons of squid. *Journal of Physiology* 95 245-271.

AULD, V.J.; GOLDIN, A.L.; KRAFTE, D.S.; CATTERALL, W.A.; LESTER, H.A.; DAVIDSON, N. & DUNN, R.J. (1990). Aneutral amino-acid change in segment IIS4 dramatically alters gating properties of the voltage-dependent sodium channel. *Proceedings of the National Academy of Sciences of USA* 87 323-327.

BADER, C.R.; BERTRAND, D.; DUPIN, E. & KATO, A.C. (1983). Development of electrical properties of cultured avian neural crest cells. *Nature* **305** 808-810.

BARISH, M.E. (1986). Differentiation of voltage-gated potassium current and modulation of excitability in cultured amphibian spinal neurones. *Journal of Physiology* 375 229-250.

BARRETT, J.N. & CRILL, W.E. (1980). Voltage clamp of cat motoneurone somata: properties of the fast inward current. *Journal of Physiology* **304** 231-249.

BEAN, B.P. (1989a). Classes of calcium channels in vertebrate cells. Annual Review

of Physiology 51 367-384.

BEAN, B.P. (1989b). Neurotransmitter inhibition of neuronal calcium currents by changes in voltage-dependence. *Nature* **340** 153-157.

BEGENISICH, T. (1988). The role of divalent cations in potassium channels. *Trends* in Neuroscience 11(6) 270-273.

BELLES, B.; MALECOT, C.O.; HESCHLER, J. & TRAUTWEIN, W. (1988). Rundown of calcium current durinh long whole-cell recordings in guinea pig heart cells: role of phosphorylation and intracellular calcium. *Pflugers Archiv* **411** 353-360.

BELLUZZI, O. & SACCHI, O. (1988). The interaction between potassium and sodium currents in generating action potentials in rat sympathetic neurone. *Journal of Physiology* **397** 127-147.

BELLUZZI, O. & SACCHI, O. (1990). The calcium-dependent potassium conductance in rat sympathetic neurones. *Journal of Physiology* **422** 561-583.

BELLUZZI, O. & SACCHI, O. (1991). A five conductance model of the action potential in the rat sympathetic neurone. *Progress in Biophysics & Molecular Biology* 55(1) 1-30.

BELLUZZI, O.; SACCHI, O. & WANKE, E. (1985). Identification of delayed potassium currents in rat sympathetic neurone under voltage-clamp. *Journal of Physiology* **358** 109-129.

BERTOLINO, M. & LLINAS, R.R. (1992). The central role of voltage-activated and receptor operated calcium channels in neuronal cells. *Annual Review of Pharmacology* & Toxicology 32 399-421.

BLATZ, A.L. & MAGLEBY, K.L. (1987). Calcium activated potassium channels. *Trends in Neuroscience* **10** 463-467.

BOSSU, J.L. & FELTZ, A. (1984). Patch clamp study of the tetrodotoxin resistant sodium current in group C sensory neurones. *Neuroscience Letters* **51** 241-246.

BRODIE, C.; BRODY, M. & SAMPSON, S.R. (1989). Characterization of the relation between sodium channels and electrical activity in cultured rat skeletal myotubes: regulatory aspects. *Brain Research* 488 186-194.

BROWN, A.M.; LEE, K.S. & POWELL, T. (1981). Sodium current in single rat heart muscle cells. *Journal of Physiology* **318** 479-500.

BROWN, D.A. (1988). M-currents. In Ion Channels Edited by Toshio Narahashi,

Plenum Press, New York & London pp 55-94.

BROWN, D.A. & ADAMS, P.R. (1980). Muscarinic suppression of a novel voltage-sensitive K<sup>+</sup>-current in a vertebrate neurone. *Nature* **283** 673-676.

BROWN, D.A. & HIGASHIDA, H. (1988). Voltage- and calcium-activated potassium currents in mouse neuroblastoma X glioma hybrid cells. *Journal of Physiology* **397** !49-165.

CATTERALL, W.A. (1988). Structure and function of voltage-sensitive ion channels. *Science* **242** 50-61.

CATTERALL, W.A. (1991). Functional subunit structure of voltage-gated calcium channels. *Science* **253** 1499-1500.

CHAD, J. (1989). Inactivation of calcium channels. Comparative Biochemistry & Physiology 93 95-105.

CHAD, J.E. & ECKERT, R. (1986). An enzymatic mechanism for calcium current inactivation in dialysed *Helix* neurones. *Journal of Physiology* **378** 31-51.

CHALAZONITIS, A.; PETERSON, E.R. & CRAIN, S.M. (1987). Nerve growth factor

regulates the action potential duration of mature sensory neurons. *Proceedings of the National Academy of Sciences of USA* 84 289-293.

COLLINS, F.; SCHMIDT, M.F.; GUTHRIE, P.B. & KATER, S.B. (1991). Sustained increase in intracellular calcium promotes neuronal survival. *Journal of Neuroscience* 11(8) 2582-2587.

CONNOR, J.A. & STEVENS, C.F. (1971). Voltage-clamp studies of a transient outward membrane current in gastropod neural somata. *Journal of Physiology* **213** 21-30.

CONSTANT: A. & BROWN, D.A. (1981). M-currents in voltage-clamped mammalian sympathetic neurones. *Neuroscience Letters* 24 289-294.

CONSTANTI, A. & GALVAN, M. (1983). M-currents in voltage-clamped olfactory cortex neurones. *Neuroscience Letters* **39** 65-70.

DASCAL, N. & LOTAN, I. (1991). Activation of protein kinase C alters voltagedependence of a Na<sup>+</sup> channel. *Neuron* 6 165-175.

DAVENPORT, R.W.; DOU, P.; REHDER, V. & KATER, S.B. (1992). Growth cone filopodia as sensors of their environment: Intracellular calcium as a second messenger. Society for Neuroscience Abstracts 18 1287.

DELCOUR, A.H. & TSIEN, R.W. (1993). Altered prevalence of gating modes in neurotransmitter inhibition of N-type calcium channels. *Science* **259** 980-984.

DI-FRANCISCO, D. (1981a). A study of the ionic nature of the pace-maker current in calf Purkinje fibres. *Journal of Physiology* **314** 359-376.

DI-FRANCISCO, D. (1981b). Characterization of the pace-maker current in calf Purkinje fibres. *Journal of Physiology* **314** 377-393.

DODD, J. & HORN, J.P. (1983). A reclassification of B- and C-cells in the ninth and tenth paravertabral sympathetic ganglion of the bullfrog. *Journal of Physiology* **334** 255-269.

DOERING, L.C. (1992). Appropriate target interactions prevent abnormal cytoskeletal changes in neurons: Astudy with intra-sciatic grafts of the septum and the hippocampus. *Journal of Neuroscience* **12(9)** 3399-3413.

DOLPHIN, A.C. & SCOTT, R.H. (1987). Calcium channel currents and their inhibition by (-) baclofen in rat sensory neurones: modulation by guanine nucleotides. *Journal* of *Physiology* **386** 1-17.

DOLPHIN, A.C. & SCOTT, R.H. (1989). Interaction between calcium channel ligands

and guanine nucleotides in cultured rat sensory and sympathetic neurones. *Journal* of *Physiology* 413 271-288.

DUBEL, S.J.; STARR, T.V.B.; HELL, J.; AHLIJANIAN, M.K.; ENYEART, J.J.; CATTERALL, W.A. & SNUTCH, T.P. (1992). Molecular cloning of the alpha-1 subunit of an w-conotoxin-sensitive calcium channel. *Proceedings of the National Academy of Sciences of USA* 89 5058-5062.

DUBOIS, J.M. (1981). Evidence for the existence of three types of potassium channels in the frog Ranvier node membrane. *Journal of Physiology* **318** 297-316.

DUBOIS, J.M. (1983). Potassium currents in the frog node of Ranvier. *Progress in Biophysics & Molecular Biology* **42** 1-20.

ECKERT, R. & CHAD, J. (1984). Inactivation of calcium channels. *Progress in Biophysics & Molecular Biology* 44 215-267.

ELMSLIE, K.S.; ZHOU, W. & JONES, S.W. (1990). LHRH and GTP&S modify calcium current activation in bullfrog sympathetic neurones. *Neuron* 5 75-80.

FAREL, P.B. (1978). Reflex activity of regenerating frog spinal motoneurones. *Brain Research* 158 331-341.

FAWCETT, J.W. & KEYNES, R.J. (1990). Perpheral nerve regeneration. *Annual Review of Neuroscience* 13 43-60.

FOEHRING, R.C.; SYPERT, G.W. & MUNSON, J.B. (1986). Properties of self-innervated motor units in medial gastrocnemius of cat: II. Axotomized motoneurones and the time course of recovery. *Journal of Neurophysiology* 55 947-965.

FOX, A.P.; NOWYCKY, M.C. & TSIEN, R.W. (1987a). Kinetic and pharmacological properties distinguishing three types of calcium currents in chick sensory neurones. *Journal of Physiology* **394** 149-172.

FOX, A.P.; NOWYCKY, M.C. & TSIEN, R.W. (1987b). Single channel recordings of three types of calcium channels in chick sensory neurones. *Journal of Physiology* **394** 173-200.

FRANKENHAEUSER, B. & HUXLEY, A.F. (1964). The action potential in the myelinated nerve fibre of *Xenopus laevis* as computed on the basis of voltage clamp data. *Journal of Physiology* 171 302-315.

FRIEL, D.D. & TSIEN, R.W. (1992a). Phase-dependent contributions from Ca<sup>2+</sup> entry and Ca<sup>2+</sup> release to caffeine-induced [Ca]; oscillations in bullfrog sympathetic neurones. *Neuron* 8 1109-1125.

FRIEL, D.D. & TSIEN, R.W. (1992b). A caffeine- and ryanodine-sensitive Ca<sup>2+</sup> store in bullfrog sympathetic neurones modulates effects of Ca<sup>2+</sup> entry on [Ca<sup>2+</sup>]<sub>i</sub>. *Journal of Physiology* **450** 217-246.

FUKUDA, J.; KAMEYAMA, M. & YAMAGUCHI, K. (1981). Breakdown ytoskeletal filaments selectively reduces Na and Ca spikes in cultured mammal neurones. *Nature* 294 82-85.

GALLEGO, R.; IVORRA, I. & MORALES, A. (1987). Effects of central or peripheral axotomy on membrane properties of sensory neurones in petrosal ganglion of the cat. *Journal of Physiology* **391** 39-56.

GOH, J.W.; KELLY, M.E.M. & PENNEFATHER, P.S. (1989). Electrophysiological function of the delayed rectifier (I<sub>K</sub>) in bullfrog sympathetic ganglion neurones. *Pflugers Archiv* 413 482-486.

GOH, J.W. & PENNEFATHER, P.S. (1987). Pharmacological and physiological properties of the afterhyperpolarization current of bullfrog ganglion neurones. *Journal of Physiology* **394** 315-330.

GONOI, T.; SHERMAN, S.J. & CATTERALL, W.A. (1985). Voltage-clamp analysis of tetrodotoxin-sensitive and -insensitive sodium channels in rat muscle cells developing

in vitro. Journal of Neuroscience 5 2559-2564.

GOODMAN, C.S. & HEITLER, W.J. (1979). Electrical properties of insect neurones with spiking and non-spiking somata: normal, axotomized and colchicine-treated.

Journal of Experimental Biology 83 95-121.

GORDON, T. (1983). Dependence of peripheral nerves on their target organs. In: Somatic and Autonima Nerve-Muscle Interaction, pp 289-325. Eds. Y. Vrbova; G. Burnstock; R. Campbell & R. Gordon. Elseviers: Amsterdam.

GORDON, T.; KELLY, M.E.M.; SANDERS, E.J.; SHAPIRO, J. & SMITH, P.A. (1987). The effects of axotomy on bullfrog sympathetic neurones. *Journal of Physiology* **392** 213-229.

GOTTMANN, K.; DIETZEL, I.D.; LUX, H.D.; HUCK, S. & ROHRER, H. (1988). Development of inward currents in chick sensory and autonomic neuronal precursor cells in culture. *Journal of Neuroscience* 8(10) 3722-3732.

GRAFSTEIN, B. (1983). Chromatolysis reconsidered: A new view of the reaction of the nerve cell body to axon injury. In *Nerve*, *Organ and Tissue Regeneration: Research Perspectives*, pp 37-50. Ed. F.O. Seil. Academic Press, New York.

GURTU, S. & SMITH, P.A. (1988). Electrophysiological characteristics of hamster dorsal root ganglion cells and their response to axotomy. *Journal of Neurophysiology* **59** 408-423.

HAGIWARA, S. (1983). Calcium channels. In Membrane potential dependent ion channels in cell membrane. Phylogenetic and developmental approaches. pp 5-47. New York: Raven. 118pp.

HALLIWELL, J.V. & ADAMS, P.R. (1982). Voltage-clamp analysis of muscarinic excitation in hippocampal neurones. *Brain Research* **250** 71-92.

HARRIS, J.B. & MARSHALL, M.W. (1973). Tetrodotoxin-resistant action potentials in newborn rat muscle. *Nature (New Biology)* **243** 191-192.

HARRIS, J.B. & THESLEFF, S. (1971). Studies on teterodotoxin resistant action potentials in denervated skeletal muscle. *Acta Physiologica Scandinavica* 83 382-388.

HARTSHORNE, R.P. & CATTERALL, W.A. (1984). The sodium channel from rat brain. Purification and subunit composition. *Journal of Biological Chemistry* **259** 1667-1675.

HENZI, V. & MACDERMOTT, A.B. (1992). Characteristics and function of Ca<sup>2+</sup>- and

inositol 1,4,5-trisphosphate-releasable stores of Ca<sup>2+</sup> in neurones. *Neuroscience* **46** 251-273.

HEPPNER, T.J. & FIEKERS, J.F. (1992). Action potential-induced alterations in cytosolic calcium in fura-2-loaded dissociated bullfrog sympathetic neurons. *Society for Neuroscience Abstracts* **18** 972.

HESS, P. (1990). Calcium channels in vertabrate cells. *Annual Review of Neuroscience* 13 337-356.

HILLE, B. (1992). Modifiers of general and an elementary channels of excitable membranes. Sinauer Associates Inc. Publishers, Sunderland, Massachusetts pp 445-471.

HODGKIN, A.L. & HUXLEY, A.F. (1952). A quantitative description of membrane currents and its application to conduction and excitation in nerve. *Journal of Physiology* 117 500-544.

HONORE, E.; ATTALI, B.; ROMEY, G.; LESAGE, F.; BARHANIN, J. & LAZDUNSKI, M. (1992). Different types of K<sup>+</sup> channels are generated by different levels of a single mRNA. *EMBO Journal* 11(7) 2465-2471.

HOSHI, T.; ZAGOTTA, W.N. & ALDRICH, R.W. (1990). Biophysical and molecular

mechanisms of Shaker potassium channel inactivation. Science 250 533-538.

HOSHI, T.; ZAGOTTA, W.N. & ALDRICH, R.W. (1990). Two types of inactivation in *Shaker* potassium channels: effects of alterations in the carboxy-terminal region.

Neuron 7 547-556.

HUGUES, M.; ROMEY, G.; DUVAL, D.; VINCENT, J.P. & LAZDUNSKI, M. (1982). Apamin as a selective blocker of the calcium-dependent potassium channel in neuroblastoma cells: Voltage-clamp and biochemical characterization of the toxin receptor. *Proceedings of the National Academy of Sciences of USA* 79 1308-1312.

IKEDA, S.R. & SCHOFIELD, G.G. (1989). Somatostatin blocks a calcium current in rat sympathetic neurones. *Journal of Physiology* **409** 221-240.

ISACOFF, E.Y.; JAN, Y.N. & JAN, L.Y. (1990). Evidence for the formation of heteromultimeric potassium channels in *Xenopus* oocytes. *Nature* **345** 530-534.

ISHIZUKA, S.; HATTORI, K. & AKAIKE, N. (1984). Separation of ionic currents in the somatic membrane of frog sensory neurons. *Journal of Membrane Biology* **78** 19-28.

ISOM, L.L.; DEJONGH, K.S.; REBBER, B.F.X.; OFFORD, J.; CHARBONNEAU, H.; WALSH, K.; GOLDIN, A.L. & CATTERALL, W.A. (1992). Primary structure and

functional expression of the beta-1 subunit of the rat brain sodium channel. *Science* **256** 839-842.

JOE, E.H. & ANGELIDES, K. (1992). Clustering of voltage-dependent sodium channels on axons depends on Schwann cell contact. *Nature* **356** 333-335.

JONES, S.W. (1985). Muscarinic and peptidergic excitation of bullfrog sympathetic neurones. *Journal of Physiology* **366** 63-87.

JONES, S.W. (1987a). Sodium currents in dissociated bullfrog sympathetic neurones. Journal of Physiology 389 605-627.

JONES, S.W. (1987b). Chicken II luteinizing-hormone releasing hormone inhibits the M-current of bullfrog sympathetic neurons. *Neuroscience Letters* **80** 180-184.

JONES, S.W. & JACOBS, L.S. (1990). Dihydropyridine actions on calcium currents of bullfrog sympathetic neurons. *Journal of Neuroscience* **10** 2261-2267.

JONES, S.W. & MARKS, T.N. (1989a). Calcium currents in bullfrog sympathetic neurons- I. Activation kinetics and pharmacology. *Journal of General Physiology* 94 151-167.

JONES, S.W. & MARKS, T.N. (1989b). Calcium currents in bullfrog sympathetic neurons- I. Inactivation. *Journal of General Physiology* **94** 169-182.

KACZMAREK, R. & LEVITAN, I.B. (1987). Neuromodulation: The biochemical control of neuronal excitability. London Oxford University Press.

KATER, S.B. & MILLS, L.R. (1991). Regulation of growth cone behaviour and calcium. *Journal of Neuroscience* 11 891-899.

KAWAI, T. & WATANABE, M. (1986). Blockade of Ca-activated K conductance by apamin in rat sympathetic neurones. *British Journal of Pharmacology* 87 225-232.

KAWAI, T. & WATANABE, M. (1989). Effects of ryanodine on the spike afterhyperpolarization in sympathetic neurones of rat superior cervical ganglion. *Pflugers Archiv* 413 470-475.

KELLY, M.E.M.; BISBY, M.A. & LUKOWIAK, K. (1988). Regeneration restores some of the altered electrical properties of axotomized bullfrog B-cells. *Journal of Neurobiology* 19 357-372.

KELLY, M.E.M.; GORDON, T.; SHAPIRO, J. & SMITH, P.A. (1986). Axotomy affects calcium sensitive potassium conductance in sympathetic neurones. *Neuroscience* 

Letters 67 163-168.

KLEINHAUS, A.L. & PRITCHARD, J.W. (1976). Sodium dependent tetrodotoxin-resistant action potentials in leech nurones. *Brain Research* **102** 368-373.

KOIKE, T. & TANAKA, S. (1991). Evidence that nerve growth factor dependence of sympathetic neurones for survival *in vitro* may be determined by levels of cytoplasmic free Ca<sup>2+</sup>. *Proceedings of the National Academy of Sciences of USA* 88 3892-3896.

KOMURO, H. & RAKIC, P. (1992). Selective role of N-type colcium channels in neuronal migration. Science 257 806-809.

KOSTYUK, P.G.; VASELOVSKY, N.S. & TSYNDRENKO, A.Y. (1981). Ionic currents in the somatic membrane of rat dorsal root ganglion neurons- I. Sodium currents. *Neuroscience* 6 2423-2430.

KUBA, K. (1980). Release of calcium ions linked to the activation of potassium conductance in a caffeine-treated sympathetic neurones. *Journal of Physiology* **298** 251-269.

KUBA, K.; MORITA, K. & NOHMI, M. (1983). Origin of calcium ions involved in the generation of a slow afterhyperpolarization in bullfrog sympathetic neurones. *Pflugers* 

Archives 399 194-202.

KUBA, K. & NISHI, S. (1976). Rythmic hyperpolarizations and depolarizations of sympathetic ganglion cells induced by caffeine. *Journal of Neurophysiology* **39(3)** 547-563.

Kuno, M.; Miyata, Y. & Munoz-Martinez, E.J. (1974). Differential reaction of fast and slow  $\alpha$ -motoneurones to axotomy. *Journal of Physiology* **240** 725-739.

KURENNY, D.E.; CHEN, H. & SMITH, P.A. (1992). Effects of somatostatin on potassium currents in bullfrog sympathetic neurons: possible role of receptor subtypes. *Neuroscience Letters* **139** 227-230.

KUWADA, J.Y. & WINE, J.J. (1981). Transient, axotomy-induced changes in the membrane properties of crayfish central neurones. *Journal of Physiology* **317** 435-461.

LANCASTER, B. & ADAMS, P.R. (1986). Calcium-dependent current generating the afterhyperpolarization of hippocampal neurones. *Journal of Neurophysiology* **55(6)** 1268-1282.

LANCASTER, B.; NICOLL, R.A. & PERKEL, D.J. (1991). Calcium activates two types of potassium channels in rat hippocampal neurons in culture. *Journal of Neuroscience* 

11(1) 23-30.

LANCASTER, B. & PENNEFATHER, P. (1987). Potassium current evoked by brief depolarizations in bullfrog sympathetic ganglion cells. *Journal of Physiology* **387** 519-548.

L. M. Y.; DOLPHIN, A.C. & DAVIES, A.M. (1992). Intracellular Ca<sup>2+</sup> regulates the standard of early sensory neurones before they become dependent on neurotrophic factors. *Neuron* **9** 563-574.

LATORRE, R.; OBERHAUSER, A.; LABARCA, P. & ALVAREZ, O. (1989). Varieties of calcium-activated potassium channels. *Annual Review of Physiology* **51** 385-399.

LAWAIND, R.; WERMAN, R. & YAROM, Y. (1988). Electrophysiology of degenerating neurones in the vagal motor nucleus of the guineapig following axotomy. *Journal of Physiology* **404** 749-756.

LI, M.; WEST, J.W.; LAI, Y.; SCHEUER, T. & CATTERALL, W.A. (1992). Functional modulation of brain sodium channels by cAMP-dependent phosphorylation. *Neuron* 8 1151-1159.

LIEBERMAN, A.R. (1971). The axon reaction: A review of the principal features of

perikaryal response to axon injury. International Review of Neurobiology 14 49-124.

LIPSCOMBE, D.; MADISON, D.V.; POENIE, M.; REUTER, H.; TSIEN, R.Y. & TSIEN, R.W. (1988). Spatial distribution of calcium channels and cytosolic calcium transients in growth cones and cell bodies of sympathetic neurons. *Proceedings of the National Academy of Sciences of USA* 85 2398-2402.

LLINAS, R.; SUGIMORI, M. & CHERKSEY, B. (1989a). Voltage-dependent calcium conductances in mammalian neurons: The P channel. *Annals of New York Academy of Sciences USA* **560** 103-111.

LLINAS, R., SUGIMORI, M., LIN, J.W. & CHERSKEY, B. (1989b). Blocking and isolation of a calcium channel from neurons in mammals and cephalopods utilizing a toxin fraction (FTX) from funnel-web spider poison. *Proceedings of National Academy of Sciences of USA* 86 1689-1693.

LOGOTHETIS, D.E.; MOVAHEDI, S.; SATLER, C.; LINDPAINTNER, K. & NADAL-GINARD, B. (1992). Incremental reductions of positive charge within the S4 region of a voltage-gated K<sup>+</sup> channel result in corresponding decreases in gating charge.

Neuron 8 531-540.

LOPEZ, G.A.; JAN, Y.N. & JAN, L.Y. (1991). Hydrophobic substitution mutations in

the S4 sequence alter voltage-dependent gating in *Shaker* K<sup>+</sup> channels. *Neuron* **7** 327-336.

LUNEAU, C.J.; WILLIAMS, J.B.; MARSHALL, J.; LEVITAN, E.S.; OLIVA, C.; SMITH, J.S.; ANTANAVAGE, J.; FOLANDER, K.; STEIN, R.B.; SWANSON, R.; KACZMAREK, L.K. & BUHROW, S.A. (1991). Alternative splicing contributes to K<sup>+</sup> channel diversity in the mammalian central nervous system. *Proceedings of the National Academy of Sciences of USA* 88 3932-3936.

MARRION, N.V.; ADAMS, P.R. & GRUNER, W. (1992). Multiple kinetic states underlying macroscopic M-currents in bullfrog sympathetic neurones. *Proceedings of the Royal Society of London* **248** 207-214.

MARRION, N.V.; ZUCKER, R.S.; MARSH, S.J. & ADAMS, P.R. (1991). Modulation of M-current by intracellular Ca<sup>2+</sup>. Neuron 6 533-545.

MARTY, A. (1981). Ca-dependent K channels with large unitary conductance in chromaffin cell membranes. *Nature* **291** 497-500.

MATTSON, M.P. & KATER, S.B. (1987). Calcium regulation of neurite elongation and growth cone motility. *Journal of Neuroscience* **7** 4043-4043.

MAYER, M.L. & WESTBROOK, G.L. (1983). A voltage-clamp analysis of inward (anomalous) rectification in mouse spinal sensory ganglion cells. *Journal of Physiology* **340** 19-45.

MCCOBB, D.P.; BEST, P.M. & BEAM, K.G. (1990). The differentiation of excitability in embryonic chick limb motoneurones. *Journal of Neuroscience* **10(9)** 2974-2984.

MCCORMACK, K.; TANOUYE, M.A.; IVERSON, L.E.; LIN, J.; RAMASWAMI, M.; MCCORMACK, T.; CAMPANELLI, J.T.; MATHEW, M.K. & RUDY, B. (1991). A role for hydrophobic residues in the voltage-dependent gating of Shicker K<sup>+</sup> channels. *Proceedings of the National Academy of Sciences of USA* 88 293 2935.

MCFARLANE, S. & COOPER, E. (1992). Postnatal development of voltage-gated K currents on rat sympathetic neurons. *Journal of Neurophysiology* 67(5) 1291-1300.

MCFARLANE, S. & COOPER, E. (1991). Kinetics and voltage-dependence of A-type currents on neonatal rat sensory neurons. *Journal of Neurophysiology* **66(4)** 1380-1391.

MCMANNUS, O.B. (1991). Calcium-activated potassium channels: Regulation by calcium. *Journal of Bioenergetics and Biomembranes* **23(4)** 537-560.

MILLER, C.; MOCZYLDOWSKI, E.; LATORR. R. & PHILLIPS, M. (1985).

Charybdotoxin, a protein inhibitor of single Ca<sup>2+</sup>-activated K<sup>+</sup> channels from mammalian skeletal muscle. *Nature* 313 316-318.

MILLER, R.J. (1991). The control of neuronal Ca<sup>2+</sup> homeostasis. *Progress in Neurobiology* 37 255-285.

MILLER, R.J. (1992). Voltage sensitive Ca<sup>2+</sup> channels. *Journal of Biological Chemistry* **267** 1403-1406.

MINTZ, I.M.; ADAMS, M.E. & BEAN, B.P. (1992a). P-type calcium channels in rat central and peripheral neurones. *Neuron* 9 85-95.

MINTZ, I.M.; VENEMA, V.J.; SWIDEREK, K.M.; LEE, T.D.; BEAN, B.P. & ADAMS, M.E. (1992b). P-type calcium channels blocked by the spider toxin omega-Aga-IVA.

Nature 355 827-829.

MOCZYLDOWSKI, E. & LATORRE, R. (1983). Gating kinetics of Ca<sup>2+</sup>-activated K<sup>+</sup> channels from rat muscle incorporated into planar lipid bilayer. *Journal of General Physiology* **82** 511-542.

MORALES, A.; IVORRA, I. & GALLEGO, R. (1985). Recovery of normal

electrophysiological properties in petrosal ganglion sensory neurones of the cat following reinnervation of carotid body. *Neuroscience Letters (Supplement)* 22 s-523.

MORAN, D. (1991). Voltage-dependent-L-type Ca<sup>2+</sup> channels participate in regulating neural crest migration and differentiation. *American Journal of Anatomy* **192** 14-22.

MORGAN, J.I. & CURRAN, T. (1988). Calcium as a modulator of the immediate-early gene cascade in neurons. *Cell Calcium* **9** 303-311.

MURPHY, T.H.; WORLEY, P.F. & BARABAN, J.M. (1991). L-type voltage-sensitive calcium channels mediate synaptic activation of immediate early genes. *Neuron* 7 625-635.

NARGEOT, J.; DASCAL, N. & LESTER, H.A. (1992). Heterologous expression of calcium channels. *Journal of Membrane Biology* **126** 97-108.

NEHER, E. (1971). Two fast transient current components during voltage-clamp on snail neurones. *Journal of Physiology* **58** 36-53.

NEHER, E.; MARTY, A.; FUDUKA, K.; KUBO, T. & NUMA, S. (1988). Intracellular calcium release mediated by two muscarinic receptor subtypes. *FEBS Letters* **240** 9988-9994.

NERBONNE, J.M.; GURNEY, A.M. & RAYBURN, H.B. (1986). Development to the fast, transient outward K<sup>+</sup> current in embryonic sympathetic neurones. *Brain Research* **378** 197-202.

NISHI, S.; SOEDA, H. & KOKETSU, K. (1965). Studies on sympathetic B and C neurones and patterns of innervation. *Journal of Cell Comparative Physiology* **66** 19-32.

NODA, M; SHIMUZU, S.; TANABE, T.; TAKAI, T.; KAYANO, T.; IKEDA, T.; TAKAHASHI, H.; NAKAYAMA, H.; KANAOKA, Y.; MINAMINO, N.; KANGAWA, K.; MATUSO, H.; RAFTERY, M; HIROSE, T.; INAYAMA, S.; HAYASHIDA, H; MIYATA, M. & NUMA, S. (1984). Primary structure of Electrophorus electricus sodium channel deduced from cDNA sequence. *Nature* 312 121-127.

OWEN, D.G.; MARSH, S.J. & BROWN, D.A. (1989). M-current noise in rat sympathetic neurones. Society for Neuroscience Abstract 15 990

PALLOTTA, B.S.; MAGLEBY, K.L. & CARRETT, J.N. (1981). Single channel recordings of Ca<sup>2+</sup>-activated K<sup>+</sup> currents in rat muscle cell culture. *Nature* **293** 471-474.

PAPPONE, P.A. (1980). Voltage-clamp experiments in normal and denervated mammmalian skeletal muscle fibres. *Journal of Physiology* **306** 377-410.

PENNEFATHER, P.S.; LANCASTER, B.; ADAMS, P.R. & NICOLL, R.A. (1985). Two distinct Ca-dependent K-currents in bullfrog sympathetic ganglion cells. *Proceedings of the National Academy of Sciences of USA* 82 3040-3044.

PEROZO, E. & BEZANILLA, F. (1991). Phosphorylation of K<sup>+</sup> channels in the squid giant axon. A mechanistic analysis. *Journal of Bioenergetics & Biomembranes* **23(4)** 599-613.

PFAFFINGER, P.J.; LEIBOWITZ, M.D.; SUBERS, E.M.; NATHANSON, N.M.; ALMERS, W. & HILLE, B. (1988). Agonists that suppress M-current elicit phosphoinositide turnover and Ca<sup>2+</sup> transients, but these events do not explain M-current suppression.

Neuron 1 477-484.

PIETROBON, D. & HESS, P. (1990). Novel mechanism of voltage-dependent gating in L-type calcium channels. *Nature* **346** 651-655.

PINTER, M.J. & VANDEN-NOVEN, S. (1989). Effects of preventing reinnervation on axotomized spinal motoneurones in the cat. I. Motoneuron electrical properties.

Journal of Neurophysiology 62 311-324.

PLUMMER, M.R. & HESS, P. (1991). Reversible uncoupling of inactivation in N-type calcium channels. *Nature* **351** 657-659

PLUMMER, M.R.; LOGOTHETIS, D.E. & HESS, P. (1989). Elementary properties and pharmacological sensitivities of calcium channels in mammalian peripheral neurons. *Neuron* **2** 1453-1463.

POLLOCK, J.D.; KREMPIN, M. & RUDY, B. (1990). Differential effects of NGF, FGF, EGF, cAMP, and dexamethasone on neurite outgrowth and sodium channel expression in PC12 cells. *Journal of Neuroscience* **10(8)** 2625-2637.

PONGS, O. (1989). Molecular basis of potassium channel diversity. *Pfluegers Archiv* **414** S71-S75.

RITTER, A.M. & MENDELL, L.M. (1992). Somal membrane properties of physiologically identified sensory neurons in the rat: effects of nerve growth factor.

numal of Neurophysiology 68(6) 2033-2041.

ROSENBERG, R.L.; HESS, P. & TSIEN, R.W. (1988). L-type channels and calcium-permeable channels open at negative membrane potentials. *Journal of General Physiology* 92 27-54.

ROY, M.L. & NARAHASHI, T. (1992). Differential properties of tetrodotoxin-sensitive and tetrodotoxin-resistant sodium channels in rat dorsal root ganglion neurons.

Journal of Neuroscience 12(6) 2104-2111.

RUDY, B. (1988). Diversity and ubiquity of K Channels. Neuroscience 25(3) 729-749.

RUPPERSBERG, J.P.; SCHROTER, K.H.; SAKMANN, B.; STOCKER, M.; SEWING, S. & PONGS, O. (1990). Heteromultimeric channels formed by rat brain potassium channel proteins. *Nature* **345** 535-537.

SANGUINETTI, M.C. & JURKIEWICZ, N.K. (1992). Role of external Ca<sup>2+</sup> and K<sup>+</sup> in gating of cardiac delayed rectifier K<sup>+</sup> currents. *Pflugers Archiv* **420** 180-186.

SCHWINDT, P.C.; SPAIN, W.J. & CRILL, W.E. (1992). Calcium-dependent potassium currents in neurons from cat sensorimotor cortex. *Journal of Neurophysiology* **67**(1) 216-226.

SCOTT, R.H. & DOLPHIN, A.C. (1986). Regulation of calcium currents in a GTP analogue: potentiation of baclofen-mediated inhibition. *Neuroscience Letters* **69** 59-64.

SCOTT, R.H. & DOLPHIN, A.C. (1990). Voltage-dependent modulation of rat sensory neurone calcium channel currents in G-protein activation: effect of a dihydropyridine antagonist. *British Journal of Pharmacology* **99** 629-630.

SELYANKO, A.A.; SMITH, P.A. & ZIDICHOUSKI, J.A. (1990a). Effects of muscarine and adrenaline on neurones from Rana pipiens sympathetic ganglia. *Journal of* 

Physiology 425 471-500.

SELYANKO, A.A.; STANSFELD, C.E. & BROWN, D.A. (1992). Closure of potassium M-channels by muscarinic acetyl-choline receptor stimulants requires a diffusible messenger. *Proceedings of Royal Society of London, Britain* **250** 119-125.

SELYANKO, A.A.; ZIDICHOUSKI, J.A. & SMITH, P.A. (1990b). A muscarine-sensitive, slow, transient outward current in frog autonomic neurones. *Brain Research* **524** 236-243.

SHAPIRO, J.; GURTU, S.; GORDON, T. & SMITH, P.A. (1987). Axotomy increases conduction velocity of C-cells in bullfrig sympathetic ganglia. *Brain Research* **410** 186-188.

SHERMAN, S.J. & CATTERALL, W.A (1982). Biphasic regulation of development of the high affinity saxitoxin receptor by innervation in rat skeletal muscle. *Journal of General Physiology* **80** 753-768.

SHERMAN, S.J. & CATTERALL, W.A. (1984). Electrical activity and cytosolic calcium regulate levels of tetrodotoxin-sensitive sodium channels in cultured rat muscle cells. *Proceedinges of the National Academy of Sciences of USA* 81 262-266.

SHERMAN, S.J., CHRIVIA, J.J. & CATTERALL, W.A. (1985). Cyclic ademosine 3':5'-monophosphate and cytosolic calcium exert opposing effects on biosynthesis of tetrodotoxin-sensitive sodium channels in rat muscle cells. *Journal of Neuroscience* 5 1570-1576.

SIGWORTH, F.J. & NEHER, E. (1980). Single sodium channel currents observed in cultured rat muscle cells. *Nature* **287** 447-449.

SILVER, R.A. LAMB, A.G. & BOLSOVER, S.R. (1990). Calcium hotspots caused by L-channel clustering promote morphological changes in neuronal growth cones.

Nature 343 751-754.

SIMONI, A.; PELLEGRINI, M.; CECCONI, C. & PELLEGRINO, M. (1990). Axotomy affects density but not properties of potassium leak channels, in leech AP neurons. Brain Research 522 118-124.

SIMS, S.M.; CLAPP, L.H.; WALSH, J.V. & SINGER, J.J. (1990a). Dual regulation of M-current in gastric smooth muscle cell: beta-adrenergic-muscarinic antagonism. *Pflugers Archiv* 417 291-302.

SIMS, S.M.; CLAPP, L.H.; WALSH, J.V. & SINGER, J.J. (1990b). Antagonistic adrenergic-muscarinic regulation of M-current in smooth muscle cells. Science 239

190-193.

SINGER, D.; BIEL, M.; LOTAN, I.; FLOCKERZI, V.; HOFMAN, F. & DASCAL, N. (1991). The roles of the subunit in the function of the calcium channel. *Science* 253 1553-1557.

SMART, T.G. (1987). Single calcium-activated potassium channels from cultured rat sympathetic neurones. *Journal of Physiology* **389** 337-360.

SNUTCH, T.P.; LEONARD, J.P.; GILBERT, M.M.; LESTER, H.A. & DAVIDSON, N. (1990). Rat brain expresse a heterogeneous family of calcium channels. *Proceedinges of the National Academy of Sciences of USA* 87 3391-3395.

SPITZER, N.C. (1979). Ion channels in development. *Annual Review of Neuroscience* **2** 263-297.

SPITZER, N.C. & LAMBORGHINI, J.E. (1976). The development of the action potential mechanism of amphibian neurones isolated in culture. *Proceedinges of the National Academy of Sciences of USA* 73 1641-1645.

STANDFELD, C.E.; MARSH, S.J. & BROWN, D.A. (1990). Putative M-channels in cultured rat superior cervical ganglion (SCG) cells. *Journal of Physiology* **426** 69P.

STORM, J.F. (1987). Action potential repolarization and a fast afterhyperpolarization in rat hippocampal pyramidal cells. *Journal of Physiology* **385** 733-759.

STUMER, W. (1990). Site-directed mutagenesis in voltage gated channels. *Biophysical Journal (Abstract)* 57 386a.

STUMER, W.; CONTI, F.; SUZUKI, H.; WANG, X.; NODA, M.; YAHADI, N.; KUBO, H, & NUMA, S, (1989). Structural parts involved in activation and inactivation of the sodium channel. *Nature* **339** 597-603.

TANG, C.M.; PRESSER, F. & MORAD, M. (1988). Amiloride selectively blocks the low threshold (T) calcium channels. *Science* **240** 213-215.

TAKATA, M.; SHOHARA, E. & FUJITA, S. (1980) The excitability of hypoglossal motoneurones undergoing chromatolysis. *Neuroscience* 5 413-419.

THAYER, S.A.; HIRNING, L.D. & MILLER, R.J. (1988). The role of caffeine-sensitive calcium stores in the regulation of the intracellular free calcium concentrations in rat sympathetic neurons *in vitro*. *Molecular Pharmacology* **34** 664-673.

THAYER, S.A. & MILLER, R.J. (1990). Regulation of the intracellular free calcium concentration in single rat dorsal root ganglion neurons in vitro. Journal of Physiology

425 85-115.

THOMPSON, S.M. & WONG, R.K.S. (1991). Development of calcium current subtypes in isolated rat hippocampal pyramidal cells. *Journal of Physiology* **439** 671-689.

TITMUS, M.J. & FABER, D.S. (1986). Altered excitability of goldfish Mauthner cell following axotomy. II. Localization and ionic basis. *Journal of Neurophysiology* 55 1440-1454.

TITMUS, M.J. & FABER, D.S. (1990). Axotomy-induced alterations in the electrophysiological characteristics of neurons. *Progress in Neurobiology* 35 1-51.

TOKIMASA, T. & AKASU, T. (1990). Cyclic AMP regulates an inwardly rectifying sodium-potassium current in dissociated bullfrog sympathetic neurones. *Journal of Physiology* **420** 409-429.

TRAUB, R.D.; WONG, R.K.S.; MILES, R. & MICHELSON, H. (1991). Amodel of a CA3 hippocampal pyramidal neuron incorporating voltage-clamp data on intrinsic conductances. *Journal of Neurophysiology* **66(2)** 635-650.

TRAYNOR, P; DRYDEN, W.F. & SMITH, P.A. (1992). Trophic regulation of action potential in bullfrog sympathetic neurones. Canadian Journal of Physiology &

Pharmacology 70 826-834.

TRIMMER, J.S. & AGNEW, W.S. (1989). Molecular diversity of voltage-sensitive Na channels. *Annual Review of Physiology* **51** 401-418.

TSIEN, R.W.; LIPSCOMBE, D.; MADISON, D.V.; BLEY, K.R. & FOX, A.P. (1988). Multiple types of neuronal calcium channels and their selective modulation. *Trends in Neuroscience* 11 431-438.

USOWICZ, M.M.; PORZIG, H.; BECKER, C. & REUTER, H. (1990). Differential expression by nerve growth factor of two types of Ca<sup>2+</sup> channels in rat pheochromocytoma cell lines. *Journal of Physiology* **426** 95-116.

VAN-DONGEN, A.M.J.; FRECH, G.C.; DREWE, J.A.; JOHO, R.H. & BROWN, A.M. (1990). Alteration and restoration of K<sup>+</sup> channel function by deletions at the N- and C-termini. *Neuron* 5 433-443.

VARADI, G.; LORY, P; SCHULZ, D.; VARADI, M. & SCHWARTZ, A. (1991). Acceleration of activation and inactivation by the beta subunit of skeletal muscle calcium channel. *Nature* **352** 159-162.

VASSILEV, P.M.; SCHEUER, T. & CATTERALL, W.A. (1988). Identification of an

intracellular peptide segment involved in sodium channel inactivation. *Science* **241** 1658-1661.

WEI, A.; COVARRUBIAS, M.; BUTLER, A. BAKER, K.; PAK, M. & SALKOFF, L. (1990). K<sup>+</sup> channel diversity is produced by an extended gene family conserved in Drosophila and mouse. *Science* **248** 599-603.

WERTZ, M.A.; ELMSLIE, K.S. & JONES, S.W. (1992). N-type channel inactivation is enhanced by phosphorylation. *Society for Neuroscience Abstract* **18** 431.

WERTZ, M.A.; ELMSLIE, K.S. & JONES, S.W. Phosphorylation enhances inactivation of N-type calcium channel current in bullfrog sympathetic neurons. *Pflugers Archiv* (in press).

WOLLNER, D.A. & CATTERALL, W.A. (1986). Localization of sodium channels in axon hillocks and initial segments of retinal ganglion cells. *Proceedings of the National Academy of Sciences of USA*. **83** 8424-8428.

XU, Z.J. & ADAMS, D.J. (1992). Resting membrane potential and potassium currents in cultured parasympathetic neurones from rat intracardiac ganglia. *Journal of Physiology* **456** 405-424.

YAMADA, W.M.; KOCH, C. & ADAMS, P.R. (1989). Multiple channels and calcium dynamics. In *Methods in Neuronal Modelling: From Synapses to Networks* Eds. Koch, C. & Seger, I. MIT, Cambridge. pp 97-133.

YANAGIHARA, K. & IRISAWA, H. (1980). Inward current activated during hyperpolarization in the rabbit sino-atrial node cell. *Pflugers Archiv* 385 11-19.

YANG, J. & TSIEN, R.W. (1993). Enhencement of N- and L-type calcium channel currents by protein kinase C in frog sympathetic neurones. *Neurons* 10 127-136.

ZAGOTTA, W.N.; HOSHI, T. & ALDRICH, R.W. (1990). Restoration of inactivation in mutatnts of *Shaker* potassium channels by a peptide derived from ShB. *Science* **250** 568-571.

## CHAPTER 2.

## CHANGES IN SODIUM AND CALCIUM CHANNEL ACTIVITY FOLLOWING AXOTOMY OF B-CELLS IN BULL-FROG SYMPATHETIC GANGLION.

Note: This chapter is a version of a paper by <u>B.S. Jassar; P.S. Pennefather & P.A.</u>

<u>Smith</u> which has been accepted for publication by *Journal of Physiology (London)*.

## 2.1 SUMMARY

- 1. Currents mediated by  $Ca^{2+}$  channels using  $Ba^{2+}$  as a charge carrier ( $I_{Ba}$ ),  $Na^+$  currents ( $I_{Na}$ ) and voltage- and  $Ca^{2+}$ -dependent  $K^+$  currents ( $I_C$ ) were recorded from bull-frog paravertebral sympathetic ganglion B-cells using whole-cell patch-clamp recording techniques. Currents recorded from control cells were compared with those from axotomized cells 13-15d after transection of post-ganglionic nerves.
- 2. Axotomy reduced peak  $I_{Ba}$  at -10mV (holding potential= -80mV) from  $3.3\pm0.3$ nA (n=42) to  $1.7\pm0.1$ nA (n=39, P<0.001). Tail  $I_{Ba}$  at -40mV following a step to +70mV from a holding potential of -80mV was also reduced in axotomized neurones (9.7±0.6nA for 42 control neurones and  $5.2\pm0.3$ nA for 39 axotomized neurones; P<0.001). Minimal changes were observed in the kinetics of activation and deactivation.
- 3. Pharmacological experiments using Bay K 8644, nifedipine and  $\omega$ -conotoxin showed that axotomy predominantly affected the N-type Ca<sup>2+</sup> channels which carry the majority of  $I_{Ca}$  in these neurones. L-type Ca<sup>2+</sup> current was little affected and T-type Ca<sup>2+</sup> currents were not observed in control or axotomized cells.
- 4. Development of inactivation at 0mV and recovery from inactivation of  $I_{\rm Ba}$  at -80mV exhibited three distinct components in both control and axotomized neurones: 'fast', 'intermediate' and 'slow'. The relative proportions of both the 'fast' and 'intermediate' components of inactivation at 0mV were almost doubled after axotomy (fast component was 15% in control and 29% in axotomized neurones; intermediate component was 17% in control and 26% in axotomized neurones).

'Fast' and 'intermediate' inactivation tended to develop more rapidly and recover more slowly after axotomy. The rate of onset of 'slow' inactivation was unaffected by axotomy but the steady-state level at -40mV was increased.

- 5. Inactivation during a 500ms pulse to +70mV was approximately 13% of the maximum inactivation seen at -20mV in control neurones. However, in axotomized neurones the level of inactivation that developed under these conditions was around 45% of maximum. Since several aspects of voltage-dependent inactivation of  $I_{\text{Ba}}$  are enhanced by axotomy, it is likely that increased inactivation is responsible for the major portion of the reduction in  $I_{\text{Ba}}$  amplitude.
- 6. Axotomy reduced  $I_C$  (measured at the end of a 3ms step from -40mV to +20mV) from  $34.5\pm4.9$ nA (n=26) to  $19.2\pm1.5$ nA (n=49, P<0.005). This reduction may be secondary to the reduction in calcium channels available for activation from -40mV following axotomy.
- 7. The TTX-sensitive and TTX-insensitive components of peak Na<sup>+</sup> conductance ( $G_{Na}$ ) were both increased after axotomy. Total  $G_{Na}$  was increased from 184.9±8.4nS to 315.2±16.4nS (n=37 for both P<0.001). Most of the kinetic and steady-state properties of  $I_{Na}$  were unchanged after axotomy.
- 8. These results suggest that the increase in spike width produced by axotomy of bullfrog sympathetic neurones involves a decrease in  $I_{Ca}$  and consequent reduction in  $I_{C}$ . The complement of ion channels expressed after axotomy is quite unlike that which might be expected in 'immature' or 'dedifferentiated' neurones.

#### 2.2 INTRODUCTION

Transection or damage to the axon of a central or peripheral neurone results in various morphological, biochemical and electrophysiological changes in the cell body (Lieberman, 1971; Titmus & Faber, 1990). This 'cell body reaction' has been interpreted as a reflection of the neurone's attempt to recenerate an axon (Grafstein & McQuarrie, 1978; but see also Carlsen, Kiff & Ryugo, 1982). If this is the case, one might expect that similar changes in neuronal properties would appear in all neuronal types as a consequence of the regenerative and degenerative mechanisms triggered by axotomy. This suggestion is difficult to reconcile with the observation that the effect of axotomy on action potential (a.p.) shape varies considerably according to neuronal type. For example, axotomy increases a.p. duration (spike width) in bullfrog sympathetic ganglion B-cells (Kelly, Gordon, Shapiro & Smith, 1986; Gordon, Kelly, Sanders, Shapiro & Smith, 1987) and in dorsal root ganglion cells of the cat cranial, carotid and glossopharyngeal nerves (Czeh, Kudo & Kuno, 1977; Gallego, Ivorra & Morales, 1987; Belmonte, Gallego & Morales, 1988) but not in hamster dorsal root ganglion cells (Gurtu & Smith, 1988). By contrast, axotomy decreases a.p. duration in guinea pig vagal motoneurones (Laiwand, Werman & Yarom, 1988). Axotomy also produces a variety of changes in different neuronal types in the amplitude and duration of the afterhyperpolarization (a.h.p.) which follows the a.p. (Titmus & Faber, 1990) whereas the rate of rise of the a.p. is increased in most cell types which have been studied (Gallego et al., 1987; Belmonte et al., 1988). Although different neuronal types express different complements of ion

channels, the variation in the electrophysiological response to axotomy could be explained by the hypothesis that specific types of ion channels are always similarly affected during the 'cell body reaction'. This is because changes in a.p. configuration in a given cell type would reflect the relative abundance and importance of 'axotomysensitive' channels for a.p. generation. This hypothesis can only be tested by using voltage and patch-clamp techniques to study specific ionic conductances in a variety of neuronal types. In the present work, we compared Ca2+, Na+ and K+ currents from control bullfrog sympathetic B-neurones with those recorded from neurones 13-15days after in vivo axotomy. Axotomy of these cells results in an increase in the width and height of the a.p. and a decrease in the amplitude and duration of the a.h.p. (Kelly et al., 1986; Gordon et al., 1987). We tested whether the previously described increase in spike width resulted from decreases in Ca2+ current and concomitant reduction of the voltage-dependent  $G_{K,Ca}$  ( $Ca^{2+}$ -activated  $K^{+}$ conductance) which repolarizes the a.p. (I<sub>C</sub>; Adams, Brown & Constanti, 1982) or whether it resulted from slowing of I<sub>Na</sub> inactivation.

Some of this work has previously appeared in abstract form (Jassar & Smith, 1991a; 1992).

### 2.3 METHODS.

Small to medium sized bullfrogs (10-12cm) were purchased from a biological supply house and stored in running water at room temperature (20°C). The surgical procedures for axotomy of spinal nerves *in vivo* were carried out under aseptic

conditions. The animals were anaesthetized by injecting a 2.5% w/v solution of 3-aminobenzoic acid ethyl ester methanesulfonate salt (MS-222) into the dorsal lymph sac. The level of anaesthesia was deemed adequate when the animal failed to respond to a noxious stimulus (forceps pinch) applied to the hindlimb toe. Unilateral axotomy of spinal nerves (on the right side of each animal) was performed by excising 5-10mm of the VIIIth, IXth and Xth (and sometimes VIIth) spinal nerves 5-10mm below the Xth paravertebral ganglion. Nerves were exposed through a 1cm dorso-lateral incision in the body wall in the middle of the lumbar region. The incision was sutured using fine silk thread. Following recovery from anaesthesia, axotomized animals were maintained in tetracycline solution (0.16g/l) in plastic tanks. This solution was changed on alternate days.

Control (unoperated) and axotomized frogs were killed by decapitation and their spinal cords destroyed by 'pithing'. The VIIth - Xth paravertebral sympathetic ganglia were removed from both sides of each control animal or from the axotomized side of two axotomized animals and dissociated using the trypsin/collagenase procedure previously described (Jassar & Smith, 1991b). The dissociated cells were resuspended in fresh '6K-external solution'. '6K external solution' contained: (in mM) NaCl 113; KCl 6; MgCl<sub>2</sub> 2; CaCl<sub>2</sub> 2; HEPES (acid) 5 and glucose 10 (pH adjusted to 7.2 with Na0H). Cells were stored at about 5°C until use and were sometimes washed with cold '6K external solution' to remove any remaining enzymes. They were placed in a small plastic petri dish under a Nikon 'Diaphot' inverted microscope and studied within 1-8h after dissociation. 'Control' data were usually obtained from

cells dissociated from the ganglia of unoperated frogs. Occasionally, ganglia from the unoperated side of axotomized frogs were used. Since the operated frogs were kept in tetracycline solution which is known to inhibit protein synthesis, this raises concerns about the effects of tetracyclines on cells from unoperated ganglia (i.e contralateral However, it has been shown that long-term continuous intravenous side). administration of tetracyclines affects only mitochondrial protein synthesis; cytoplasmic protein synthesis is not affected and this fails to produce any obvious 'side effects' (Bogert and Kroon, 1981). Since no obvious differences were discernible between the action potential characteristics and the currents recorded from the two control groups in this study (i.e cells from unoperated frogs and cells from the contralateral ganglia of axotomized frogs which were maintained in tetracyclines), the data from the two groups were pooled. Ba<sup>2+</sup> was used as the charge carrier to study currents through Ca2+ channels. For these experiments, the 'external' solution contained (in mM); N-methyl-D-glucamine (NMG) chloride 117.5; NMG-Hepes 2.5; BaCl<sub>2</sub> 2.0; (pH7.2). 'Internal' solution consisted of (in mM) NMG-Cl 76.5; HEPES 2.5; tris-BAPTA 10, tris-ATP 5; MgCl<sub>2</sub> 4; (pH7.2; Jones & Marks 1989a). For sodium currents, 'external' solution contained (in mM): NaCl 97.5; TEA-Br 20; MnCl<sub>2</sub> 4; tris-Cl 2.5 (pH 7.2) and the 'internal' solution contained (in mM): CsCl 103; NaCl 9; TEA-Br 5; Cs-HEPES 2.5; Cs-EGTA 1 (pH 7.2; Jones 1987). To study I<sub>C</sub>, 'external' solution contained KCl 2; CaCl<sub>2</sub> 4; NMG-Cl 40; Tris-Cl 2.5; sucrose 134; D-glucose 10. CaCl<sub>2</sub> was replaced with MgCl<sub>2</sub> in this external solution and 50µM CdCl<sub>2</sub> was added to block Ca<sup>2+</sup> influx which normally is responsible for activating I<sub>C</sub>. 'Internal solution' contained (in mM): KCl 110; NaCl 10; MgCl<sub>2</sub> 2; CaCl<sub>2</sub> 0.4; EGTA 4.4; HEPES 5; D-glucose 10; cyclic-AMP 0.125; leupeptin 0.1 (pH 7.2). External solutions were 250mOsM/kg and internal solutions were 240mOsM/kg. The petri dishes were superfused with external solutions at a flow rate of 2ml/min. This flow rate allowed exchange of solutions within about 2min. Drugs were applied by superfusion. All solutions containing dihydropyridines were administered under subdued lighting conditions from light-proof reservoirs. Bay K 8644 and nifedipine were dissolved in DMSO to make 3mM and 10mM stock solutions, respectively. These solutions were diluted 1 in 10,000 in external solution for application to ganglion cells.

Cells of intermediate size (usual input capacitance,  $(C_{in})$  40 - 80pF) were selected for recording. These were presumed to be B-cells (Dodd & Horn, 1983). An Axopatch 1B amplifier was used to record Ba<sup>2+</sup> currents ( $I_{Ba}$ ) and data collection usually started 15min after establishing whole-cell recording conditions. Series resistance measured following break-through was 3-12 M $\Omega$  (usually 5-8 M $\Omega$ ). Data were analyzed only from cells in which there was no run-down of  $I_{Ba}$  within the first 15min of data collection. In such cells, the amplitude of  $I_{Ba}$  was 60-80% of its original value even after 75 minutes of recording. To limit reduction in successive responses due to slow  $I_{Ba}$  inactivation (Jones & Marks, 1989b), the interval between successive depolarizing voltage commands was 15s and the interval between successive experimental protocols was at least 3min (Jassar & Smith, 1991b). Cells were held at -80mV during these intervals. Series resistance compensation was

monitored and re-adjusted throughout the experiment (always at 80%). The error in clamp potential in recording a current of 6 nA, due to series resistance of 8M $\Omega$  at 80% compensation would be approximately 10 mV. This would reflect a maximum error for peak Ba<sup>2+</sup> currents which were <6nA. Greater voltage errors would be expected for the larger  $I_{Ba}$  tail currents. Cancellation of capacity transients and leak subtraction was done by applying 25% amplitude hyperpolarizing pulses, multiplying responses by 4 and addition (Jones & Marks, 1989a). Membrane capacitance was compensated at the start of recording and  $C_{in}$  was estimated by reading the dial used to compensate the capacitance. Whole-cell capacitance compensation was disabled prior to data collection.

I<sub>Na</sub> and I<sub>C</sub> were recorded using an Axoclamp 2A amplifier in the single-electrode, discontinuous voltage-clamp mode (Jones, 1987). These currents, which were typically >20nA, are too large to study with the Axopatch 1B amplifier. Also, the use of a 'switching amplifier' minimises series resistance problems associated with large, rapidly activating currents because the amplifier headstage is clamped to the recorded membrane voltage and the electrode itself does not contribute to the series resistance. Using low resistance patch electrodes coated with 'Sigmacote'® (Sigma, St. Louis, MO, USA), it was possible to achieve switching frequencies between 35 and 55kHz (usually 45-50kHz) and a clamp gain between 12 and 25nA.mV<sup>-1</sup> (usually 16-20 nA.mV<sup>-1</sup>). The steady-state voltage error (V<sub>S</sub>) reported by an electrode in recording 30nA current from a 70pF cell with a clamp gain of 16nA/mV and a switching frequency of 45kHz will be <1mV, as estimated from the equation

$$V_S = I/gFC_{in}$$

where I = current, g = clamp gain, F = switching frequency and  $C_{in}$  = whole cell capacitance (Finkel & Redman, 1984; Jones 1987). Peak clamp voltage error ( $V_{I:}$ ) is given by the expression

$$V_E = I(d/FC_{in})$$

where d = 1 - 'duty cycle' ( = 0.7 for Axoclamp 2A). For a 30nA current recorded from a 70pF cell using a 45kHz switching frequency, the error would be 6.7mV.

Data were digitized using a Labmaster DMA interface and stored on an IBM compatible computer (Northgate 386) fitted with removable hard disk systems (Bernoulli drive, Iomega Corp. Roy, UT, U.S.A.). During data acquisition, the corner frequency of the filter was set to 5kHz for  $I_{Ba}$  and the bandwidth of the filter was 10 or 30kHz for  $I_{Na}$  and  $I_{C}$ . Permanent records were made from the hard disk using an XY plotter. Data were acquired and analyzed using 'Pclamp' software (Axon Instruments, Burlingame, CA., USA). Tail current amplitudes were measured at  $500\mu s$  (for  $I_{Ba}$ ) or at peak amplitude of the tail (for  $I_{C}$ ) after the termination of a command pulse following subtraction of capacity currents. This procedure seemed appropriate for estimating the peak amplitudes of the relatively slow tail currents which would flow at the test potential of -40mV (see Fig 1). All data are presented as mean  $\pm$  s.e.m. In graphs where no error bars are visible, the error bars are smaller than the symbols used to designate the data points.

All drugs and chemicals were purchased from Sigma (St. Louis, MO., USA) except for Bay K 8644 and nifedipine which were gifts from Dr. Susan Dunn.

### 2.4 RESULTS.

All data on the effects of axotomy were obtained 13-15d after section of the postganglionic nerves. Axotomy-induced changes in the a.p. characteristics of bullfrog sympathetic ganglion (BFSG) cells seem to be maximal at this time (Gordon *et al.*, 1987).

## 2.4.1.1 Effects of Axotomy on IBa

Figure 1 illustrates  $I_{Ba}$  evoked in a control and in an axotomized neurone following a series of depolarizing voltage commands from a holding potential of -80mV.  $I_{Ba}$  tails (at -40mV) were recorded at the end of each depolarizing pulse. The current in the axotomized cell is obviously much smaller than that recorded in the control neurone. Figure 2A illustrates the average I-V relationship obtained from peak  $I_{Ba}$  in 42 control and 39 axotomized cells (13-15d after axotomy). Axotomy reduced peak  $I_{Ba}$  at -10mV from  $3.3\pm0.3$ nA (n=42) to  $1.7\pm0.1$ nA (n=39, P<0.001). Figure 2C, which illustrates the average tail current amplitudes from 42 control and 39 axotomized cells, gives a measure of the extent of  $I_{Ba}$  activation by the various voltage commands in control and axotomized cells. This reduction in peak  $I_{Ba}$  and in  $I_{Ba}$  tails was also obvious when the data were replotted as current densities (Figs. 2B and D) and suggests that our selection of cells within a particular range of diameters minimized the variability of the total current which could result from differences in cell size. This observation justifies the use of raw current amplitude

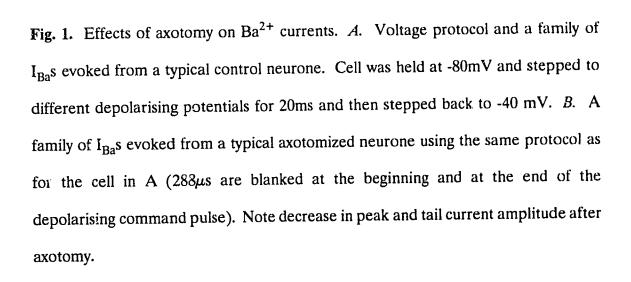
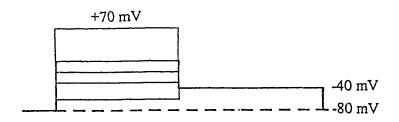
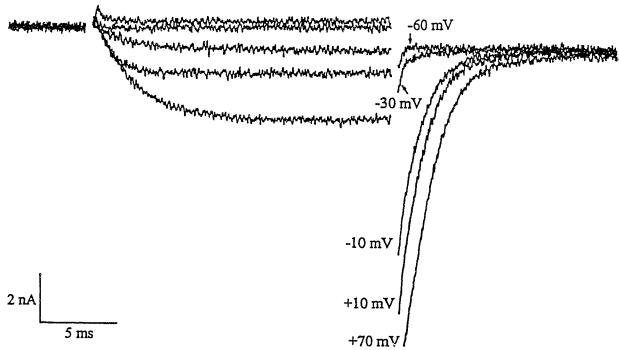


Figure 1.

# A Control





# B Axotomized

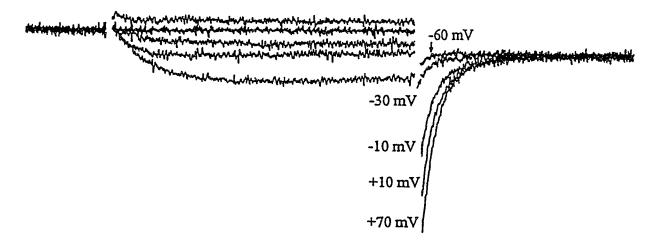
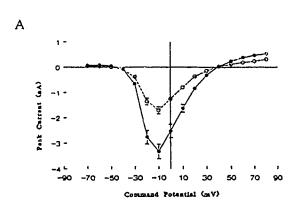
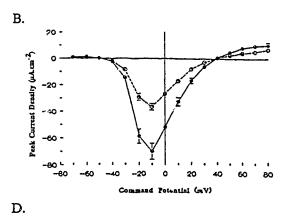


Fig. 2. Comparison of I<sub>Ba</sub> in control and axotomized neurones. A. Current-voltage relationship for peak I<sub>Ba</sub> from 42 control (\*) and 39 (o) axotomized cells. B. Data from cells used in A replotted as current-density-voltage relationship. Current density was calculated from  $C_{in}$  assuming a specific membrane capacitance of  $1\mu F.cm^{-2}$ . C. Current-voltage relationship for tail  $I_{Ba}$  current from 42 control ( $\blacksquare$ ) and 39 axotomized (0) cells. D. Data from cells used in C replotted as current-densityvoltage relationship as in B. E. Normalized tail-current amplitudes from control and axotomized cells plotted as a function of command potential. Symbols represent the observed data points and the solid line is a plot of the Boltzmann equation of the form  $I_{t(v)}/I_{t(max)} = G_{(v)}/G_{(max)} = \left\{ 1 + \exp^{-ze(Vo + V)/kT} \right\}^{-1}$  where  $I_{t(v)}$  is the amplitude of the  $I_{Ba}$  tails following a command to voltage, V,  $I_{l(max)}$  is the maximum amplitude of I<sub>Ba</sub> tails seen following commands to positive voltages. The ratio of these currents is equal to the ratio of  $Ba^{2+}$  conductances  $G_{(v)}/G_{(max)}$  which is an index of the fraction of  $Ca^{2+}$  channels open. z = valency of the gating particle, <math>e = valency of the gating particle, <math>e = valency of the gating particleelementary electronic charge (1.602 x  $10^{-19}$  C), k = Boltzman's constant (1.381 x  $10^{-23}$ V C K<sup>-1</sup>), T = absolute temperature and  $V_o$  is the potential for half maximal activation.

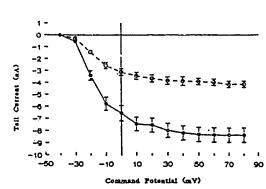
Figure 2.

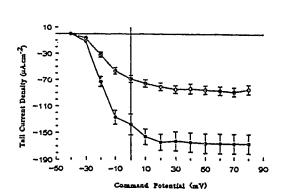
## **Barium Currents**



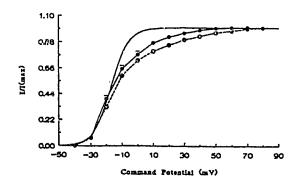


C.





E.



for comparison of data for other currents between control and axotomized cells reported in this study. The mean data points from Figs 2C have been normalized and replotted in Fig 2E. The solid line in figure 2E describes a Boltzmann equation in which z was set to 4.6 and  $V_o$  to -17mV. The line corresponds well to both axotomized and control data only at relatively negative potentials (see figure legend). The deviation at more positive membrane potentials probably reflects, in part, fast inactivation which develops during 20ms test pulses. Inactivation is most pronounced between -40 and 0mV and is reduced at  $\div$ 70mV (see Fig. 7D & E; Jones & Marks, 1989b).

# 2.4.1.2 Pharmacology of Ba2+ currents before and after axotomy.

Although single channel conductances characteristic of both N and L-type  $Ca^{2+}$  channels have been described in bullfrog sympathetic ganglion B-cells (Lipscombe, Madison, Poenie, Reuter, Tsien & Tsien, 1988a), it has been reported that less than 10% of the channels are of the L-type (Jones & Marks 1989a; Jones & Jacobs, 1990). The effect of  $\omega$ -conotoxin GVIA on whole cell  $I_{Ba}$  was examined to test whether the proportion of L to N type current changed after axotomy. Some typical data records illustrating the reversible inhibition of  $I_{Ba}$  in a control neurone by 200nM  $\omega$ -contoxin are shown in Figure 3A (cf. Morrill, Boland & Bean, 1991). The effect of the toxin on the I-V relationship of 14 control cells is shown in Figure 3B and in 14 axotomized cells in Figure 3C. In control neurones at -10mV,  $\omega$ -conotoxin reduced the peak  $I_{Ba}$  to  $1.7\pm0.1$ nA (n=14) and after axotomy to

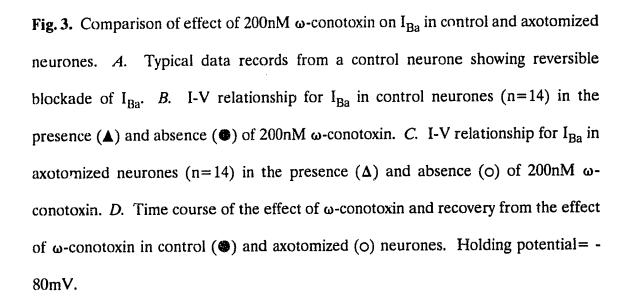
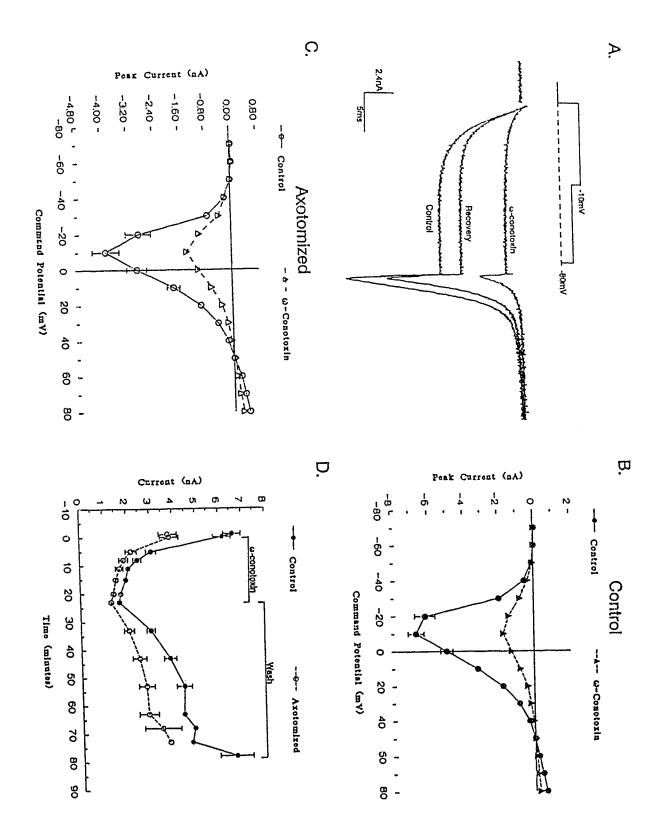


Figure 3.

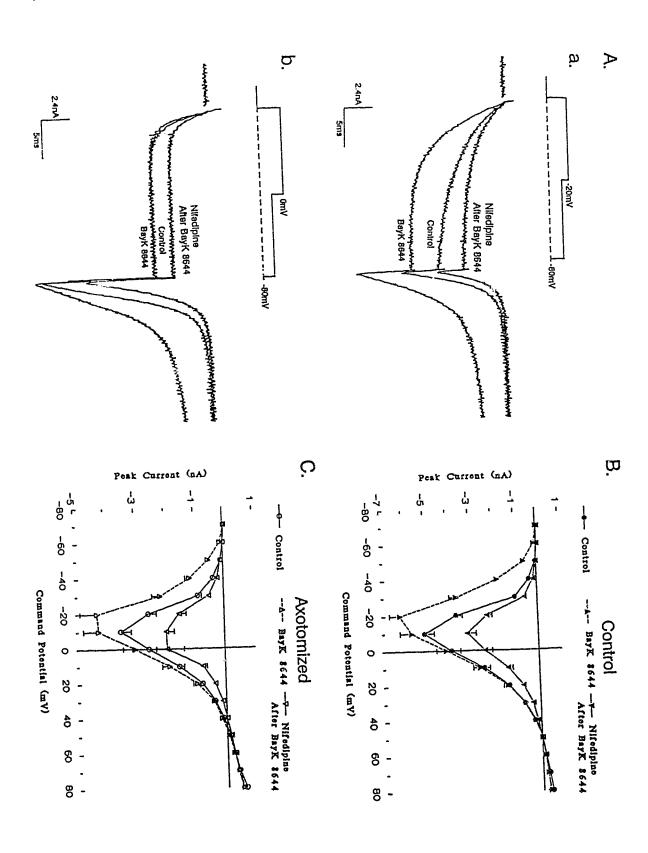


1.4±0.1nA (n=14). Thus, there was little or no change in the amount of ω-conotoxin-resistant current remaining after axotomy (0.1>P>0.05). This point is illustrated further by the data in Figure 3D which shows the time course of the effect of ω-conotoxin on  $I_{Ba}$  (at -10mV) in control and axotomized neurones. In both situations, the inhibition of the current takes 20-25min to reach a steady-state and the effect is almost completely reversed after about 1h. Although the toxin reduces  $I_{Ba}$  (at -10mV) to 26.5±1.4% in control cells and to 38.5±2.5% in axotomized cells, there is more total current in the control neurones than in the axotomized neurones and the amount of ω-conotoxin-resistant current is unchanged.

If this  $\omega$ -conotoxin resistant fraction of the total current is carried by L-type channels (Jones & Marks, 1989a; Jones & Jacobs, 1990) and the numbers of L-channels are unchanged after axotomy, then dihydropyridines would be expected to affect the total  $I_{Ba}$  by the same absolute amount in both control and axotomized neurones. Nifedipine ( $1\mu$ M) failed to affect  $I_{Ba}$  in control or axotomized cells whereas the current was potentiated in both situations by Bay K 8644 (300nM). The additional amount of current seen in control neurones at -20mV, ( $2.5\pm0.4$ nA; n=11) was similar to that seen in axotomized cells ( $1.7\pm0.5$ nA, n=12; P>0.2). This was accompanied by a shift in the activation curve to more hyperpolarized potentials. When the solution containing Bay K 8644 was replaced by one containing  $1\mu$ M nifedipine,  $I_{Ba}$  was reduced to levels less than its initial value in control and axotomized cells at all voltages. Nifedipine after Bay K 8644 reduced the control  $I_{Ba}$  at -10mV by  $1.9\pm0.1$ nA (n=11) in control cells, and by  $1.5\pm0.3$ nA (n=12) (P>0.2)

Fig. 4. Voltage-dependence of the effects of dihydropyridines on  $I_{Ba}$  in control and axotomized neurones. A. a. Bay K 8644 (300nM) potentiates  $\overline{\iota}_{Ba}$  evoked by stepping from -80mV to -20mV and subsequent application of nifedipine ( $1\mu$ M) reduces the potentiated current to less than initial level. b. Bay K 8644 (300nM) does not potentiate  $I_{Ba}$  evoked by stepping from -80mV to 0mV but subsequent application of nifedipine ( $1\mu$ M) still reduces the current to less than the control value. Traces in A and B were obtained from a control neurone. B. I-V relationship for  $I_{Ba}$  in control neurones (n=11) prior to the addition of dihydropyridines ( $\bullet$ ), in the presence of Bay K 8644 ( $\blacktriangle$ ) and in the presence of nifedipine (after exposure to Bay K 8644) ( $\blacktriangledown$ ). C. I-V relationship for  $I_{Ba}$  in axotomized neurones (n=12) prior to the addition of dihydropyridines ( $\circ$ ), in the presence of nifedipine (after exposure to Bay K 8644) ( $\bullet$ ) and in the presence of nifedipine (after exposure to Bay K 8644) ( $\bullet$ ). Holding potential= -80mV.

Figure 4.



after axotomy. Again, there was no difference in the amount of current affected. Typical data records for currents activated in a control cell at 0 and -20mV are shown in Figures 4Aa and 4Ab. The I-V plots for 11 control and 12 axotomized cells (Figs. 4B and C) show the potentiation of  $I_{Ba}$  by Bay K 8644 and its subsequent supression by nifedipine. The potentiation produced by Bay K 8644 was most apparent at potentials negative to -20mV whereas the depression produced by nifedipine was most apparent at potentials positive to -20mV. This effect is also quite evident from the data records illustrated in Figs 4Aa and 4Ab. These effects of dihydropyridines and  $\omega$ -conotoxin suggest that axotomy predominantly affects N-type and not L-type  $Ca^{2+}$  channels.

### 2.4.1.3 Effects of Axotomy on Inactivation of $I_{Ba}$

To investigate the effects of axotomy on steady-state inactivation properties,  $I_{Ba}$  was evoked from three different holding potentials of -90, -60 and -40mV (Fig. 5). The I-V relationship for peak  $I_{Ba}$  clearly shows that shifting the holding potential from -60 to -90mV has a larger effect on peak  $I_{Ba}$  in the axotomized cells than in the control cells. After axotomy, such a shift in holding potential almost doubles  $I_{Ba}$  at -10mV (from  $0.85\pm0.11$ nA, n=8 to  $1.75\pm0.12$ nA, n=8, P<0.001; Fig. 5B) whereas in the control situation, changing the holding potential has little effect on  $I_{Ba}$  recorded at -10mV (0.3>P>0.2; Fig. 5A). This effect is attributable to increased slow inactivation in axotomized neurones (see below). Figures 5C and 5D illustrate the I-V relationship for  $I_{Ba}$  tails (at -40mV) evoked from different holding potentials from

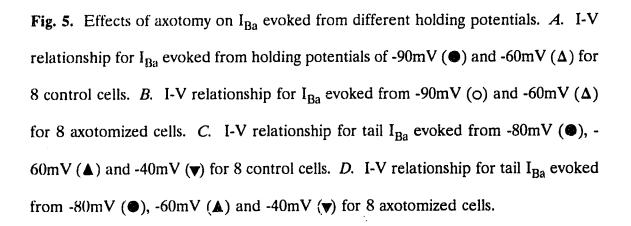
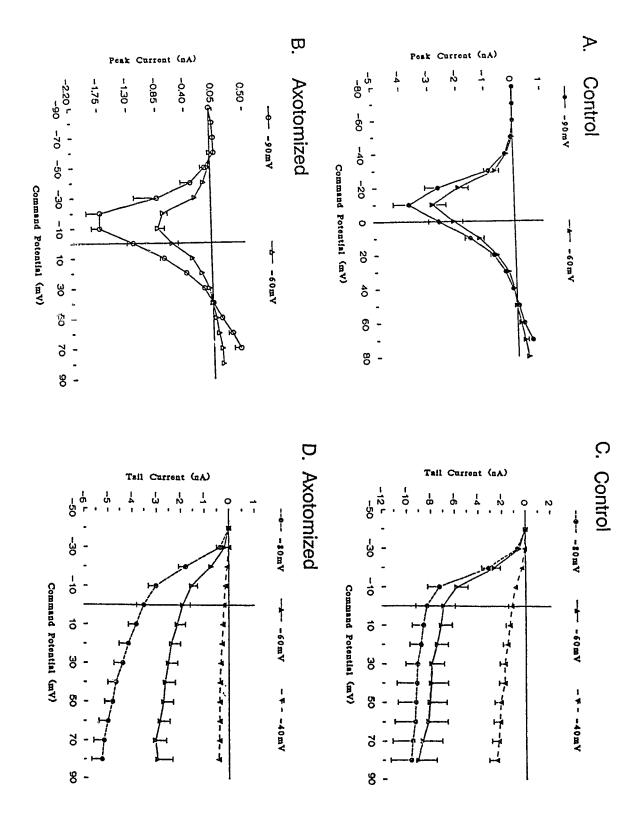


Figure 5.



control and axotomized neurones. Changing the holding potential has a far stronger effect on the relative amplitude of  $I_{Ba}$  tails in axotomized neurones than in control neurones. Assuming that inactivation is negligible at -80mV in both control and axotomized neurones, the effect of holding potential on  $I_{Ba}$  tails following a 20ms pulse to +70mV suggests that the mid-point voltage for inactivation is shifted from -48mV to approximately -58mV after axotomy (cf. Jones & Marks, 1989b).

Figure 6 illustrates the onset and recovery from inactivation of I<sub>Ba</sub> following a 1s conditioning pulse to 0mV. The experimental protocol and typical current records from a control and an axotomized neurone are illustrated in Fig 6A. The current remaining at the end of the 1s pulse was  $64\pm2\%$  in control neurones ( $36\pm2\%$ inactivation; n=39) and  $40\pm2\%$  ( $60\pm2\%$  inactivation; n=35) for axotomized neurones. I<sub>Ba</sub> evoked by 1s pulses to 0mV from a holding potential of -80mV, shows two components of inactivation- 'fast' and 'intermediate'. The contribution of these two components was quantified by fitting the decay phase to the sum of two exponential components plus an offset and the data are summarized in table 1. The amplitude of the 'fast' inactivating component (A<sub>1</sub>) contributes 15±2% of total I<sub>Ba</sub> evoked in control cells ( $\tau_1$ =58±4ms; n=39) and 29±2% for axotomized neurones ( $\tau$ =45±2ms; n=35). The extrapolated values of the amplitude of the 'intermediate' component (A<sub>2</sub>) comprised  $40\pm2\%$  of total I<sub>Ba</sub> in control neurones ( $\tau_2=746\pm30$ ms) and  $44\pm1\%$  in axotomized neurones ( $\tau_2$ =479±15ms). When these 1s pulses were evoked every 15s, there was decrement of current between successive responses (see Fig. 6Aa1). This decrement appears to be due to build up of a 'slow' form of inactivation. In Fig 6B the normalized peak  $I_{Ba}$  is plotted against pulse number. The data can be described by an exponential approach to a new steady-state value. The rates of onset  $(k_+)$  and recovery  $(k_-)$  of slow inactivation can be estimated from the parameters describing the decrement (see appendix). If x is the steady-state fractional decrement due to 'slow' inactivation and  $1/\lambda$  is the number of pulses required to reach  $e^{-1}$  of this steady-state value then

$$(1 - x) * k_{+} * 1s = x * k_{-} * 15s$$

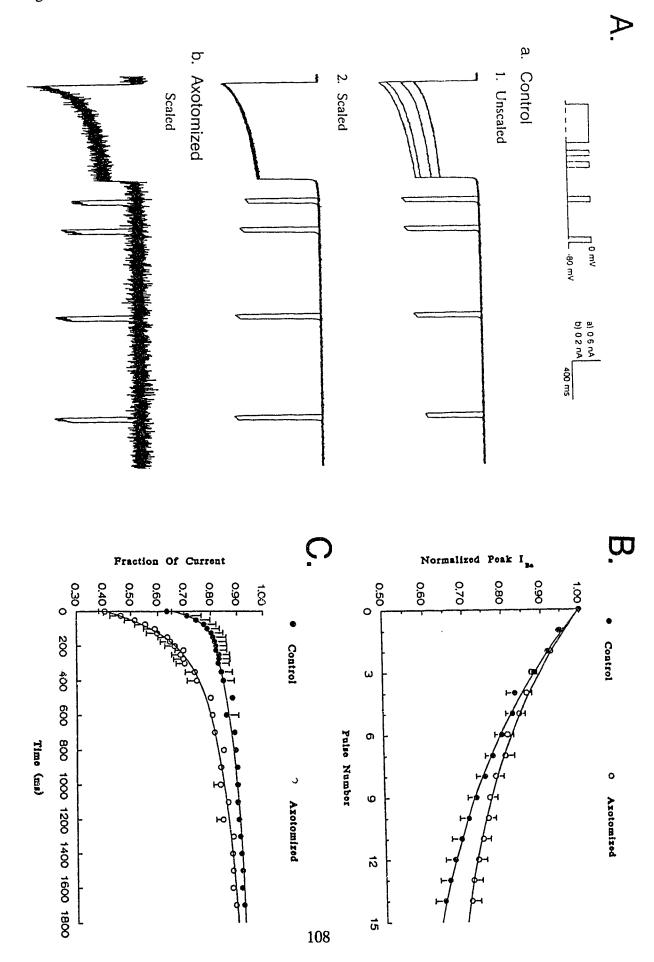
and

$$\lambda = k_{+} * 1s + k_{.} * 15s.$$

Thus, knowing the values of  $\lambda$  and the steady-state decrement one can derive  $k_+$  and  $k_-$ . The extrapolated steady-state decrement was 49% for control cells and 37% for axotomized cells. The values of  $\lambda$  estimated from Fig. 6B were 0.09 for control cells and 0.108 for axotomized cells. The derived values of  $k_+$  and  $k_-$  are 0.043.s<sup>-1</sup> and 0.0031.s<sup>-1</sup> in control; and 0.04.s<sup>-1</sup> and 0.0045.s<sup>-1</sup> in axotomized neurones. These values yield the time constants for onset (at 0mV) and offset (at -80mV) of the 'slow' component ( $\tau_3$ ) of inactivation in table 1. Fig. 6B also shows that a single 1s pulse is associated with about 6% slow inactivation (A<sub>3</sub>). Once the 'fast' and 'slow' components of the total inactivation during the 1s pulse are accounted for, the total

Fig. 6. Effects of axotomy on time-dependence of onset and recovery from inactivation. ... Cells were stepped to 0mV for 1s from a holding potential of -80mV during the conditioning pulsa is flower by a 75ms test pulses to 0mV applied at increasing intervals from 25ms to 1700ms every 15c (0.66 Hz). a. & b. show IBas evoked using the voltage protocols illustrated in the upper panel from a control and an axotomized neurone, respectively. al shows the raw data records illustrating the decrement of current between successive pulses in a control neurone. In a2 and b, the amplitudes of the currents evoked in three successive pulses have been scaled to superimpose extents evoked during the conditioning pulse in the first trial for comparison. Four traces and superimposed, each conditioning pulse followed by its test pulse. The calibration is correct for current amplitudes shown in al and for the first pulse only in a2 and b. B. Onset of 'slow' inactivation of IBa (at 0mV) in control ( ) and axotomized (o) neurones. The peak I<sub>Ba</sub> during each 1s conditioning pulse is normalized to the peak IBa observed during first 1s conditioning pulse and plotted against the pulse number (see al). Solid lines through the data describe the relative decrement of current between successive pulses for the control cells by the equation I(n)/I(0) = 0.51 + 0.49 \* exp<sup>-0.091n</sup> and by the expression I(n)/I(0) = 0.63 + 0.37 \* exp<sup>-0.108n</sup> for axotomized cells, where I(n) refers to the peak  $I_{Ba}$ evoked in the nth conditioning pulse and I(0) refers to peak IBa evoked in the first pulse of the train and n is the pulse number, the first one designated as 0. C. Rate of recovery from inactivation (at -80mV) measured from the amplitude of 75ms test pulses in control ( ) and axotomized (o) neurones. Solid lines are plots of the equation  $I_0/I_{0(max)} = 1 - (0.06 * exp^{-0.0000031t}) - (0.16 * exp^{-0.0013t})$  $(0.12 * exp^{-0.020t})$  for control data and by  $I_0/I_{0(max)} = 1 - (0.06 * exp^{-0.0000045t}) - (0.25 * exp^{-0.0010t})$ -  $(0.28 * exp^{-0.0070t})$  for axotomized data where  $I_0$  is peak  $I_{Ba}$  during test pulse,  $I_{0(max)}$  is peak  $I_{Ba}$ during conditioning pulse and t is the delay between the conditioning and test pulses.

Figure 6.



inactivation observed suggests that 17% and 26% 'intermediate' inactivation developed during the 1s pulse in control and axotomized cells respectively (see table 1 for details). However, using the time constants and extrapolated amplitude of the 'intermediate' component estimated from the fits of the decay of  $I_{Ba}$  and subtracting the 'slow' component one predicts 24% and 30% intermediate component in control and axotomized neurones respectively. It is likely that the pulse duration (1s) is not long enough to define accurately the 'intermediate' component. Using 3s pulses, a 1.5s time constant is observed in the inactivation of  $I_{Ba}$  (Wertz, Elmslie & Jones, in press).

The three components of inactivation are also apparent in the kinetics of recovery (Fig. 6C). The peak current during test pulse is expressed as a fraction of the peak of the corresponding conditioning pulse. The amplitudes of the 'fast', 'intermediate' and 'slow' components observed during recovery corresponds to those observed during onset of inactivation.

Data presented in Table 1 illustrates that axotomy increases both 'fast' and 'intermediate' components of inactivation. Onset of slow inactivation at 0mV and recovery at -80mV do not appear to be affected much. It should be recalled, however, that Fig. 5 suggests that some form of 'slow' inactivation is enhanced in axotomized neurones such that the half inactivation voltage is shifted from -48mV to approximately -58mV after axotomy. It is instructive to consider how the two observations can be reconciled. If recovery from 'slow' inactivation is not voltage-dependent and only the rate of onset of inactivation increases with depolarization,

Table I. Components of Inactivation of IBa-

		Total in	A <sub>1</sub>	$\tau_1$	A <sub>2</sub>	$ au_2$ (ms)	Α <sub>3</sub>	$\tau_{\mathfrak{Z}}$
		Is (%)	(%)	(ms)	(%)		(%)	(s)
Onset at 0mV	Control	44±2 <sup>1</sup>	15±2	58±4	40±2	746±30	-	235
	Axotomized	68±2 <sup>1</sup>	29±2	45±2	44±1	479±15	~	255
Recovery at -80mV	Control	36±2 <sup>2</sup>	14	50	17 <sup>3</sup>	746	64	326 <sup>5</sup>
	Axotomized	60±2 <sup>2</sup>	29	143	26.3	1000	64	220 <sup>5</sup>

For onset of inactivation at 0mV the values for time constants and relative amplitudes were obtained by fitting two exponential components plus an offset to the decay of the current during the 1s pulse. A similar analysis was applied to average data for recovery from inactivation at 80mV (see Fig. 6C and legend). 'A' refers to % amplitude and '\tau' refers to time constant.

Subscripts 1, 2 & 3 refer to 'fast', 'intermediate' and 'slow' components of inactivation respectively.

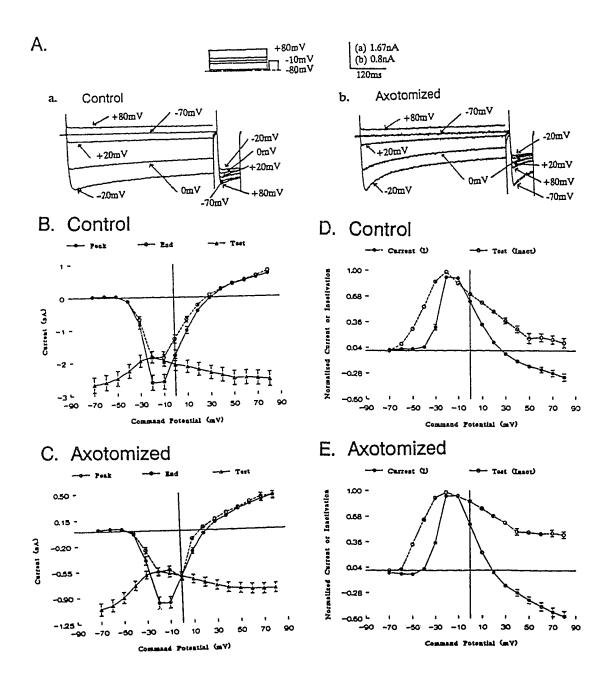
- 1. Estimated using values of  $A_1$ ,  $\tau_1$ ,  $A_2$  and  $\tau_2$  derived from bi-exponential fits to the inactivation during 1s commands to 0mV from -80mV.
- 2. Determined from the ratio of amplitudes of  $I_{\rm Ba}$  at the end of the 1s pulse over the peak  $I_{\rm Ba}$  for the pulse.
- Obtained by subtracting the relative amplitude of 'fast' and 'slow' components from the amount
  of total inactivation during the 1s pulse.
  - 4. Determined from the decrement of the peak  $I_{\mbox{\footnotesize{Ba}}}$  between successive pulses.
  - 5. Estimated from decrement of peak  $I_{\mbox{\footnotesize{Ba}}}$  during 0.067Hz train of 1s commands to 0mV.

then the voltage-dependence of that rate would have to be e-fold per 18mV in control and e-fold per 27mV in axotomized cells. This would allow for the rate of onset to equal the rate of offset of 'slow' inactivation at -48mV in control cells and at -58mV in axotomized neurones. More experiments using different test potentials will be required to explore this possibility.

The effects of axotomy on voltage-dependence of inactivation of  $I_{Ba}$  were studied using a voltage protocol which involved a 500ms conditioning pulse followedby a 75ms test pulse (Jones & Marks, 1989b). Typical traces are illustrated in Fig 7A. Maximal peak I<sub>Ba</sub> flows during conditioning pulses to -10 or -20mV and this current displays obvious decrement by the end of the 500ms conditioning pulse which is more pronounced in the axotomized neurone (Fig 7Ab). inactivation of  $I_{\text{Ba}}$  (at -10mV during a 500ms depolarizing pulse) was 29.6 $\pm$ 2.2 in control neurones (n=44) and  $46.8\pm1.6$  in axotomized neurones (n=57; P<0.001). Figure 7B shows that the current available for activation in the 75ms test pulse is minimal when the conditioning pulse is associated with maximal current (i.e. maximal inactivation is seen following pulses to -10 or -20mV). Inactivation is reduced at positive potentials where IBa is reduced. This result is suggestive of 'currentdependent' inactivation. However, significant inactivation is observed at -50mV where little I<sub>Ba</sub> is apparent. Jones and Marks (1989b) have suggested that the current-dependence is only apparent and, in fact, represents the voltage-dependence of inactivation such that less inactivation develops at positive potentials. Figure 7C illustrates the data for inactivation of  $I_{\text{Ba}}$  from 57 axotomized neurones. A more

Fig. 7. Effects of axotomy on voltage-dependence of inactivation of  $I_{Ba}$ . A. Voltage protocol and series of current responses from a control neurone (a) and axotomized neurone (b). Each conditioning step from the holding potential of -80mV to a depolarized potential was followed by a 'test' pulse to -10mV. Calibration (a) refers to control records (a) and calibration (b) refers to records from the axotomized cell (b). Note that the smaller currents in the axotomized neurone inactivate to a greater extent and have a higher rate of inactivation as compared to those in the control neurone. B. Peak (●), end of pulse (o) and test pulse current (▲) from 44 control neurones plotted as a function of the command potential used for the conditioning pulse. C. Peak (♠), end of pulse (o) and test pulse current (♠) from 57 axotomized neurones plotted as a function of the command potential in the conditioning pulse. D. Data from control neurones (B, n = 44) normalized and re-plotted. Maximum peak current flowing during the conditioning pulse was defined as 1 for each cell and peak current at different depolarizing potentials (1) normalized to this value. Minimum current elicited for each cell for a test pulse (to -10mV) was taken as maximum inactivation ( =1 ) and other values were normalized to this value to give an index or inactivation (o). E. Data from axotomized neurones (C) normalized and repletted for conditioning pulse current ( $\bullet$ ) and inactivation (o; n=57).

Figure 7.



convenient method of illustrating inactivation in control and axotomized cells is shown in Figs 7D and E. Currents recorded during the conditioning pulses were normalized to their maximum values and plotted against voltage. Minimum current during test pulses was defined as maximum inactivation. Inactivation at various potentials was normalized to this value. This yields a more direct comparison of conditioning current amplitude and the amount of inactivation (cf. Jones & Marks 1989b). The data illustrate that the enhanced inactivation seen in axotomized neurones is especially apparent at positive potentials (P<0.001 for voltages from 0 to +50mV).

Unlike the data presented in Figs 2 & 3, currents illustrated in Fig 7 were not leak-subtracted. The apparent reversal potential for  $I_{Ba}$  in control cells (Figs 7B and D) is more positive than that for axotomized cells (Fig. 7C and E). This difference may result from a greater contribution of outward leak current in axotomized cells because it is opposed by a weaker inward  $I_{Ba}$  under these conditions. Leak current is not altered by axotomy (B.S. Jassar, P.S. Pennefather & P.A. Smith, *submitted*).

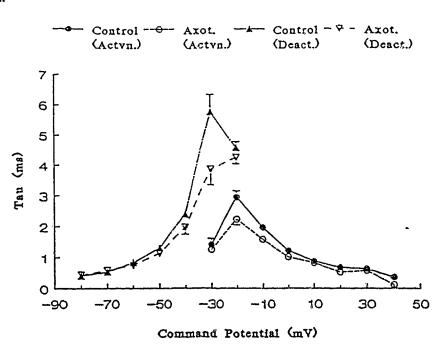
## 2.4.1.4 Effects of Axotomy on activation and deactivation of $I_{B\alpha}$

The kinetics of activation and deactivation of  $I_{Ba}$  were examined to further explore any changes in the properties of  $Ca^{2+}$  channels which might be induced by axotomy. Figure 8A illustrates the voltage-dependence of the rate of activation and deactivation of  $I_{Ba}$ . Activation time constants ( $\tau_{act}$ ) were obtained by applying single exponential fits to currents recorded from experiments such as that illustrated in Fig 1 (n=42 for control cells and n=39 for axotomized cells). Deactivation time

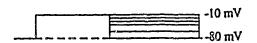
Fig. 8. Effects of axotomy on kinetics of activation and deactivation of  $I_{Ba}$ . A. Voltage-dependence of  $\tau$  for activation (for control n=42;  $\bullet$ , and for axotomized n=39; 0) and deactivation (for control n=14;  $\bullet$ , for axotomized n=15;  $\forall$ ).  $\tau_{act}$  (time constant of activation) was measured by fitting single exponential curves to currents evoked by using the protocol shown in figure 1. B. Upper panel shows voltage protocol for studying deactivation. Cells were stepped to -10 mV for 20ms and then stepped back to a series of less depolarized potentials to observe tail currents. Lower panel shows a family of  $I_{Ba}$ s and tail currents evoked from a control neurone by using this protocol.  $\tau_{deact}$  (time constant of deactivation) was measured by fitting single exponential curves to the tail currents. Holding potential= -80mV.

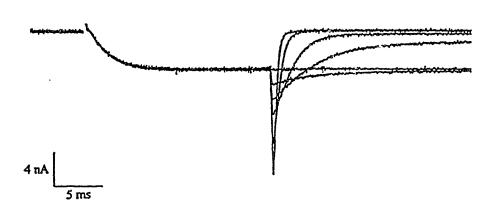
Figure 8.





## В.





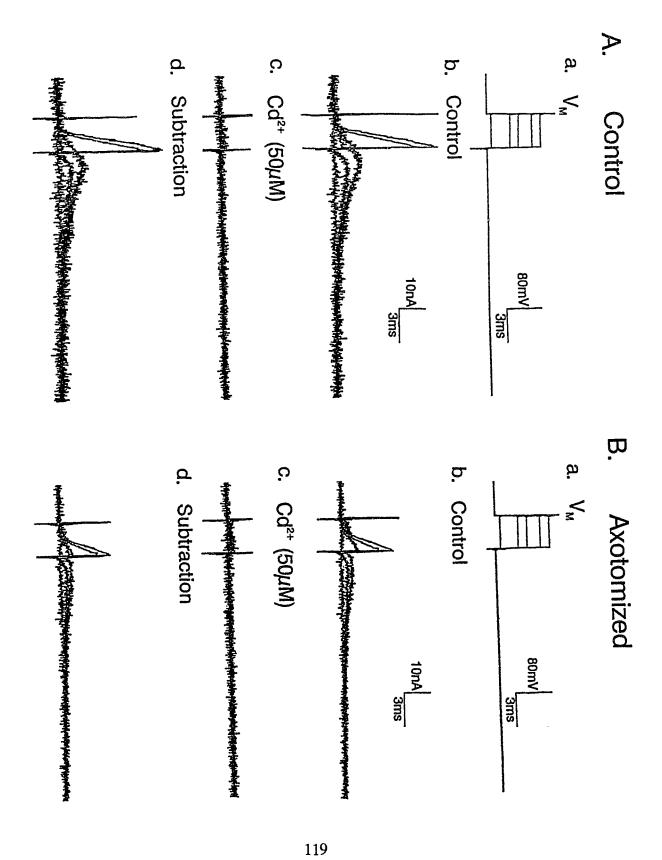
constants ( $\tau_{deact}$ ) were obtained from single exponential fits to tail currents recorded at various potentials following a step command to -10mV (n=17 for control cells and n=16 for axotomized cells). An experiment of this type is illustrated in Fig 8B. The difference in magnitude of deactivation and activation time constants at -30mV (Fig. 8A) and the initial delay in activation of  $I_{Ba}$  (Fig 8B) may indicate that multiple closed states precede opening of  $Ca^{2+}$  channels (Sala, 1991). Axotomy appears to increase the rate of  $I_{Ba}$  activation at relatively negative potentials (e.g. at -20mV; P<0.005) whereas at more positive voltages (e.g. +30mV), little or no effect could be detected (P>0.6). After axotomy, the rate of deactivation at -30mV appeared to be increased (P<0.02) yet axotomy seemed to have little effect at more hyperpolarized membrane potentials (P>0.2 at -60mV). Given the amplitude ( $\approx13$ nA, Fig 8B) and time course of  $I_{Ba}$  tail currents (<2ms at -80mV), the data on deactivation must be viewed with caution because such large, rapid currents are subject to significant voltage and time-course errors imposed by the series resistance.

# 2.4.2 Effects of axotomy on I<sub>C</sub>

The  $Ca^{2+}$ -dependent  $K^{+}$  current,  $I_{C}$ , plays a major role in the repolarization of the a.p. in bull-frog sympathetic ganglion B-cells (Lancaster & Pennefather, 1987). Since  $Ca^{2+}$  current is decreased, a decrease in  $I_{C}$  would be expected after axotomy.  $I_{C}$  was evoked by applying brief (3ms) depolarizing commands from a holding potential of -40mV. Extracellular solution contained 4mM  $Ca^{2+}$  but no  $Na^{+}$  (see Methods). This protocol should minimize contamination of the current by the

Fig. 9. Comparison of  $I_C$  in a typical control (A) and a typical axotomized (B) neurone. a. Voltage protocol for evoking  $I_C$ . Cells were held at -40mv and stepped to depolarized potentials for 3ms.  $V_M$  shows the membrane voltage which the cell membrane attained in response to a step command pulse to depolarized potentials. b. A family of currents evoked in response to a series of depolarising command pulses ( $[Ca]_O = 4mM$ ). c. A family of currents evoked by same depolarizing commands as used in c but in the presence of  $50\mu$ M Cd<sup>2+</sup> and  $[Ca]_O = 0mM$  to block  $I_{Ca}$  and calcium-dependent K<sup>+</sup>-currents. d.  $I_C$ , in relatively pure form, obtained by subtracting current in 0mM Ca<sup>2+</sup> and  $50\mu$ M Cd<sup>2+</sup> from that obtained in 4mM Ca<sup>2+</sup>.

Figure 9.



delayed rectifier (IK) which should be largely inactivated at this potential (Adams et al., 1982). The decrease in I<sub>C</sub> after axotomy is apparent from the typical current records illustrated in Figure 9. I<sub>C</sub> appears as a rapidly activating outward current and the rate of activation increases with increasing depolarization. The current is almost completely eliminated by replacement of  $Ca^{2+}$  with  $Mg^{2+}$  and addition of  $50\mu M$ Cd2+ to the external solution. For analysis of I<sub>C</sub>, the very small currents remaining in Cd2+ were subtracted from the original currents. Data obtained from peak currents at the end of a 3ms pulse to various depolarized potentials and the tail currents measured at peak amplitude following this pulse has been replotted as current-voltage relationship in Figure 10A and B respectively. The maximum amount of  $I_C$  is activated by depolarization to +20 or +30mV. Peak and tail current values for a 3ms step to +20mV were 19.2±1.5nA and 5.5±0.5nA for axotomized cells (n=49) and  $34.5\pm4.9$ nA and  $10.2\pm2.1$ nA for control cells (n=26) respectively. There was therefore a significant decrease in peak and tail current amplitude after axotomy (P < 0.005 for peak currents and P < 0.05 for tails). Since the 3ms pulse used in these experiments is too short for I<sub>C</sub> to approach its maximum, it is possible that the reduction in current amplitude seen in axotomized neurones results from slowed activation kinetics. However, experiments using longer (50ms) voltage commands have shown that axotomy reduces steady-state I<sub>C</sub> and that the rate of activation is unchanged (Jassar et al., submitted).

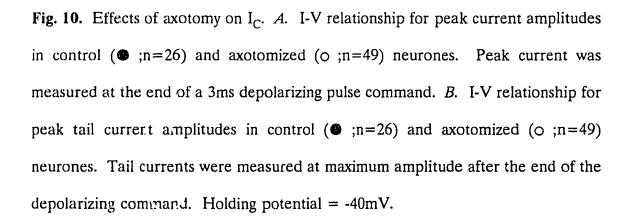
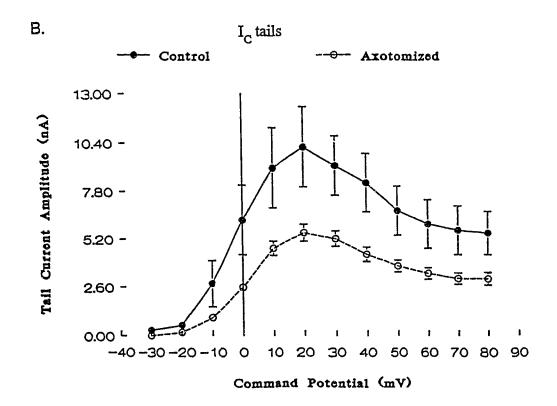


Figure 10.

A.  $I_C$  peak --0-- Axotomized Control 40 -Peak Current Amplitude (nA) 32 -24 -16 -8 -0 -30 40 60 70 80 90 50 10 20 -40 -30 -20 -10 Command Potential (mV)



## 2.4.3 Effects of Axotomy on $I_{Na}$

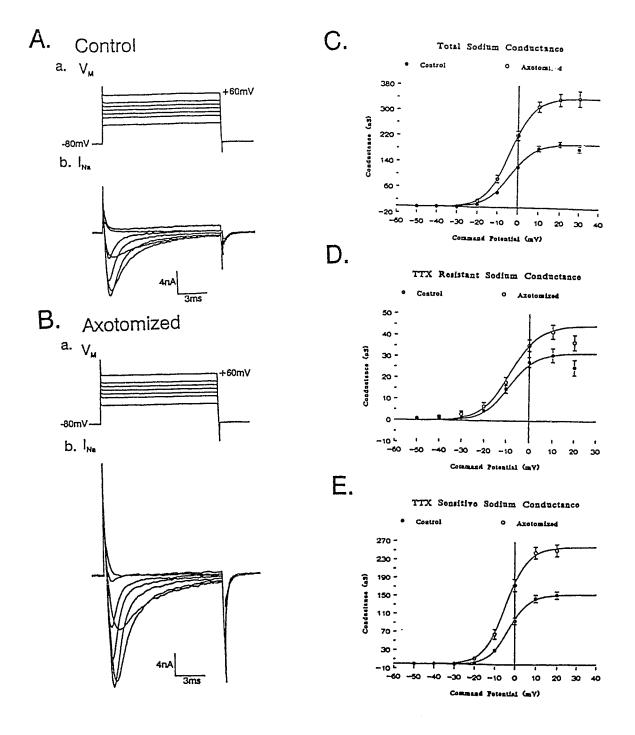
Axotomy produced a marked potentiation of total  $I_{Na}$ . This effect is illustrated in the typical data records shown in Figure 11. The data from the current-voltage relationship for total peak  $I_{Na}$  in 37 control and 37 axotomized cells were converted into conductance data. The resulting activation curves are plotted in Fig 11C. Since part of the  $G_{Na}$  of bull-frog sympathetic ganglion B-cells is TTX-resistant (Jones, 1987),  $I_{Na}$  was studied in the presence of  $I_\mu M$  TTX in 34 of the 37 control cells and 34 of the 37 axotomized cells.  $I_\mu M$  TTX blocked 75-80% of the total  $I_{Na}$  at -10 to +30 mV in both control and axotomized cells. The conductance-voltage relationship for the peak, TTX-resistant  $I_{Na}$  is shown in Fig 11D. The TTX-resistant current appears to be slightly less affected by axotomy than the total  $I_{Na}$ . For example at +10 mV, TTX-resistant  $G_{Na}$  is increased by about 35% from 31.0±3.2nS to  $42.0\pm3.2 \text{nS}$  (Fig 11D) whereas the total  $G_{Na}$  at the same voltage is increased by 71% (from  $184.9\pm8.4 \text{nS}$  to  $315.2\pm16.4 \text{nS}$ ; Fig 11C).

To illustrate more clearly the effect of exctomy on the TTX-sensitive component of  $I_{Na}$ , current-voltage plots and activation curves were replotted using data from 34 control and 34 axotomized cells following subtraction of the TTX-resistant current from the total  $I_{Na}$  in each cell. These data are presented in Fig. 11E. The averaged control and axotomized data in Figs. 11C, D and E are well described by a Boltzmann equation and there is no obvious shift in the voltage-dependence of  $G_{Na}$  following axotomy.

The development of inactivation of  $I_{Na}$  is a time and voltage-dependent

Fig. 11. Effects of axotomy on I<sub>Na</sub>. Cells were held at -80mV and step commanded to different depolarized potentials for 12ms and peak currents measured after filtering digitally at 4KHz. A and B are typical recordings from a control and an axotomized neurone respectively. Panel a shows the membrane potential  $(V_{\underline{M}})$  which cell membrane attained in response to a series of voltage-command pulse and panel  ${\bf b}$  shows family of  $I_{Na}s$  elicited in response to depolarizing commands.  $I_{Na}$  was converted to  $G_{Na}$  using the equation  $G_{Na(v)} = I_{Na(v)}/(V - E_{Na})$  where  $G_{Na(v)}$  and  $I_{Na(v)}$  are peak Na<sup>+</sup> conductance and current at the command potential, V and  $E_{Na}$  (for  $[Na^+]_0 = 97.5 \text{mM}$  and  $[Na^+]_i = 9mM$ ) = +60mV. Symbols represent the observed data points and the solid line are plots of the Boltzmann equation (described in legend to figure 2) in figures 11C, D & E. C. Conductancevoltage relationship calculated from total peat  $I_{Na}$  in control ( $\bullet$ ; n=37) and axotomized ( $\circ$ ; n=37) neurones elicited in response to commands to various depolarized potentials.  $V_0 = -3.7 \text{mV}$  and slope factor = 6mV per e-fold change in potential for both control and axotomized cells. D. Conductancevoltage relationship estimated from TTX-resistant  $I_{\hbox{Na}}$  measured in the presence of  $1\mu\hbox{M}$  TTX in control ( $\odot$ ; n=34) and axotomized (o; n=34) neurones.  $V_0 = -8.7 \text{mV}$  and -8.2 mV; and slope factor = 5.75mV and 6.3mV per e-fold change in potential for control and axotomized neurones respectively. E. Conductance-voltage relationship calculated from TTX-sensitive  $I_{Na}$  in control ( $\bullet$ ; n=34) and axotomized (o; n=34) neurones. TTX-sensitive current was obtained by subtracting TTX-resistant component from total  $I_{Na}$ .  $V_0 = -3mV$  and -4.5mV; and slope factor = 5mV and 5.5mV per e-fold change in potential for control and axotomized neurones respectively.

Figure 11.



process (Hodgkin & Huxley, 1952; Jones, 1987). The rate of onset of inactivation at different potentials was studied using protocols such as that illustrated in Fig 12. The cell was clamped to a series of relatively positive holding potentials (from -50 to  $\pm 10$ mV) for 1,4,7,10 and 20ms to allow inactivation to develop prior to the application of a 12ms test pulse to  $\pm 10$ mV. The amplitude of  $I_{Na}$  generated during this test pulse provided a measurement of the amount of inactivation which developed at various holding potentials. These data are plotted in Fig 12C as the ratio of the peak current flowing in the test pulse to the maximal current which was evoked from a holding potential of -80mV. There is no apparent difference between the data from 34 control and 34 axotomized cells. Axotomy failed to affect the voltage dependence of inactivation which was studied using a 10ms prepulse prior to a test pulse to  $\pm 10$ mV. These data are expressed as a standard  $h_{\infty}$  plot in Fig 12D. The solid line is a Boltzmann plot for fast inactivation assuming z = 2.6 and  $V_0 = \pm 10$ mV.

In order to examine the possible role of changes in  $I_{Na}$  inactivation in axotomy-induced spike broadening, the inactivation time constants ( $\tau_{inact}$ ) were measured from data such as that shown in Fig. 11. The relationship between rate of inactivation and voltage for 37 control and 37 axotomized cells is plotted in Fig 12D. The current appeared to inactivate slightly more rapidly in axotomized cells but this effect may have been secondary to increased clamp-error associated with the larger currents in axotomized neurones.

 $I_{\mbox{Na}}$  recovers from inactivation very quickly and recovery is almost complete in

Fig. 12. Effects of axotomy on voltage and time-dependence of development of inactivation of I<sub>Na</sub>. A. Upper panel (left) is the voltage protocol. The first part of the protocol is the conditioning pulse during which time cells were held at relativaly depolarized potentials for 1,4,7,10 or 20ms. The amount of inactivation developed by this conditioning pulse was then tested by applying a 12ms test pulse to +10mV. Lower panel shows raw data records of I<sub>Na</sub> evoked from a typical control cell using a series of 20ms conditioning pulses to -40,-30,-20,-10,0 and +10mV followed by a test pulse to +10mV. The first and largest current record was recorded by a test pulse to +10mV from the holding potential of -80mV. R. A family of I<sub>Na</sub>s evoked from a typical axotomized neurone by using the same series of voltage protocols as for the control cell in A. C. Comparison of voltage and time-dependence of I<sub>Na</sub> inactivation in control (n=37) and axotomized (n=37) neurones. Current elicited in each test pulse was converted to percent of the maximum current elicited from the holding potential of -80mV. D.  $h_{\infty}$  plot for  $I_{Na}$  obtained from data such as that in C for 10ms prepulses to different potentials. The solid line indicates a plot of the Boltzmann equation as indicated in the text. • represents control data and o represents data from axotomized cells in all graphs. Relationship between rate of inactivation of  $I_{Na}$  and command potential in control ( $\blacktriangle$ ; n=37) and axotomized ( $\Delta$ ;n=37) neurones (y-axis on the right side). Rate of inactivation was calculated from  $\tau_{inact}$  measured by single exponential fits to the decay of current during 12ms depolarising pulses (similar to those shown in Fig. 11Ab & Bb). Note that the rate of inactivation of I<sub>Na</sub> was slightly enhanced in axotomized neurones.

Figure 12.

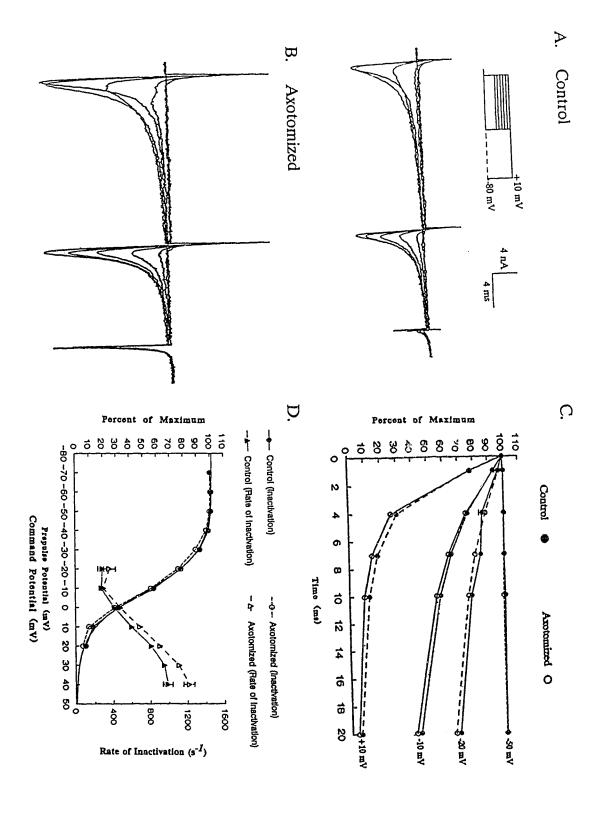
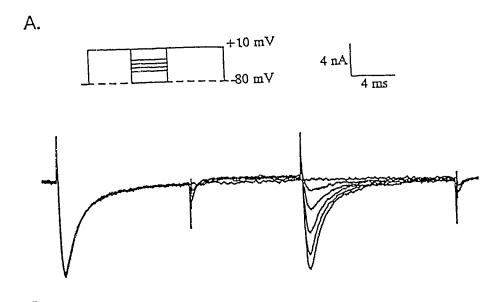
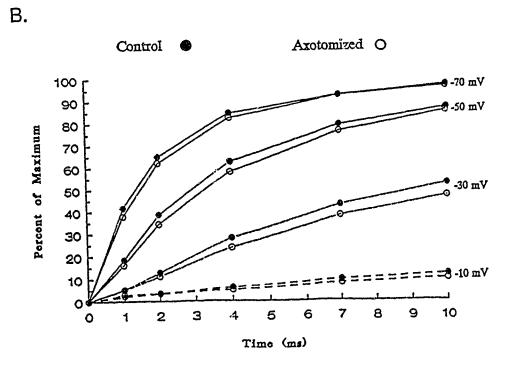


Fig. 13. Effects of axotomy on voltage and time-dependence of recovery from inactivation of INa. A. Upper panel (left) is the voltage protocol. The first part of the protocol is the conditioning pulse for inactivating  $I_{Na}$  during which the cells were stepped from the holding potential of -80mV to +10mV for 12ms. The second part of the protocol is for studying time course and voltage-dependence of the recovery from this inactivation. During this time, the cell was held at a series of different depolarized potentials for 1,2,4,7 or 10ms. The amount of recovery from inactivation remaining after this second part of the protocol was then tested by applying a test pulse to  $+10 \,\mathrm{mV}$ . Lower panel shows raw data records of  $I_{Na}$  evoked from a typical control cell. In this part of the experiment, the test pulse to +10mV assessed the amount of inactivation persisting after 10ms at various potentials. B. Comparison of voltage and time-dependence of recovery of  $I_{Na}$  inactivation in control ( ;n=37) and axotomized (0; n=37) neurones. Current elicited in each test pulse was converted to percent of the maximum current elicited at +10mV from the initial -80mV holding potential.

Figure 13.





less than 10ms. The rate of recovery from inactivation was studied using the protocol shown in Figure 13. The cell was held at -80mV and stepped to +10mV for 12ms to allow  $I_{Na}$  to activate and inactivate. The cell was then held at a variety of potentials for 1,2,4,7 and 10ms to allow for recovery from inactivation. The amount of inactivation remaining at various potentials and at various time intervals was assessed by applying a test pulse command to +10mV. The data from 37 control and 37 axotomized cells are shown in Fig 13B. Inactivation is expressed as the ratio of the current in the test pulse to the amplitude of the maximal  $I_{Na}$  in the conditioning pulse. Apart from some small difference at -30mV, the rate of recovery from inactivation was little altered by axotomy.

#### 2.5 DISCUSSION.

## 2.5.1 Mechanism of Axotomy-Induced Spike Broadening.

These experiments show that the increase in spike width seen after axotomy of bull-frog sympathetic ganglion cells involves a reduction in  $I_{Ca}$  and concomitant reduction of  $I_{C}$  rather than from a slowing in the rate of  $I_{Na}$  inactivation. This is because the rate of  $I_{Na}$  inactivation, if anything, is increased after axotomy predicting a reduction, rather than an increase in the duration of the a.p.

In a previous study from this laboratory (Kelly et al., 1986) it was found that regenerative Ca<sup>2+</sup>-spikes could be elicited both in control and in axotomized neurones. The interpretation of that study was that axotomy does not affect Ca<sup>2+</sup>

channels and that the increase in spike width and reduction in a.h.p. amplitude and duration resulted from functional loss of  $Ca^{2+}$ -activated  $K^+$  channels. However, the present study shows that  $I_{Ca}$  is significantly reduced in axotomized neurones. The difference between these results and those of Kelly *et al.* (1986) presumably reflects the inherent non-linearities associated with using regenerative  $Ca^{2+}$  spikes as indices of  $Ca^{2+}$  channel function.

# 2.5.2 Changes in $I_{Ba}$ and $Ca^{2+}$ channels

Both N- and L-type  $Ca^{2+}$  channels are present in bull-frog sympathetic neurones (Lipscombe *et al.*, 1988). Based on the sensitivity of whole cell  $I_{Ba}$  to  $\omega$ -conotoxin (100nM), Bay K 8644 (1 $\mu$ M) and nifedipine (10 $\mu$ M), Jones & Marks (1989a) and Jones & Jacobs (1990) suggested that N-type  $Ca^{2+}$  channels carry approximately 90% of the  $Ca^{2+}$  current in bullfrog sympathetic neurones. In our hands, only 75-80% of the average whole cell  $I_{Ba}$  in control cells was sensitive to  $\omega$ -conotoxin (200nM) and we observed more obvious effects of Bay K 8644 (300nM) and nifedipine (1 $\mu$ M). This difference may result from the lack of absolute specificity of  $\omega$ -conotoxin and dihydropyridines and from the different concentrations used in the two studies. Reversible inhibition of N-type  $I_{Ca}$  by  $\omega$ -conotoxin in bullfrog sympathetic ganglion cells has been previously described by Morrill *et al.*, (1992).

Although the total  $I_{Ba}$  was reduced after axotomy, there are no obvious differences in the shape of the I-V relationship. Interestingly,  $\omega$ -conotoxin reduces the total current to about the same absolute level in both control and axotomized

cells. This suggests that the effects of axotomy are restricted to changes in N-type Ca<sup>2+</sup> channels. This idea is supported by the observation that Bay K 8644 was able to induce a similar amount of L-type Ca<sup>2+</sup> current in control and axotomized neurones and this additional current was subject to a similar amount of reduction by nifedipine in both situations.

It has often been suggested that axotomy causes differentiated neurones to revert to an 'immature' state (Lieberman, 1971; Gurtu & Smith, 1988). It has been reported that during development of several neuronal types, 'low-voltage-activated' (T-type) Ca<sup>2+</sup> channels are expressed either before 'high-voltage-activated' Ca<sup>2+</sup> channels or transiently (Gottmann, Dietzel, Lux, Huck & Rohrer, 1988; Pirchio, Lightowler & Crunelli, 1990; Thompson & Wong, 1991). There was no indication of the presence of a T-type Ca<sup>2+</sup> conductance either from the shape of the I-V curve between -60 and -20mV (Fig 5B & 5D) as is seen in sensory neurones (see Fig 1D and E in Fox, Nowycky & Tsien, 1987; and Fig 4B in Gottmann et al., 1988) or from the I<sub>Ba</sub> traces shown in figure 1B.

The small changes in the rate of  $I_{Ba}$  activation and deactivation observed after axotomy must be interpreted with caution, because the currents seen after axotomy are smaller and thus less susceptible to distortion as a result of series resistance. The lack of effect of axotomy on the voltage-dependence of  $I_{Ba}$  activation (Fig. 2E) and the doubtful significance of the small changes in kinetics (Fig. 8), suggest, that at least in terms of their activation parameters, the  $Ca^{2+}$  channels present in axotomized cells are similar to those in control cells. The simplest interpretation for the decrease in

 $I_{\text{Ba}}$  is that fewer activatable channels are present in the neuronal cell body after axotomy at normal membrane potentials.

By contrast with the slight effects of axotomy on I<sub>Ba</sub> activation, inactivation is clearly enhanced in axotomized neurones. We have observed at least three components of inactivation in both control and axotomized neurones- 'fast', 'intermediate' and 'slow'. 'Fast' and 'intermediate' inactivation is almost completely absent during 500ms steps to +70mV in control cells (13.8±5.2%; Fig. 7D) whereas a significant amount of inactivation is exhibited at this voltage in axotomized cells (45.6±3.9%; Fig. 7E). Tail currents carried by Ba<sup>2+</sup> at -40mV following a 20ms step command to +70mV from a holding potential of -80mV are also reduced by approximately 41% in axotomized neurones (9.2±1.2nA in control neurones, Fig. 5C; 5.4±0.4nA in axotomized neurones, Fig. 5D). Inactivation should be minimal with this protocol in control neurones. However, a combination of enhanced resting inactivation at -80mV (see Fig. 5) and increased 'fast' and 'intermediate' inactivation at +70mV (see Table 1 & Fig. 7) in axotomized neurones may account for this difference. We therefore propose that a major portion of the decrease in amplitude of IBa can be accounted for by the enhanced inactivation after axotomy.

Although some effect on the time course of 'fast' and 'intermediate' components were observed, the primary effects was on the relative proportion of these components at a given membrane potential after axotomy. Thus axotomy may cause more of the Ca<sup>2+</sup> channels to switch from a 'non-inactivating' to an 'inactivating mode' after axotomy (Plummer & Hess, 1991). Although the factors that

phosphorylation has recently been shown to increase the proportion of inactivating Ca<sup>2+</sup> channels in BFSG neurones (Wertz, Elmslie & Jones, *in press*). It is therefore possible that the changes in inactivation seed after axotomy result from alterations in Ca<sup>2+</sup> channel phosphorylation.

Another possibility is that another produces a change in subsect structure or stoichiometry of different subunits in the channel macromolecule as a result of changes at the transcriptional or post-transcriptional level. Precedence for this idea comes from the observation that heterologous expression of different subunits of L-type  $Ca^{2+}$  channels from skeletal muscle in LCa.11 cells induces  $Ca^{2+}$  channels which exhibit  $I_{Ca}$  with different kinetic properties. Expression of  $\alpha$ -subunit alone results in the induction of  $I_{Ca}$  with slow activation and inactivation kinetics whereas co-expression of  $\alpha$  and  $\beta$  subunits induces channels which have faster kinetics (Varadi, Lory, Schultz, Varadi & Schwartz, 1991). This suggests that different functions of the channel are vested in different subunits. A third possibility is that increased  $I_{Ba}$  inactivation results from axotomy-induced cytoskeletal disruption (Fukuda, Kameyama & Yamaguchi, 1981; Johnson & Byerly, 1993).

# 2.5.3 Changes in I<sub>Na</sub>

The increase in amplitude of I<sub>Na</sub> may be responsible for the small, yet significant increase in spike height seen in axotomized BFSG neurones (Gordon *et al.*, 1987). Indeed, this effect may be a general characteristic of axotomized cells

because the rate of rise of the a.p. is known to increase in a wide variety of vertebrate and invertebrate neuronal types after axotomy (Gallego *et al.*, 1987; Titmus & Faber, 1990). As with the  $Ca^{2+}$  channels, the molecular mechanism underlying the increased  $G_{Na}$  could result from changes in channel subunit expression, post translational modification or changes in channel distribution.

## 2.5.4 Effects of axotomy on ion channels.

During development, several types of nerve cells express TTX-resistant Na<sup>+</sup> channels. Also, some types of immature cells exhibit Ca<sup>2+</sup>-dependent rather than Na<sup>+</sup>-dependent a.p.s (Spitzer, 1979; Nerbonne & Gurney, 1989 but see also Barish, 1986) whilst others may transiently express T-type Ca<sup>2+</sup> currents (Gottmann et al., 1988; Pirchio et al., 1990; Thompson & Wong, 1991). One working hypothesis which seeks to explain the 'cell body reaction' is that it reflects de-differentiation of neurones towards an immature state which is more amenable to growth processes (Lieberman, 1971; Titmus & Faber, 1990). This 'de-differentiation' concept does not fit with the observed effects of axotomy on ion channels in BFSG. This is because axotomy did not potentiate TTX-resistant I<sub>Na</sub> any more than TTX-sensitive I<sub>Na</sub>. Furthermore, I<sub>Ba</sub> was decreased rather than increased and no T-type Ca<sup>2+</sup> current was seen after axotomy.

Increases in the rate of rise and amplitude of the a.p. is a fairly consistant observation following axotomy of a variety of neuronal types (Gallego et al., 1987) whereas changes in a.h.p. amplitude and duration and spike width are more variable

(Titmus & Faber, 1990). It is possible, however, that N-type Ca<sup>2+</sup> channels are always affected and tend to assume an 'inactivating' mode after axotomy. The differential effects of axotomy on the a.p. in various neuronal types would then reflect the expression and level of inactivation of N-type Ca<sup>2+</sup> channels in each type of neurone. It will obviously be necessary to examine a wide variety of neuronal types before one can advance a general hypothesis relating changes in ion channels to the axotomy-induced cell body reaction.

#### 2.6 APPENDIX

The kinetics of the slow component of  $I_{Ba}$  inactivation were deduced from the use-dependent build-up of 'slow' inactivation during a train of commands to 0mV from a holding potential of -80mV where few channels are open and few channels are in the 'slow' inactivated state at equilibrium. At a potential (0mV) where all of the channels can open and 'slow' inactivation can be complete, the proportion  $(O_n)$  of  $Ca^{2+}$  channels activated by the nth pulse in a train will be equal to the proportion  $(R_{n-1})$  of channels that are in non-inactivated, resting state at -80mV just before that pulse (i.e.  $R_{n-1} = O_n$ ). If  $k_+$  is the rate constant of inactivation at 0mV, during the command inactivation will proceed at a rate initially equal to  $O_n * k_+$  and decrease to  $O_{n+1} * k_+$  at the end of the pulse. This assumes that all states of the channel enter the slow inactivation state at the same rate. Provided the fraction of the peak current that undergoes 'slow' inactivation during the pulse is not large (e.g.  $O_{n+1} * O_n$ ), the amount of inactivation that develops during a pulse of duration,  $t_1$ , will be  $O_n * k_+ * t_1$  which can also be written as  $R_{n-1} * k_+ * t_1$ . Similarly, if  $k_-$  is the rate constant for recovery from inactivation at -80mV and the interval between pulses,  $t_2$ , is such that there is little recovery before the next pulse is initiated, the proportion of inactivated channels that does recover will equal  $(1 - R_n)$ 

$$\therefore R_{n-1} - R_n = R_{n-1} * k_+ * t_1 - (1 - R_n) * k_- * t_2$$
 (1)

Eventually, the total decrement will approach a limiting value  $(1 - R_{\infty})$  where  $R_{n-1} - R_n = 0$ . Thus, from equation 1

$$R_{\infty} * k_{+} * t_{1} = (1 - R_{\infty}) * k_{-} * t_{2}$$
and
$$R_{\infty} = \frac{k_{-} * t_{2}}{k_{+} * t_{1} + k_{-} * t_{2}}$$
(2b)

The decrement per pulse appears to decline exponentially. This means that

$$\ln \left( \frac{R_n - R_{\infty}}{R_{n-1} - R_{\infty}} \right) = -\lambda$$

where  $\lambda$  is a constant. For small values of  $\lambda$ 

$$\ln (1 - \lambda) = -\lambda$$

Therefore 
$$\frac{R_n - R_{\infty}}{R_{n-1} - R_{\infty}} = 1 - \lambda$$

and  $\lambda = \frac{R_{n-1} - R_n}{R_{n-1} - R_{\varpi}}$ 

Substituting Eqn. 1 and 2b one obtains

$$\lambda = \frac{R_{n-1} * k_{+} * t_{1} - (1 - R_{n}) * k_{-} * t_{2}}{R_{n-1} - [k_{-} * t_{2} / (k_{-} * t_{2} + k_{+} * t_{1})]}$$

$$= (k_{-} * t_{2} + k_{+} * t_{1}) \begin{bmatrix} R_{n-1} * k_{+} * t_{1} - (1 - R_{n}) * k_{-} * t_{2} \\ R_{n-1} * k_{+} * t_{1} - (1 - R_{n-1}) * k_{-} * t_{2} \end{bmatrix}$$

Again, if  $\lambda$  is small then

$$R_{n-1} = R_n$$
 and,

$$\lambda = k_1 * t_2 + k_+ * t_1$$
 (3)

## 2.7 REFERENCES

ADAMS, P.R. BROWN, D.A. & CONSTANTI, A. (1982). M-currents and other potassium currents in bullfrog sympathetic neurones. *Journal of Physiology* **330**, 537-572.

BARISH, M.E. (1986). Differentiation of voltage-gated potassium current and modulation of excitability in cultured amphibian spinal neurones. *Journal of Physiology* **375**, 229-250.

BELMONTE, C., GALLEGO, R. & MORALES, A. (1988). Membrane properties of primary sensory neurones of the cat after peripheral reinnervation. *Journal of Physiology* **405**, 219-232.

BOGERT, C. & KROON, A.M. (1981). Tissue distribution and effects on mitochondrial protein synthesis of tetracyclines after prolonged continuous intravenous administration to rats. *Biochemical Pharmacology* **30(12)**, 1706-1709.

CARLSEN, R.C., KIFF, J. & RYUGO, K. (1982). Suppression of the cell body response in axotomized frog spinal neurones does not prevent initiation of nerve regeneration.

Brain Research 234, 11-25.

CZEH, G., KUDO, N. & KUNO, M. (1978). Membrane properties and conduction velocity in sensory neurones following central and peripheral axotomy. *Journal of Physiology* **270**, 165-180.

DODD, J. & HORN, J.P. (1983). A reclassification of B- and C-cells in the ninth and tenth paravertebral sympathetic ganglion of the bullfrog. *Journal of Physiology* **334** 255-269.

FINKEL, A.S. & REDMAN, S.J. (1984). Theory and operation of a single microelectrode voltage clamp. *Journal of Neuroscience Methods* 11 101-127.

FOX, A.P., NOWYCKY, M.C. & TSIEN, R.W. (1987). Kinetic and pharmacological properties distinguishing three types of calcium currents in chick sensory neurones. *Journal of Physiology* **394**, 149-172.

FUKUDA, J., KAMEYAMA, M. & YAMAGUCHI, K. (1981). Breakdown of cytoskeletal filaments selectively reduces Na and Ca spikes in cultures mammal neurones. *Nature* **294**, 82-85.

GALLEGO, R., IVORRA, I. & MORALES, A. (1987). Effects of central or peripheral axotomy on membrane properties of sensory neurones in the petrosal ganglion of the cat. *Journal of Physiology* **391**, 39-56.

GOH, J.W., KELLY, M.E.M. & PENNEFATHER, P.S. (1989). Electrophysiological function of the delayed rectifier  $(I_K)$  in bullfrog sympathetic ganglion neurones. *Pflugers Archiv* 413, 482-486.

GORDON, T., KELLY, M.E.M., SANDERS, E.J., SHAPIRO, J. & SMITH P.A. (1987). The effect of axotomy on bullfrog sympathetic neurones. *Journal of Physiology* **392**, 213-229.

GOTTMANN, K., DIETZEL, I.D., LUX, H.D., HUCK, S. & ROHRER, H. (1988). Development of inward currents in chick sensory and autonomic neuronal precursor cells in culture. *Journal of Neuroscience* **8**, 3722-3732.

GRAFSTEIN, B. & MCQUARRIE, E.I. (1978). Role of nerve cell body in axonal regeneration. In *Neuronal Plasticity*, pp 155-195. Ed. C.W. Cotman. Raven Press: New York.

GURTU, S. & SMITH, P.A. (1988). Electrophysiological characteristics of hamster DRG cells and their response to axotomy. *Journal of Neurophysiology* **59**, 408-423.

GUSTAFSSON, B. & PINTER, M.J. (1984). Effects of axotomy on distribution of passive electrical properties of cat motoneurones. *Journal of Physiology* 356, 433-442.

HODGKIN, A.L. & HUXLEY, A.F. (1952). A Quantitative description of membrane current and its application to conduction and excitation in nerve. *Journal of Physiology* 117, 500-544.

JASSAR, B.S. & SMITH, P.A. (1991a). Role of target organ in the maintenance of calcium currents in bullfrog sympathetic neurones. *Society for Neoroscience Abstracts* 17, 67.

JASSAR, B.S. & SMITH, P.A. (1991b). Slow frequency-dependence of action potential afterhyperpolarization in bullfrog sympathetic ganglion neurones. *Pflugers Archiv* 419, 478-485.

JASSAR, B.S. & SMITH, P.A. (1992). Mechanism of axotomy-induced spike broadening in bullfrog sympathetic neurones. *Society for Neoroscience Abstracts* 18, 42.

JOHNSON, B.D. & BYERLY, L. (1993). A cytoskeletal mechanism for calcium channel rundown and block by intracellular calcium. *Biophysical Journal* 64 A116.

JONES, S.W. (1987). Sodium currents in dissociated bull-frog sympathetic neurones. Journal of Physiology 389, 605-627. JONES, S.W. & JACOBS, L.S. (1990). Dihydropyridine actions on calcium currents of frog sympathetic neurones. *Journal of Neuroscience* **10**, 2261-2267.

JONES, S.W. & MARKS, T.N. (1989a). Calcium currents in bullfrog sympathetic neurones; I Activation, kinetics and pharmacology. *Journal of General Physiology* **94**, 151-167.

JONES, S.W. & MARKS, T.N. (1989b). Calcium currents in bullfrog sympathetic neurones; II Inactivation. *Journal of General Physiology* **94**, 169-182.

KELLY, M.E.M., GORDON, T., SHAPIRO, J. & SMITH P.A. (1986). Axotomy affects calcium-sensitive potassium conductance in sympathetic neurones. *Neuroscience Letters* 67, 163-168.

LAIWAND, R., WERMAN, R. & YAROM, Y. (1988). Electrophysiology of degenerating vagal motor nucleus of the guinea-pig following axotomy. *Journal of Physiology* **404**, 749-766.

LANCASTER, B & PENNEFATHER, P. (1987). Potassium currents evoked by brief depolarizations in bull-frog sympathetic ganglion cells. *Journal of Physiology* **387**, 519-548.

LIEBERMAN, A.R. (1971). The axon reaction: A review of the principal features of perikaryal responses to axon injury. *International Review of Neurobiology* **14**, 49-124.

LIPSCOMBE, D., MADISON, D.V., POENIE, M., REUTER, H., TSIEN, R.Y. & TSIEN, R.W. (1988). Spatial distribution of calcium channels and cytosolic calcium transients in growth cones and cell bodies of sympathetic neurones. *Proceedings of the National Academy of Sciences of the U.S.A.* 85, 2398-2402

MORRILL, J., BOLAND, L.M. & BEAN, B.P. (1991). ω-Conotoxin block of calcium channels in peripheral neurons: Reversibility and the influence of divalent cation concentration. Society for Neuroscience Abstracts 17, 1160.

NERBONNE, J.N. & GURNEY, A.M. (1989). Development of excitable membrane properties in mammalian sympathetic neurons. *Journal of Neuroscience* 9, 3272-3280.

PIRCHIO, M.; LIGHTOWLER. S. & CRUNELLI, V. (1990). Postnatal development of the T calcium current in cat thalamocortical cells. *Neuroscience* 38(1) 39-45.

PLUMMER, M.R. & HESS,P. (1991). Reversible uncoupling of inactivation in N-type calcium channels. *Nature* 351, 657-659.

SALA, F. (1991). Activation kinetics of calcium currents in bull-frog sympathetic

neurones. Journal of Physiology 437, 221-238.

SPITZER, N.C. (1979). Ion channels in development. *Annual Review of Neuroscience* **2**, 263-297.

THOMPSON, S.M. & WONG, R.K.S. (1991). Development of calcium current subtypes in isolated rat hippocampal pyramidal cells. *Journal of Physiology* **439**, 671-689.

TITMUS, M.J. AND FABER, D.S. (1990). Axotomy-induced alterations in the electrophysiological characteristics of neurones. *Progress in Neurobiology* 35, 1-51.

VARADI, G., LORY, P., SCHULTZ, D., VARADI, M. & SCHWARTZ, A. (1991). Acceleration of activation and inactivation by the β subunit of the skeletal muscle calcium channel. *Nature* 352, 159-162.

WERTZ, M.A.; ELMSLIE, K.S. & JONES, S.W. (1993). Phosphorylation enhances inactivation of N-type calcium channel current in bullfrog sympathetic ganglion neurones. *Pflugers Archiv* (in press).

# CHAPTER 3.

# CHANGES IN POTASSIUM CHANNEL ACTIVITY FOLLOWING AXOTOMY OF B-CELLS IN BULL-FROG SYMPATHETIC GANGLION.

Note: This chapter is a version of a paper by <u>B.S. Jassar; P.S. Pennefather & P.A.</u>

<u>Smith</u> which has been submitted to *Journal of Physiology (London)*.

### 3.1 SUMMARY

- 1. Voltage-dependent and Ca<sup>2+</sup>-activated K<sup>+</sup> currents were recorded from bull-frog paravertebral sympathetic ganglion B-cells using whole-cell patch-clamp and single-electrode voltage-clamp recording techniques. Currents recorded from control cells were compared with those from axotomized cells 13-15d after transection of the post-ganglionic nerve.
- 2. M-conductance ( $G_M$ ; muscarine-sensitive, voltage and time-dependent K<sup>+</sup> conductance) at -30mV was increased from 8.5±0.9nS in control neurones (n=28) to 11.5±0.9nS in axotomized neurones (n=32, P<0.05) with slowing of the deactivation kinetics whereas leak conductance ( $G_{leak}$ ; between -70 and -100mV) was unchanged (around 2nS for both control and axotomized neurones). The fast, transient outward K<sup>+</sup> current ( $I_A$ ) and the slow, transient outward K<sup>+</sup> current ( $I_{SA}$ ) were present in only 5 of 48 axotomized neurones as compared with 20 of 28 control neurones.
- 3. The delayed-rectifier  $K^+$  current  $(I_K)$  was reduced in axotomized neurones (P<0.001) without any apparent effect on time course of activation and deactivation. Maximal conductance  $(G_K)$  elicited by 50ms command pulses (at +50mV) was  $220\pm19$ nS for control neurones (n=16) and  $136\pm10$ nS after axotomy (n=52).
- 4. Steady-state intracellular  $Ca^{2+}$  levels (measured by Fura-2 microspectrofluorometry) were similar in control (57.5±5.5nM; n=53) and axotomized neurones (57.4±5.2nM; n=58; P<0.001).
  - 5. The fast, voltage-sensitive, Ca<sup>2+</sup>-activated K<sup>+</sup> current, I<sub>C</sub>, evoked with 50ms

command pulses from a holding potential of -40mV was significantly decreased in axotomized neurones (peak  $I_C$  at +30mV was 69.7±6.1nA for 27 control neurones and  $48.1\pm2.9$ nA for 52 axotomized neurones; P<0.005) with little change in its rate of activation.

- 6. After axotomy the peak amplitude of  $I_C$  evoked with 3ms command pulses to different potentials from a holding potential of -80mV were comparable to control values. Significant differences were observed only at a few potentials. Even less difference was observed between  $I_C$  tail currents following these brief commands in control and axotomized neurones. The similarity in magnitude and time course of  $I_C$  between control and axotomized neurones suggest that the properties of  $I_C$  channels are not changed after axotomy. Tail  $I_C$  following a command to +20mV and recorded at -40mV had peak amplitudes of 9.1±1.4nA in control (n=15) and 7.6±0.7nA (n=50) in axotomized neurones, despite a 50% reduction of  $I_{Ca}$  after axotomy. The discrepancy between reduction of  $I_{Ca}$  and decrease in  $I_C$  suggests that  $I_C$  is activated near maximally during the tail current and that the maximal  $G_C$  at 0mV is about 550nS.
- 7. The voltage-insensitive  $Ca^{2+}$ -dependent  $K^+$  current  $(I_{AHP})$  could not be recorded in dissociated neurones but could be recorded in intact ganglion cells using 'sharp' microelectrodes. In axotomized neurones, voltage-clamp commands (to +10mV) had to be extended by 16ms to evoke  $I_{AHP}$  responses that were similar in magnitude to those observed in control cells. For  $I_{AHP}$  responses of similar magnitudes the time constant of decay was not significantly different between the

control (143.9 $\pm$ 5.9ms; n=32) and axotomized neurones (126.0 $\pm$ 10.2ms; n=34; P>0.1). This suggests that neither the number of  $I_{AHP}$  channels nor the Ca<sup>2+</sup> buffering capacity of cytoplasm is changed in axotomized neurones.

8. The reduction is  $I_C$  and  $I_{AHP}$  as well as the increase in the duration of the action potential and the decrease in the amplitude and duration of the afterhyperpolarization which is seen after axotomy can be accounted for by the previously-documented decrease in  $I_{Ca}$  due to increased inactivation.

#### 3.2 INTRODUCTION

Transection or damage to an axon results in a variety of changes in the biochemical, morphological and electrophysiological properties of the neuronal cell body (Gordon, 1983). These may be a part of the regenerative pro esses essential to, and specifically geared for axonal outgrowth (Graftein, 1983). The observed changes in neuronal electrophysiological properties provoked by axo y are widely variable and have diverse time courses and sequelae (Titmus & Faber, 1990). For example, there is an increase in the duration of the afterhyperpolarization (ahp) that F-type medial gastrocnemius (MG) follows the action potential (a.p.) in motoneurones (Foehring, Sypert & Munson, 1986; but see also Kuno, Miyata & Munoz-Martinez, 1974) and in lumbar motoneurones (Pinter & Vanden-Noven, 1989). By contrast, ahp duration decreases in S-type MG motoneurones (Foehring et al., 1986), cat cranial glossopharyngeal neurones (Gallego, Ivorra & Morales, 1987), guinea pig vagal motoneurones (Lawaind, Werman & Yarom, 1988) and bull-frog sympathetic ganglion (BFSG) B-cells (Gordon, Kelly, Sanders, Shapiro, & Smith, 1987). Axotomy produces no change in the ahp of hamster spinal dorsal root ganglion neurones (Gurtu & Smith, 1988).

Since the contribution and relative abundance of the conductances responsible for various electrophysiological properties of the neurones differ in different neuronal types, the apparent diversity in electrophysiological response to axotomy may be secondary to these differences. Alternatively, the variety in response in various neuronal types may result from different effects of axotomy on the properties of

similar currents. A comprehensive and systematic study of the effect of axotomy on ion channel properties in any single neuronal type is thus a first step towards identifying a unified hypothesis for the basic mechanism/s of axotomy-induced changes.

Axotomy of B-neurones in BFSG results in a well-defined set of changes in membrane properties. These include an increase in the height and duration of the a.p. and a decrease in the amplitude and duration of the ahp (Gordon et al., 1987). There is also an increase in the rheobase current (Gordon et al., 1987) whereas the conduction velocity remains unchanged (Shapiro, Gurtu, Gordon & Smith, 1987). The ionic conductances underlying the membrane properties of BFSG B-cells are well understood (Adams, Brown & Constanti, 1982; Goh & Pennefather, 1987; Jones, 1987; Lancaster & Pennefather, 1987; Goh, Kelly & Pennefather, 1989; Jones & Marks, 1990a & b) and we have established that axotomy increases peak sodium currents (I<sub>Na</sub>); and increases the inactivation while decreasing the overall amplitude of Ca2+ currents (I<sub>Ca</sub>; Jassar, Pennefather & Smith, in press). In the present study we report on the effects of axotomy on various K+ currents in BFSG cells. Together with our previous results (Jassar et al., in press) this provides a comprehensive description of the axotomy-induced changes in ion channel properties. These studies aim at understanding the molecular mechanisms that underlie the changes in membrane properties associated with axotomy.

#### 3.3 METHODS

The methods used for axotomy, cell dissociation and electrophysiological recordings have been described in detail elsewhere (Selyanko, Smith & Zidichouski, 1990a; Jassar et al., in press). Briefly, small to medium sized bullfrogs were axotomized under general anaesthesia with MS-222 (3-aminobenzoic acid ethyl ester methanesulfonate salt; 0.5ml of 25mg/ml solution injected into the dorsal lymph sac) and 5-10mm pieces were excised from VIII, IX & Xth spinal nerves of the right side (sometimes VII & XIth also). Animals were kept in 0.16g.l<sup>-1</sup> tetracycline solution in ordinary tap water (changed on alternate days) for 13-15 days prior to use.

#### 3.3.1 Electrophysiological Recording

On the day of experiment (electrophysiological recording), the VIII, IX & Xth paravertebral sympathetic ganglia were removed from the axotomized side or from 'unoperated' side of two axotomized animals or from both sides of a control unoperated frog. Ganglia were dissociated for electrical recordings using the method described by Selyanko *et al.*, 1990a). The acutely dissociated cells were suspended in '6K-external solution' and visualized under a Nikon 'Diaphot' inverted microscope in a plastic Petri dish for recordings. '6K external solution' contained: (in mM) NaCl 113; KCl 6; MgCl<sub>2</sub> 2; CaCl<sub>2</sub> 2; HEPES (acid) 5 and glucose 10 (pH adjusted to 7.2 with NaOH). Intermediate-sized cells (40-80 $\mu$ m diameter) were selected for electrical recordings which were made with patch electrodes. Recordings were initiated in bridge-balance current-clamp mode and membrane time constants ( $\tau_m$ ) determined

from exponential fits to the time course of voltage changes (to between -65 to -130 mV) elicited by hyperpolarizing current injections. Input resistance ( $R_{in}$ ) was calculated from the linear portion of the voltage-current relationship obtained from current-clamp data. Membrane capacitance (C<sub>m</sub>) which is a measure of the membrane surface area, was calculated from  $R_{\rm in}$  and  $\tau_{\rm m}$  for every neurone using the equation  $C_m = \tau_m/R_{in}$ . For recording currents, the amplifier (Axoclamp-2A; Axon Instruments, Burlingame, California, U.S.A.) was switched to discontinuous singleelectrode voltage-clamp mode. To study potassium currents, the cells were bathed in an external solution containing (in mM): KCl 2; CaCl<sub>2</sub> 4; NMG-Cl 40; Tris-Cl 2.5; sucrose 134; D-glucose 10 and internal solution contained (in mM): KCl 110; NaCl 10; MgCl<sub>2</sub> 2; CaCl<sub>2</sub> 0.4; EGTA 4. ; All PLS 5; D-glucose 10; leupeptin 0.1; cyclic-AMP 0.125 (pH 7.2). External solutions were 250mOsm.kg<sup>-1</sup> and internal solutions were 240mOsm.kg<sup>-1</sup>. The petri dishes were superfused with external solution at a flow rate of 2ml.min<sup>-1</sup> which allowed exchange of solutions within about 2 minutes. Patch electrodes coated with 'Sigmacote' were used to record I<sub>C</sub> (Ca<sup>2+</sup>-activated, voltage-dependent K+ currents), IK (delayed rectifier K+ current), IM (a voltage- and time-dependent muscarine-sensitive  $K^+$  current),  $I_A$  (transient outward  $K^+$  current) and the slow transient outward K+ current, I<sub>SA</sub> (Adams et al., 1982; Selyanko, Zidichouski & Smith, 1990b). Usually a clamp gain of >16nA.mV<sup>-1</sup> and a cycling frequency of >35KHz could be achieved and this reduced the peak clamp voltage error to 6.7mV and steady-state clamp voltage error to <1mV for recording a 30nA current from a 70pF cell (Jones, 1987; Jassar et al., in press).

 $I_{AHP}$  (Ca<sup>2+</sup>-activated, voltage-insensitive K<sup>+</sup> current) was studied in intact ganglia which were treated with 10mg.ml<sup>-1</sup> collagenase for 15 minutes to facilitate penetration by microelectrodes. External solution for  $I_{AHP}$  contained NaCl 115; KCl 2; CaCl<sub>2</sub> 4; Tris-Cl 2.5 and D-glucose 10 (pH 7.2; 250mOsm.kg<sup>-1</sup>). Glass 'sharp' microelectrodes, coated with sylgard and filled with 3M KCl (resistance between 30-50m $\Omega$ ), were used for electrical recording. Only those cells which had resting membrane potential of at least -50mV, spike height >75mV and which gave stable recording for >15minutes, were used to record  $I_{AHP}$ . The clamp gain that could be achieved with these relatively higher resistance electrodes was usually >6nA.mV<sup>-1</sup> and cycling frequency was always greater than 12KHz. The bandwidth of the filter was set to 100Hz during data acquisition.

Data were digitized using a Labmaster DMA interface and stored on an IBM compatible computer (Northgate 386) fitted with a removable hard disk system (Bernoulli drive, Iomega Corya, Roy, UT, U.S.A.). During data acquisition, the bandwidth of the filter was set to 10 or 30KHz for I<sub>C</sub> and I<sub>K</sub> and to 300Hz for I<sub>M</sub> and I<sub>A</sub>. Permanent records were made using an XY plotter. Data were acquired and analyzed using 'Pclamp' software (Axon Instruments, Burlingame, CA, U.S.A.). Data are presented as mean±s.e.m.. In graphs where no error bars are visible, the error bars are smaller than the symbols used to designate the data points. Significance of differences between the control and the axotomized data was determined using Student's two-tailed, unpaired *t*-test.

#### 3,3.2 Intracellular Calcium Measurements

Acutely-dissociated neurones (Goh *et al.*, 1989) were loaded with the Ca<sup>2+</sup>-indicator dye, Fura-2 through incubation with  $10\mu$ M Fura-2AM in frog Ringer for 50-60 minutes at room temperature (20°C). After loading, the cells were observed under an epifluorescence microscope. Continuous perfusion was maintained. Intracellular calcium levels were measured by using a PTI microspectrofluorometer (Deltascan 4000 series model; Photon Technology Instruments Inc., South Brunswick, NJ, U.S.A.). The ratio (R) of fluorescence intensity at 350nm (F<sub>350</sub>) and 380nm (F<sub>380</sub>) was measured to calculate the free Ca<sup>2+</sup> levels ([Ca<sup>2+</sup>]<sub>i</sub>). [Ca<sup>2+</sup>]<sub>i</sub> was then calculated using the formula

$$[Ca^{2+}]_i = K_d.C(R-R_{min})/(R_{max}-R)$$

where  $K_d$  is the effective dissociation constant for the  $Ca^{2+}$ -Fura-2 complex (224nM) and C is the ratio of  $F_{380}$  for  $R_{max}$  and  $R_{min}$  conditions.  $R_{min}$  was the minimum ratio measured by changing the perfusing Ringer solution to one which had 0mM  $CaCl_2$  and 2.5mM EGTA and  $10\mu$ M 4,Bromo-A23187.  $R_{max}$  was the maximum ratio obtained by perfusing the cells with normal Ringer to which  $10\mu$ M 4,Bromo-A23187 was added. The values used in our calculations were 0.7 for  $R_{min}$ ; 7.5 for  $R_{max}$ ; and 1200nM for  $C.K_d$ .

All drugs and chemicals were purchased from Sigma Chemical Company (St. Louis, MO, USA) except for 4,Br-A23187 and Fura-2AM which were from Molecular Probes (Eugene, OR, USA).

### 3.3.3 Modelling

Currents were modelled using 'Axon Engineer<sup>TM</sup>' software (Aeon Software, Eugene, OR, USA). Values of transition variables (activation, deactivation or inactivation) were adjusted to simulate the currents evoked in isolation by voltage-clamp commands under various conditions. These simulated currents were then coupled with a model of intracellular Ca<sup>2+</sup> diffusion and buffering based on one dimensional movement of Ca<sup>2+</sup> between concentric intracellular compartments (see legend to Fig. 9).

#### 3.4.1 RESULTS

Data on the effects of axotomy were obtained 13-15 days after section of the postganglionic nerves as the axotomy-induced changes in the a.p. characteristics of BFSG neurones seem to be maximal at this time (Gordon et al., 1987).

Before voltage-clamping, the resting membrane potential (RMP) of every cell was recorded just after establishing whole-cell recording. RMP was not affected by axotomy (-52.0 $\pm$ 1.3mV for 28 control neurones and -49.1 $\pm$ 0.9mV for 52 axotomized neurones; P>0.05).  $R_{in}$ , measured from the linear portion of the current-clamp V-I relationship (at potentials negative to -65mV) was 412.0 $\pm$ 27.2M $\Omega$  in control neurones (n=28) and 432.1 $\pm$ 27.8M $\Omega$  in axotomized neurones. Thus axotomy does not affect the input resistance of the neurones (P>0.5). Since the cells from which recordings were made had no differences in their  $C_m$  (68.6 $\pm$ 3.8pF for 28 control cells and 70.5 $\pm$ 2.8pF for 48 axotomized neurones; P>0.6), visual size matching was effective

in selecting cells of similar size. This allows direct comparison of currents recorded from control and axotomized neurones in the present study without normalization for surface area. Given a specific membrane capacitance of  $1\mu\text{F.cm}^{-2}$ , the mean diameter of the cells was around  $48\mu\text{m}$ .

# 3.4.2 Effects of axotomy on $I_M$ and $I_{leak}$

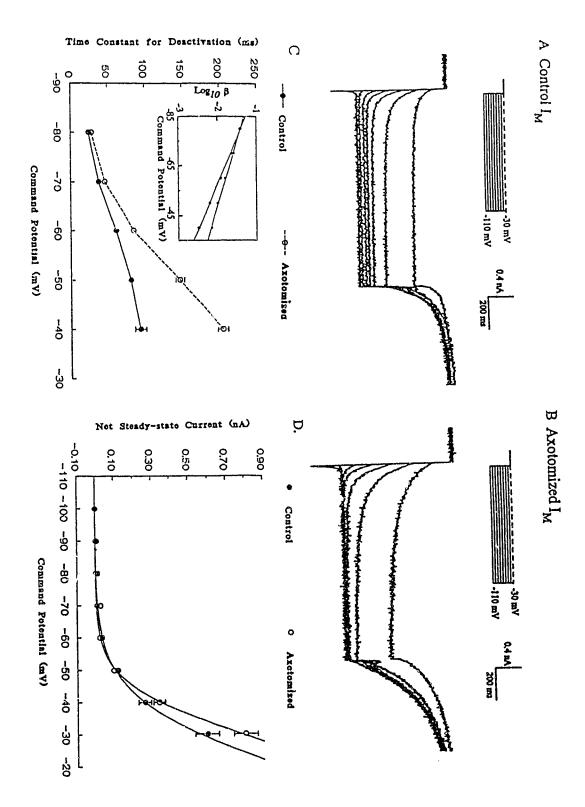
Hyperpolarizing command pulses from a holding potential of -30mV promote deactivation of  $I_M$ . The current then reactivates upon repolarization to -30mV (Adams et al., 1982). Figure 1A & 1B show representative current responses evoked from a control and an axotomized neurone, respectively. The most obvious difference between the recordings is that the time course of deactivation of  $I_M$  is slower to axotomized neurones. Time constants ( $\tau_M$ ) at different potentials were determined by single exponential fits to the current relaxations.

Recently Marrion, Adams & Gruner (1992) fitted  $I_M$  with more than one kinetic component. In our procedure the first 4ms following the voltage command were ignored and fits obtained over the time course of 1s. This yielded r values >0.9. Cursory examination of 'r' values obtained with bi-exponential fits suggested that a single exponential fit was adequate to describe data acquired under the conditions of our experiments.

The relationship between voltage and  $\tau_{\rm M}$  measured from 28 control and 32 axotomized neurones is shown in figure 1C. The data show an obvious increase in the  $\tau_{\rm M}$  in axotomized neurones ( $\tau_{\rm M}$  at -50mV was 80.9±4.8ms control neurones and

Figure 1. Effects of axotomy on I<sub>M</sub>. A. A family of I<sub>M</sub> responses elicited in a control neurone in response to 1s hyperpolarizing commands from a holding potential of -30 mV. The upper panel shows the voltage command protocol. B. A family of  $I_{\text{M}}$ responses clicited in an axotomized neurones in response to a similar voltage command protocol as that for the control neurone in A. Note the slower deactivation of I<sub>M</sub> during the command pulse and slower activation on repolarization in the axotomized neurone as compared with the control neurone. C. Voltage-dependence of deactivation time constants of  $I_M$  in control ( $\odot$ ) and axotomized ( $\odot$ ) neurones. The inset shows the voltage dependence of rate of deactivation of I<sub>M</sub> which was derived using the equation  $\beta = 1/(1 + \exp(-0.1^*(V-35)))/\tau_m$  (see text for details). **D.** The net steady-state I-V relationship for 28 control ( ) and 32 axotomized ( ) neurones. The net steady-state current at different potentials was calculated by subtracting the extrapolated linear leak between -70 and -100mV from the total steady-state current. Note that though the net steady-state I<sub>M</sub> at -30mV is increased, there is no difference in  $I_{M}$  at potentials <-50mV. The solid line through the data is defined by the equation  $I_M = \{15nS*V_K*BV*(exp[B(V-V_K)] - 1)/(exp[BV] - 1)\}*\{1/(1+exp[-2.6B(-1)])\}*(1/(1+exp[-2.6B(-1)])$ 35mV-V)])} for the data from control cells and  $I_M = \{15nS*V_K*BV*(exp[B(V-V_K)]-V)\}$ 1)/ $(\exp[BV]-1)$ }\* $\{1/(1+\exp[-3.4B(-40mV-V)])\}$  for the data from axotomized cells, where V = command potential and  $V_K = the K^+$  reversal potential (-100 mV) and B = RT/F = 1/25.7mV. These relations combine expressions describing GHK rectification and Boltzmann activation.

Figure 1.



140.6 $\pm$ 6.9ms for axotomized neurones; P<0.001). The time constants were converted into true rates of deactivation by multiplying the apparent rates of deactivation ( $1/\tau_{\rm M}$ ) by the estimated fraction of channels that will be in the closed state at that potential (Pennefather, Oliva & Mulrine, 1992). The latter number was estimated using parameters for the voltage-dependence of steady-state  $I_{\rm M}$  measured by Adams *et al.* (1982; e-fold change per 10mV). The half maximal activation was assumed to be - 35mV in control and -40mV after axotomy. This analysis indicated that axotomy increases the voltage-dependence of the deactivation rate constant ( $\beta$ ) from e-fold per 21mV to e-fold per 14mV (*see inset* Figure 1C). Reanalysis with a steeper voltage-dependence of steady-state activation (e-fold per 8.5mV which reflects the change in  $\beta$ ) did not change the conclusion.

The I-V curve for each cell fell into two distinct regions- a region of relatively high conductance in which  $I_M$  activates (i.e. between -60 and -30mV) and a region of lower conductance where most of the current flows through leak channels (i.e. below -70mV,  $I_{leak}$ ). The latter region (between -70 and -100mV) was fitted with a linear function. The leak conductance, calculated from the slope of this linear fit was not significantly different in axotomized neurones (1.8±0.2nS for 28 control neurones and 2.2±0.2nS for 32 axotomized neurones; P>0.1) and was comparable to  $R_{in}$  estimated from the initial current-clamp measurements (see methods).

 $I_{\rm M}$  at potentials positive to -70mV was estimated by subtracting the extrapolated values of the leak current from the total current (assuming that the leak is linear). The net steady-state I-V relationship for 28 control and 32 axotomized

neurones is shown in Figure 1D. The estimated average M-conductance at -30mV was significantly increased after axotomy  $(8.5\pm0.9\text{nS} \text{ for } 28 \text{ control and } 11.5\pm0.9\text{nS} \text{ for } 32 \text{ axotomized neurones; } P<0.05)$ . This increase could reflect a 30% increase in the number of M-channels or a change in their kinetics. The latter is possible given that the voltage-dependence of the rate of deactivation is 1.5 fold greater after axotomy. Indeed, the data could be well described by a function in which the midpoint for activation was shifted from -35mV to -40mV and voltage-dependence increased by 1.5 fold without changing the maximal conductance as shown by solid lines in figure 1D.

Hyperpolarizing commands to negative potentials result in the activation of a slow, inward  $Na^+/K^+$  current known as H-current ( $I_H$ , Tokimasa & Akasu, 1990). Under the conditions of our experiments ( $[K]_o = 2mM$ ),  $I_H$  was either undetectable or very small relative to  $I_M$ . No further analysis was therefore made of  $I_H$  in control and axotomized neurones.

# 3.4.3 Effects of axotomy on $I_A$ and $I_{SA}$

Repolarization to a holding potential of -30mV after a prolonged hyperpolarization often results in the activation of a transient outward  $K^+$  current,  $I_A$ , in BFSG neurones.  $I_A$  is almost completely inactivated near the resting membrane potential i.e around -50mV (Adams *et al.*, 1982). The membrane has to be hyperpolarized to remove inactivation prior to activation by a subsequent depolarization.  $I_A$  at -30mV following a 1s command to -110mV was present in 20

of 28 control neurones but in only 5 of 48 axotomized neurones.

 $I_{SA}$  is another transient K<sup>+</sup>-current which activates on repolarization to a holding potential of -30mV after a prolonged hyperpolarization but exhibits slower kinetics than  $I_A$ . This current is not normally detected in microelectrode voltage-clamped BFSG neurones (Adams *et al.*, 1982) and appears after long term recording or in the presence of muscarine in sympathetic neurones of *Rana pipiens* (Selyanko *et al.*, 1990b).  $I_{SA}$  was observed in 20 of 28 control BFSG B-neurones and 4 of 48 axotomized neurones. With one exception where only  $I_A$  was observed, the axotomized cells that exhibited  $I_A$  also exhibited  $I_{SA}$ . This result suggests that  $I_A$  and  $I_{SA}$  are similarly regulated by axotomy and may be generated by similar channels.

## 3.4.4 Effects of axotomy on I<sub>C</sub>

 $I_C$  is responsible for fast repolarization of the action potential (Adams *et al.*, 1982; Pennefather, Lancaster, Adams & Nicoll, 1985; Lancaster & Pennefather, 1987). We were able to evoke  $I_C$  when intracellular  $Ca^{2+}$  was buffered to 40nM using 4.4mM EGTA.  $I_C$  was absent when extracellular  $Ca^{2+}$  was removed indicating that its activation requires influx of  $Ca^{2+}$  influx through  $Ca^{2+}$  channels. High concentration of EGTA did not prevent activation of  $I_C$  presumably because of the slow rate of  $Ca^{2+}$  binding to this chelator (Smith, Liesegang, Berger, Czerlinski & Podolsky, 1984). It nevertheless clamped basal levels of  $[Ca^{2+}]_i$  during recording period. After axotomy,  $I_{Ca}$  is both reduced and subject to increased inactivation (Jassar *et al.*, *in press*): these changes complicate attempts to determine any effect on

I<sub>C</sub> per se.

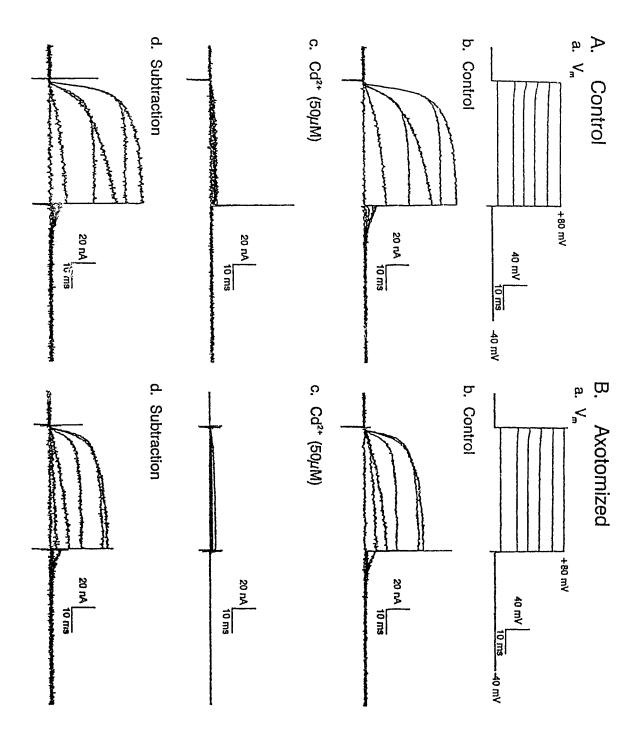
Although  $I_{Ca}$  is subject to run down in whole-cell recordings (Chad & Eckert, 1986; Belles, Malecot, Hescheler & Trautwein, 1988), the currents recorded in BFSG B-neurones are relatively stable when ATP and leupeptin are included in the internal solution (Jassar & Smith, 1991). In the present experiments, using leupeptin and cyclic AMP,  $I_{C}$  was well-maintained during 1.5 -2h of recording (i.e. >75% of that elicited at the beginning of the recordings). Sufficient ATP may have been produced by the cell since D-glucose was present in the patch-pipette filling solution.

# 3.4.4.1 I<sub>C</sub> evoked with 50ms pulses from -40mV

In the first series of experiments,  $I_C$  was evoked by a series of 50ms pulses from a holding potential of -40mV. This procedure minimizes contamination by  $I_K$  which is largely inactivated at that potential (Adams *et al.*, 1982; Xu & Adams, 1992). Pronounced slow inactivation of N-type  $Ca^{2+}$ -current at that potential (Jones & Marks, 1989b) will reduce  $Ca^{2+}$  influx that occurs in response to a depolarizing voltage command and thereby limits the amplitude of  $I_C$ . Smaller currents pose less practical problems relating to the control of the membrane voltage. Current responses recorded in a control and an axotomized neurone are shown in Figures 2A and 2B. Figures 2Ab and 2Bb show the total outward current elicited. Outward tail currents accompany repolarization to the holding potential. Changing the external solution to one containing 0mM  $Ca^{2+}$ , 4mM  $Mg^{2+}$  and  $50\mu$ M  $Cd^{2+}$  blocks most of the outward current (Fig. 2Ac and 2Bc) confirming that  $I_K$  was mostly inactivated at

Figure 2.  $I_C$  evoked in a typical control (A) and a typical axotomized neurone (B) by applying 50ms depolarizing command pulses from a holding potential of -40mV. a.  $V_m$  refers to the membrane voltage achieved in response to depolarizing command pulses. b. Total outward currents elicited in response to depolarizing command pulses. c. Currents elicited in a solution in which  $Ca^{2+}$  was replaced with equimolar concentration of  $Mg^{2+}$  and  $50\mu M$   $Cd^{2+}$  added. Note that the currents are markedly attenuated in such a solution. d. Relatively pure form of  $I_C$  obtained by subtracting the currents recorded in 0mM  $Ca^{2+}$ , 4mM  $Mg^{2+}$  and  $50\mu M$   $Cd^{2+}$  (c) from the total outward currents elicited in 4mM  $Ca^{2+}$  in the external solution (b). Note the slower activation of  $I_C$  at +60mV and at +80mV in both the control and the axotomized neurone.

Figure 2.



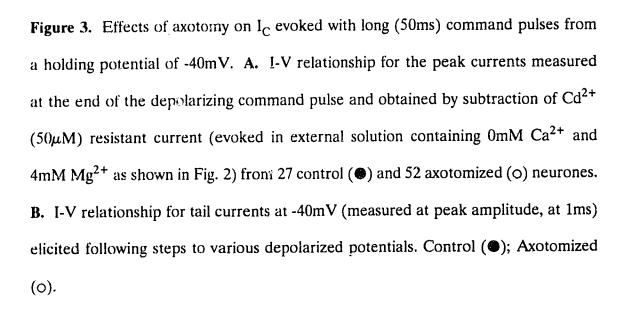
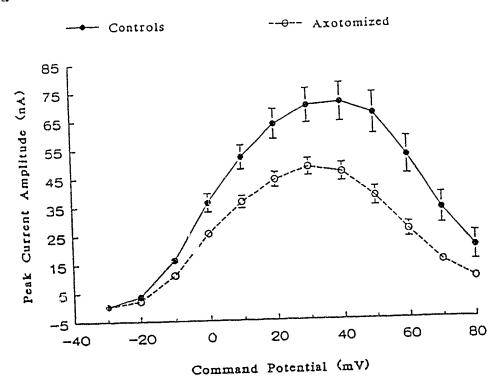
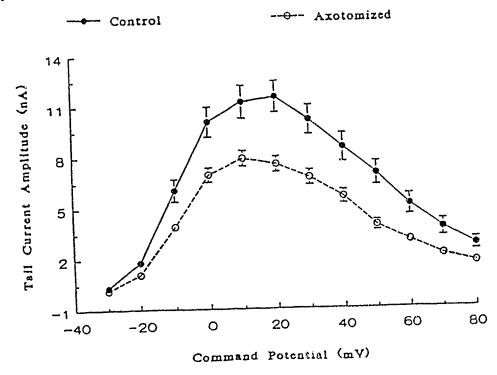


Figure 3.

A.



B.



-40mV. Figures 2Ad and 2Bd show the isolated and relatively pure form of  $I_C$  obtained by subtracting the  $Cd^{2+}$ -resistant current  $(I_K)$  from the total outward current. The  $Cd^{2+}$ -sensitive currents, which are presumed to reflect  $I_C$  start to activate with commands to -30mV and reach a maximum at +30mV. The currents activate with a delay of few hundred microseconds. The time required for  $I_C$  to increase from 25% to 75% of maximum was around 5ms for all potentials between 0 and +50mV and was not significantly different between the control and axotomized neurones (P>0.1). With commands to potentials >+40mV, a slowly activating component becomes apparent (see Fig. 2Ad & 2Bd).

The relationship between voltage and peak and tail currents (from  $\mathbb{Z}^3$  control and 52 axotomized neurones) is shown in Fig 3A and 3B respectively. The data show that when  $I_C$  (obtained after subtraction) is evoked from -40mV, the current is significantly decreased after axotomy (P < 0.005 for both steady-state and tail currents). At +30mV, the values for peak currents were 69.7±6.1nA for 27 control neurones and 48.1±2.9nA for 52 axotomized neurones. Both peak and tail current amplitudes exhibited a pronounced decrement with increasing depolarization above +30mV. This results in a negative slope in the I-V relationship because  $I_{Ca}$  becomes very small due to rectification as the command potential becomes more positive (Jones & Marks, 1989a; Sala, 1991; Jassar *et al.*, *in press*); the increase with depolarization in potency of  $Ca^{2+}$  to activate  $I_C$  (Moczydlowski & Latorre, 1983) is inadequate to compensate for that decrease in the  $Ca^{2+}$  influx. The small  $I_{Ca}$  at +70mV is nevertheless still important in  $I_C$  generation as  $Cd^{2+}$  blocks  $I_C$  at that

potential. Differences in  $I_C$  between control and axotomized neurones are not due to differences in resting levels of  $[Ca^{2+}]_i$  because this is fixed by the EGTA in our recording pipette. Resting levels of  $[Ca^{2+}]_i$  in non-dialysed cells are also not affected by axotomy. Direct measurements of  $[Ca^{2+}]_i$  from fura-2 loaded control cells were not different from that in axotomized neurones (57.5±5.5 nM for 53 control neurones and 57.4±5.2nM for 58 axotomized neurones; P<0.001).

### 3.4.4.2 I<sub>C</sub> evoked with short pulses

Since the duration of the depolarizing phase of the normal a.p. is brief (<3ms), we carried out a second series of experiments using shorter command pulses (3ms) to assess the influence of  $I_C$  in determining the time course of a.p.s. In addition, these commands were generated from a holding potential of -80mV to minimize the influence of inactivation of  $I_{Ca}$  (Jones & Marks, 1989b; Jassar *et al.*, *in press*). Because  $I_K$  activates slowly, a short command pulse evokes a current which comprises mainly  $I_C$ . Also, the voltage control of brief currents evoked from -80mV is improved over long currents because  $I_C$  is only partially activated by 3ms commands. Some typical data records from a control and an axotomized neurone are illustrated in Fig. 4A and 4B respectively.  $I_C$  in a relatively pure form, was again obtained by subtracting the currents recorded in 0mM  $Ca^{2+}$ , 4mM  $Mg^{2+}$  and  $50\mu M$   $Cd^{2+}$  from that recorded in normal Ringer (4mM  $Ca^{2+}$ ). Figure 5A shows the I-V plot for 15 control and 50 axotomized neurones for the currents activated with 3ms voltage commands. Again, a negative slope conductance in peak currents I-V

Figure 4.  $I_C$  recorded from a typical control (A) and a typical axotomized neurone (B) by applying 3ms depolarizing command pulses from a holding potential of -80° V. a.  $V_C$  refers to the voltage command protocol. b.  $V_m$  refers to the membrane voltage achieved in response to depolarizing command pulses. c. Total outward currents elicited in response to depolarizing command pulses. d. Currents elicited in a solution in which extracellular  $Ca^{2+}$  was replaced with  $Mg^{2+}$  and  $50\mu M$   $Cd^{2+}$  was added. Note that the currents are markedly attenuated in such a solution. e. Relatively pure form of  $I_C$  obtained by subtracting the currents recorded in 0mM  $Ca^{2+}$ , 4mM  $Mg^{2+}$  and  $50\mu M$   $Cd^{2+}$  (d) from the total outward currents elicited in 4mM  $Ca^{2+}$  in the external solution (c). Note that peak  $I_C$  at the end of the pulse is smaller in the axotomized neurone at +30mV but is not very different at +70mV.

Figure 4.

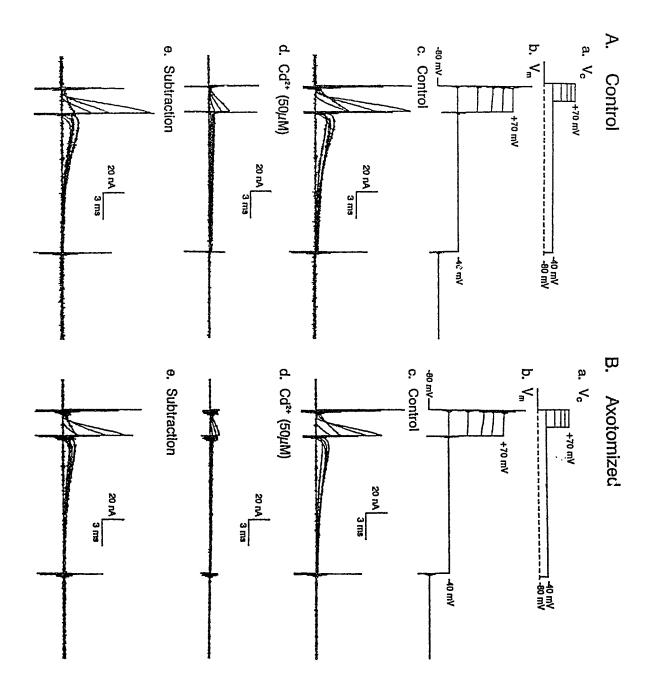
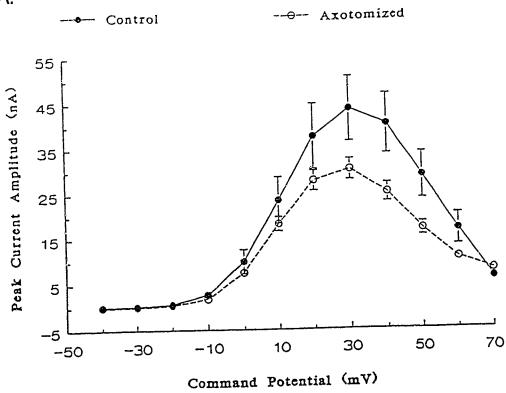


Figure 5. Effects of axotomy on I<sub>C</sub> evoked with brief (3ms) command pulses from a holding potential of -80mV. A. I-V relationship for the peak currents measured at the end of the depolarizing command pulse and obtained by subtraction of Cd<sup>2+</sup> (50μM) resistant current (evoked in external solution containing 0mM Ca<sup>2+</sup> and 4mM Mg<sup>2+</sup> as shown in Fig. 4) from 15 control (⑤) and 50 axotomized (o) neurones.

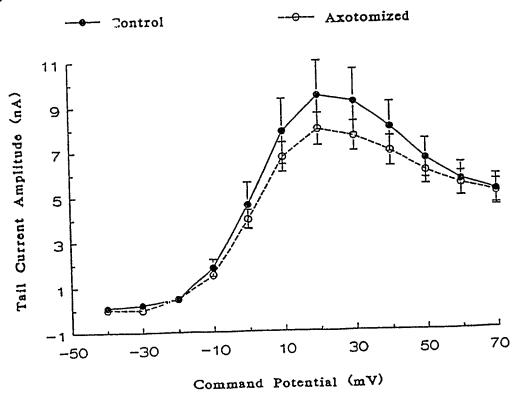
B. I-V relationship for tail currents for the same neurones as in A at -40mV (measured at peak amplitude, usually between 1-2ms) elicited following steps to various depolarized potentials. Control (⑥); Axotomized (o).

Figure 5.





# B.



relationship is observed. Analysis of peak  $I_C$  shows that the currents are significantly smaller in axotomized neurones only at few potentials (P < 0.05 at +40 and +50mV); at most potentials the differences are not statistically significant (P > 0.05 at +30mV and +60mV).

I<sub>C</sub> tail currents were recorded at -40mV. These exhibited a rising phase during the first 1-2ms following repolarization and had a decay time constant of about 6ms. The rising phase may reflect in part, contamination by inward I<sub>Ca</sub> tail currents. In addition, the large influx of Ca<sup>2+</sup> during I<sub>Ca</sub> tail currents may increase [Ca]<sub>i</sub> sufficiently to activate additional I<sub>C</sub> channels despite the reduced affinity of the voltage-dependent channels for Ca2+ at -40mV. That the latter possibility needs to be considered is supported by a comparison between expected and observed amplitudes of tail currents due to  $I_C$ . The observed amplitude of  $I_C$  tail currents following 3ms pulses from -80mV is greater than that predicted by GHK rectification from the amplitude of I<sub>C</sub> at the end of the pulse (see Fig. 8). For example, assuming  $E_{K} = -100 mV$ , GHK rectification predicts a 3.8 fold instantaneous decrease in current with the two-fold change in driving force which occurs when the voltage is changed from +20 to -40 mV. Such a change was in fact seen with  $I_K$  (see Fig. 6). Yet, in the present experiments if the I<sub>C</sub> tail current is extrapolated to the time just after the 3ms command has ended, the data suggest that the instantaneous decrease in current is only 3.0 fold. This indicates that the tail current is at least 25% greater than the expected value and suggests that additional channels are activated during repolarization to -40mV. With pulses to +70mV there appears to be little if any instantaneous decrease in current upon stepping to -40mV suggesting that more than 75% of the  $I_C$  tail current following a command to +70mV is generated by  $Ca^{2+}$  entering the cell during the  $I_{Ca}$  tail current (see Lancaster & Pennefather, 1987).

Given the activation kinetics for I<sub>Ca</sub> (Jones & Marks, 1989a; Sala, 1991), this current will be maximally activated within 3ms with commands to potentials >+30mV. The expected amount of Ca<sup>2+</sup> entering during the I<sub>Ca</sub> tails will therefore be similar following these commands. The observation that  $I_{\mathbb{C}}$  tail currents in response to commands to +30mV was approximately two-fold greater than that following commands to +70mV suggests that as much as 50% of I<sub>C</sub> tail currents following the 3ms commands to +20mV reflects channels that are activated by new  $Ca^{2+}$  entering during  $I_{Ca}$  tails (see Lancaster & Fennefather, 1987). In control cells there is little difference between I<sub>C</sub> tail current following brief commands from -80mV and long commands from -40mV. There is also little difference in  $I_C$  tail currents following the brief command in control and axotomized neurones again despite a substantial reduction of I<sub>Ca</sub> in axotomized cells. We suggest that saturation of I<sub>C</sub> activation may explain the resistance of I<sub>C</sub> to reductions in I<sub>Ca</sub>. If we accept this hypothesis, then maximal G<sub>C</sub> (under our ionic gradients and at 0mV) must be around 550nS. The fact that there is little difference in time course of  $I_{\rm C}$  or in maximal conductance implies that I<sub>C</sub> channels per se are minimally affected by axotomy.

I<sub>C</sub> tail currents shown in Fig. 5B exhibit no significant differences between control and axotomized neurones and reinforce the same conclusion.

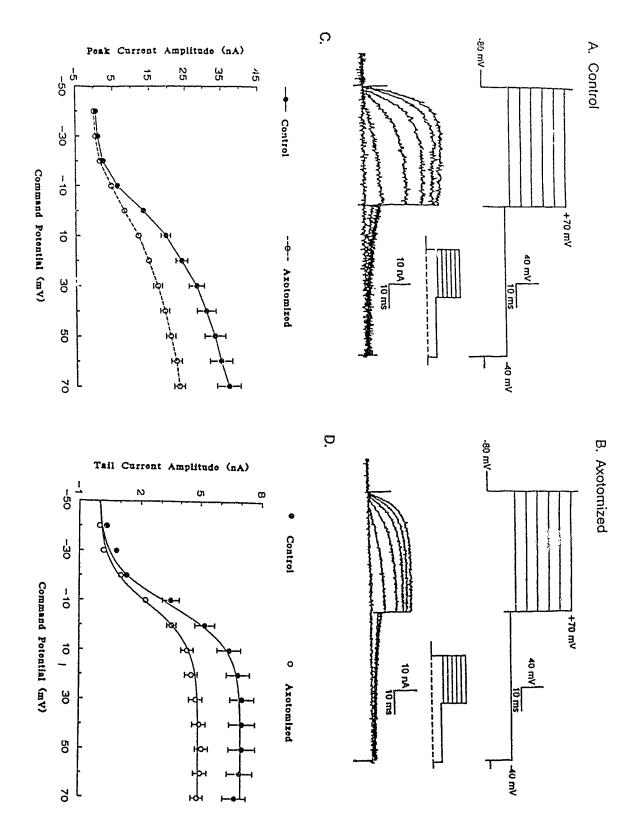
## 3.4.5 Effects of axotomy on $I_K$

 $I_K$  was recorded in a solution in which  $I_{Ca}$  and hence  $I_C$  was blocked. Current responses from a control and an axotomized neurone are illustrated in Fig. 6A and 6B respectively. I<sub>K</sub> started to activate at -20mV and increased with increasing depolarization. The currents did not inactivate during a 50ms command pulse duration. I<sub>K</sub> tail currents at -40mV could be fitted with a single exponential with a time constant of ≈22ms. There was no significant difference in the time constant at -40mV between the control and the axotomized neurones (P>0.2). relationship for data for steady-state peak currents from 16 control and 52 axotomized neurones is shown in Fig 6C. Steady state  $I_K$  was significantly decreased in axotomized neurones (P < 0.05 at -20mV and -10mV; P < 0.001 at potentials  $\ge 0$ mV). The average peak conductance (at +50mV) estimated from steady-state  $I_K$  was  $219.6 \pm 19.0$ nS for 16 control neurones and  $136.3 \pm 10.0$ nS for 52 axotomized neurones. For both control and axotomized neurones the instantaneous reduction in current with the steps from +20mV to -40mV was 3.9 fold as expected from GHK predictions (see above).

 $I_K$  tail currents were also decreased after axotomy as shown in Fig. 6D (P < 0.005 at potentials > 0 mV). The voltage-dependence of steady-state activation of  $I_K$  was deduced from the relationship between the amplitude of  $I_K$  tail currents at 40 mV and the preceding command potential. The points in Fig. 6D were well described by a Boltzmann's activation curve with a half activation potential of -8 mV and a slope factor of e-fold per 8.3 mV. These results again suggest that  $G_K$  is

Figure 6. Effects of axotomy on  $I_K$ . A & B show the a family of currents evoked with 50ms depolarizing command pulses from a holding potential of -80mV from a corol and an axotomized neurone respectively. The Ringer's solution contained  $I_{cd}M$   $Ca^{2+}$ , 4mM  $Mg^{2+}$  and  $50\mu M$   $Cd^{2+}$ . The upper panel shows the membrane voltage attained in response to the depolarizing command pulses. The inset on the right shows the voltage command protocol beside each recording. C. The I-V relationship for the peak currents measured at the end of the depolarizing command pulse for 16 control ( $\textcircled{\bullet}$ ) and 52 axotomized (o) neurones. D. The I-V relationship for tail currents measured at 1ms after the end of the depolarizing command pulse from 16 control ( $\textcircled{\bullet}$ ) and 52 axotomized (o) neurones. The solid lines through the data represent the Boltzmann's fit described by the equation  $G_{K(max)}/(1+\exp[(-8mV-V)/8.3mV])$ .  $G_{K(max)}$  was calculated from the data for control and axotomized neurones using a reversal potential of -100mV.

Figure 6.



decreased by 30% in axotomized neurones. Axotomy did not appear to induce any change in the voltage-dependence of steady-state activation or in time course of  $I_K$ .

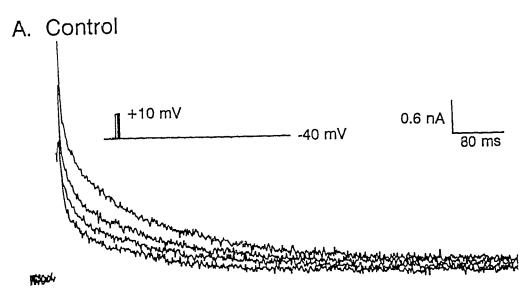
# 3.4.6 Effect of axotomy on I<sub>AHP</sub>

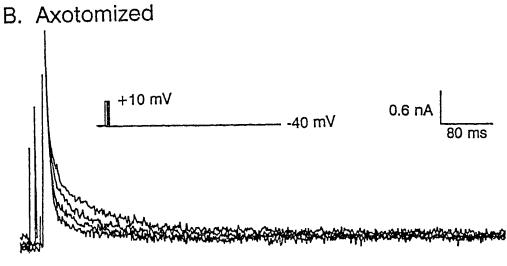
 $I_{AHP}$  is a voltage-insensitive  $Ca^{2+}$ -sensitive  $K^+$ -current that contributes to the slow ahp which follows the a.p. in BFSG neurones (Pennefather et al., 1985; Lancaster & Pennefather, 1987). Attempts to record I<sub>AHP</sub> in whole-cell configuration were unsuccessful and the effects of axotomy on this current were assessed in vitro with 'sharp' intracellular microelectrodes in intact ganglia. IAHP was activated following depolarizations for various intervals (2.25ms to 27ms) to +10mV from a holding potential of -40mV (Fig. 7A & 7B) to evoke  $Ca^{2+}$  influx via  $Ca^{2+}$  channels. The total current elicited from -40mV is relatively small due to inactivation of  $I_K$  and  $I_{Ca}$ . Since  $I_K$  is almost completely inactivated and  $I_C$  decays completely in much less than 40ms (see Figures 2 & 4; Goh & Pennefather, 1987), we measured I<sub>AHP</sub> at 41.5 ms after the end of the depolarizing command. The duration of depolarization can be considered an index of  $Ca^{2+}$  influx. We observed that the amount of  $I_{AHP}$  elicited in both control (n=32) and axotomized (n=34) neurones (Figure 7C) increased to the same extent with duration of depolarization. As expected from reduced Ca2+ influx evoked by depolarization after axotomy, longer depolarizations were required to produce an I<sub>AHP</sub> of a given amplitude after axotomy.

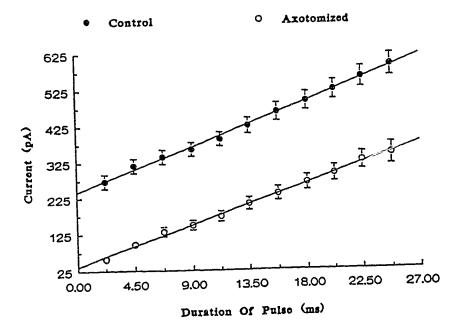
The decay of the total outward currents following depolarizing commands of increasing duration (from 2.25ms to 27ms) to +10mV exhibited two exponential

**Figure 7.** Effects of axotomy on  $I_{AHP}$ . **A.** Outward currents evoked in a control neurone following 4.5; 9.0; 15.75 and 27ms voltage command pulse to +10mV from a holding potential of -40mV. **B.** Outward currents evoked in an axotomized neurone using exactly the same set of protocols as that for control cell in **A. C.** The relationship between the duration of the depolarizing command pulse and the  $I_{AHP}$  evoked.  $I_{AHP}$  was measured at 41.5ms after the end of the depolarizing command. Note the linear relationship for both the control (n=32) and the axotomized (n=34) neurones; and the parallel shift to the right in the relationship for the axotomized cells.

Figure 7.







components. The time constants of these components had 30-40 fold difference and the slower component pertains to  $I_{AHP}$  (Pennefather & Goh, 1988). The time constant of decay of  $I_{AHP}$  contains information about the time course of changes in  $[Ca^{2+}]_i$  concentration in the vicinity of  $I_{AHP}$ -channels (Lancaster & Pennefather, 1987; Pennefather & Goh, 1988; Pennefather, Sala & Hernandez-Cruz, 1990; Goh, Sanchez-Vives & Pennefather, 1992; Sah, 1993). A comparison of the time constant of decay of  $I_{AHP}$  of equal amplitudes in control (evoked by a 6.75ms command pulse) and axotomized neurones (evoked by a 22.5ms command pulse; see Fig. 7C) revealed no significant difference between the values from the two populations of cells (143.9±6ms for 32 control neurones and  $126\pm10.2$ ms for 34 axotomized neurones; P<0.2).

#### 3.5 DISCUSSION

#### 3.5.1 Resting Membrane Potential and Excitability.

In the present study we observed that  $G_{leak}$  and the RMP were not altered by axotomy. RMP was around -50mV and the  $G_{leak}$  (between -70 and -100mV) around 2nS in both control and axotomized BFSG neurones. These findings are consistent with previous studies (Hunt & Riker, 1966; Gordon *et al.*, 1987). In the same cells but under different conditions (e.g. 5mM Na<sub>2</sub>-ATP inside and 2mM Mn<sup>2+</sup> outside) Jones (1990), reported a leak conductance of 3nS and a RMP of -70mV. Our observations of a more positive RMP and a smaller leak conductance might suggest

fewer  $K^+$  leak channels under our conditions. Also the electrogenic sodium pump current may have been smaller under our experimental conditions because our pipettes did not contain high levels of ATP. At the RMP, we recorded approximately 2nS of  $G_M$  and a comparable amount of  $G_{leak}$  in both control and axotomized BFSG neurones. Thus, even if  $I_M$  makes a significant contribution to the RMP (Adams *et al.*, 1982 *but see also* Jones, 1990), the unaltered resting levels of  $I_M$  at RMP (Fig. 1D) are consistent with the unchanged RMP in axotomized neurones.

In the threshold region for a.p. generation i.e. around -30mV,  $G_M$  is increased in axotomized neurones by about 30%. Since maximal  $G_M$  was not determined in the present study, we are unable to distinguish whether this increase is due to changes in kinetics versus changes in number of channels. Despite the increase in outward current due to  $I_M$ , excitability of axotomized cells in response to constant current injection is not altered (Gordon *et al.*, 1987). The unchanged excitability may be explained by changes in currents other than  $I_M$ ;  $I_K$  is decreased after axotomy whereas  $I_{Na}$  is increased (Jassar *et al.*, *in press*). Also, there is a decrease in  $I_C$  and  $I_{AHP}$  which can be accounted for by the previously reported changes in  $I_{Ca}$  in axotomized neurones (*see below*). These diverse changes presumably compensate for each other in such a way that excitability appears unchanged after axotomy.

Gordon et al. (1987) have reported rheobasic currents of 0.16 and 0.5nA for control and axotomized neurones, respectively, with intracellular recording with sharp microelectrodes from intact BFSG. However, the value of rheobasic current predicted by modelling of the currents was of the order of 0.5nA for control and

slightly lower for axotomized cells (Jassar, Pennefather & Smith, unpublished observations). The discrepancy could result from the fact that the dissociated cells have a higher threshold for a.p. generation (Jones, 1987) because they lack the boost provided by Na<sup>+</sup> channels in the "initial segment" or "first node" region of the axon; this region expresses Na<sup>+</sup> channels with activation curves centered at potentials more negative than those in the soma (see Frankenhauser & Huxley, 1964; Jones, 1987). Our results suggest that the increase in rheobase seen in intact, axotomized BFSG neurones does not arise from changes in soma membrane properties and may therefore be attributable to changes in the properties of the axon or "initial segment".

Our extrapolated maximal  $G_M$  was around 15nS which is small relative to the values observed in microelectrode recordings from intact ganglia (Adams *et al.*, 1982) and in dissociated ganglion neurones (Kelly & Pennefather, 1990). In the latter study, ATP was included in the patch pipette and [Ca]<sub>i</sub> was 100nM whereas in our experimental conditions  $[Ca^{2+}]_i$  was estimated to be  $\approx$ 40nM and the pipettes contained  $125\mu$ M cyclic AMP rather than ATP. It is known that the maximal  $G_M$  can be modified by  $[Ca]_i$  (Yu, Adams & Rosen, 1991; Marrion, Zucker, Marsh & Adams, 1992). The differences observed in channel properties between the control and the axotomized neurones in the present study are not due to differences in  $[Ca^{2+}]_i$  or ATP. However differences between the two groups in responsiveness to this kind of modulation by these agents can not be ruled out.

### 3.5.2 Changes in $I_C$ after axotomy

We have shown that  $I_{\text{Ca}}$  is reduced after axotomy and its inactivation is enhanced (Jassar et al., in press). Since I<sub>C</sub> is a Ca<sup>2+</sup>-activated K<sup>+</sup> conductance, the changes in  $I_{Ca}$  should be reflected as changes in  $I_{C}$ . In the present study we observed that the amount of I<sub>C</sub> evoked by 3ms commands from a holding potential of -80mV is not significantly different between the control and the axotomized neurones for most potentials (Fig. 5). By contrast, we have previously shown that the I<sub>C</sub> evoked by a 3ms command pulse to +30mV from a holding potential of -40mV is significantly reduced by axotomy (Jassar et al., in press; see also Fig. 2 & 3). A comparison of the present and previous data shows that  $I_{\text{C}}$  is reduced by  $\approx\!\!33\%$  by changing the holding potential from -80 to -40 mV in axotomized neurones whereas it reduces by  $\approx 20\%$  in control neurones. As a result of slow inactivation of  $I_{Ca}$  (Jones & Marks, 1989b), the shift in holding potential from -80mV to -40mV results in ≈64% reduction in  $I_{\rm Ca}$  tails at -40mV in control and  $\approx\!\!90\%$  reduction in axotomized cells (Jassar et. al., in press). There is thus a three fold discrepancy between the reduction of I<sub>Ca</sub> and I<sub>C</sub> in both control and axotomized cells. In addition, as I<sub>Ca</sub> in axotomized neurones is already only 52% of control when activated from -80mV,  $I_{Ca}$  activated from -40mV in axotomized neurones will be only 17% of the magnitude of I<sub>Ca</sub> evoked from -40mV in control neurones. These calculations ignore the very significant differences in recording conditions used by us to examine  $I_{Ca}$  and  $I_{C}$ .

In order to explore this non-linear relationship, and to examine whether all of the observed changes in  $I_C$  were simply reflective of changes in  $I_{Ca}$ , we used a

computer simulation of the ion fluxes and channel gating in BFSG neurones. The basic model of  $I_C$  was similar to that described by Moczydlowski and Lattorre (1983). The basic model of I<sub>Ca</sub> was the same as that described by Sala (1991). A number of constraints limited our model of  $I_{\rm C}$  activation. The densities of  $I_{\rm Ca}$  and  $I_{\rm C}$  channels were scaled to give peak current densities comparable to those observed in the control and the axotomized neurones. There also must be rapid activation of I<sub>C</sub> at potentials between 0 and +40mV, rapid deactivation at potentials negative to -20mV. Yamada, Koch and Adams (1989) were able to simulate the properties of  $I_C$  provided that the Ca2+ sensitivity was orders of magnitude greater than that observed by Moczydlowski and Lattore (1983) and that there was no saturation of I<sub>C</sub> during an a.p. However our data suggest that there is saturation of I<sub>C</sub> during I<sub>C</sub> tail currents following brief commands from -80 mV. In other cell types the I<sub>C</sub> channels have been shown to be co-localized with Ca2+ channels (Roberts, Jacobs & Hudspeth, 1990). This co-localization ensures that the Ca<sup>2+</sup> entering the cells has a greater chance of encountering I<sub>C</sub> channels before diffusing away or interacting with endogenous buffers and transporters; co-localization could account for the insensitivity of I<sub>C</sub> due to reduction of I<sub>Ca</sub> observed here. We therefore thought it worthwhile to simulate the consequences of co-localization of I<sub>C</sub> and I<sub>Ca</sub> channels. In order to approximate such a situation without resorting to elaborate models involving three dimensional diffusion, we have considered very thin shells (5nm thick) just below the membrane in which diffusion of Ca2+ is reduced twenty thousand fold relative to the other concentric shells used to divide up the intracellular space. This modification in our model of one dimensional diffusion between the concentric shells, allows most of the  $Ca^{2+}$  entering the cell during a command to remain in the outer most shell for sufficient time to activate  $I_C$  channels. Yet within a few milliseconds turning off  $I_{Ca}$ , most  $Ca^{2+}$  ions can still escape from that shell despite the restricted diffusion because of its narrow width and because of the large initial concentration gradient.

Figure 8 illustrates the instantaneous I-V relationship assumed in our model for  $I_C$  and  $I_{Ca}$ . The rectification of  $I_C$  arises from simple GHK considerations. The normalized peak chord conductance at 0mV that we have used for  $I_C$  is 5mS/cm<sup>2</sup>. Because ions are unevenly distributed on either side of the membrane there will be different amounts of ions to carry current through activated channels in one direction versus the other. This simple form of rectification is described by the GHK equation

$$I = G_{X,0} - [X]_{0} - [X]_{i} \exp [Z_{X} F V_{m} / RT]$$

$$[X]_{0} - [X]_{i} - \exp [Z_{X} F V_{m} / RT]$$

$$[X]_{0} - [X]_{i} - \exp [Z_{X} F V_{m} / RT]$$
(1)

where  $G_{X,0}$  is the maximal chord conductance at 0mV,  $V_X$  is the reversal potential,  $V_m$  is the membrane potential and  $Z_X$ , F, R and T have their usual meanings.

In order to account for the greater than GHK rectification observed for  $I_{Ca}$  by Sala (1991) when calcium is a charge carrier, we used a modified GHK equation in which surface potentials on the outside and the on the inside of the membrane are considered (see Lewis, 1979). This modified GHK equation will have the same form

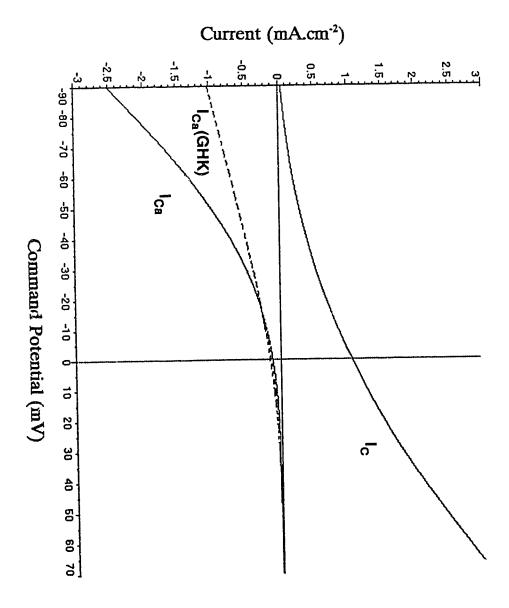
**Figure 8.** I-V curves of  $I_C$  and  $I_{Ca}$  used in our simulations. The solid outward current I-V curve is for  $I_C$  and is generated (*see text*) by the equation:

If one assumes a single channel conductance at 0 mV of 100 pS with 110mM internal and 2mM external K<sup>+</sup> this corresponds to a channel density of  $0.5 \,\mu\text{m}^{-2}$  (see Lancaster and Pennefather, 1987). The solid inward I-V curve is for I<sub>Ca</sub> assuming an external surface potential of -20mV (see Lewis, 1979) and is generated (see text) by the equation:

$$\frac{4.0\text{mS}}{\text{cm}^2} \times \frac{(145\text{mV})}{4\text{mM}} \times \frac{\exp[2B(-20\text{mV} + 145\text{mV})] - \exp[-2B(V_m + 20\text{mV})]}{\exp[2B(V_m + 20\text{mV})] - 1}$$

If one assumes a single channel current of 0.1 pA at -12mV in 4 mM Ca<sup>2+</sup> this corresponds to a channel density of 22. $\mu$ m<sup>-2</sup> (see Sala, 1991). The dashed inward I-V relation is for I<sub>Ca</sub> with a conductance of 1.0 mS/cm<sup>2</sup> at 0mV that exhibits simple GHK rectification (i.e. channel surface potential = 0). [B = RT/F = 1/25.7mV].

Figure 8.



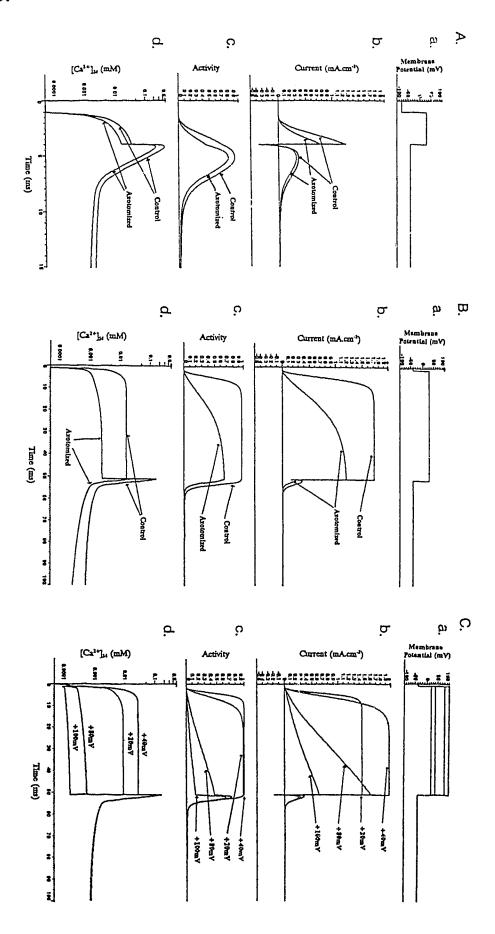
as equation 1 only  $V_m$  becomes  $(V_m - V_{so} + V_{si})$  and  $[X_o]$  and  $[X]_i$  becomes  $[X]_o$  exp[- $Z_X$  F  $V_{so}$  / RT) and  $[X_i]$  exp [- $Z_X$  F  $V_{si}$  / RT]. The latter modification takes into account the influence of surface potential on the concentration of ion X at the membrane. The modified GHK equation generates an I-V relation that agrees well with that observed by Sala (1991) when we set an external surface potential of -20mV and peak chord conductance of 4mS.cm<sup>-2</sup> at the effective zero potential (e.g. -20mV). For comparison, Fig. 8 also shows the I-V curve expected from simple GHK rectification of  $I_{Ca}$  with a maximal chord conductance at 0mV of 1.0 mS/cm<sup>2</sup>.

Fig. 9A shows the results of our simulation of the response to a 3 ms command to +30 ms from -80 mV with the  $I_C$  tail current measured at -40 mV. It shows that there is sufficient calcium entering the  $I_{Ca}$  channel to generate local activities greater than  $10~\mu\text{M}$  during the command and almost 0.5~mM just after the pulse when a large  $I_{Ca}$  tail current is active. The model suggests that the high  $Ca^{2+}$  activity during the pulse could be sufficient to activate 60% of  $I_C$  channels within 3 ms. After the pulse, an even higher activity of  $Ca^{2+}$  could allow new  $I_C$  channels to be activated despite their lower affinity of  $Ca^{2+}$  at -40~mV. This effect, together with the large  $I_{Ca}$  tail current generates the experimentally observed rising phase of the calcium-dependent outward tail current. Reducing  $I_{Ca}$  by half as is observed after axotomy (Jassar *et al.*, *in press*) leads to a 30% reduction in peak  $I_C$  and a 10% reduction in the amplitude of the outward tail current at -40~mV.

Figure 9B shows the results of using exactly the same model parameters but with new values of maximal  $G_{Ca}$  to simulate the response to a 50 ms command to

Figure 9. Results of I<sub>C</sub> simulation. Only 3 currents are considered in this simulation: I<sub>C</sub>, I<sub>Ca</sub> and  $I_{leak}$ . The conductance properties of  $I_{C}$  and  $I_{Ca}$  are illustrated in fig. 8.  $I_{leak}$  was assumed to exhibit a linear I-V with a conductance of 0.034mS.cm<sup>-2</sup> and a reversal potential of -30mV. The equation describing the gating of these channels are given in the Appendix. The basic strategy for the model of intracellular buffered diffusion is similar to that used by Sala & Hernandez-Cruz (1990) where one dimensional diffusion between concentric shells is solved numerically. We obtain results equal to theirs when the same parameters are used. In our model the intracellular space is divided into 3 banks of shells and differences in spacing and diffusion coefficient between these banks of shells is allowed. The three banks consist of 6, 9 and 9 shells respectively with width of 0.005, 0.5 and  $2.17\mu m$  and diffusion coefficients of 0.00001, 0.2 and 0.2 $\mu$ m<sup>2</sup>.ms<sup>-1</sup>. In each column panel a is the membrane potential, panel b is a plot of the total outward current, normalized for surface area, panel c is a plot of the fractional activation of  $I_C$  channels and panel d is a semilogarithmic plot of the calcium concentration in the outermost 5nm wide shell of cytoplasm just below the membrane. A. Response to a 3 ms command to +30mV from -80mV followed by a command to -40mV. In each plot the greater curves are those predicted for control neurones with a maximal  $G_{Ca}$  of 4.0mS.cm<sup>-2</sup> at -35mV. The lesser curves are those for axotomized neurones with a maximal  $G_{\text{Ca}}$  of 2.1mS.cm<sup>-2</sup> at -35mV. B. Response to a 50ms command to +30mV from -40mM. As the result of slow inactivation maximal G<sub>Ca</sub> is expected to be reduced to 1.4mS.cm<sup>-2</sup> in control neurons and to 0.21mS.cm<sup>-2</sup> in axotomized neurones. The peak activity of I<sub>C</sub> channel and peak outward I<sub>C</sub> are both reduced to about 2 fold of control while the steady state level of  $[Ca^{2+}]_i$  is reduced 6 fold by the reduction of  $I_{Ca}$ . C. Response to 50ms commands of increasing amplitude (to 20, 40, 80, 100 mV) from -40mV in control neurones. As the command potential becomes more positive the steady-state level of [Ca<sup>2+</sup>]<sub>i</sub> during the command becomes less. At +100mV there is little increase in [Ca<sup>2+</sup>]<sub>i</sub> during the command.

Figure 9.



+30 mV from a holding potential of -40 mV. As we observed experimentaly, the reduction of G<sub>Ca</sub> to 1.4 mS.cm<sup>-2</sup> and 0.18 mS.cm<sup>-2</sup> in control and axotomized neurones respectively by holding at -40 mV is sufficient to allow a pronounced difference to exist between these two types of cells in the amount of  $I_{\mathbb{C}}$  that can be evoked by such commands. Notice also, despite the reduction of G<sub>Ca</sub> in control cells from 4 to 1.4 mS.cm<sup>-2</sup>, the peak  $I_{\rm C}$  evoked by a 50 ms command from -40 mV is greater than that during a 3 ms command from -80 mV. This too is observed experimentally and reflects the fact that I<sub>C</sub> is incompletely activated by 3ms. Fig. 9C illustrates the predicted time course of I<sub>C</sub> with 50 ms commands of increasing amplitude. Since I<sub>Ca</sub> rectifies and elevation of [Ca<sup>2+</sup>]<sub>i</sub> during the commands is reduced, the rise time of I<sub>C</sub> is slowed. This effect arises because at sufficiently positive potentials, even low levels of [Ca<sup>2+</sup>]<sub>i</sub> will be adequate to fully activate I<sub>C</sub>. However, this activation rate will be limited by the ability of Ca<sup>2+</sup> molecules to find I<sub>C</sub> channels which in turn will be a function of [Ca]<sub>i</sub>. A slow component in the activation time course of I<sub>C</sub> is observed at positive potentials in our experimental records (see Fig. 5). However the fast component (see Fig. 2d) that also is observed experimentally during pulses to +60mV is not reproduced by our model.

Although the results of our simulation qualitatively agree with our observation and show that axotomy-induced changes in  $I_C$  may be explicable in terms of changes  $I_{Ca}$ , exact quantitative agreement is yet to be achieved. There are several reasons for this, not the least of which is the crudeness of our approach to estimating the activity of  $Ca^{2+}$  in the vicinity of  $I_C$  channels, as well as the ill-defined conductance

properties and reversal potential of  $I_{Ca}$  at positive potentials. Also, the model of  $I_{C}$  activation was based on results obtained with  $I_{C}$  channels purified from muscle sarcoplasmic reticulum and studied in an artificial lipid bilayer (Moczydłowski & Latorre, 1983). Further experiments and simulations are required to confirm the tentative conclusions presented above.

# 3.5.3 Changes in $I_K$

Although the voltage-dependence of activation of I<sub>K</sub> was not altered, the amplitude of steady-state I<sub>K</sub> evoked in response to 50ms command pulses from a holding potential of -80mV was decreased in axotomized neurones to approximately 67% of that observed in control neurones. By contrast, other currents that also activate with depolarization like  $I_M$  (this study) and  $I_{Na}$  (Jassar et al., in press) were increased. It is therefore likely that the effects of axotomy are not a simple result of changes in surface potential. By contrast with parasympathetic neurones (Xu & Adams, 1992),  $I_K$  does not make a significant contribution to the resting current nor is it likely to play any role in the repolarization phase of the action potential in these cells as action potential duration is not affected even when >70% of total  $I_K$  is blocked with 3,4-diaminopyridine (Goh et al., 1989). Therefore the decrease in I<sub>K</sub> is not likely to contribute to the increased duration of the a.p. or the attenuation of the ahp. The lack of effect of axotomy on the voltage-dependence of activation of  $I_K$  is consistent with two possibilities. One is that the numbers of  $I_K$  channels are reduced. Alternatively, the steady-state inactivation curve for  $I_K$  could be shifted by axotomy such that 33% of  $I_K$  channels are inactivated at -80mV. It is notable that  $I_{Ca}$  shows a shift in inactivation that contributes to the reduction in  $I_{Ca}$  recorded from axotomized neurones (Jassar *et al.*, *in press*).

# 3.5.4 Changes in I<sub>AHP</sub>

Since  $I_{AHP}$  is a  $Ca^{2+}$ -activated K+ current, changes in  $I_{Ca}$  should also promote changes in this current. We estimated that the combined effect of enhanced slow inactivation and reduced  $I_{Ca}$  leads to a 80% reduction in  $Ca^{2+}$  influx by voltage-clamp commands from a holding potential of -40mV in axotomized neurones. We observed a decrease in  $I_{AHP}$  in axotomized neurones in response to depolarizations of the equal magnitude and duration. However if the duration is increased sufficiently to compensate for reduced  $I_{Ca}$ , the amplitude of  $I_{AHP}$  was restored. This suggests that the number of AAP channels is unchanged in axotomized neurones. For ahps of similar magnitudes in control and axotomized neurones, the time constants of decay were comparable. This suggests that intracellular buffering was not dramatically modified by axotomy. We therefore conclude that the reduction in ahp observed in current-clamp studies with axotomy (Kelly *et al.*, 1986; Gordon *et al.*, 1987) could result from the reduced amplitude and time constant of  $I_{AHP}$  that is a consequence of reduced  $Ca^{2+}$  influx.

## 3.5.5 Concluding Comments

Axotomy of BFSG B-neurones promotes increases in the duration and

amplitude of the a.p., a reduction in the amplitude and duration of ahp and an increase in rheobase (Gordon et al., 1987). We have used voltage-clamp analysis to determine the changes in ion currents that underlie these effects. In a previous study (Jassar et al., in press) we focussed on Ca2+ and Na+ channels while the present study deals with effects on the various K<sup>+</sup> channels. The characteristics of all K<sup>+</sup> channels were modified by axotomy. The results strongly suggest that the properties of the ion channels found in BFSG B-cells are differentially regulated after axotomy. We observed small increase in  $I_M$ , small decreases in  $I_K$  and  $I_C$ ; and larger decreases in  $I_{AHP}$ . The changes in  $Ca^{2+}$ -dependent currents ( $I_C$  and  $I_{AHP}$ ) appear to be secondary to reduction in  $I_{Ca}$  after axotomy. We estimate that the reduction in  $I_{Ca}$  and the concomitant reduction in I<sub>C</sub> activated during an action potential are responsible for the observed increase in the duration of the a.p. Similarly the reduction in I<sub>Ca</sub> is sufficient to account for the decrease in amplitude and duration of ahp. The effects on a.p. amplitude result from the increase in  $I_{Na}$  whereas the effects on rheobase can not be accounted for by our observations on isolated cell bodies.

Current-clamp studies carried out on other neuronal types have attempted to determine which ionic conductances are affected by axotomy. For example, decreases in  $I_A$  in degenerating vagal motoneurones of the guinea pig may account for changes in the time course of repolarization following large hyperpolarizing pulses (Lawaind et al., 1988). Decreases in  $I_C$  in cat cranial glossopharyngeal neurones (Gallego et al., 1987) may be responsible for prolongation of a.p. duration associated with axotomy. In the same cells, decreases in  $I_{AHP}$  may account for the decrease in ahp duration

(Gallego et al., 1987; Lawaind et al., 1988). Since there are only a few voltage-clamp studies which directly deal with the effects of axotomy on ion channels (Simoni, Pellegrini, Cecconi & Pellegrino, 1990; Jassar et al., in press) it is not possible to know whether the effects of axotomy are restricted to certain channel types or whether the same channels exhibit different sensitivities to axotomy in different neuronal types. In the first case, the diversity of the response would reflect the differential contribution of various ion channels to the passive and active membrane properties in different neuronal types. Clearly, additional voltage-clamp studies of the effects of axotomy on a variety of neuronal are required before a unifying hypothesis can be generated.

3.6 APPENDIX.

Equations describing the gating of the currents involved in the simulations are given below. These currents are considered;  $I_{Ca}$ ,  $I_{C}$  and  $I_{leak}$ .  $I_{Ca}$ ; based on the model of Sala (1991).

I<sub>C</sub>; based on the model of Moczydlowski & Latorre (1983).

where 
$$k_1 = 50$$
/mM/ms,  $k_{-1} = 0.5$  exp [-0.039 (V-0)],  $k_2 = 2$ /ms,  $k_{-2} = 4$ /ms,  $k_3 = 50$ /mM/ms,  $k_{-3} = 0.5$  exp [-0.039 (V-0)]. Also  $K_1 = k_1 / k_{-1} = 100\mu$ M and  $K_3 = k_3 / k_{-3} = 10\mu$ M. Note that we have arbitrarily assumed that the differences of affinity between  $K_1$  and  $K_3$  arise from the differences in the forward rate constants  $k_1$  and  $k_3$  and that the voltage dependence of  $Ca^{2+}$  binding is restricted to the offrate so that  $k_1$  and  $k_3$  are voltage independent.

I<sub>leak</sub>; (no gating).

Assumptions regarding channel permeability are given in the legend to Fig. 8. Parameters defining the transport and buffering of intracellular  $Ca^{2+}$  are similar to those used by Sala and Hernandez-Cruz (1990). Fast buffer concentration was set at  $50\mu M$ . Slow buffer was set at  $300\mu M$ . Neither was allowed to diffuse.

#### 3.7 REFERENCES

ADAMS, P.R.; BROWN, D.A. & CONSTANTI, A. (1982). M-currents and other potassium currents in bull-frog sympathetic neurones. *Journal of Physiology* **330** 537-572.

BELLES, B.; MALECOT, C.O.; HESCHELER, J. & TRAUTWEIN, W. (1988). "Rundown of the Ca current during long whole-cell recordings in guinea pig heart cells: role of phosphorylation and intracellular calcium. *Pflugers Archiv* **411** 353-360.

CHAD, J.E. & ECKERT, R. (1986). An enzymatic mechanism for calcium current inactivation in dialysed *Helix* neurones. *Journal of Physiology* **378** 31-51.

FOEHRING, R.C.; SYPERT, G.W. & MUNSON, J.B. (1986). Properties of self-innervated motor units in medial gastrocnemius of cat: II. Axotomized motoneurones and the time course of recovery. *Journal of Neurophysiology* 55 947-965.

FRANKENHAEUSER, B. & HUXLEY, A.F. (1964). Action potential myelinated nerve fiber of *Xenopus laevis* as computed on the basis of voltage clamp data. *Journal of Physiology* 171 302-315.

GALLEGO, R.; IVORRA, I. & MORALES, A. (1987). Effects of central or peripheral

axotomy on membrane properties of sensory neurones in the petrosal ganglion of cat. *Journal of Physiology* **391** 39-56.

GOH, J.W.; KELLY, M.E.M. & PENNEFATHER, P.S. (1989). Electrophysiological function of the delayed rectifier ( $I_K$ ) in bull-frog sympathetic ganglion neurones. *Pflugers Archiv* 413 482-486.

GOH, J.W. & PENNEFATHER, P.S. (1987). Pharmacological and physiological properties of the afterhyperpolarization current of bull-frog ganglion neurones. *Journal of Physiology* **394** 316-336.

GOH, J.W., SANCHEZ-VIVES, M.V. & PENNEFATHER, P.S. (1992). Influence of Na/Ca exchange and mobilization of intracellular calcium on the time course of the slow afterhyperpolarization current (I<sub>AHP</sub>) in bullfrog sympathetic ganglion neurons. *Neuroscience Letters* 138 123-127.

GORDON, T. (1983). Dependence of peripheral nerves on their target organs. In Somatic and Autonomic Nerve-Muscle Interactions, pp. 289-325. Eds. Y. Vrbova, G. Burnstock, R. Campbell and R. Gordon. Elseviers: Amsterdam.

GORDON, T.; KELLY, M.E.M.; SANDERS, E.J.; SHAPIRO, J. & SMITH, P.A. (1987). The effects of axotomy on bull-frog sympathetic neurones. *Journal of Physiology* 392

GRAFSTEIN, B. (1983). Chromatolysis reconsidered: A new view of the reaction of nerve cell body to axon injury. In: *Nerve, Organ and Tissue Regeneration: Research Perspectives*, pp. 37-50. Ed. F.O. Seil. Academic Press: New York.

GURTU, S. & SMITH, P.A. (1988). Electrophysiological properties of hamster dorsal root ganglion cells and their response to axotomy. *Journal of Neurophysiology* **59** 408-423.

HUNT, C.C. & RIKER, W.K. (1966). Properties of frog sympathetic neurones in normal ganglia and after axon section. *Journal of Neurophysiology* **29** 1096-1114.

JASSAR, B.S., PENNEFATHER, P.S. & SMITH, P.A. Changes in sodium and calcium channel activity following axotomy of B-cells in bull-frog sympathetic ganglion. *Journal of Physiology (in press)*.

JASSAR, B.S. & SMITH, P.A. (1991). Slow frequency-dependence of action potential afterhyperpolarization in bull-frog sympathetic ganglion neurones. *Pflugers Archiv* **419** 478-485.

JONES, S.W. (1987). Sodium currents in dissociated bull-frog sympathetic neurones.

Journal of Physiology 389 605-627.

JONES, S.W. (1990). On the resting potential of isolated frog sympathetic neurones.

Neuron 3 153-161.

JONES, S.W. & MARKS, T.N. (1989a). Calcium currents in bull-frog sympathetic neurones. I. Activation kinetics and pharmacology. *Journal of General Physiology* **94** 151-167.

JONES, S.W. & MARKS, T.N. (1989b). Calcium currents in bull-frog sympathetic neurones. I. Inactivation. *Journal of General Physiology* **94** 169-182.

KUNO, M.; MIYATA, Y. & MUNOZ-MARTINEZ, E.J. (1974). Differential reaction of fast and slow alpha motoneurones to axotomy. *Journal of Physiology* **240** 725-739.

LANCASTER, B. & PENNEFATHER, P.S. (1987). Potassium currents evoked by brief depolarizations in bull-frog sympathetic ganglion cells. *Journal of Physiology* **387** 519-548.

LAWAIND, R.; WERMAN, R. & YAROM, Y. (1988). Electrophysiology of degenerating neuornes in the vagal motor nucleus of the guinea pig following axotomy. *Journal of Physiology* **404** 749-766.

LEWIS, C.A. (1979). Ion concentration dependence of the reversal potential and the single channel conductance of ion channels at the frog neuromassissist function.

Journal of Physiology 286 417-445.

MARRION, N.V.; ADAMS, P.R. & GRUNER, W. (1992). Multiple kinetic states underlying macroscopic M-currents in bullfrog sympathetic neurones. *Proceedings of the Royal Society of London* **248** 207-214.

MARRION, N.V.; ZUCKER, R.S.; MARSH, S.J. & ADAMS, P.R. (1991). Modulation of M-current by intracellular Ca<sup>2+</sup>. Neuron 6 533-545.

MOCZYDOLWSKI, E. & LATORRE, R. (1983). Gating of Ca<sup>2+</sup>-activated K<sup>+</sup> channels from rat muscle incorporated into black lipid bilayer: Evidence for two voltage-dependent Ca<sup>2+</sup> binding reactions. *Journal of General Physiology* 82 511-542.

PENNEFATHER, P.S. & GOH, J.W. (1988). Relationship between calcium load and the decay rate of I<sub>AHP</sub> in bullfrog ganglion neurons. *Society for Neuroscience Abstract* 14 1089.

PENNEFATHER, P.S.; LANCASTER, B.; ADAMS, P.R. & NICOLL, R.A. (1985). Two distinct Ca-dependent K-currents in bullfrog-sympathetic ganglion cells. *Proceedings* 

of the National Academy of Sciences of U.S.A. 82 3040-3044.

PENNEFATHER, P.; OLIVA, C. & MULRINE, N. (1992). Origin of the potassium and voltage dependence of cardiac inwardly rectifying K-current (I<sub>K1</sub>). *Biophysical Journal* **61** 448-462.

PENNEFATHER, P.; SALA, F. & HERNANDEZ-CRUZ, A. (1990). Computer simulations of I<sub>AHP</sub> kinetics. Society for Neuroscience Abstract 16 187.

PINTER, M.J. & VANDEN-NOVEN, S. (1989). Effects of preventing reinnervation on axotomized spinal motoneurones in the cat. I. Motoneuron electrical properties.

Journal of Neurophysiology 62 311-324.

ROBERTS, W.M.; JACOBS, R.A. & HUDSPETH, A.J. (1990). Colocalization of ion channels involved in frequency selectivity and synaptic transmission at presynaptic active zones of hair cells. *Journal of Neuroscience* **10(11)** 3664-3684.

SAH, P. (1993). Kinetic properties of a slow pamin-insensitive Ca<sup>2+</sup>-activated K<sup>+</sup> current in guinea pig vagal neurones. *Journal of Neurophysiology* **69(2)** 361-366.

SALA, F. (1991). Activation kinetics of calcium currents in bull-frog sympathetic neurones. *Journal of Physiology* **437** 221-238.

SALA, F. & HERNANDEZ-CRUZ, A. (1990). Calcium diffusion modelling in a spherical neuron. Significance of buffering properties. *Biophysical Journal* **57** 313-324.

SELYANKO, A.A.; SMITH, P.A. & ZIDICHOUSKI, J.A. (1990a). Effects of muscarine and adrenaline on neurones from *Rana Pipiens* sympathetic ganglia. *Journal of Physiology* **425** 471-500.

SELYANKO, A.A.; ZIDICHOUSKI, J.A. & SMITH, P.A. (1990b). A muscarine-sensitive, slow, transient outward current in frog autonomic neurones. *Brain Research* **524** 236-243.

SHAPIRO, J.; GURTU, S.; GORDON, T. & SMITH, P.A. (1987). Axotomy increases the conduction velocity of C-cells in bull-frog sympathetic ganglia. *Brain Research* **410** 86-88.

SIMONI, A.; PELLEGRINI, M.; CECCONI, C. & PELLEGRINO, M. (1990). Axotomy affects density but not properties of potassium leak channels, in the leech AP neurones. *Brain Research* 522 118-124.

SMITH, P.D.; LIESEGANG, G.W.; BERGER, R.L.; CZERLINSKI, G. & DODOLWSKY, R.J. (1984). A stopped-flow investigation of calcium ion binding by ethyleneglycol bis(β-aminoethyl ether)-N,N'-tetraacetic acid. *Annals of Biochemistry* **143** 188-195.

TITMUS, M.J. & FABER, D.S. (1990). Axotomy-induced alterations in the electrophysiological characteristics of neurons. *Progress in Neurobiology* **35** 1-51.

TOKIMASA, T. & AKASU, T. (1990). Cyclic AMP regulates an inwardly rectifying sodium-potassium current in dissociated bull-frog sympathetic neurones. *Journal of Physiology* **420** 409-429.

YAMADA, W.M.; KOCH, C. & ADAMS, P.R. (1989). Multiple channels and calcium dynamics. In *Methods in Neuronal Modelling "From Synapses to Networks"* Eds. KOCH, C. & SEGER, I. pp 97-133, MIT Cambridge.

YU, S.P., ADAMS, P.R. & ROSEN, A.D. (1991). Effects of arachidonic acid pathway inhibitors on calcium regulated M-current enhancement. *Society for Neuroscience Abstract* 17 67.

XU, Z.J. & ADAMS, D.J. (1992). Resting membrane potential and potassium currents in cultured parasympathetic neurones from rat intracardiac ganglia. *Journal of Physiology* **456** 405-424.

# CHAPTER 4.

# SLOW FREQUENCY-DEPENDENCE OF ACTION POTENTIAL AFTERHYPERPOLARIZATION IN BULLFROG SYMPATHETIC GANGLION NEURONES.

Note: This chapter is a version of a paper by <u>B.S. Jassar & P.A. Smith</u> which has been published in *Pflugers Archiv* (1991) **419** 478-485.

#### 4.1 SUMMARY

- 1. The afterhyperpolarization (a.h.p.) which follows the action potential (a.p.) in bullfrog sympathetic ganglion B-cells involves activation of  $Ca^{2+}$ -sensitive  $K^+$  conductances following  $Ca^{2+}$  influx via  $Ca^{2+}$  channels. The duration of a.h.p.'s evoked at 2s stimulus intervals were  $70.05\pm3.76\%$  of those evoked at 90s stimulus intervals (n=35).
- 2. Since there was no consistent effect of ryanodine  $(5\mu M)$ , ruthenium red,  $(300\mu M)$  or dantrolene Na  $(35\mu M)$  on this frequency-dependence, it is unlikely to result from release of Ca<sup>2+</sup> from intracellular stores.
- 3.  $Ca^{2+}$  currents, studied by means of the whole-cell patch-clamp technique, exhibited a slow frequency-dependence as a reallt of a slow inactivation process which was independent of  $Ca^{2+}$ -induced  $I_{Ca}$  inactivation and  $I_{Ca}$  run-down.
- 4. The duration of Ca<sup>2+</sup> spikes recorded with microelectrodes also showed frequency-dependence. The average duration of Ca<sup>2+</sup> spikes evoked at 5s stimulus interval was 39.2±4.0% of that evoked at 90s stimulus interval.
- 5. There was excellent correlation (r = 0.964) between the estimated changes in Ca<sup>2+</sup> influx and the expected activation of the Ca<sup>2+</sup>-sensitive K<sup>+</sup> current, I<sub>AHP</sub>. This result is consistent with the hypothesis that the frequency-dependence of the a.h.p. is a consequence of the slow inactivation of I<sub>Ca</sub>.

#### 4.2 INTRODUCTION.

In many neurones, the action potential (a.p.) is followed by an afterhyperpolarization (a.h.p.) which can have profound effects on repetitive discharge characteristics and accommodation (Kuno, Miyata & Munoz-Martinez, 1974; Krnjevic, Puil & Werman, 1978; Lux & Hofmeier, 1982a; Tokimasa 1984a; Pennefather, Lancaster, Adams & Nicoll, 1985; Fowler, Green & Weinreich, 1985; Adams, Jones, Pennefather, Brown, Koch & Lancaster, 1986; Madison & Nicoll, 1986; Gordon, Kelly, Sanders, Shapiro & Smith, 1987). This a.h.p. often results from  $activation \ of \ Ca^{2+} - dependent \ K^+ \ conductances \ following \ depolarization-induced \ Ca^{2+}$ influx (Lux & Hofmeier, 1982a & b; Pennefather et al., 1985; Lancaster & Pennefather, 1987; Goh & Pennefather, 1987). The amplitude and duration of the a.h.p. may be influenced by 'extrinsic' factors such as neuromodulators (Madison & Nicoll, 1986; Tokimasa, 1984b), trophic factors (Czeh, Gallego, Kudo & Kuno, 1978; Gordon et al., 1987; Titmus & Faber, 1990) and by 'intrinsic' mechanisms such as frequency-dependence of Ca<sup>2+</sup> influx (Lux & Fleyer, 1977). Although such mechanisms have been well-studied in molluscan neurones (Lux & Heyer, 1977) little is known about 'intrinsic' mechanisms which might operate and affect a.h.p. amplitude and duration in vertebrate neurones. In the present experiments on bullfrog sympathetic ganglion (BFSG) B-cells, we noticed that the duration of the a.h.p. decreased with increasing stimulus frequency and have investigated the mechanism of this phenomenon.

Two possible mechanisms were considered; 1) the involvement of a Ca<sup>2+</sup>-

induced  $Ca^{2+}$  release process (Kuba, Morita & Nohmi, 1983; Lipscombe, Madison, Poenie, Reuter, Tsien & Tsien, 1988) and 2) a frequency-dependence of  $Ca^{2+}$  influx as a result of slow inactivation of  $I_{Ca}$  (Jones & Marks 1989b).

If Ca<sup>2+</sup>-induced Ca<sup>2+</sup> release were involved, the influx of Ca<sup>2+</sup> accompanying each a.p. would trigger the release of additional Ca<sup>2+</sup> from intracellular stores. The frequency-dependence of a.h.p. duration would then be explained in terms of the time taken for refilling of these stores; when stimuli were applied at short time intervals there would be insufficient time for the stores to refill. By contrast, when stimuli were applied at long time intervals (>23s, Kuba, 1980) the stores would be fully refilled and the amount of Ca<sup>2+</sup> released would be correspondingly larger. Two lines of evidence suggest that a Ca<sup>2+</sup>-induced Ca<sup>2+</sup> release mechanism is available in BFSG: 1) it can be demonstrated following extensive Ca<sup>2+</sup> loading as a result of prolonged depolarization (Lipscombe et al., 1988), 2) it probably accounts for spontaneous, rhythmic hyperpolarizations and frequency dependence of the a.h.p. following treatment with caffeine (Kuba & Nishi 1976; Kuba, 1980; Kuba et al., 1983; Lipscombe et al., 1988). Despite this, it remains to be established whether such a mechanism is invoked during a single action potential and whether it can account for frequency dependence of the a.h.p. in the absence of caffeine (see Thayer, Hirning & Miller, 1988). To test this possibility, we examined whether ryanodine and other drugs which influence Ca2+-induced Ca2+ release, influenced the frequencydependence of a.h.p. duration.

Jones and Marks (1989b) have shown that there is a partial inactivation of  $I_{Ca}$ 

in BFSG during a 1.0s depolarizing voltage command and that there is also a slow inactivation process which develops and recovers in about 10s. To test whether this slow inactivation of  $I_{Ca}$  could account for the frequency-dependence of the a.h.p, we estimated the changes in  $Ca^{2+}$  influx which would occur at different stimulus frequencies and attempted to correlate them with the observed changes in a.h.p. duration. A preliminary report of some of this data has appeared (Jassar & Smith, 1990).

#### 4.3 MATERIALS AND METHODS.

Medium sized bullfrogs (10-12cm) were purchased from a biological supply house and stored in running water at room temperature (20°C).

## 4.3.1 Intracellular Recording.

Methods for intracellular recording from BFSG neurones have been published previously (Smith & Weight, 1986) and only a brief description will be presented. The paravertebral sympathetic chain, including the 6th to 10th paravertebral ganglia, was removed along with the 9th or 10th spinal nerve from pithed bullfrogs and placed in an appropriate recording chamber. To facilitate microelectrode penetration, the preparation was exposed to 10mg/ml collagenase (Sigma, Type IA) for 15 min. B-neurones were impaled with glass microelectrodes filled with 3M KC1 (resistance -  $40\text{-}100\text{M}\Omega$ ) and identified by their antidromic conduction velocity. Supramaximal, antidromic stimuli were delivered to the postganglionic spinal nerve at intervals of

2,3,5,10,15,20,25,30,45,60 and 90s. 6 to 10 shocks were applied at each simulus interval and the a.p.'s recorded in bridge-balance mode using a Dagan 8100 amplifier. Resting potential (r.m.p.) was monitored on a Gould-Brush model 2400 rectilinear pen recorder (filters set to -3dB at 5Hz). The last a.p. generated by the last stimulus at each stimulus interval was recorded on a Nicolet storage oscilloscope which was fitted with a floppy disk storage device. Hard records were obtained by using an X-Y plotter. The preparation was maintained in normal Ringer's solution which contained: (in mM) NaCl 100; CaCl<sub>2</sub> 1.8; KCl 2.0; Tris HCl 16; and D-Glucose 1g/l; pH 7.2). In some experiments, 5mM caffeine or 5μM ryanodine or 300μM ruthenium red was added directly to this solution. For recording Ca<sup>2+</sup> spikes, 2μM TTX was added to the Ringer solution in which 100mM TEA.Br replaced NaCl.

Data were collected from cells which had a.p. amplitude (spike height) > 75mV and (total) a.h.p. duration > 250ms. In some cells, a.h.p. duration progressively increased following microelectrode penetration (Kuba *et al.*, 1983; Gordon *et al.*, 1987). Studies of frequency-dependence in such cells were only initiated after the a.h.p. duration stabilized. This process took up to 30min. If a.h.p. duration had not stabilized at this time, no measurements of a.h.p. frquency-dependence were attempted. A.h.p. amplitude was measured from r.m.p. to peak of the a.h.p., spike height was measured from r.m.p. to peak, spike width was measured at the base of the a.p. and a.h.p. duration was measured at 50% a.h.p. amplitude. A.h.p. duration at 50% repolarization was used because it is hard to measure full duration as the voltage trajectory decays asymptotically. Changes in a.p. parameters were normalized

to the values recorded at the 90s stimulus interval.

## 4.3.2 Whole-Cell Patch-Clamp Recording

Bullfrog sympathetic ganglion cells were dissociated using trypsin/collagenase procedure previously described for Rana pipiens cells by Selyanko, Smith & Zidichouski (1990). The dissociated cells were resuspended in fresh '6Kexternal solution' and kept at about 5°C until use and were sometimes washed with cold '6K external solution' to remove any remaining enzymes. The cells were placed in a small plastic petri dish and observed under a Nikon 'Diaphot' inverted microscope. '6K external solution' contained: (in mM) NaCl 113; KCl 6; MgCl<sub>2</sub> 2; CaCl<sub>2</sub> 2; HEPES (acid) 5 and glucose 10 (pH adjusted to 7.2 with Na0H). Prior to recording Ca2+ currents, the superfusion was switched to a solution containing (in mM); TEA bromide 112; MgCl<sub>2</sub> 2.0; CaCl<sub>2</sub> 2.0; HEPES.Na0H 5.0; glucose 10.0, sucrose 22.0 (pH7.2; osmolarity 250 mosm/kg). BaCl<sub>2</sub> replaced CaCl<sub>2</sub> in some experiments. Internal patch solution consisted of (in mM) CsCl 110; NaCl 5; MgCl<sub>2</sub> 0.4, HEPES 5, EGTA 4.4, Na<sub>2</sub>ATP 5; leupeptin 0.1; (pH7.2;240 mosm/kg). Fresh Na<sub>2</sub>ATP and leupeptin were added to the solution each day. Cells of intermediate size (i.e. input capacitance, C<sub>in</sub> between 40 and 60pF) were selected for recording and held at -55mV using patch electrodes of 2-10 MΩ resistance (electrode resistance was usually between 4 and 6 M $\Omega$ ). Voltage was stepped from -55mV to 0mV at 4,5,10,20,30,45,60 or 90s intervals. 6-10 responses were recorded at each stimulus interval and data measurements made on the last response of each series. Data were not collected from cells in which there was an obvious run-down of Ca<sup>2+</sup> current. Also data were sometimes collected from experiments in which the stimulus frequency was progressively decreased (i.e. from a 4s interval to a 90s interval; see results and discussion sections).

Series resistance compensation was always at 80%. The error in clamp potential in recording a current of 6 nA, due to series resistance of 5M $\Omega$  at 80% compensation would be 6 mV. This would reflect a maximum error as most measured currents were <6nA. Cancellation of capacity transients and leak subtraction was done by applying mirror-image hyperpolarizing pulses stepping from -55mV to -110mV and adding.

Data were aquired using an Axoclamp 1B amplifier and stored on an IBM-XT computer fitted with a removable hard disk system (Bernoulli drive, Iomega Corp. Roy, UT, U.S.A.). The corner frequency of the filter was set to 2KHz during data acquisition. Steady-state currents and voltage commands were stored on a Gould-Brush 2400 pen recorder (pen rise time < 8ms). Permanent records were made from the hard disk using an XY plotter. Peak, end-of-pulse Ca<sup>2+</sup> currents were measured using Pclamp software (Axon Instruments, Burlingame, CA., USA). Tail current amplitudes were measured at their apparent peaks following subtraction of capacity currents and filtering at 2kHz. This procedure seemed appropriate for estimating the peak amplitudes of the relatively slow tail currents which would flow at the holding potential of -55mV. The integrals of Ca<sup>2+</sup> tail currents were determined using an area measuring programme (kindly provided by Prof. T. Gordon).

All drugs and chemicals were purchased from Sigma (St. Louis, MO., USA) except for ryanodine which was from Calbiochem (La Jolla, CA., USA).

#### 4.4 RESULTS.

## 4.4.1 Frequency-dependence of the a.h.p.

43 cells were studied using current-clamp microelectrode recording. 35 of these cells showed a reduction in a.h.p. duration as the interval between antidromic stimuli was decreased. When stimuli were elicited once every 90s, a.h.p. duration (at 50% amplitude) was 176.9±15.6ms (n=35). This was reduced to 70.1±3.8% of control when the stimulus interval was reduced to 2s. Recordings from a typical cell are shown in Fig 1A and all data (from 35 cells) are summarized graphically in Fig. 1B. After the decrease in duration at 2s stimulus interval, the rate and extent of the recovery of a.h.p. duration was somewhat variable. When the stimulus frequency was reduced to once per 90s, the a.h.p. duration recovered completely after 9 to 12 minutes in some cells whereas in others, it did not. The mean recovery at 15min was 94.6±3.2% (n=23; Fig 1B).

A.h.p. amplitude recorded at the 90s stimulus interval was  $31.3\pm5.2$ mV (n=35) and there was no significant change as the stimulus interval was shortened except for a slight decrease at stimulus intervals shorter than 5s (to  $93.32\pm0.9\%$  of control at 2s stimulus interval, n=35).

The amplitude and duration of the a.p. (spike height and spike width) did not show any significant change with increasing frequency of stimulation.

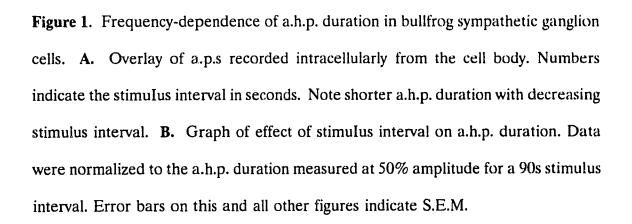
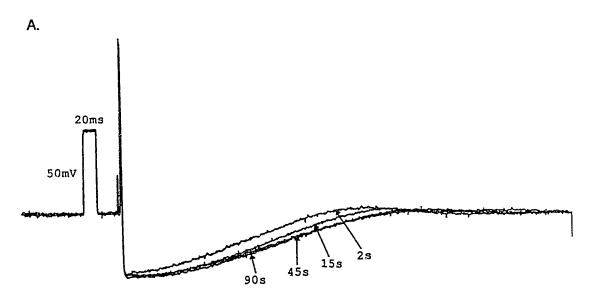
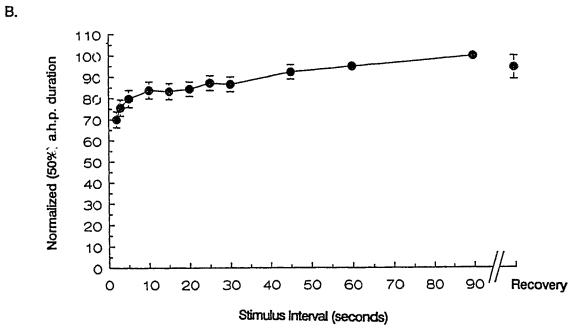


Figure 1



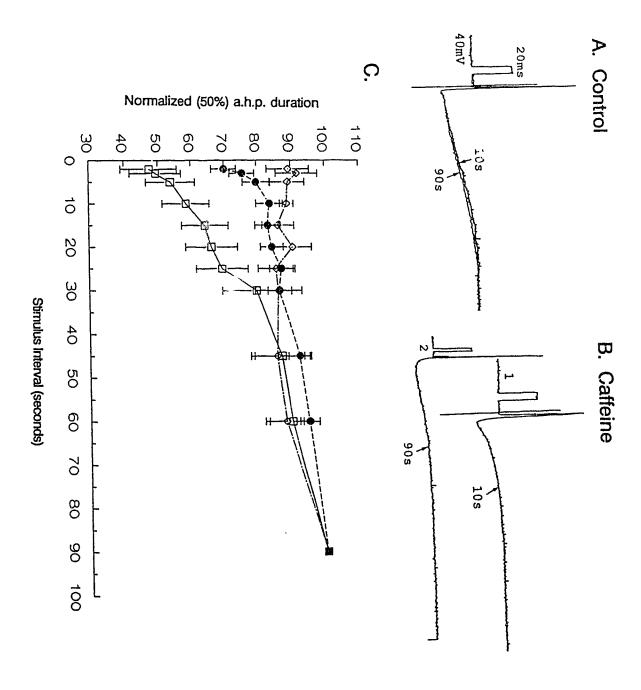


## 4.4.2 Effects of drugs on the frequency-dependence of the a.h.p.

In skeletal muscle sarcoplasmic reticulum, ryanodine (5µM) blocks the Ca<sup>2+</sup>release channel in an open state (Nagasaki & Fleischer, 1988) and 1µM ryanodine blocks the caffeine-induced elevation of intracellular Ca2+ in rat sympathetic neurones (Thayer et al., 1988). Prior to testing the effect of this drug on a.h.p. frequency-dependence in BFSG, it was necessary to establish that ryanodine affected the Ca<sup>2+</sup> induced-Ca<sup>2+</sup> release mechanism in this tissue. We therefore examined the effect of  $5\mu M$  ryanodine on the frequency-dependence of the a.h.p. which is seen in caffeine-treated cells. Under these conditions, a.h.p. frequency-dependence is known to depend on Ca<sup>2+</sup>-induced Ca<sup>2+</sup> release (Kuba, 1980; Kuba et al., 1983). Fig. 2A illustrates the small but significant frequency-dependence of the a.h.p. duration prior to the application of caffeine. After 5mM caffeine (Fig. 2B), the a.h.p. duration is increased and the frequency-dependence is accentuated. This effect, which was seen in all 11 cells tested, is illustrated graphically in Fig 2C; the normalized a.h.p. duration is reduced to less than 50% of control at the 2s time interval. However, when 2 cells were treated with  $5\mu$ M ryanodine + 5mM caffeine, the frequency-dependence of the a.h.p. was blocked (Fig 2C). This suggests that  $5\mu M$  ryanodine affects the  $Ca^{2+}$ release channel in BFSG neurones. Examination of the effects of ryanodine on a.h.p. frequency-dependence in normal (caffeine free) were terminated after just four cells had been examined because only small and variable effects were seen. Similar small and inconsistent effects were seen in two cells tested with ruthenium red  $(300\mu M)$ 

Figure 2. Effect of caffeine and ryanodine on frequeny-dependence of a.h.p. duration. A. Intracellular recordings from a typical cell prior to addition of caffeine, note that the a.h.p. of the a.p. recorded at the 10s stimulus interval is shorter than that recorded at 90s stimulus interval. B. Enhancement of the a.h.p. frequency-dependence in the presence of 5mM caffeine. Trace 1 recorded from the same cell as that in A. at 10s stimulus interval, Trace 2 recorded at 90s stimulus interval. Note difference in time base for these two records. C. Graphs to show effects of caffeine and caffeine + ryanodine on effect of stimulus interval on a.h.p. duration. Data were normalized to the a.h.p. duration measured at 50% amplitude for a 90s stimulus interval. • Control frequency-dependence.  $\Box$  Frequency-dependence seen in the presence of 5mM caffeine.  $\diamondsuit$  Frequency-dependence seen in the presence of 5mM ryanodine.

Figure 2.



and in two others tested with dantrolene Na (35 $\mu$ M). The inconsistent effect of ryanodine was unlikely to result from the 'use-dependent' nature of its action (Thayer et al., 1988) because in 2 of the cells tested, ryanodine failed to influence a.h.p. frequency-dependence after 4h of superfusion, during which time 4 tests of a.h.p. frequency-dependence were made.

# 4.4.3 Frequency-dependence of Ca<sup>2+</sup> influx.

If frequency-dependence of Ca2+ influx contributes to the frequencydependence of a.h.p. duration, this should be manifested in the frequencydependence of I<sub>Ca.</sub> This was examined using whole-cell recording from cells which were clamped at -55mV, which is close to the r.m.p. normally recorded with microelectrodes (Gordon et al., 1987). Ca2+ currents were elicited using 20 ms pulses to 0mV. Under these conditions, the peak, end-of-pulse and tail current amplitudes were reduced with increasing stimulus frequency. Some typical data records from experiments in which Ca2+ was used as a charge carrier are illustrated in Fig 3A and graphical data from 25 measurements on 17 cells is shown in Fig 3B. Data from 6 of the 17 cells were obtained starting at 4s intervals and increasing to 90s intervals and vice-versa; in 2 cells double measurements of frequency dependence were made using 90s intervals and decreasing to 4s intervals; in 2 cells data were obtained using increasing stimulus intervals only and in the remaining 7 cells, a single determination of frequency dependence was made using decreasing stimulus intervals only. All data were then pooled in an attempt to minimize any effects of  $I_{\text{Ca}}$  run-down (see Belles,

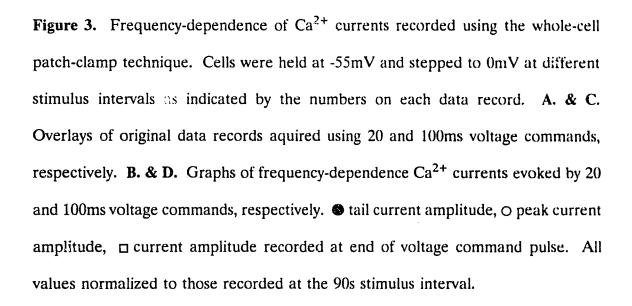
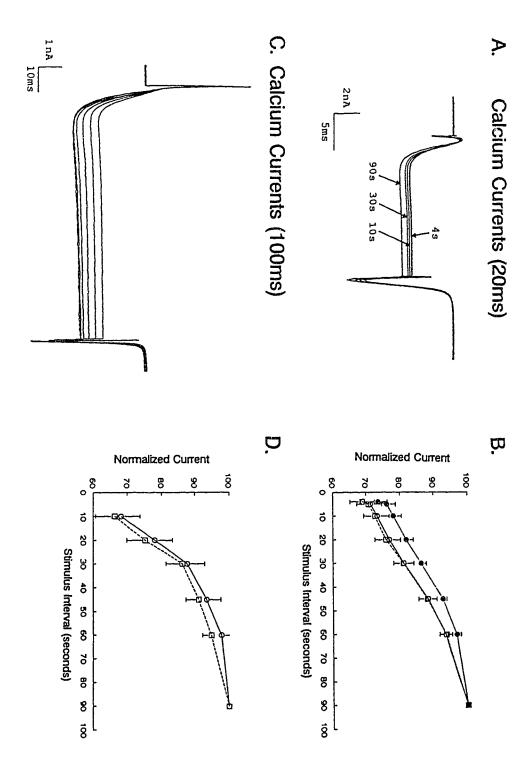


Figure 3.



Malecot, Heschler & Trautwein, 1988). At the 5s time interval, peak  $I_{Ca}$  was reduced to 71.5±3.6% of control, and tail current amplitude to 76.3±2.6% of control. A more pronounced frequency-dependence was seen when  $I_{Ca}$  was elicited using 100mspulses (Figs 3C & D). At the 10s time interval, the percentage changes in peak and end-of-pulse current amplitudes were significantly greater than those seen with the shorter, 20ms commands (P<0.005 and <0.001 respectively). Attempts were again made to minimize possible effects of  $I_{Ca}$  run-down and data were pooled from 17 determinations on 13 cells. For 100ms pulses, data from 4 of 13 cells were obtained starting at 4s intervals and increasing to 90s intervals and *vice-versa*; in 5 cells data were obtained using increasing stimulus intervals only and in the remaining 4 cells, a single determination of frequency-dependence was made using decreasing stimulus intervals only.

Since the frequency-dependence of  $I_{Ca}$  is a function of pulse length, this raises the possibility that accumulation of intracellular  $Ca^{2+}$  is responsible for the slow inactivation process (Eckert & Tillotson, 1981). This would seem unlikely because frequency-dependence was still observed when 2mM  $Ba^{2+}$  was used as a charge carrier (Fig. 4 cf. Jones & Marks, 1989b). For 100ms voltage commands, peak  $I_{Ba}$  was reduced to 62.9  $\pm$  3.7% of control at the 10s stimulus interval (n=5). There was, in fact more depression of  $I_{Ba}$  than  $I_{Ca}$  when both currents were compared at similar stimulus frequencies (P<0.01, for 100ms commands at 10s stimulus intervals, compare Figs 3 & 4).

At 0mV, Ca<sup>2+</sup> currents activate within 3ms (Adams, 1981; Jones & Marks,

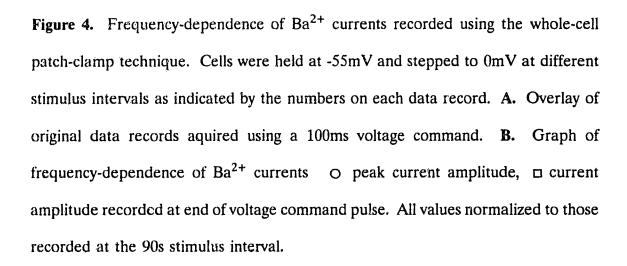
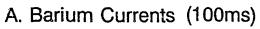
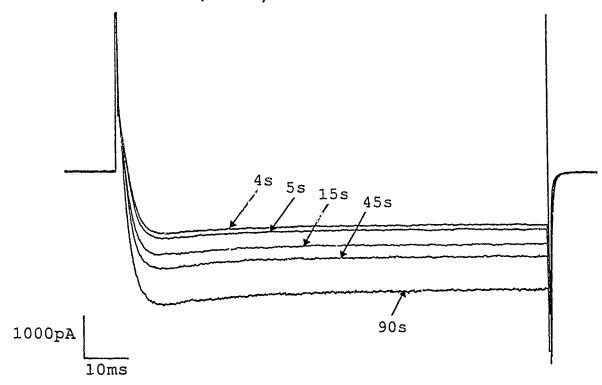
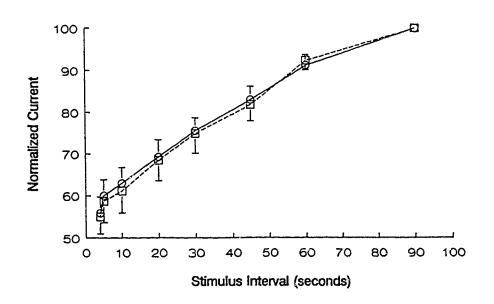


Figure 4.





B.



1989a), but since the a.p. only lasts 2-3ms, most of the  $Ca^{2+}$  influx accompanying the a.p. flows as a tail current during the initial phase of the a.h.p. (Lancaster & Pennefather 1987). An estimate of expected  $Ca^{2+}$  influx during an a.p. may therefore be obtained from measurements of tail current areas because the product of current and time (charge) is directly related to the amount of  $Ca^{2+}$  which enters. Fig 5A shows mean changes in tail current area seen in 14 cells in response to increasing stimulus frequency (duration of depolarizing voltage command was 20ms). Data on the frequency-dependence of the a.h.p. (as in Fig. 1B) are included for comparison. At the 5s stimulus interval, tail current area was reduced to 72.3  $\pm$  4.1% of control.

The amplitude and duration of the a.h.p. in BFSG B-cells is determined by two  $Ca^{2+}$  dependent  $K^+$  currents;  $I_C$  and  $I_{AHP}$  (Pennnefather et al.,1985; Lancaster et al.,1987; Goh and Pennefather,1987).  $I_C$  repolarizes the membrane after the a.p. and may determine a.h.p. amplitude whereas  $I_{AHP}$  is the primary determinant of a.h.p. duration. Since the amount of activation of  $I_{AHP}$  is dependent on the square of the intracellular  $Ca^{2+}$  concentration (Yamada, Koch & Adams, 1989) there should be a correlation between the square of the  $I_{Ca}$  tail area and a.h.p. duration, if the frequency dependence of a.h.p. is determined by the frequency-dependence of  $I_{Ca}$ . When these two parameters were compared at each stimulus frequency, an excellent correlation was observed (r = 0.94; see Fig 5B).

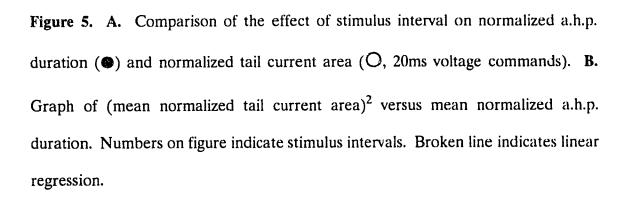
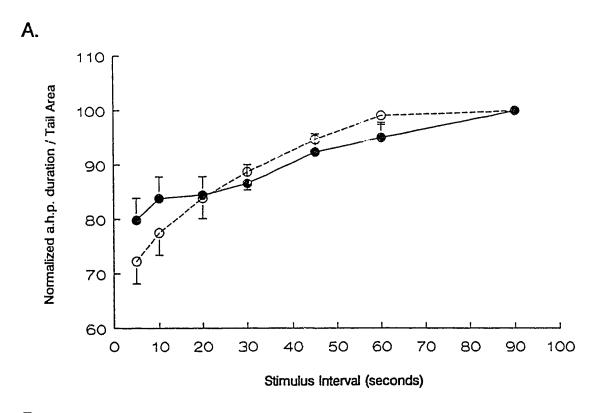
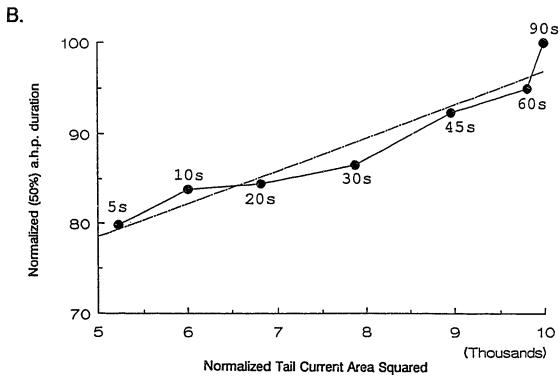


Figure 5.





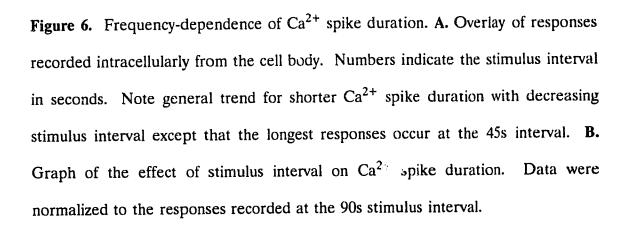
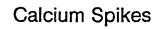
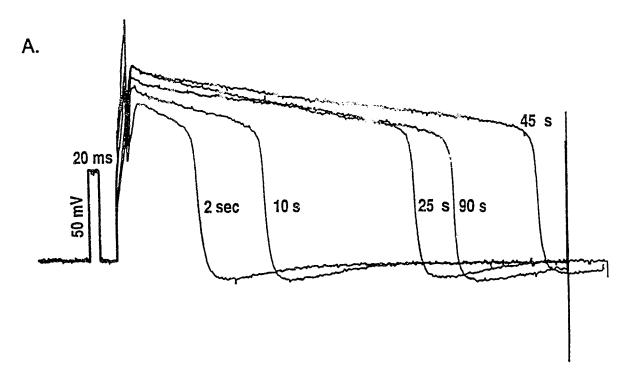
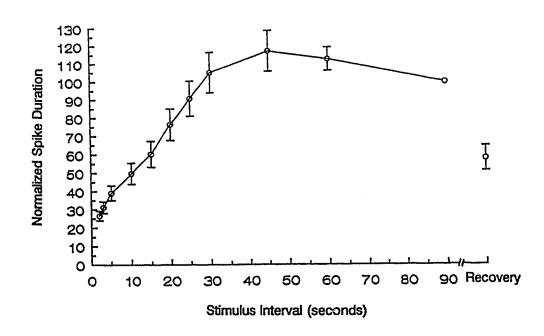


Figure 6.





В.



## 4.4.4 Frequency-dependence of Ca<sup>2+</sup> spikes

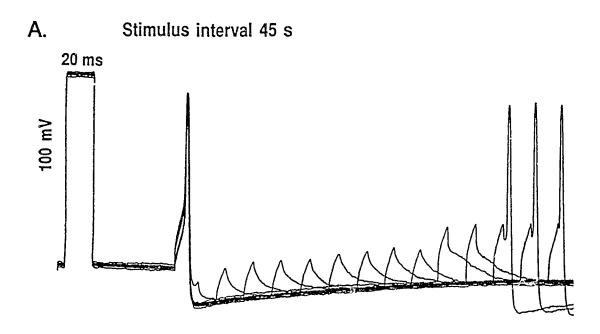
Despite the randomization of the stimulus paradigms, apparent frequency-dependence of  $Ca^{2+}$  currents recorded during whole-cell recording inevitably leads to concerns relating to current run-down and/or improvement of currents as the intracellular solution diffuses into the cell. We therefore used microelectrodes to record  $Ca^{2+}$  spikes from intact BFSG cells and examined their frequency-dependence. As shown in Fig. 6, the duration of the  $Ca^{2+}$  spikes exhibited a strong frequency-dependence. The mean spike duration was  $429\pm41.2$  ms at 90s stimulus interval and was reduced to  $39.2\pm4\%$  (n=12) of this control value at the 5s stimulus interval. Unlike the frequency-dependence of  $I_{Ca}$  amplitude,  $Ca^{2+}$  spikes reached a maximum duration at the 45s stimulus interval.

## 4.4.5 Significance of a.h.p. frequency-dependence.

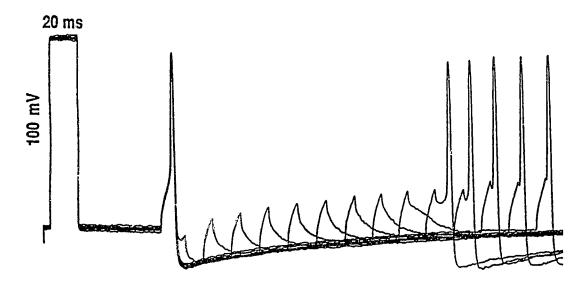
If a.h.p. frequency-dependence is important for the operation of an intact neuronal system, it should be shown that changes in a.h.p. duration can affect neuronal integrative properties. An experiment of this type is shown in Fig 7. A.p.'s were elicited by injecting brief, depolarizing current pulses via the microelectrode. The pulses were paired, and the delay between the pulses increased by 20ms in each succesive trial. When trials were performed once every 45s (Fig 7A), the a.h.p. was long and many of the injected current pulses which were paired with the first stimulus pulse failed to elicit a second a.p. Suprathreshold a.p.'s were only elicited at the three longest stimulus delays. On the other hand, when trials were performed every

Figure 7. Effect of frequency-dependence of a.h.p. duration on excitability. A. Overlay of responses to paired intracellular stimulation using 8ms 0.3nA current commands. Pairs of stimuli were delivered once every 45s and the delay between the two stimuli increased by 20ms for each succesive trace. B. As in A except that paired stimuli with increasing interstimulus delays were delivered once every 3s. Note that the a.h.p.'s in B are shorter than those seen in A and this is reflected in the generation of a.p.'s at shorter interstimulus delays. Traces in A & B recorded from the same cell.

Figure 7.







3s, the a.h.p. was shorter and the current pulses paired with the first stimulus were slightly more effective in eliciting a.p.'s. Under these conditions, the five longest intervals were effective in bringing the membrane to threshold for a.p. generation (Fig 7B).

#### 4.5 DISCUSSION.

The present results show that the a.h.p. duration of BFSG B-cells is frequency-dependent and that this phenomenon can be observed under conditions where the neurones have not been manipulated pharmacologically so as to enhance Ca<sup>2+</sup>-induced Ca<sup>2+</sup> release (cf. Kuba et al., 1983).

Accumulation of extracellular K<sup>+</sup> (Lancaster & Pennefather, 1987; Yamada et al., 1989) is unlikely to account for the frequency-dependence of a.h.p. duration because, for most stimulus intervals, a.h.p. amplitude was unchanged. Some accumulation of K<sup>+</sup> may have occurred at short stimulus intervals (2-5s) because both a.h.p. amplitude and duration were affected at these frequencies.

The absence of clear effects of ryanodine, dantrolene and ruthenium red argue against the hypothesis that  $Ca^{2+}$ -induced  $Ca^{2+}$  release is a major determinant of a.h.p. frequency-dependence under normal conditions. On the other hand, the excellent correlation between  $Ca^{2+}$  influx and a.h.p. duration in BFSG favours the explanation that the frequency-dependence is entirely attributable to slow inactivation of  $I_{Ca}$ .

If this hypothesis is accepted, it is difficult to explain why ryanodine, which fails

to affect control cells, promotes *total* loss of a.h.p. frequency-dependence in caffeine-treated cells (Fig 2C). Although this result suggests that ryanodine blocks frequency-dependence resulting from to  $Ca^{2+}$ -induced  $Ca^{2+}$  release, the slow inactivation of  $I_{Ca}$  should still persist such that *some* frequency-dependence of the a.h.p. should be retained under these conditions. Another concern relates to the effect of pulse length on  $I_{Ca}$  frequency-dependence because the frequency-dependence for 20ms voltage commands is less than that for 100ms commands (see Fig 3). Since the exact mathematical relationship between pulse length and frequency-dependence is unknown, it is impossible to predict whether the brief (2-3ms)  $Ca^{2+}$  currents, which would be evoked during normal a.p's, would exhibit frequency-dependence. Nevertheless, the correlation between frequency-dependence of  $I_{Ca}$  tails which follow 20ms voltage commands and the frequency-dependence of a.h.p. duration suggests that the frequency dependence must be maintained for short-duration  $Ca^{2+}$  currents.

The lack of involvement of Ca<sup>2+</sup>-induced Ca<sup>2+</sup> release in the generation of the frequency-dependence of the a.h.p. in BFSG contrasts with results from rat sympathetic neurones where it has been reported that ryanodine suppresses the frequency-dependent component of the a.h.p. (Kawai & Watenabe 1991 but see also Thayer *et al.*, 1988).

Despite the randomization of the stimulus paradigms and the demonstration that  $I_{Ca}$  exhibits frequency-dependence with both increasing and decreasing stimulus intervals, data obtained using whole-cell recording inevitably raises concerns relating to current run-down and/or improvement of currents as the intracellular solution

### 4.6 REFERENCES

ADAMS, P.R. (1981). The calcium current of a vertebrate neuron. Advances in Physiological Sciences 4 In Physiology of excitable membranes Ed. J. Salanki, Pergamon, New York, pp 135-138.

ADAMS, P.R.; JONES, S.W.; PENNEFATHER, P.; BROWN, D.A.; KOCH, C. & LANCASTER, B. (1986). Slow synaptic transmission in frog sympathetic ganglia. Journal of Experimental Biology 124 259-285.

BELLES, B.; MALECOT, C.O.; HESCHLER, J. & TRAUTWEIN, W. (1988) Run-down of the Ca<sup>2+</sup> current during whole-cell recordings in guinea pig heart cells: role of phosphorylation and intracellular calcium. *Pflugers Archiv* **411** 353-360.

CZEH, G.; GALLEGO, R.; KUDO, N. & KUNO, M. (1978) Evidence for the maintenance of motoneuronal properties by muscle activity. *Journal of Physiology* **281** 239-251.

ECKERT, R. & TILLOTSON, D. (1981) Calcium mediated inactivation of the calcium conductance in caesium loaded giant neurones of *Aplysia californica*. *Journal of Physiology* **314** 99-108.

FOWLER, J.C.; GREEN, B. & WEINREICH, D. (1985) Two calcium sensitive spike afterhyperpolarizations in visceral sensory neurones of the rabbit. *Journal of Physiology* **365** 59-75.

GOH, J.W. & PENNEFATHER, P.S. (1987) Pharmacological and physiological properties of the afterhyperpolarization current of bullfrog ganglion neurones. *Journal of Physiology* **394** 315-330.

GORDON, T.; KELLY, M.E.M.; SANDERS, E.J.; SHAPIRO, J. & SMITH, P.A. (1987). The effect of axotomy on bullfrog sympathetic neurones. *Journal of Physiology* **392** 213-229.

JASSAR, B.S. & SMITH, P.A. (1990) Frequency-dependence of afterhyperpolarization in bullfrog sympathetic neurones. *Society for Neuroscience Abstracts* **16** 678.

JONES, S.W. & MARKS, T.N. (1989a) Calcium currents in bullfrog sympathetic neurones; I Activation kinetics and pharmacology. *Journal of General Physiology* 94 151-167.

JONES, S.W. & MARKS, T.N. (1989b) Calcium currents in bullfrog sympathetic neurones; II Inactivation. *Journal of General Physiology* **94** 169-182.

KAWAI, T. & WATANABE, M. (1991) Ryanodine suppresses the frequency-dependent component of the spike after-hyperpolarization in the rat superior cervical ganglion. *Japanese Journal of Pharmacology* **55** 367-374.

KRNJEVIC, K.; PUIL, E. & WERMAN, R. (1978) EGTA and motoneuronal afterpotentials. *Journal of Physiology* **275** 199-223.

KUBA, K. (1980) Release of calcium ions linked to the activation of potassium conductance in a caffeine-treated sympathetic neurone. *Journal of Physiology* **298** 251-269.

KUBA, K.; MORITA, K. & NOHMI, M. (1983) Origin of calcium ions involved in the generation of a slow afterhyperpolarization in bullfrog sympathetic neurones. *Pflugers Archives* **399** 194-202.

KUBA, K. & NISHI, S. (1976) Rhythmic hyperpolarization and depolarization of sympathetic ganglion cells induced by caffeine. *Journal of Neurophysiology* **39** 547-563.

KUNO, M.; MIYATA, Y. & MUNOZ-MARTINEZ, E.J. (1974) Differential reactions of slow and fast motoneurones to axotomy. *Journal of Physiology* **240** 725-739.

LANCASTER, B. & PENNEFATHER, P. (1987). Potassium currents evoked by brief

depolarizations in bull-frog sympathetic ganglion cells. *Journal of Physiology* **387** 519-548.

LIPSCOMBE, D.; MADISON, D.V.; POENIE, M.; REUTER, H., TSIEN, R.W. & TSIEN, R.Y. (1988). Imaging of cytosolic Ca transients arising from Ca stores and Ca channels in sympathetic neurones. *Neuron* 1 335-365.

LUX, H.D. & HEYER, C.E. (1977). An aequorin study of a facilitating calcium current in bursting pacemaker neurons of Helix. *Neuroscience* 2 585-592.

LUX, H.D. & HOFMEIER, G. (1982a) Properties of a calcium- and voltage-activated potassium current in *Helix pomatia* neurons. *Pflugers Archiv* **394** 61-69.

Lux, H.D. & Hofmeier, G. (1982b) Activation characteristics of the calciumdependent outward potassium current in Helix. *Pflugers Archiv* 394 70-77.

MADISON, D.V. & NICOLL, R.A. (1986) Actions of noradrenaline recorded intracellularly in rat hippocampal Cal pyramidal neurones in vitro. *Journal of Physiology* 372 221-244.

NAGASAKI, K. & FLEISCHER, S. (1988) Ryanodine sensitivity of the calcium release channel of sarcoplasmic reticulum. *Cell Calcium* 9 1-7.

PENNEFATHER, P.; LANCASTER, B.; ADAMS, P.R. & NICOLL, R.A. (1985). Two distinct Ca<sup>2+</sup> dependent K<sup>+</sup> currents in bullfrog sympathetic ganglion cells. *Proceedings of the National Academy of Sciences of USA* 82 3040-3044.

SCHOUTEN, V.J.A. & MORAD, M. (1989). Regulation of Ca<sup>2+</sup> current in frog ventricular myocytes by the holding potential, cyclic AMP and frequency. *Pflugers Archiv* 415 1-11.

SELYANKO, A.A.; SMITH, P.A. & ZIDICHOUSKI, J.A. (1990). Effects of muscarine and adrenaline on neurones from *Rana pipiens* sympathetic ganglion. *Journal of Physiology* 425 471-500.

SMITH, P.A. & WEIGHT, F.F. (1986). The synaptic pathway for the slow inhibitory postsynaptic potential in amphibian sympathetic ganglia. *Journal of Neurophysiology* **56** 823-834.

THAYER, S.A.; HIRNING, L.D. & MILLER, R.J. (1988). The role of caffeine-sensitive calcium stores in the regulation of the intracellular free calcium concentration in rat sympathetic neurones *in vitro*. *Molecular Pharmacology* **34** 664-673.

TITMUS, M.J. & FABER, D.S. (1990) Axotomy-induced alterations in the electrophysiological characteristics of neurones. *Progress in Neurobiology* 35 1-51.

TOKIMASA, T. (1984a) Calcium dependent hyperpolarization in bullfrog sympathetic neurones. *Neruoscience* 12 929-937.

TOKIMASA, T. (1984b) Muscarinic agonists depress calcium dependent gk in bullfrog sympathetic neurones. *Journal of Autonomic Nervous System* **10** 107-116.

YAMADA, W.M.; KOCH, C. & ADAMS, P.R. (1989) Multiple channels and calcium dynamics, in *Methods in Neuronal Modeling: from Synapses to Networks* Ed. C KOCH and Segev I. MIT Press Cambridge pp97-133.

# CHAPTER 5.

GENERAL DISCUSSION.

#### 5.1 Introduction.

The work presented in this thesis is concerned with 'exogenous' and 'endogenous' of regulation of the action potential (a.p.) and its afterhyperpolarization (ahp) in bullfrog sympathetic ganglion (BFSG) cells. The experiments on effects of axotomy on ion channels suggest that alteration of, at least one aspect of, 'exogenous' regulation which is normally present due to the continuity of the axon and or the interaction between the neurone and its target, is responsible for the axotomy-induced changes in ion channels. In addition, the data on the frequency-dependence of ahp duration demonstrate the presence of 'endogenous' regulation which results from the intrinsic properties of the membrane  $Ca^{2+}$  channels. Many of the more specific points which can be raised or explained have been discussed along with the data in previous chapters (2, 3 & 4). Here, the general points which have not been addressed or described will be discussed.

### 5.2 Frequency-dependence of action potential afterhyperpolarization

When the frequency of stimulation is increased from 0.012Hz to 0.5Hz the duration of ahp is decreased. The possible physiological relevance of this effect is discussed in chapter 4. Thus ahp frequency-dependence represents a way of modulating the excitability of the neurone. This 'endogenous' means of modulation results from intrinsic properties of Ca<sup>2+</sup> channels (slow inactivation).

Axotomy results in a decrease in the amplitude and duration of the ahp that follows a 'single' a.p. in BFSG B-cells. Since caffeine enhances Ca<sup>2+</sup>-induced Ca<sup>2+</sup>

release and thereby prolongs ahp duration (Kuba & Nishi, 1976; Kuba, 1980), this raises concerns about the possible contribution of Ca<sup>2+</sup>-induced Ca<sup>2+</sup> release to the generation of the normal ahp (Kuba, Morita & Nohmi, 1983) and the modification of this process after axotomy. However, results of the present study on the frequency-dependence of ahp clearly show that the Ca<sup>2+</sup>-induced Ca<sup>2+</sup> release is not primed by a single a.p. Also the time constants of decay of I<sub>AHP</sub> as well as intracellular Ca<sup>2+</sup> level is not altered in axotomized neurones (Chapter 3) which suggests that the mechanisms of sequestration of Ca<sup>2+</sup> are not changed. Therefore the changes in intracellular Ca<sup>2+</sup> dynamics should not be a matter of concern in investigating the mechanisms underlying axotomy-induced changes in ahp following single a.p.

### 5.3 Axotomy-induced changes in ion channels

Axotomy affects almost all of the voltage- and  $Ca^{2+}$ -activated channels, either increasing or decreasing the whole-cell currents in BFSG B-cells. However, all the currents are not affected in the same way. There is a decrease in whole-cell  $I_{Ca}$ ,  $I_{K}$ ,  $I_{A}$ ,  $I_{C}$  and  $I_{AHP}$  whereas  $I_{Na}$  and  $I_{M}$  are increased. This shows that these different currents are differentially regulated by 'exogenous' influences which act upon these cells. This type of regulation of ion channels could occur at the pre-translational or at post-translational level. Pre-translational modification can result in structural modification of single channels through mechanisms such as up- or down-regulation of mRNAs encoding for a channel or channel subunit. This would result in a change

in the absolute number of ion channels in the membrane or in a change in the subunit stoichiometry of the channel macromolecule. In addition, changes may reflect alternative splicing of the mRNA or change in mRNA structure. Post-translational mechanisms might include changes in single channel properties due a change in the level of second-messengers or destabilization of channel macromolales resulting from disruption or loss of cytoskeletal elements.

# 5.3.1 Changes in Ca<sup>2+</sup> channels

The prominent change observed in currents mediated by  $Ba^{2+}$  through  $Ca^{2+}$  channels ( $I_{Ba}$ ) was a decrease in whole-cell currents and an enhancement of inactivation. Although the increased inactivation could certainly account for the major portion of the reduction in  $I_{Ba}$ , a decrease in the absolute number of membrane  $Ca^{2+}$  channels can not be ruled out by these experiments. Possible mechanism/s for the decrease in the whole-cell currents which may result from changes in channel macromolecule itself or a changes in phosphorylation status or a decrease in the number of  $Ca^{2+}$  channels are discussed below.

### 5.3.1.1 Phosphorylation state of channels

Since an increase in phosphorylation increases inactivation of N-type Ca<sup>2+</sup> channels in BFSG B-cells (Wertz, Elmslie & Jones, 1993), it is possible that an increased level of phosphorylation of N-type Ca<sup>2+</sup> channels may be responsible for the axotomy-induced reduction in I<sub>Ba</sub>. This possibility is difficult to reconcile with the

recently reported enhancement of  $I_{Ba}$  suggested to be mediated by activation of protein kinase C (Yang & Tsien, 1993). However, the two opposite effects may be seen if the phosphorylation in these two instances involves two different consensus sequences located in different parts of the molecule each one having a different effect. The concentrations of phorbol-dibutyrate (1 $\mu$ M), nimodipine (10 $\mu$ M), Bay K 8644 (1 $\mu$ M) and  $\omega$ -conotoxin used in this study by Yang and Tsien were relatively higher than required for the specific actions of these compounds (*see* Jones & Jacobs, 1990). This leads to concerns relating to non-specific pharmacological effects of these compounds.

### 5.3.1.2 Change in channel macromolecule and/or G-protein activation

As mentioned in chapter 1 (section 1.2.2), co-expression of  $\alpha 1$ ,  $\alpha$ -2/ $\delta$ ,  $\beta$  and  $\gamma$  subunits of L-type Ca<sup>2+</sup> channels in Xenopus oocyte and in LCa.II cell lines results in an increase in the absolute amount of the whole-cell  $I_{Ca}$  along with an increase in rate of activation and inactivation compared to expression of  $\alpha$ -1 subunit alone (Singer, Biel, Lotan, Flockerzi, Hoffman & Dascal, 1991; Varadi, Lory, Schulz, Varadi & Schwartz, 1991). Thus a change in stoichiometry of channel subunits does not seem to be the basis for axotomy-induced changes in BFSG B-cells because such a change would affect both the activation and inactivation profiles of  $I_{Ba}$  The data show that only inactivation is enhanced and activation/ deactivation kinetics are not significantly altered. This also rules out the involvement of G-protein activation in  $I_{Ba}$  reduction because this process would be expected to change the activation kinetics

of the current (Elmslie, Zhou & Jones, 1990).

# 5.3.1.3 Cytoskeleton and Ca<sup>2+</sup> channels

Inclusion of ATP in the patch pipette reduces 'rundown' of  $I_{Ba}$  in excised patches; destabilization of cytoskeletal elements by colchicine and cytochalasin B blocks the reduction of "rundown" by inclusion of ATP in the patch pipette. Moreover addition of the cytoskeletal stabilizers, taxol and phalloidin reduce rundown even in the absence of ATP and also decrease Ca2+-dependent inactivation of I<sub>Ca</sub> (Johnson & Byerly, 1993). This data suggests that Ca<sup>2+</sup> channels might be attached to an interconnected network of microtubules and microfilaments which might be subject to regulation by some phosphorylation mechanism/s. Thus, disruption of this cytoskeleton may be responsible for channel rundown and increased Ca2+-dependent inactivation of  $Ca^{2+}$  channels. Further, the selective reduction of  $V_{max}$  of the  $Ca^{2+}$ spikes by colchicine also suggests an association between Ca2+ channels and microtubules (Fukuda, Kamayema & Yamaguchi, 1981). Since axotomy results in disruption of cytoskeletal elements (Hoffman & Lasek, 1980; Hall, Virginia, Lee & Kosik, 1991), it is tempting to suggest that at least part of the reduction in  $I_{\text{Ba}}$  may be due to the disruption of cytoskeletal elements in axotomized neurones. This possibility can be tested experimentally (see 5.8).

### 5.3.2 Changes in Na<sup>+</sup> channels.

The axotomy-induced increase in  $I_{\mathrm{Na}}$  is unlikely to reflect increases in

phosphorylation because at least in squid axon, phosphorylation causes substantial decrease in Na<sup>+</sup> currents (Dascal & Lotan, 1991; Li, West, Lai, Scheuer & Catterall, 1992). The increase in  $I_{Na}$  also cannot be explained by a disruption of cytoskeletal elements because that might be expected to decrease I<sub>Na</sub> (Fukuda, Kamayema & Yamaguchi, 1981). The co-expression of  $\alpha$  and  $\beta$  subunits is necessary for inducing channels with kinetic properties similar to those of native Na<sup>+</sup> channels (Catterall, 1988; Isom, DeJongh, Rebber, Offord, Charbonneau, Walsh, Goldin & Catterall, 1992). Since the activation and inactivation properties of whole-cell currents were unchanged after axotomy, the axotomy-induced increase in  $I_{Na}$  is unlikely to result from changes in subunit stoleans and the in channel structure. If an increased number of Na+ channels appear in the cell membrane of the soma, this would reflect increased synthesis or decreased degradation of the channels. This possibility was not examined in this study. Alternatively, it may simply be a redistribution and localization of channels (Wollner & Catterall, 1986) in soma membrane due to loss of axon or a part of the neurone where these (extra) channels would be inserted normally.

# 5.3.3 Changes in Ca<sup>2+</sup>-activated K<sup>+</sup> channels

As shown in chapter 3, the axotomy-induced changes in  $I_{Ba}$  predict the observed reduction in  $I_{C}$  and  $I_{AHP}$ . This suggests that the changes observed in both of these  $Ca^{2+}$ -activated  $K^+$  conductances are due to the changes in  $I_{Ca}$ . Moreover, the amplitude of  $I_{C}$  tails following depolarization to +70 mV from a holding potential

of -80mV (where  $Ca^{2+}$  influx is already saturated and the sensitivity of  $I_C$  channels to  $Ca^{2+}$  is increased) is not affected by axotomy. Also, the amplitude of  $I_{AHP}$  is similar for  $Ca^{2+}$  influxes of similar magnitude in control and axotomized neurones (see Fig. 7; Chapter 3). Since microspectrofluorometric measurements of intracellular  $Ca^{2+}$  using Fura-2 showed that the levels were not changed and the rate of decay of  $I_{AHP}$  for responses of similar amplitude was also not affected, this suggests that the number of  $I_C$  and  $I_{AHP}$  channels is not changed after axotomy i.e. these particular conductances are not altered following interruption of the contact of neurone with its target. Using mathematical model for various currents we show that the changes observed in  $I_{Ba}$  ( $I_{Ca}$ ) and the concomitant reduction in  $I_C$  and  $I_{AHP}$  can explain the prominent changes observed in the action potential (i.e. an increase in duration of action potential and a decrease in the amplitude and duration of the afterhyperpolarization) after axotomy.

An interesting observation from the modelling results is the requirement for high local concentration of  $Ce^{2\pi}$ , in the vicinity of the  $I_C$  channels, for their optimum activation. As suggested in discussion in chapter 3 this could result either from slow diffusion or from co-localization of the  $Ca^{2+}$  and maxi- $K^+$  channels. Such a co-localization of these two types of channels has been reported in the presynaptic active zones of hair cells (Roberts, Jacobs & Hudspeth, 1990). This kind of co-localization of  $Ca^{2+}$  and  $Ca^{2+}$ -activated  $K^+$  channels might be a common mechanism in many different neuronal types for keeping the excitability under check, and for limiting the duration of the depolarization phase of the a.p. This would restrict the entry of

extracellular Ca2+ which is potentially cytotoxic (Young, 1992).

# 5.3.4 Changes in voltage-activated K<sup>+</sup> channels

Phosphorylation of M-channels and delayed rectifier-type  $K^+$  channels can affect the amount of current available for activation at a given voltage. For example, larger  $I_M$  can be elicited by including higher levels of ATP in the patch pipette (P.S. Pennefather, *personal communications*). At least in perfused squid giant axon, higher levels of ATP in the internal solution leads to larger amounts of  $I_K$  with slower activation kinetics (Augustine & Bezanilla, 1990; Perozo & Bezanilla, 1991). Thus, although the increase in  $I_M$  could be explained by increased phosphorylation, it can not explain the decrease in  $I_K$ . Moreover, since the activation/deactivation kinetics of  $I_K$  are not changed, it is likely that the decrease in  $I_K$  results from a decrease in the number of channels or a shift to the left in steady-state inactivation curve.

 $I_A$  and  $I_{SA}$  was practically absent after axotomy. It is very interesting to note that all cells which failed to express  $I_A$  also failed to express  $I_{SA}$ . This suggests that the two channels may be regulated similarly and perhaps comprise very similar channel macromolecules. They may arise from same gene and the differences may be due to very small changes in the gene either at transcriptional or post-transcriptional level. A single  $K^+$  channel cDNA when expressed in a *Xenopus* oocyte can exhibit different gating modes. A low level of expression results in fast inactivating A-type current and high level of expression leads to induction of  $K^+$  channels with delayed rectifier type, slowly inactivating macroscopic currents (Moran,

Schreibmayer, Weigl, Dascal & Lotan, 1992). Thus, the same cRNA can give rise to two different kinds of K<sup>+</sup> channels. There is a significant degree of sequence homology between cDNAs for different voltage-gated K<sup>+</sup> channels. Therefore, it is likely that a slight change in expression level or in alternative splicing (Luneau, Williams, Marshall, Levitan, Oliva, Smith, Antanavage, Folander, Stein, Swanson, Kaczmarek & Buhrow, 1991) can lead to changes in ion channel expression which can be manifested as the changes observed in currents through different voltage-gated K<sup>+</sup> channels i.e. A-type, the delayed rectifier K<sup>+</sup> and the muscarine-sensitive K<sup>+</sup> (M-) channels.

### 5.4 Intracellular Calcium

Since steady-state intracellular Ca<sup>2+</sup> level in the cell body was not chronically changed after axotomy, reduction in Ca<sup>2+</sup>-currents may be a mechanism for limiting Ca<sup>2+</sup>-influx in the already injured neurone. The cytotoxic effects of high levels of intracellular Ca<sup>2+</sup> are well documented (Young, 1992). On the other hand, the increase in the duration of a.p. resulting from slowing of the fast repolarization phase may compensate for the decreased number of activatable Ca<sup>2+</sup> channels and thus ensure an optimum influx of Ca<sup>2+</sup>. An increase in Ca<sup>2+</sup> is required to turn on 'immediate early genes' (Morgan & Curran, 1988; Murphy, Worley & Baraban, 1991) which might be for responsible for initiating some of changes in ionic conductances as well as the processes essential for regeneration and repair. Only a transient increase in intracellular Ca<sup>2+</sup> is required for turning on these genes because

pharmacological blockade of depolarization-induced Ca<sup>2+</sup> influx into cortical neurones after 15min of influx is not effective in inhibiting the expression of immediate early genes (Morgan & Curran, 1988; Murphy *et al.*, 1991). Intracellular Ca<sup>2+</sup> has been reported to increase transiently for 5-10min after axon transection in snail neurones (Davenport, Dou, Rehder & Kater, 1992). This type of transient increase can not be ruled out in the present study because the intracellular Ca<sup>2+</sup> levels were not monitored over the whole time period of the response (only levels 13-15d after axotomy were measured). Results on Ca<sup>2+</sup>-activated K<sup>+</sup> currents suggest that buffering capacity of the cytoplasm was not altered after axotomy as the time constant of decay of I<sub>AHP</sub> and kinetics of I<sub>C</sub> were not altered. The reduced Ca<sup>2+</sup> influx and the unaltered Ca<sup>2+</sup> buffering will keep the intracellular Ca<sup>2+</sup> levels more stable of the periods of time which will be beneficial for the already vulnerable neurone.

### 5.5 Dedifferentiation and Axotomy

Axotomy results in a stereotypic pattern of morphological responses as well as a reordering of protein synthesis in neuronal perikaryon ('axon reaction'; Lieberman, 1971) which might be specifically geared for axonal outgrowth and regeneration (Grafstein & McQuarrie, 1978). Thus, axotomy shifts a neurone from a 'mature transmitting' mode to a 'growing regenerating' mode. Based on this hypothesis the effects of axotomy are often discussed in terms of reversion of the mature neurone to an 'immature state'. This dedifferentiation is assumed to

recapitulate the developmental pattern of growth (Hoffman & Cleveland, 1988 but see also Svensson & Aldskogius, 1992). However many of the present results fail to lend support to this hypothesis.

In many neuronal types, during development, the action potential changes from a Ca<sup>2+</sup>-dependent one to a Na<sup>+</sup>-dependent one (Spitzer, 1979). However, axotomy of BFSG B-cells results in a decrease in  $I_{\text{Ca}}$  and an increase in  $I_{\text{Na}}$ . The changes observed in steady-state inactivation of IBa after axotomy also argue against such a dedifferentiation hypothesis since the steady-state inactivation for  $I_{\text{Ba}}$  shifts to the left when PC12 cells are stimulated to acquire a neuronal phenotype following NGF treatment (Streit & Lux, 1990). Although the evidence suggests that axotomy does not result in dedifferentiation, no firm conclusion can be drawn in the absence of data on developmental timetable of the expression of ion channels in BFSG Bcells. Moreover, exceptions to the general rule of switching of the ionic-dependence of a.p. from a Ca2+-dependent to Na+-dependent have already been reported (Bader, Bertrand, Dupin & Kato, 1983; Barish, 1986) and the developmental timetable of different neuronal types has to be worked out better than it is today to reach any unified general hypothesis about expression of ion channels during differentiation.

### 5.6 Dependence of ion channels on an intact axon.

The effects of axotomy strongly suggest that the membrane ion channels are differentially regulated by some 'exogenous' influences. However, this regulation is

differential in that Ca<sup>2+</sup>, Na<sup>+</sup>, M-type, A-type and delayed rectifier-type channels are subject to regulation whereas maxi K<sup>+</sup> channels and AHP channels are not. Regeneration restores some of the altered properties of the axotomized BFSG cells (Kelly, Bisby & Lukowiak, 1988). The onset of the changes is rapid and recovery is slow after a cut lesion; and *vice versa* for crush lesions. Ahp duration returns to control values in about 8 weeks after a crush lesion whereas the duration of the action potential (longer than control) and the amplitude of ahp (smaller than control) do not. The data thus suggests a differential regulation of these parameters of a.p. and thus indirectly of the conductances underlying them. The physiological correlates of 'exogenous' influences could not be ascertained in this study and further experiments are necessary to delineate the involvement and exact role of various possible factors.

### 5.7 Possible mechanisms of axtromy-induced changes

Axotomy of a neurone results in several responses which include morphological, biochemical and electrophysiological alterations. Furthermore, each one of these categories includes several different components. The complex nature of response suggests that there may be many factors involved in axotomy-induced response, each one playing a specific role. The possible factors involved in some of the axotomy-induced changes are discussed below.

### 5.7.1 Trophic factors

Axotomy leads to loss of interaction between the neurone and its target tissue. Since target-derived trophic factors have been shown to be responsible for survival, regeneration and sprouting of different neuronal types (Meakin & Shooter, 1992), it is possible that axotomy prevents retrograde transport of the trophic factor/s to soma. Several neurotrophic factors have been identified in brain and peripheral nerves which include nerve growth factor (NGF), brain-derived neurotrophic factor (BDNF), neurotrophin-3 (NT-3), neurotrophin-4 (NT-4), acidic fibroblast growth factor (FGF), basic FGF, ciliary neurotrophic factor (CNTF) etc. Out of these factors NGF, FGF and possibly also BDNF are potential candidates which may be involved in survival, differentiation and regeneration of sympathetic neurones (Rich, 1992).

Since NGF has been shown to regulate a.p. duration in mature sensory neurones (Chalazonitis, Peterson & Crain, 1987), it is possible that the loss of retrograde supply of this trophic factor may be responsible for axotomy-induced changes in BFSG cells. These cells show axotomy-like changes when grown in explant cultures in the absence of NGF i.e. there is an increase in the duration of the a.p. and a decrease in the amplitude and duration of ahp. However NGF can be only partly responsible for maintenance of these properties. Although addition of NGF to the culture medium attenuates decrease in ahp amplitude, the increase in spike width seen in control explants was enhanced by both NGF and NGF antibodies. The decrease in ahp duration was neither attenuated by exposure to NGF nor enhanced by NGF antibodies (Traynor, Dryden & Smith, 1992). The results thus

show that NGF alone is not responsible for regulation of a.p. and there might be additional factors involved in 'exogenous' regulation of a.p. in BFSG cells.

### 5.7.2 Activity and activity-dependent changes in second messengers

Since no physical connection exists between the axotomized neurone and its target, the second type of interaction which is lost may be some activity or activitydependent factor/s. Electrical activity and increased cytosolic Ca<sup>2+</sup> have been shown to decrease the level of mRNA for α-subunit of Na<sup>+</sup> channels and cyclic AMP increases its level in parallel with changes in the number of Na<sup>+</sup> channels (Offord & Catterall, 1989). Moreover blockade of electrical activity and complete elimination of neuromuscular transmission by application of botulinum toxin can produce axotomy-like changes in cat motoneurones (Pinter, Vanden-Noven, Muccio & Wallace, 1991). Also, it has been reported that cyclic AMP analogs working through protein kinase A (PKA), independent of NGF, may promote survival and neurite outgrowth in cultures of rat sympathetic and sensory neurones (Rydel & Greene, 1988). Thus, it is possible that axotomized neurones may induce expression of some mechanisms whereby the PKA-dependent phosphorylation is enhanced or potentiated. Although the effects of axotomy on delayed rectifier channels suggest that phosphorylation is not enhanced, there might be a differential regulation of different isozymes of kinases.

### 5.7.3 Changes in gene expression and cytoskeletal disruption

Axotomy leads to stereotypic changes in genes encoding for the cytoskeletal These changes include a down-regulation of neurofilament and an elements. upregulation of actin and T  $\alpha$ 1 tubulin and growth associated protein (GAP-43; Oblinger & Lasek, 1988; Miller, Tetzlaff, Bisby, Fawcett & Miner, 1989; Hall, Virginia, Lee & Kosik, 1991; Tetzlaff, Alexander, Miller & Bisby, 1991; Wong & Oblinger, 1991). Axotomy of lamprey giant central neurones close to their somata results in appearance of highly phosphorylated form of neurofilament protein in the sprouts which leads to downregulation of neurofilament production (Hall et al., 1991). This ectopic form of neurofilament may compete for MAPs and thus interfere with stability of microtubules. Thus, a destabilization of microtubules may result from a generalized increase in phosphorylation since such an increase in whosphorylation has been proposed from the increased inactivation of IBa observed in axotomized neurones (Chapter 2). Destabilization and loss of microtubules may in some way permit neurofilament invasion of the dendrites and axonal regeneration. Appropriate target interaction has been reported to be necessary for maintenance of cytoskeleton (Doering, 1992). Since neurofilaments are major intrinsic determinants of axonal caliber (Hoffman, Cleveland, Griffin, Landes, Cowan & Price, 1987) axotomy results in changes in conduction velocity in large myelinated fibers (Titmus & Faber, 1990).

### 5.7.4 Inflammation and axonal transport

Those peripheral neurones which survive axotomy extend neurites and regrow

and regenerate to reconnect back to the target organ. Axonal regeneration is enhanced by inflammation near the nerve cell body (Lu & Richardson, 1991) and the regeneration can be impeded by interleukin-1 (IL-1) receptor antagonist (Guenard, Dinarello, Weston & Aebischer, 1991). This suggests that macrophages brought in the area of injury as a result of inflammation play an essential role in peripheral nerve regeneration through the release of stimulatory and/ or inhibitory molecules.

Axotomy has also been shown to enhance the faster subcomponent of slow axonal transport which transports cytomatrix proteins (clathrin, fodrin, actin, and calmodulin), tubulin, and glycolytic enzymes (velocity 2-8 mm/day; Jacob & McQuarrie, 1991). This acceleration is consistent with the increased requirement of various materials for repair and regeneration. Any role of these processes in the 'exogenous' regulation of ion channels in neurones remains to be investigated.

### 5.8 Conclusions and Future Experiments

The present study shows that the electrophysiological properties of BFSG B-cells are subject to 'endogenous' and 'exogenous' regulation. This study deals with one aspect of 'exogenous' regulation of ionic currents i.e. effects of axotomy. Axotomy results in loss of contact with target organ, injury and subsequently inflammation and repair. The effects of axotomy are most probably a result of combination of these factors. The changes observed in various different currents following axotomy suggest a differential regulation of ion channels. Further, mathematical modelling of currents shows that the changes in currents can explain

the changes observed in a.p. and other electrophysiological properties (Gordon, Kelly, Sanders, Shapiro & Smith, 1987).

Axotomy induces a series of complex changes in neurones including changes in ion channels. The main changes observed in ion channels relate to changes in  $Ca^{2+}$  channels. The two basic mechanisms most likely to explain the changes in  $I_{Ca}$  are an increased phosphorylation and disruption of the cytoskeleton. Both of these mechanisms have been shown to decrease  $I_{Ca}$  in neurones. Destabilization and disruption of cytoskeleton (Hoffman & Lasek, 1980, Tetzlaff et al., 1991) seems to be a more commonplace response than increased phosphorylation (Fukuda, Kamayema & Yamaguchi, 1981; Johnson & Byrely, 1993). Since cytoskeletal disruption decreases  $I_{Ca}$  and the reduction in  $I_{Ca}$  has been suggested to be responsible for changes in  $I_{C}$  and  $I_{AHP}$ , the present evidence is consistent with the idea that axotomy-induced disruption or destabilization of cytoskeleton is likely to be responsible for most of the changes in a.p. shape (increase in duration of spike and a decrease in amplitude and duration of a.h.p.).

Based on the discussion presented above in sections 5.3 and 5.7 some questions arise which should be addressed in order to understand more clearly the response of neurones to injury and the 'exogenous' regulation of ion channels. The following paragraphs describe the main questions and the strategic experiments which can be carried out to test hypotheses based on these questions.

Co-localization of  $Ca^{2+}$  and  $Ca^{2+}$ -activated  $K^+$  channels is an important aspect of regulation of the action potential. However, it is not known yet whether

these channels are co-localized in BFSG B-cells and other neuronal types. To investigate this, intracellular Ca<sup>2+</sup> transients and channel molecules would have to be visualized simultaneously. This can be done using an appropriate fluorescent probe such as Fura-2, Fluo-3 or Indo-3 and channel molecules can be visualized by using appropriate fluorescent or tagged ligand molecules like charybdotoxin, apamin etc. which bind to the channel macromolecules. Confocal microscopy can be utilized to visualize such transients and molecules (Roberts, Jacobs & Hudspeth, 1990; Robitaille, Adler & Charlton, 1990).

Although the 'exogenous' influences that differentially regulate ion channels were not investigated systematically, the potential candidates include the activity-dependent changes in second messenger levels, cytoskeletal disruption and trophic factors. Prior to investigating these mechanisms, the axotomy-induced changes will have to be investigated at single channel level to ascertain the exact nature of the change i.e whether the changes in currents are due to changes in channel number or due to changes in single channel properties following changes in channel macromolecules or changes in the level of the second messengers. Single channel recording from excised inside-out or outside-out patches will be helpful in resolving the issue. The present study has identified that the prime candidate for investigation is Ca<sup>2+</sup> channels, though other channels should also not be overlooked.

The question of the change in channel numbers can be addressed by using autoradiographic techniques with specific ligand;  $\omega$ -conotoxin for N-type Ca<sup>2+</sup> channels; dihydropyridines for L-type Ca<sup>2+</sup> channels; TTX/ STX for Na<sup>+</sup> channels.

Since cDNAs for most of the channels have already been cloned and are available (Catterall, 1988; Snutch, Leonard, Gilbert, Lester & Davidson, 1990; Dubel, Starr, Hell, Ahlijanian, Enyeart, Catterall & Snutch, 1992), molecular biological techniques like *in situ* hybridization using specific probes (mRNA or cDNA for the specific channel) can also be used to investigate the expression of which particular type of ion channel has been up- or down-regulated.

Since the data suggest that the most important change in Ca2+ channels is the change in inactivation, further experiments should include those designed to test the mechanism/s of this change. Recently it has been reported that augmentation of phosphorylation or an inhibition of the phosphatases can increase inactivation of I<sub>Ca</sub> in BFSG cells (Wertz, Elmslie & Jones, in press). Thus one working hypothesis will be that the axotomy-induced reduction of I<sub>Ca</sub> results from inactivation due to increased phosphorylation. Therefore agents which can activate different phosphorylating mechanisms like forskolin for the protein kinase A system and phorbol myristate acetate (PMA) or phorbol-dibutyrate (PDA) for protein kinase C would be expected to produce larger changes in IBa in control cells as compared with that in axotomized neurones. The situation will be analogous to the one in pharmacological experiments showing occlusion of the response, thus suggesting commonality and convergence of the transduction mechanism. Similarly, phosphatase inhibitors like calyculin A and okadaic acid will exert same effects by potentiating the effects of the phosphorylation mechanism/s. Alternatively, the axotomized neurones can be exposed to specific kinase inhibitors (like calphostin D and chelerythrin for

protein kinase C; and A3 or peptide inhibitors for protein kinase A) to see if the changes can be reversed. Similarly, chronic exposure to PMA can be utilized to down-regulate protein kinase C. These interventions when combined with whole-cell or single channel recordings of different currents in isolation should clarify the issue whether the changes observed are due to changes in phosphorylation or due to changes in channel numbers. Furthermore, if these changes are the result of loss of 'exogenous' regulation, this can also be tested (see below).

Since agents which promote cytoskeletal disruption (e.g. colchicine) have been shown to promote axotomy-like changes, an alternative hypothesis for the reduction is that the axotomy-induced disruption of cytoskeleton is responsible for the axotomyinduced changes in various ionic conductances. This would predict that treatment of an axotomized neurone with a cytoskeleton stabilizing agent like taxol and or phalloidin should attenuate or inhibit axotomy-induced changes. experiment to test this hypothesis will be to treat the axotomized neurones (in vivo or in vitro) with cytoskeleton stabilizing agent/s starting immediately or 14 days after axotomy and compare the ionic currents among control, axotomized and axotomized neurones treated with the cytoskeleton stabilizing agent. The purpose of having two treatment groups (one where treatment will be initiated right after axotomy and the other in which treatment will be started 1-2 weeks later) will be to investigate whether these agents can only block the development of these changes or they can also reverse these changes. This mechanism might be exploited in future for developing pharmacological interventions for better regeneration or recovery after axonal injury or axonopathy.

The factors involved in 'exogenous' regulation of ion channels were not investigated systematically in this study. Trophic factors which may be of importance in survival, maintenance, sprouting and regeneration include NGF, FGF and possibly also BDNF. Involvement of these factors needs to be investigated in detail since this might provide a clue to the modulation of the function/s which might be under their control and thus provide a potential therapeutic means of modulating regeneration. The experiments which can be conducted to delineate the role of each of these can In vivo experiments would involve be conducted either in vivo or in vitro. investigation whether the injection of the trophic factor into the animal would reverse or interfere with the axotomy-induced changes and whether the injection of antibodies to the specific trophic factor would accentuate these changes. Although this will be a good way of examining the role of the trophic factor in the animal, the access versus excess (i.e. too little versus too much) issue will be a matter of concern. Similar experiments can also be conducted on explant cultures of sympathetic ganglia and/ or in primary cultures of sympathetic neurones where the trophic factors or antibodies can be incorporated in the culture medium or the perfusate as desired. Acute treatments like application of activators or inhibitors of second messenger cascade can be done equally readily on primary cultures or acutely dissociated neurones and whole-cell patch clamping offers the additional advantage by allowing us to change the internal or external solution as desired.

The effects on a.p. and various ionic conductances in BFSG B-cells have

already been investigated. Therefore the next step will be to investigate the effects on ion channels at single channel level. Since enough information is now available about the electrophysiology, biophysics, trophic regulation and morphology of ganglionic neurones, this knowledge can be exploited further to understand better the relationship between electrical activity, cell body reaction and re-establishment of functional synaptic connections and thus gain a better understanding of the response of neurones to injury and the mechanisms of regeneration and repair.

## 5.9 REFERENCES

AUGUSTINE, C.K. & BEZANILLA, F. (1990). Phosphorylation modulates potassium conductance and gating current of perfused giant axons of squid. *Journal of Physiology* **95** 245-271.

BADER, C.E.; BERTRAND, D.; DUPIN, E. & KATO, A.C. (1983). Development of electrical properties of cultured avian neural crest cells. *Nature* **305** 808-810.

BARISH, M.E. (1986). Differentiation of voltage-gated potassium current and modulation of excitability in cultured amphibian spinal neurones. *Journal of Physiology* **375** 229-250.

CATTERALL, W.A. (1988). Structure and function of voltage-sensitive ion channels. *Science* **242** 50-61.

CHALAZONITIS, A.; PETERSON, E.R. & CRAIN, S.M. (1987). Nerve growth factor regulates the action potential duration of mature sensory neurons. *Proceedings of the National Academy of Sciences of USA* 84 289-293.

DASCAL, N. & LOTAN, I. (1991). Activation of protein kinase C alters voltagedependence of a Na<sup>+</sup> channel. *Neuron* 6 165-175. DAVENPORT, R.W.; DOU, P.; REHDER, V. & KATER, S.B. (1992). Growth cone filopodia as sensors of their environment: Intracellular calcium as a second messenger. Society for Neuroscience Abstracts 18 1287.

DOERING, L.C. (1992). Appropriate target interactions prevent abnormal cytoskeletal changes in neurons: A study with intra-sciatic grafts of the septum and the hippocampus. *Journal of Neuroscience* **12(9)** 3399-3413.

DUBEL, S.J.; STARR, T.V.B.; HELL, J.; AHLIJANIAN, M.K.; ENYEART, J.J.; CATTERALL, W.A. & SNUTCH, T.P. (1992). Molecular cloning of the alpha-1 subunit of an ω-conotoxin-sensitive calcium channel. *Proceedings of the National Academy of Sciences of USA* 89 5058-5062.

ELMSLIE, K.S.; ZHOU, W. & JONES, S.W. (1990). LHRH and GTP&S modify calcium current activation in bullfrog sympathetic neurones. *Neuron* 5 75-80.

FUKUDA, J.; KAMEYAMA, M. & YAMAGUCHI, K. (1981). Breakdown of cytoskeletal filaments selectively reduces Na and Ca spikes in cultured mammal neurones. *Nature* **294** 82-85.

GORDON, T. (1983). Dependence of peripheral nerves on their target organs. In: Somatic and Autonmic Nerve-Muscle Interaction, pp 289-325. Eds. Y. Vrbova; G.

Burnstock; R. Campbell & R. Gordon. Elseviers: Amsterdam.

GORDON, T.; KELLY, M.E.M.; SANDERS, E.J.; SHAPIRO, J. & SMITH, P.A. (1987). The effects of axotomy on bullfrog sympathetic neurones. *Journal of Physiology* **392** 213-229.

GRAFSTEIN, B. & McQuarrie, E.I. (1978). Role of the nerve cell body in axonal regeneration. In *Neuronal Plasticity* pp 155-195. Eds. C.W. Cottman. *Raven press* New York.

GUENARD, V.; DINARELLO, C.A.; WESTON, P.J. & AEBISCHER, P. (1991). Peripheral nerve regeneration is impeded by interleukin-1 receptor antagonist released from a polymeric guidance channel. *Journal of Neuroscience* **29** 396-400.

HALL, G.F.; VIRGINIA, M.; LEE, Y. & KOSIK, K.S. (1991). Microtubule destabilization and neurofilament phosphorylation precede dendritic sprouting after close axotomy of lamprey central neurones. *Proceedings of the National Academy of Sciences of USA*. 88 5016-5020.

HOFFMAN, P.N. & CLEVELAND, D.W. (1988). Neurofilament and tubulin expression recapitulates the developmental programme during axonal regeneration: induction of specific β-tubulin isotype. *Proceedings of the National Academy of Sciences of USA* 85

4530-4533.

HOFFMAN, P.N.; CLEVELAND, D.W.; GRIFFIN, J.W.; LANDES, P.W.; COWAN, N.J. & PRICE, D.L. (1987). Neurofilament gene expression: a major determinant of axonal caliber. *Proceedings of the National Academy of Sciences of USA* 84 3472-3476.

HOFFMAN, P.N. & LASEK, R.J. (1980). Axonal transport of cytoskeleton in regenerating motor neurones: Constancy and change. *Brain Research* 202 317-333.

HONORE, E.; ATTALI, B.; ROMEY, G.; LESAGE, F.; BARHANIN, J. & LAZDUNSKI, M. (1992). Different types of K<sup>+</sup> channels are generated by different levels of a single mRNA. *EMBO Journal* 11(7) 2465-2471.

ISACOFF, E.Y.; JAN, Y.N. & JAN, L.Y. (1990). Evidence for the formation of heteromultimeric potassium channels in *Xenopus* oocytes. *Nature* **345** 530-534.

ISOM, L.L.; DEJONGH, K.S.; REBBER, B.F.X.; OFFORD, J.; CHARBONNEAU, H.; WALSH, K.; GOLDIN, A.L. & CATTERALL, W.A. (1992). Primary structu. and functional expression of the beta-1 subunit of the rat brain sodium channel. *Science* **256** 839-842.

JACOB, J.M. & McQuarrie, I.G. (1991). Axotomy accelerates slow component b of

axonal transport. Journal of Neurobiology 22(6) 570-582.

JOHNSON, B.D. & BYRELY, L. (1993). A cytoskeletal mechanism for calcium channel rundown and block by intracellular calcium. *Biophysical Journal* **64** A116

JONES, S.W. & JACOBS, L.S. (1990). Dihydropyridine actions on calcium currents of bullfrog sympathetic neurons. *Journal of Neuroscience* **10** 2261-2267.

KELLY, M.E.M.; BISBY, M.A. & LUKOWIAK, K. (1988). Regeneration restores some of the altered electrical properties of axotomized bullfrog B-cells. *Journal of Neurobiology* **19** 357-372.

KUBA, K. (1980). Release of calcium ions linked to the activation of potassium conductance in a caffeine-treated sympathetic neurones. *Journal of Physiology* **298** 251-269.

KUBA, K.; MORITA, K. & NOHMI, M. (1983). Origin of calcium ions involved in the generation of a slow afterhyperpolarization in bullfrog sympathetic neurones. *Pflugers Archives* 399 194-202.

KUBA, K. & NISHI, S. (1976). Rythmic hyperpolarizations and depolarizations of sympathetic ganglion cells induced by caffeine. *Journal of Neurophysiology* 39(3) 547-

LI, M.; WEST, J.W.; LAI, Y.; SCHEUER, T. & CATTERALL, W.A. (1992). Functional modulation of brain sodium channels by cAMP-dependent phosphorylation. *Neuron* 8 1151-1159.

LIEBERMAN, A.R. (1971). The axon reaction: A review of the principal features of perikaryal response to axon injury. *International Review of Neurobiology* **14** 49-124.

LU, X. & RICHARDSON, P.M. (1991). Inflammation near the nerve cell body enhances axonal regeneration. *Journal of Neuroscience* **11(4)** 972-978.

LUNEAU, C.J.; WILLIAMS, J.B.; MARSHALL, J.; LEVITAN, E.S.; OLIVA, C.; SMITH, J.S.; ANTANAVAGE, J.; FOLANDER, K.; STEIN, R.B.; SWANSON, R.; KACZMAREK, L.K. & BUHROW, S.A. (1991). Alternative splicing contributes to K<sup>+</sup> channel diversity in the mammalian central nervous system. *Proceedings of the National Academy of Sciences of USA* 88 3932-3936.

MEAKIN, S.O. & SHOOTER, E.M. (1992). The nerve growth factor family of receptors. *Trends in Neuroscience* 15 (9) 323-331.

MILLER, F.D.; TETZLAFF, W.; BISBY, M.A.; FAWCETT, J.W. & MILNER, R.J. (1989).

Rapid induction of the major embryonic  $\alpha$ -tubulin mRNA, T $\alpha$ 1, during nerve regeneration in adult rats. Journal of Neuroscience 9(4) 1452-1463.

MORAN, D. (1991). Voltage-dependent-L-type Ca<sup>2+</sup> channels participate in regulating neural crest migration and differentiation. *American Journal of Anatomy* **192** 14-22.

MORAN, O.; SCHREIBMAYER, W.; WEIGL, L.; DASCAL, N. & LOTAN, I. (1992). Level of expression controls gating of a K<sup>+</sup> channel. FEBS Letters 302(1) 21-25.

MORGAN, J.I. & CURRAN, T. (1988). Calcium as a modulator of the immediate-early gene cascade in neurons. *Cell Calcium* 9 303-311.

MURPHY, T.H.; WORLEY, P.F. & BARABAN, J.M. (1991). L-type voltage-sensitive calcium channels mediate synaptic activation of immediate early genes. *Neuron* **7** 625-635.

OBLINGER, M.M. & LASEK, R.J. (1988). Axotomy-induced alterations in the synthesis and transport of neurofilaments and microtubules in dorsal root ganglion cells.

Journal of Neuroscience 8(5) 1747-1758.

OFFORD, J. & CATTERALL, W.A. (1989). Electrical activity, cAMP, and cytosolic calcium regulate mRNA encoding sodium channel α subunits in rat muscle cells.

Neuron 2 1447-1452.

PEROZO, E. & BEZANILLA, F. (1991). Phosphorylation of K<sup>+</sup> channels in the squid giant axon. A mechanistic analysis. *Journal of Bioenergetics & Biomembranes* **23(4)** 599-613.

PINTER, M.J.; VANDEN-NOVEN, S. & WALLACE, N. (1991). Axotomy-like changes in cat motoneuron electrical properties elicited by botulinum toxin depend on the complete elimination of neuromuscular transmission. *Journal of Neuroscience* 11(3) 657-666.

RICH, K.M. (1992). Neuronal death after trophic factor deprivation. *Journal of Neurotrauma* **9** S61-S69.

ROBERTS, W.M.; JACOBS, R.A. & HUDSPETH, A.J. (1990). Colocalozation of ion channels involved in frequency selectivity and synaptic transmission at presynaptic activa zones of hair cells. *Journal of Neuroscience* **10(11)** 3664-3684.

ROBITAILLE, R.; ADLER, E.M. & CHARLTON, M.P. (1990). Strategic location of calcium channels at transmitter release sites of frog neuromuscular synapses. *Neuron* 5 773-779.

RYDEL, R.E. & GREENE, L.A. (1988). cAMP analogs promote survival and neurite outgrowth in cultures of rat sympathetic and sensory neurones independently of nerve growth factor. *Proceedings of the National Academy of Sciences of USA* 85 1257-1261.

SINGER, D.; BIEL, M.; LOTAN, I.; FLOCKERZI, V.; HOFMAN, F. & DASCAL, N. (1991). The roles of the subunit in the function of the calcium channel. *Science* 253 1553-1557.

SNUTCH, T.P.; LEGNARD, J.P.; GILBERT, M.M.; LESTER, H.A. & DAVIDSON, N. (1990). Rat brain expresses a heterogeneous family of calcium channels. *Proceedings* of the National Academy of Sciences of USA 87 3391-3395.

SPITZER, N.C. (1979). Ion channels in development. *Annual Review of Neuroscience* **2** 263-297.

STREIT, J. & LUX, H.D. (1990). Calcium current inactivation during nerve growth factor induced differentiation of PC12 cells. *Pflugers Archives* 416 368-374.

SVENSSON, M. & ALDSKOGIUS, H. (1992). The effect of axon injury on microtubule associated proteins MAP2, 3 and 5 in the hypoglossus nucleus of the adult rat. *Journal of Neurocytology* **21** 222-231.

TETZLAFF, W.; ALEXANDER, S.W.; MILLER, F.D. & BISBY, M.A. (1991). Response of rubrospinal neurones to axotomy: changes in mRNA expression for cytoskeletal proteins and GAP-43. *Journal of Neuroscience* 11(8) 2528-2544.

TITMUS, M.J. & FABER, D.S. (1990). Axotomy-induced alterations in the electrophysiological characteristics of neurons. *Progress in Neurobiology* **35** 1-51.

TRAYNOR, P; DRYDEN, W.F. & SMITH, P.A. (1992). Trophic regulation of action potential in bullfrog sympathetic neurones. *Canadian Journal of Physiology & Pharmacology* **70** 826-834.

VARADI, G.; LORY, P; SCHULZ, D.; VARADI, M. & SCHWARTZ, A. (1991). Acceleration of activation and inactivation by the beta subunit of skeletal muscle calcium channel. *Nature* 352 159-162.

WERTZ, M.A.; ELMSLIE, K.S. & JONES, S.W. Phosphorylation enhances inactivation of N-type calcium channel current in bullfrog sympathetic neurons. *Pflugers Archiv* (in press).

WOLLNER, D.A. & CATTERALL, W.A. (1986). Localization of sodium channels in axon hillocks and initial segments of retinal ganglion cells. *Proceedings of the National Academy of Sciences of USA*. **83** 8424-8428.

WONG, J. & OBLINGER, M.M. (1991). NGF rescues substance P expression but not neurofilament or tubulin gene expression in axotomized sensory neurones. *Journal of Neuroscience* 11(2) 543-552.

YANG, J. & TSIEN, R.W. (1993). Enhencement of N- and L-type calcium channel currents by protein kinase C in frog sympathetic neurones. *Neurons* 10 127-136.

YOUNG, W. (1992). Role of calcium in central nervous system injuries And Cofficient Neurotrauma 9 S9-S25.